Population structure and dynamics
of polyphosphate accumulating organisms
in a communal wastewater treatment plant

DISSERTATION

zur Erlangung des akademischen Grades

Doctor rerum naturalium

(Dr. rer. nat.)

vorgelegt

der Fakultät Mathematik und Naturwissenschaften

der Technischen Universität Dresden

von

Dipl. Biol. Susanne Günther

geboren am 26.05.1983 in Leipzig

Leipzig, 2011

Dissertation der Technischen Universität Dresden

Datum der mündlichen Prüfungen: 12.12.2011

Gutachter: Prof. Dr. Isolde Röske

                    Prof. Dr. Thomas Bley

Table of contents

Abbreviations

µS	micro Siemens
9-AA	9-aminoacridine
a. p.	air pressure
a. r.	aeration regime
a. v.	air velocity
A/O	anaerobic/oxic
A²/O	anaerobic/anoxic/oxic
ADP	adenosine diphosphate
amount $_{r.s.}$	amount of return sludge (reused sludge from AT 1 and 2)
ARDRA	amplified rDNA restriction analysis
AT	aeration tank
ATP	adenosine triphosphate
aut. part.	autofluorescent particles
b. w.	bidestilled water
Bardenpho	wastewater treatment process for subsequent (de)nitrification and phosphorous removal developed by Barnard
Biodenipho	biological (de)nitrification and phosphorous removal
BLAST	basic local alignment search tool
BP	band pass
CARD FISH	catalysed reporter deposition fluorescence –in situ- hybridisation
CDP	cytidine diphosphate
COD	chemical oxygen demand
CV	coefficient of variation
DAPI	4',6-diamidino-2-phenylindole dihydrochloride
DNA	desoxyribonucleic acid
DPAO	denitrifying polyphosphate accumulating organisms
DSMZ	Deutsche Sammlung von Mikroorganismen und Zellkulturen - German Collection of Microorganisms and Cell Cultures
e.c.	electrical conductivity
e.g.	*exempla gratia* – for example
EASC	extended anaerobic sludge contact
EBPR	enhanced biological phosphorous removal
EPS	extracellular polymeric substance
et al.	*et alii / et aliae / et alia* – and others
EW	Einwohnergleichwert - population equivalent
FISH	fluorescence –in situ- hybridisation
FSC	forward scatter
g	gram
GAO	glycogen accumulating organisms
GDP	guanidine nucleoside diphosphate
h	humidity
Heatphos	elution of intracellular polyphosphoric acid by sludge heating
i.e.	*id est* – that means
IC	inorganic carbon
kDa	kilo Dalton
LP	long pass
MAR FISH	microautoradiographic fluorescence –in situ- hybridization
MLSS	mixed liquor suspended solids
ML-UV	multi line ultraviolet
MLVSS	mixed liquor volatile suspended solids

n.l.l.c.	neutral lipid like compounds
NAD	nicotinamide adenine dinucleotide
NH_4-N	ammonia-nitrogen
n-MDS	non-parametric multidimensional scale
NMR	nuclear magnetic resonance
ORP	oxidation-reduction potential
P	phosphate
PAO	polyphosphate accumulating organism
PAST	paleontological statistics
PBS	phosphate buffered saline
PC	primary clarifier
PCR	polymerase chain reaction
PHB	poly hydroxy butyrate
Phoredox	phosphorus reduction oxidation
PMT	photo multiplier tube
polyP	polyphosphate
ppk	polyphosphate kinase
ppm	parts per million
ppx	exopolyphosphatase
RDP	recombination detection program
RNA	ribonucleic acid
rpm	rotation per minute
rRNA	ribosomal ribonucleic acid
SBR	sequenced batch reactor
SCB	sodium cacodylate buffer
SSC	sideward scatter
SSCP	single strand conformation polymorphism
T	temperature
Tc	tetracycline hydrochloride
TC	total carbon
TEM	transmission electron microscopy
Tg	terra gram
TN	total nitrogen
TOC	total organic carbon
T-RF	terminal restriction fragment
T-RFLP	terminal restriction fragment length polymorphism
TSS	total suspended solids
UDP	uridine diphosphate
VSS	volatile suspended solids
WW	wastewater
WWTP	wastewater treatment plant
x g	standard gravity

List of Figures

List of Tables

Introduction

The world population is expected to grow from now 6.8 to approximately 9.2 billion people by the year 2050, putting high pressure on the productive capacity of agriculture and industry. Moreover, such an increase presents an enormous risk for the environment, since human activities are the etiologic agent for widespread and exponentially increasing changes in species distribution and abundances, as well as the climate. For instance about 30% of the vertebrates and 20% of the higher plants in Europe are classified as 'threatened' and the current extinction rates are estimated to be 100-1,000 times higher than in pre-human times [PIMM *et al.*, 1995; LAWTON *et al.*, 1995]. The fossil fuel combustion and deforestation have increased the concentration of atmospheric carbon dioxide by 30% within the past 300 years with more than 50% of the increase occurring in the last 40 years [CHAPIN *et al.*, 2000]. According to literature, the mean growth rate of the atmospheric CO_2 concentration for the previous 20 years was about 1.5 ppm per year (ppm = parts per million) with 387 ppm at the end of 2009. Compared to the concentration at the start of the industrial revolution in 1750 (280 ppm) it showed an increase of 39%. It is also stated, that the present concentration is the highest during at least the last 2 million years [GLOBAL CARBON PROJECT, 2011]. This, and the rising concentrations of methane (doubled) and other gases may lead to a rapid climate change called global warming. Moreover, it is reported that up to 54% of the available fresh water is used by humans and this percentage will increase to 70% by 2050 [CHAPIN *et al.*, 2000].

Not only the excessive use of fertilizers for crop production or the waste produced by humans are considered as human activities that are extremely harmful to the environment, but also the consumption of meat (global consumption expected to rise by 54% between 2002 and 2030), aquaculture production (worldwide increase over 600% within the last 30 years), and the use of fossil fuels for energy production (expected to rise over 50% between 2005 and 2030) [SELMAN and GREENHALGH, 2009].

1. Eutrophication and the phosphorous cycle

One of the problems caused by human activity is the eutrophication of marine and freshwater systems all over the world. Eutrophication, defined as the increase of nutrients in an ecosystem, can be a natural process or caused by human activities (anthropogenic). Natural eutrophication is a common phenomenon, known to be part of the normal aging process of water ecosystems. It is a slow (time span up to several hundred years) and gradual process, occurring because production and consumption within the ecosystem are for some reasons not levelled out, leading from eutrophic water bodies to shallow water bodies and, in the following to swamps or fens and eventually to woods. Non-natural eutrophication is mainly caused by the excess influx of nitrogen and phosphate, with phosphate being the major cause for eutrophication of freshwater systems. In most (fresh-) water ecosystems phosphate is a growth limiting factor, since it is mostly bound to metals or soil particles.

Figure 1 shows the reservoirs and general fluxes of phosphate over the year.
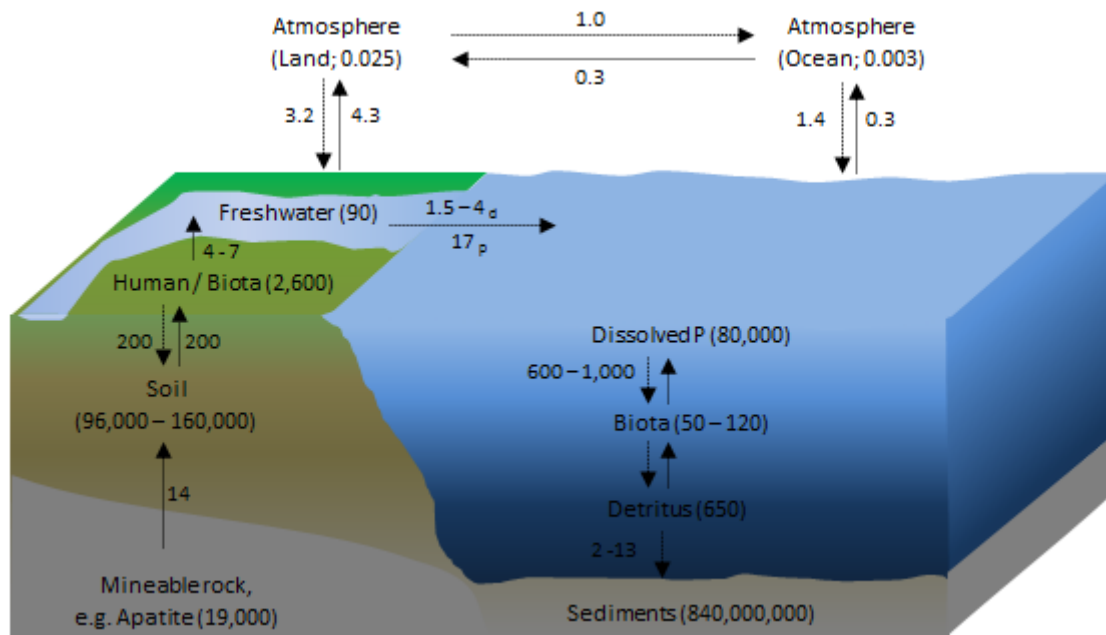
Figure 1. Phosphorous cycle with general reservoirs (in brackets) and fluxes (numbers at the arrows) of phosphate (numbers given in Tg P per year). d: dissolved, p: particular [Data from RICHEY, J.E., WOLLAST, R., DUCE, R.A.; chapter 2, Scope 21, 1983]. In marine environments phosphate is mostly found in form of salts in sediments or bound in rocks (e.g. Apatite: $Ca_5(PO_4)_3(F,Cl,OH)$). Due to weathering or mining of the rocks phosphate can be absorbed and incorporated by primary biomass producers entering the biotic food and degradation chain. Degraded phosphorous compounds re-enter the soil or, as runoff, the ocean. The native phosphorous cycle is very slow but due to low natural supply of phosphate, relative to the requirements for plants and animals, humans accelerate the turnover of phosphate compounds by using fertilizers leading to eutrophication of water systems.

In the eutrophication process the massive increase in nutrient concentration (e.g. dissolved phosphorous) enhances the primary productivity (defined as the production of organic compounds e.g. biomass from atmospheric or aquatic carbon dioxide) like the excessive growth of phytoplankton and algae. This leads to a loss of sub-aquatic vegetation which is the reason for oxygen deprivation and the development of so called 'dead' (hypoxic) zones. Hypoxia, as the most severe symptom of eutrophication, has escalated over the last 50 years from 10 documented cases in 1960 to over 169 in 2007. The Gulf of Mexico is the most popular example, containing a growing hypoxic, biological nearly dead area, which comprised about 5,000 km² in the year 2000 and over 22,000 km² only two years later. Some of the hypoxic areas are expected to recover, like the Black Sea, which was the greatest hypoxic zone in the world until the economic collapse of the former Soviet Union in the 1990's reduced the influx of nutrients drastically, others are expected to be still growing due to extensive use of fertilizers [SELMAN et al., 2008]. It is estimated that about 54% of the lakes in Asia, 53% in Europe, 48% in North America, 41% in South America and, 28% in Africa are eutrophic [ILEC, 1994]. Phosphate fluxes in rivers have also increased dramatically. The natural flux of dissolved phosphate of all rivers into the ocean per year lies between 0.45 and $0.5 * 10^{12}$ g P. Because of the growth of the human population and the excessive use of fertilizers the flux value has risen to over $2.3 * 10^{12}$ g P per year [WOLLAST, 1983].

Since the average amount of organic bound phosphate released by one person per day is about 2 g, phosphate elimination from wastewater to prevent eutrophication events is a big challenge, especially when considering the predicted human population growth. But not only excess influx of phosphorous into water systems is a big problem. Extensive use of phosphorous as fertilizer has had a high impact on the natural resources. It is estimated, that the remaining resources may last for only 90 more years [STUMPF *et al.*, 2007]. So recycling of phosphates from wastewater presents an important challenge to stabilize and increase the quality of surface water systems and to obtain new phosphorus resources for sustainable and economic use in several areas of agriculture and industry.

2. Wastewater treatment and phosphate elimination

Conventional wastewater treatment plants (WWTPs) remove approximately 30-40% of the influent phosphate concentration due to bacterial growth, cell maintenance and incorporation or adsorption to the Extracellular Polymeric Substances (EPS) [OOSTHUIZEN and CLOETE, 2001]. For further phosphate elimination, the first step to phosphate recycling, several methods are known, ranging from chemical precipitation using metals to Enhanced Biological Phosphorous Removal (EBPR).

2.1 General wastewater treatment

The inflowing raw wastewater is in the first step screened by bars and racks (Figure 2, a) to remove the larger objects that are carried in the stream. Removed particulate matter is either collected and later disposed or chopped into small particles which are degraded further in the downstream process. In the grit chamber (Figure 2, b) the velocity of the wastewater is adjusted to facilitate the settlement of stones, grit and sand. After the grit chamber the wastewater flows into the primary clarifier (Figure 2, c), were the primary sludge is allowed to settle while grease and oil are skimmed of at the surface. Typically over 60% of the suspended solids are removed after this treatment step. The next step is the elimination of nitrogen via denitrification in the non-aerated activated sludge tank (Figure 2, d). Phosphate and a major part of the organic compounds which are still remaining are eliminated in the aerated activated sludge tank (Figure 2, e). The final step for the now nearly carbon, nitrogen and phosphorous free wastewater is the secondary clarifier (Figure 2, f) where microbial flocs are allowed to settle. Some of the settled sludge is reused for the activated sludge tanks. Settled sludge that is not re-used and biodegradable substances from the other treatment stages are collected and degraded at the anaerobic digestion chamber (Figure 2, h), which is designed to produce methane. The methane can be stored in the gas reservoir (Figure 2, i) and used for energy production. Now the water should have levels of organic compounds, phosphorous and nitrate below the limits claimed by the local authorities. To test this and to raise the quality of the effluent the water is passed through a control station (Figure 2, g) before it is discharged into the environment. When the value of e.g. phosphorous at the control station is not within the permitted limit, chemical precipitates are added to the activated sludge tanks to remove the phosphorous.
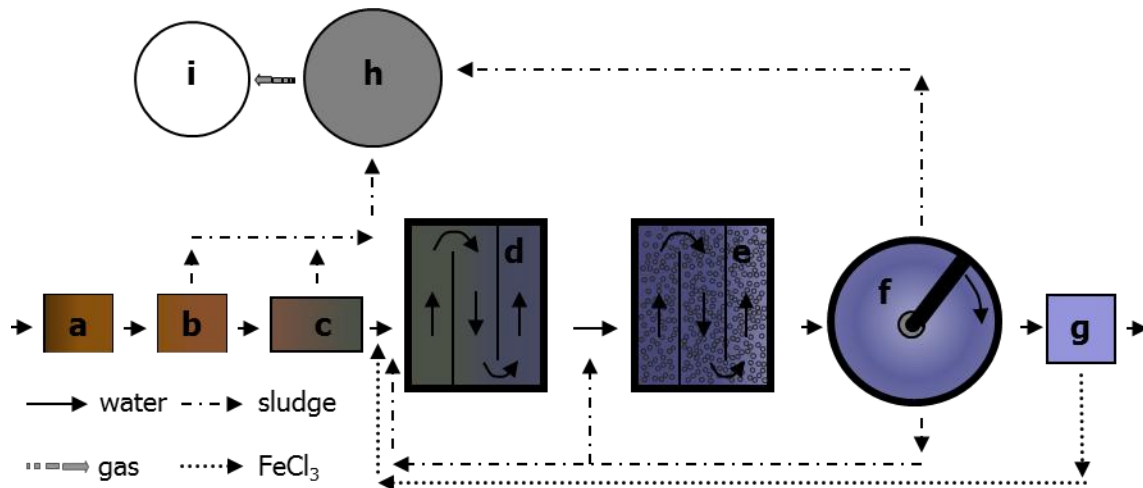
Figure 2. The general flow of water, sludge, gas and FeCl$_3$ for chemical phosphate elimination in a WWTP operating via the A/O process. a: screening (bars/racks), b: grit removal, c: primary clarifier, d: anaerobic activated sludge tanks for denitrification, e: aerated activated sludge tank, f: secondary clarifier, g: control station for effluent water, h: anaerobic digestion chamber, i: gas reservoir

2.2 Phosphate removal

Chemical phosphate removal strategies via addition of precipitants like FeCl$_3$, FeClSO$_4$, Fe$_2$(SO$_4$)$_3$, NaAl(COH)$_4$, Al$_2$(SO$_4$)$_3$ are widely used and secure the observance of phosphate emission levels. But they are expensive in the long term run. Also, they have a high environmental impact, since they produce enormous amounts of metal contaminated sludge which cannot be re-used as fertilizers. More economical and environmentally compatible is the EBPR process. It is nowadays an accepted and frequently applied technique for phosphate removal in the wastewater treatment processes [MARTIN GARCIA et al., 2006].

There is a multitude of operational designs feasible for a WWTP that operates (at least partly) via EBPR. Bardenpho, Biodenipho, Phoredox, A/O, A²/O, Extended Anaerobic Sludge Contact (EASC) are just some of them. Roughly simplified, the EBPR process is supposed to work on the basis of alternating anaerobic and aerobic cycles, with substrate supply at the anaerobic stage. Phosphate removal from wastewater is achieved by withdrawing the Polyphosphate Accumulating Organisms (PAOs, see below) as excess sludge [BLACKALL et al., 2002]. Unfortunately, the process varies highly in efficiency and is prone to failure, so that most WWTPs operating in EBPR mode have chemical precipitation as backup technique. In a survey of 182 WWTPs in Germany with wastewater influent higher than 100,000 EW, 45.1% used chemical precipitation methods, 50% EBPR and chemical precipitation, and only 4.9% EBPR [MONTAG et al., 2008].

3. Polyphosphates and organisms responsible for the phosphate elimination

It is known from literature, that only 1-2 mg of the normal influent phosphorous concentration of wastewater (10-15 mg L^{-1}) are consumed by growing microorganisms. The remaining phosphate is stored in the EBPR process by the PAOs as so called polyphosphate granules and eliminated in the further process of wastewater treatment (see below).

3.1 Ubiquitous distribution of polyphosphates and their cellular localization

Polyphosphates of inorganic origin have been found in volcanic condensates and oceanic steam vents. They are so far found in every living organism, but only microorganisms are known to accumulate high quantities in form of intracellular granules [GAWIGAN *et al.*, 1999]. In microorganisms polyphosphates have been found in the cytoplasm, periplasm, at the flagellar pole, in the cell membrane and on the cell surface. PAOs accumulate excess phosphorous and store it in form of osmotically inert intracellular polyphosphate granules, which are usually located in the nucleoplasmic region or in association with other cell components like multienzyme complexes (e.g. RNA polymerase [KUSANO and ISHIHAMA, 1997], the degradosome [BLUM *et al.*, 1997]), ribosomes, cytosceleton, cell membrane, and cell wall. They are in a size range between 48 nm and 1 µm and may constitute over 50% of the total cell phosphorous [SHIVELY, 1974]. Frequently two or more granules per cell are observed (e.g. in Zoogloea ramigera, [ROINESTAD and YALL, 1970]), depending on species and cell age (young cells with many small granules, older ones with few, big granules [STREICHAN *et al.*, 1990]).

3.2 Molecular composition of polyphosphate granules

Polyphosphate granules consist of linear or circular orthophosphate chains with chain lengths ranging from very few to several hundred residues. The residues are linked by energy rich phosphoanhydride bonds (see Figure 3). As a polyanion the polyphosphate chains need counter ions to neutralize the negative charge. The most important counter ions are Mg^{2+}, Ca^{2+} and K^+, but several other cations like Mn^{2+}, Al^{3+}, Fe^{3+}, small basic proteins and nucleic acids have also been proven to be incorporated to a lesser extent, depending on growth conditions and microorganism under investigation [VAN GROENESTIJN *et al.*, 1988; SCHÖNBORN *et al.*, 2001].
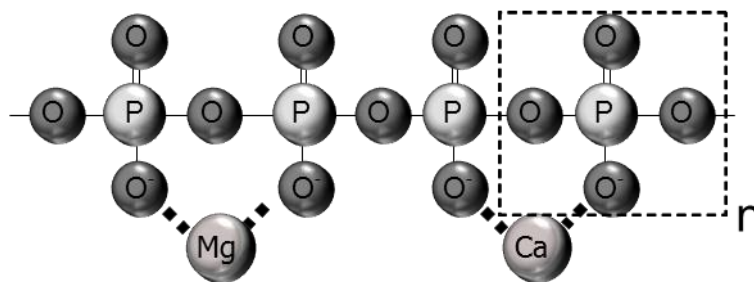
Figure 3. Simplified structure of the orthophosphate chains with associated cations.

3.3 Enzymes involved in polyphosphate synthesis and degradation

There are many enzymes involved in polyphosphate metabolism, some remotely conserved like the polyphosphate kinase, and others highly diverse like the exopolyphosphatases. Since little is known about microorganisms in their natural environment, especially the uncultivable ones, the following list of enzymes is not complete, but is designed to give a rough overview [for further information see for instance KULAEV and KULAKOVSKAYA, 2000 or KORNBERG *et al.*, 1999].

Polyphosphate kinase (ppk): The polyphosphate kinase is an extensively studied enzyme, which is responsible for the processive synthesis of polyphosphate chains, but it also acts as a polyphosphate degrading enzyme. It can convert GDP and other nucleoside diphosphates to the respective nucleoside triphosphates, with preferences in the following order: ADP>GDP>UDP/CDP. This enables the *ppk* to modulate the cellular ribonucleoside triphosphate and desoxyribonucleotide triphosphate levels and therewith to participate in the regulation cell division and stationary phase survival. As a component of different multienzyme complexes *ppk* has been found to participate in enzyme activity regulation. As an example, the *ppk* isolated from *Escherichia coli* is a membrane bound homotetramer with a molecular weight of 80 kDa per subunit. It is also part of the degradosome, responsible for the processing and degradation of RNA (*ppk* binds either to the RNA or to ATP thereby regulating the enzyme activity).

Other systems for polyP synthesis: In *ppk*-null-mutants polyphosphate containing membrane complexes have been found in many organisms, indicating the presence of another polyphosphate synthesising enzymes. It is speculated that the enzyme 3-phosphoglycerolphosphate-polyphosphate-phospho-transferase could use 1,3-diphosphoglycerate to form polyphosphates in *ppk* deficient cells.

Exo- and endopolyphosphatases: These enzymes are mainly responsible for the polyphosphate degradation. Exopolyphosphatases split orthophosphate ions from the chain ends and have despite their high diversity some common characteristics like the high requirement for K^+ or the low activity with short-chain polyphosphates. Endopolyphosphatases split up the polyphosphate chains from the inside, providing action sites for the exoplolyphosphatases.

Triphosphatases: In *Thermobacterium autotrophicum* a specific triphosphatase has been found which also requires K^+ for maximum activity and has a low specific activity for short-chain polyphosphates probably due to the reverse action of the polyphosphate kinase.

Other polyphosphate degrading enzymes: In many bacteria other enzymes for polyphosphate degradation have been found. Examples are: polyphosphate-adenosine monophosphate-phosphotransferase, polyphosphate glucokinase, polyphosphate fructokinase, and phosphate dependent NAD-kinase.

Even with enzymes from the few cultivable species, there are still many questions to answer, for instance with regard to the expression status of the enzyme (inducible or constitutive) or the genetic regulation involved in the expression.

3.4 Polyphosphate functions
As polyfunctional compounds, polyphosphates have various errands within the cell. They are phosphate and energy sources, sequester toxic metal ions, store cations and influence their functions, participate in cell envelope formation and function, pathogenicity, motility, biofilm formation and quorum sensing.

Furthermore, they are known to be regulators of gene and protein activity and play an important role in stress response and stationary phase adaption. In addition to this, they are part of membrane channels which are supposed to act as some kind of DNA-transport systems and phosphate or calcium pumps [Kulaev and Kulakovskaya, 2000]. Most of the above mentioned functions have been evaluated using null mutants. A list of those mutants and the resulting phenotypes can be found in Seufferheldt et al. (2008).

3.5 Probable evolutionary functions of polyphosphates

The ubiquitous distribution of polyphosphates and their structure has led researches to the assumption that they may have had an important role in abiogenic synthesis of nucleic acids and other macromolecules on the primordial earth (earth before the existence of the first life forms). It could have provided a polyanionic, energy-rich scaffold to assemble or orient macromolecules. Due to its phosphorylating properties, polyphosphates could donate to alcohols, sugars, nucleosides, and proteins, as well as react with activated alkyl and amino acids to generate fatty acids and polypeptides [Brown and Kornberg, 2004]. Belozersky and other authors suggested that polyphosphates in phylogenetically very ancient and primitive microorganisms perform the functions of energy rich compounds like ATP does in 'modern' microbial cells. In many microorganisms there are still many biochemical reactions were polyphosphates serve as phosphorous donor e.g. ATP regeneration. Some enzymes found in phylogenetic ancient microorganisms have been shown to have a higher activity with polyphosphates than with ATP (e.g. glucokinase) [Kulaev et al., 2000]. In phylogenetically more modern microorganisms it is vice versa.

4. Microorganisms participating in the EBPR Process

Although polyphosphates as intracellular compounds are well investigated, the microorganisms in the EBPR process are still unknown. Chemical models which are predicting the PAO behaviour in EBPR sludges are mainly based on experiments on transformations of organic compounds and phosphorous in labscale EBPR-systems with enriched microbial communities or pure cultures.

Many pure cultures have been isolated which showed partly the properties expected from PAOs, but none of them could be shown to have great significance in wastewater treatment plants operating via EBPR [Nakamura et al., 1995; Blackall et al., 2002; Serafim et al., 2002]. For instance Acinetobacter species have long been expected to be responsible for EBPR and they have therefore been extensively studied, but later studies showed that they neither exhibit typical PAO-features (e.g. carbon transformation patterns) nor are adequately represented in EBPR sludges [Cloete and Steyn 1987; Wagner et al., 1994; Tandoi et al., 1998]. This may be due to the cultivation bias, since unfortunately only those microorganisms were studied which would grow under laboratory conditions. Those cultivable microorgamisms represent just about 1-10% of the overall microbial community present in the WWTP [Ritz, 2007].

New insights in the wastewater treatment processes suggest that mainly uncultivable bacterial species are responsible for accumulating polyphosphates [LEMOS *et al.*, 2003; WAGNER *et al.*, 2006]. Since those organisms cannot be investigated in pure culture on a laboratory scale, techniques need to be involved which enable to follow individual bacterial performances without cultivation.

5. Detection of PAOs

Many researchers have been trying to overcome the cultivation bias by studying the organisms thought to be the ones responsible for phosphate elimination from wastewater *in situ* and there are many possible methods to do this, each with its own advantages and limitations. The following section should give a short overview over the most frequently applied techniques.

5.1 Polyphosphate granule visualization and detection of possible PAOs

Dyes: There are quite a number of staining techniques for polyphosphate granules described in literature for use in light or fluorescence microscopy. The Neisser staining and Loeffler's Methylene Blue staining (both relying on the dye Methylene Blue) as well as the fluorescent dye 4',6-DiAmidino-2-PhenylIndole dihydrochloride (DAPI) are the most frequently used ones. Most of the staining techniques depend on the polyanionic nature of the polyphosphate granules and despite the frequent utilization of these dyes unspecific staining has been reported [SERAFIM *et al.*, 2002].

Labelled substrates (^{31}P): Labelled substrates in combination with Nuclear Magnetic Resonance (NMR) techniques allow non-invasive and non-destructive investigation of microbiological physiology. The labelled substrates are incorporated into the target molecules facilitating the observation of substrate consumption, end-product and metabolite formation within one sample [SERAFIM *et al.*, 2002].
However, due to the requirement of external substrate addition and the incubation time needed this technique might have influences on the microbial community under investigation. Another restriction is the limited availability of labelled substrates and the costs for devices needed to use this technique on the single cell level (e.g. microscope equipped with NMR detectors).

Fluorescence In Situ Hybridisation (FISH) techniques: Labelled probes for the detection of DNA or RNA molecules *in situ* are one of the most important advances in microbial ecology, since they allow the detection and localization of a specific target within the cell and can be routinely used for identification of microorganisms, studies of gene expressions and to explore the ecophysiology of the habitat. To enhance the signal intensity and spatial resolution methods like Catalysed Reporter Deposition (CARD) FISH [SANZ and KÖCHLING, 2007] and microautoradiographic (MAR) FISH [KONG *et al.*, 2005] are available. Despite the usefulness of those methods there are a few limitations of all FISH techniques. Firstly, the need for the sequence of the target molecules and their abundance in the cell and secondly, the often incomplete permeabilization of the cells followed by the limited penetration of the probes.

Antibodies: SAITO *et al.* (2005) employed fluorescence labelled antibodies to directly label polyphosphate granules at the ultrastructural level. They used the affinity of the polyphosphate binding domain of *Escherichia coli* exopolyphosphatase to selectively stain polyphosphate granules in *Saccharomyces cerevisiae*. The use of labelled antibodies is feasible for the visualization of polyphosphate granules at the ultrastructural level, but not for routine analysis due to the amount of time consuming preparation steps.

PCR-based and other molecular techniques: Molecular techniques for the investigation of possible PAOs in WWTPs like the comparative observation of functional and deteriorated WWTPs operating on EBPR via Single Strand Conformation Polymorphism (SSCP) analysis and clone libraries or full cycle rRNA analysis have been proposed in many studies [HESSELMANN *et al.*, 1999; DABERT *et al.*, 2001]. They reveal the microbial diversity in the investigated microbial system, but they do not give any information about metabolic functions of the organisms present. Furthermore, they only work within the boundaries of the primers used. MARTIN GARCIA *et al.* (2006) used metagenomic analysis to investigate activated sludge communities which were dominated by the yet-uncultured bacterium 'Candidatus Accumulibacter phosphatis' and applied shot gun sequencing to elucidate the EBPR related metabolism and the genome of this bacterium which is supposed to be one of the key players in the EBPR process. This technique was applied for enriched cultures, since investigation of quickly changing compositions of WWTP samples would be much more time and cost intensive. Use of the omnipresent enzymes from the polyphosphate metabolism for investigation of PAOs (e.g. *ppk* and *ppx*) have been another often employed way for analysis of activated sludge, but like other bulk measurements they do reveal nothing about the actual function of single organisms participating in the EBPR process.

5.2 Combinations of the afore mentioned techniques and their application

There are many combinations of the afore mentioned methods which can be applied directly to the activated sludge, therefore avoiding the cultivation bias and allowing analysis on the single cell level.

Most frequently the combination of FISH and DAPI staining is applied to investigate PAOs from activated sludge systems and nearly always this is done via light and fluorescence microscopy [WAGNER *et al.*, 1994; KAWAHARASAKI *et al.*, 1999; CROCETTI *et al.*, 2000 and 2002], but some researchers have also used polyphosphate staining in combination with electron microscopy. Electron microscopic methods (e.g. Transmission Electron Microscopy (TEM)) reach higher resolution, but it is frequently reported that normal preparation and staining techniques can displace, transform and dissolve many elements within a sample (e.g. polyphosphate granules), so that they provide only a limited representation of the *in vivo* situation [BUCHAN, 1980]. Although the analyses of stained samples (with respect to the limitation of each single technique) are applicable in most laboratories, microscopic analysis is an extremely time consuming way of analysis, since stained cells have to be counted by the observer and results may be impaired by cell clusters or low signal intensities as well as the subjective view of the observer.

A faster and more reliable analysis of stained or labelled cells is provided by the use of flow cytometry which, in addition to speed and accuracy, allows the separation of cells with certain properties (e.g. cells exhibiting polyphosphate granules stained with DAPI) and their follow-up analysis (used for instance by ZILLES et al., 2002a). This technique has its limitations when it comes to flocs of microbial cells which are not easily dispersed and withstand separation steps like sonication. A technique similar to flow cytometry is the so called laser microdissection where stained cells are excised and separated after microscopic observation for subsequent DNA analysis [GLOESS et al., 2008]. This method worked well for analysis of lake sediments and activated sludge samples, but it is a laborious method since the cells have to be excised and collected one by one and a special protocol for small amounts of PCR products is needed.

6. Phosphate recycling from wastewater

The following section aims to give a short overview over some of the phosphate recycling forms described in literature. According to MONTAG and colleagues [MONTAG et al., 2008] the potential of phosphate recovery from wastewater in German WWTPs varies from 30 to 85% depending on the phosphorous load, WWTP type and operation as well as phosphate removal efficiency.

Most of the known processes for phosphate recovery rely on the formation of hydroxyapatite. Tobermorite crystals, a seed material consisting of calcium silicate hydrate, are used for crystallization of hydroxyapatite from sludge side streams of a WWTP by MORIYAMA [MORIYAMA et al., 2001]. These crystals are described by to be usable as fertilizer and directly applicable to soils. Hydroxyapatite is also formed when TiO_2 fibers [NAGAMINE et al., 2003] or blast furnace slag (in the presence of calcium [JOHANSSON et al., 2000]) are used to remove phosphate from wastewater. Leaching of phosphate from sludge incineration ash (with acid or base dependent methods and subsequent precipitation with calcium) is another way to recover phosphate but it is only feasible if low amounts of chemical precipitation agents are used during WWTP operation [HIROTA et al., 2010].

Also described by HIROTA is the so called 'Heatphos' process where heating at 70°C of phosphate rich sludges results in the release of polyphosphates from bacterial cells into the surrounding liquid. These polyphosphates can be precipitated by calcium without the need for pH adjustments which is required for the precipitation of orthophosphate. The precipitate called 'biophosphorite' consist of 16% phosphate and 18% calcium and has therefore a higher phosphate content compared to the typical rock phosphate with 8-13% phosphate and 26-33% calcium.

Struvite, ammonium magnesium phosphate crystals with high phosphate content, is also used to produce a fertilizer called MAP (Magnesium Ammonium Phosphate). HIROTA describes the production of struvite from the ammonium and phosphate rich filtrate of the slurry derived from the anaerobic sludge digestion process by addition of magnesium hydroxide at pH between 8.2-8.8. Highest struvite production occurs at a low concentration of suspended solids, pH higher than 7.5 and molecular ratios of ammonium, magnesium and phosphate of 1:1:1.

Aim of this study

Since little is known about the uncultivable microorganisms participating in the EBPR process, it is important to gain more knowledge about them to optimize the whole process of phosphate elimination from wastewater and make it better accessible to control strategies.

Flow cytometric analysis of PAOs in combination with other molecular and chemical techniques will be useful to shed light on the EBPR processes in a WWTP and the microorganisms involved in biological phosphorous removal. Furthermore, it will help to answer questions about conditions favouring the enrichment of PAOs.

Therefore the aim of this study was to detect PAOs quantitatively in wastewater sludges, to determine their phylogenetic affiliation and to follow their dynamics in a WWTP.

To achieve this, cultivation independent, flow cytometry based techniques were used to obtain knowledge on PAO distribution in wastewater on the single cell level. Since most of the fixation protocols in existence are not suitable for analysis of community dynamics via flow cytometry new fixation protocols which implement a high structural cell stability of the various species involved in the wastewater treatment process needed to be developed. Even more important, a polyphosphate staining technique appropriate for combined analysis of polyphosphate and DNA content is necessary for analysis of the PAO community dynamics as well as for the separation and identification of up to date uncultivable PAOs.

Analysis of the overall community dynamics combined with the observation and identification of the main PAOs may be an important tool for EBPR bioprocess optimization. Therefore, this study will also focus on following community dynamics from samples harvested directly from a WWTP to determine changes in the WWTP process that lead to deterioration of phosphate elimination at an early stage. It may be useful to detect failures in the EBPR process on the microbiological scale and develop process strategies to make EBPR more stable in the long term run.

Material and Methods

1. Microorganisms and culture conditions

1.1 Pure cultures

To fulfil the demands of the later described experiments it was necessary to cultivate test organisms (bacteria, archaea) to estimate the fixation efficiency and to evaluate methods for polyphosphate staining. A list of these organisms, their sources and culture conditions is given in Table 1.

Table 1. List of species used, their sources, culture conditions and time of the harvest (growth phase). For the list of media and solutions see Annex I (A. I).

name	source	medium (see A. I)	cultivation parameters	growth phase
Methanomonas methylovora	UFZ strain collection	1	30 °C, 150 rpm	early exponential
Paracoccus denitrificans	UFZ strain collection	2	30 °C, 150 rpm	early exponential
Shewanella putrefaciens	UFZ strain collection	2	30 °C, 150 rpm	early exponential
Desulfovibrio desulfuricans	UFZ strain collection	3	anaerobic, 30 °C, 0 rpm	early exponential
Paracoccus denitrificans	UFZ strain collection	4	anaerobic, 30 °C, 0 rpm	early exponential
Methanosarcina barkeri (DSM 800)	DSMZ	5	anaerobic, 37 °C, 0 rpm	early exponential
Microlunatus phosphovorus NM-1 (DSM 10555)	DSMZ	6	30 °C, 150 rpm	lag, exponential, stationary
Pseudomonas sp.	wastewater isolate (TU Dresden)	6	30 °C, 150 rpm	exponential, stationary
Paracoccus sp.	wastewater isolate (TU Dresden)	6	30 °C, 150 rpm	exponential, stationary
Escherichia coli K12	UFZ strain collection	7	30 °C, 150 rpm	stationary
Methylobacterium rhodesianum MB126	UFZ strain collection	1	30 °C, 150 rpm	stationary
Micropruina glycogenica Lg2^T (DSM 15918)	DSMZ	8	30 °C, 150 rpm	stationary
Bacillus subtilis	UFZ strain collection	7	30 °C, 150 rpm	stationary
Acinetobacter calcoaceticus 69-V	UFZ strain collection	9	30 °C, 150 rpm	stationary

Aerobic strains were cultivated in batches of 300 mL each on a rotary shaker whilst anaerobic cultures were set up in 118-mL serum bottles which were filled with 85-90 mL medium and 10-15% inoculum, closed tightly with thick black rubber stoppers (Ochs, Bovenden/Lenglern, Germany) and cultivated statically in the dark. Strictly anaerobic cultures were prepared in an anoxic glove box (gas atmosphere 95% nitrogen, 5% hydrogen; Coy Laboratory Products Inc., Grass Lake, MI, USA).

Cultures were checked regularly for purity by streaking aliquots on agar plates of the respective medium (given above) as well as microscopic observation. Growth was measured spectro-photometrically at 700 nm (Model Ultrospec III Amersham Biosciences Europe, $d_{cuvette}$ = 0.5 cm).

Table 2 shows the most important properties of afore mentioned organisms and the rationale for usage in various experiments.

Table 2. Rationale for usage of the species in Table 1. Tc: tetracycline hydrochloride

name	properties	used as
Methanomonas methylovora	methanol oxidising bacterial strain	test organism for fixation efficiency
Paracoccus denitrificans	grown under aerobic conditions: non-nitrate reducing	test organism for fixation efficiency
Shewanella putrefaciens	iron reducing bacterial strain	test organism for fixation efficiency
Desulfovibrio desulfuricans	sulphate reducing bacterial strain	test organism for fixation efficiency
Paracoccus denitrificans	grown under aerobic conditions: nitrate reducing bacterial strain	test organism for fixation efficiency
Methanosarcina barkeri (DSM 800)	methanogenic archaeon	test organism for fixation efficiency
Microlunatus phosphovorus NM-1 (DSM 10555)	polyphosphate production	model organism for polyphosphate-production
Pseudomonas sp.	polyphosphate production	model organism for polyphosphate-production
Paracoccus sp.	polyphosphate production	model organism for polyphosphate-production
Escherichia coli K12	quickly growing	negative control (Tc-binding to DNA)
Methylobacterium rhodesianum MB126	PHB production	negative control (Tc-binding to PHB)
Micropruina glycogenica Lg2^T (DSM 15918)	glycogen production	negative control (Tc-binding to glycogen)
Bacillus subtilis	spore formation	negative control (Tc-binding to spores)
Acinetobacter calcoaceticus 69-V	polyphosphate production	test organism for Tc fluorescence spectra

To stimulate polyphosphate production the test organisms (*M. phosphovorus* NM1, *Pseudomonas* sp., *Paracoccus* sp.) were cultivated in 500-mL shake flasks with tightly closed screw caps on 100 mL synthetic wastewater described in HRENOVIC *et al.*, 2003 (medium 6, see Annex I). They were subjected to alternating aerobic and anaerobic conditions (changing every 12 hours). For every new anaerobic process interval the medium was replenished with 0.26 mM propionate, 0.1 g L^{-1} peptone and 54 µM CaCl$_2$ as well as 83 µM MgSO$_4$ and 1.6 mM KH$_2$PO$_4$.

To establish aerobic conditions, the culture was flushed with sterile air and under anaerobic conditions with sterile nitrogen of highest purity for at least 60 minutes. *Acinetobacter calcoaceticus* 69-V was cultivated for 5 to 6 days at the parameters given in Table 1 until polyphosphate granules could be detected microscopically via DAPI staining (see Material and Methods, section 4.2, p. 17).

1.2 Mixed cultures

1.2.1 Batch experiments

Activated sludge from the wastewater treatment plant (WWTP) Kaditz (Dresden, Germany) was cultivated for 2 weeks in batches on a rotary shaker at 30°C and 150 rpm under aerobic and anaerobic conditions, alternating every 12 hours. Synthetic wastewater medium (10% vol/vol, medium 6, see Annex I) was supplied in the anaerobic phase and the culture sparged with nitrogen for at least 30 minutes. After 12 hours the culture was sparged with air for at least 30 minutes.

1.2.2 Bench top bioreactor experiments

For lab-scale bioreactor experiments activated sludge from the aerobic treatment phase of the WWTP Elsterwerda (Brandenburg, Germany) was harvested and cultivated in a 7-liter laboratory bioreactor with a working volume of 5 liter (New Brunswick BioFlow III, New Brunswick Scientific, USA) at 300 rpm (except for the settling period) and 20°C at the TU Dresden (Institute of Food Technology and Bioprocess Engineering and the Institute of Microbiology, Dresden University of Technology, Germany). The pH value of 7 ± 0.05 was automatically regulated by titration with either 0.6 M HCl or 0.5 M NaOH. The reactor was operated as Sequenced Batch Reactor (SBR) with a cycle time of 6 h four times a day, consisting of an aerobic period (2 h, aerated), followed by a settling and refilling period for restoring anaerobic conditions (2 h, manual feed) and an anaerobic period (2 h). The initial Mixed Liquor Suspended Solids (MLSS) were set to 2.5 g L^{-1} by appropriate dilution with cultivation medium (medium 10, OECD synthetic wastewater, see Annex I).

For overnight SBR operation, settling and refilling was replaced by automated feeding of concentrated medium (43 mL/6 h) to result in a final concentration equal to that of the manual feed. The concentrations of phosphate and other components of the medium were changed during the cultivation as indicated according to the demands of the experiments. The oxygen was recorded by an oxygen sensor (Applicon, The Netherlands). The pH was analyzed by a sensor from Mettler-Toledo (Switzerland).

1.2.3 Direct sampling from WWTP Eilenburg

Municipal wastewater from the city Eilenburg and the surrounding communities Doberschütz, Zschepplin, Naundorf, Krippehna, and Krostiz as well as industrial wastewater from the brewery Krostiz and other industrial and business parks is being treated in the WWTP Eilenburg. This treatment plant was designed to treat wastewater up to 49,000 EW. The usual retention time for sludge in the WWTP is 8 days [personal communication, Feb. 2010].
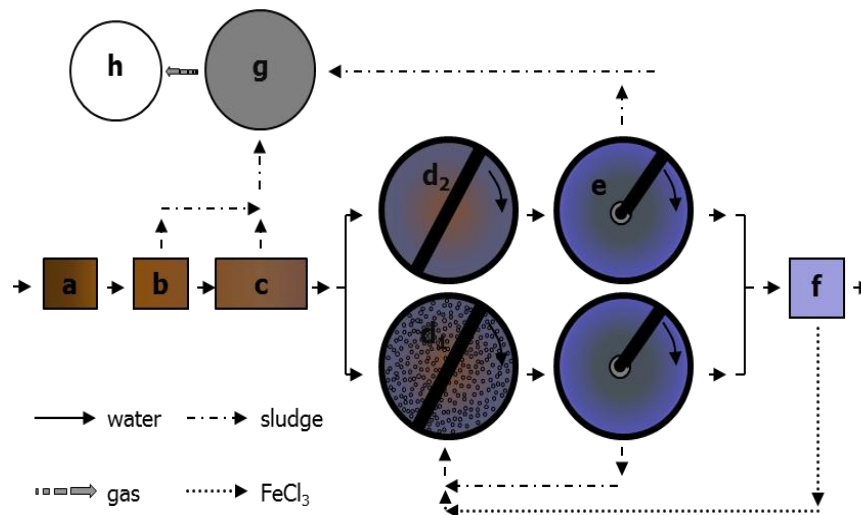
Figure 4. Schematic drawing of the WWTP Eilenburg. The general flow of water, sludge, gas and FeCl$_3$ for chemical phosphate elimination is shown via arrows. a: screening (bars/racks), b: grit removal, c: primary clarifier, d: activated sludge tanks (d$_1$: aerated, d$_2$:non-aerated; alternating every 90 minutes), e: secondary clarifier, f: control station for effluent water, g: anaerobic digestion chamber, h: gas reservoir

After rough mechanical treatment, the wastewater flows through a primary clarifier (PC) where it stays 30 min before its purification in about 4 hours within two parallel activated sludge tanks (AT 1 and 2) set to sequential anaerobic and aerobic phases, altering in a 90 min mode for intermittent nitrification/ denitrification processes (but with an aeration regime which is inverse). Subsequently, the purified effluent is directed into the secondary clarifier (for 3 hours) whereas the activated sludge is reused or channelled into the digestion tank. Samples were taken at 3 points: the primary clarifier c, the activated sludge tank d$_1$ and the activated sludge tank d$_2$. Immediately after harvesting the samples were either stored in ice-cooled, airtight bottles or fixed for flow cytometric analysis. The amount of activated sludge harvested was depended on the method used for analyses of various abiotic parameters. 2 mL of the respective sample were used for flow cytometric measurements, 500 mL were sampled for determination of chemical parameters (redox potential, pH, electrical conductivity, COD, TC, IC, TOC, TN, NH$_4$-N, inorganic phosphate, NO$_3$, NO$_2$).

2. Cell fixation

Table 3. Fixation protocols for follow-up analysis (flow cytometry, cell sorting, microscopy and TEM).

step	flow cytometric analysis / microscopy	cell sorting / microscopy		TEM
		phylogenetic analysis	further cultivation	
1	sampling (batch cultivaton, bioreactor, WWTP)			
2	10% NaN$_3$, 5 mM BaCl$_2$ and 5 mM NiCl$_2$ in PBS	10% NaN$_3$ (in PBS)	no fixation	3% glutaraldehyde in 0.1 M SCB
3	transport in ice-cooled devices (glas flasks and vials)			immobilization with 4% Agar in SCB
4	3 washing steps in PBS			
5	activated sludge samples: 10 min sonication			4 washing steps with SCB
6	adjustment of the cell suspension (cell density: 3*10^8 cells mL^{-1})			
7	further preparation (e.g. staining)			

2.1 Test of fixation efficiency

Cells of pure cultures were harvested and washed twice with phosphate-buffered saline (PBS: 0.4 M Na_2HPO_4/NaH_2PO_4, 150 mM NaCl, pH 7.2) by centrifugation at 3,200xg (5 min). Activated sludge samples were taken from the aerobic and anaerobic phases and washed twice with PBS by centrifugation at 3,200xg (10 min). The remaining pellets were resuspended in an appropriate amount of fixation buffer (1 mL for app. $3x10^8$ cells mL^{-1}) and the samples stored in glass tubes at 4°C.

Fixation of pure cultures was done by using the following metal salts as fixatives: aluminium nitrate nonahydrate ($Al(NO_3)_3*9H_2O$; Fluka, Switzerland), barium chloride 2-hydrate ($BaCl_2*2H_2O$; Laborchemie Apolda, Germany), sodium molybdate 2-hydrate ($Na_2MoO_4*2H_2O$; Riedel-de Haën, Seelze, Germany), sodium tungstate (Na_2WO_4; Berlin-Chemie, Germany), bismuth nitrate oxide ($Bi(O)NO_3$; Fluka, Switzerland), nickel (II) chloride hexahydrate ($NiCl_2*6H_2O$; Merck, Germany) and cobalt (II) nitrate hexahydrate ($Co(NO_3)_2*6H_2O$; Riedel-de Haën, Seelze, Germany). Each of the metal salts was dissolved to give a concentration of 5 mM in PBS. Sodium azide (Merck, Germany) was added to give a 10% solution. The pH was adjusted to 7.0 with either NaOH or HCl. A solution of 10% sodium azide in PBS and selected mixtures of metal ions ($BaCl_2$, $NiCl_2$, $Bi(O)NO_3$ or $BaCl_2$, $NiCl_2$; 5 mM each in PBS) with 10% sodium azide were also tested. Activated sludge samples from the batch culture (see section 1.2.1, p. 14) were taken after four days of continued shifts between aerobic and anaerobic conditions from both phases, two hours after the respective shifts. After washing, the samples were treated with four metal combinations, each containing 10% sodium azide (in PBS) and respectively: (1) 5 mM $BaCl_2$ and 5 mM $NiCl_2$, (2) 15 mM $BaCl_2$ and 15 mM $NiCl_2$, (3) 5 mM $BaCl_2$, 5 mM $NiCl_2$ and 0.41 mM Tween 20 (Merck, Germany), or (4) 15 mM $BaCl_2$, 15 mM $NiCl_2$ and 0.41 mM Tween 20. Cryopreservation involving resuspending the cells in ice-cold PBS or ice-cold PBS containing 15% glycerine (Laborchemie Apolda, Germany) followed by storing aliquots of 1 mL at -20°C was also tested. Unfixed cells harvested at both phases served as controls. They were washed and resuspended in the same volume of PBS as above. All tests were carried out in duplicates. Flow cytometric measurements were performed on all samples repeatedly over at least 30 days.

2.2 Polyphosphate staining experiments and WWTP samples

All cells, with exception of those to be sorted, were fixed in a 10% sodium azid solution (in PBS) amended with 5 mM $BaCl_2$ and 5 mM $NiCl_2$ and stored at 4°C maximally for 9 days. A 10% sodium azide solution without added metals was used for fixation of the cells that were to be sorted.

3. Cell preparation

Aliquots of the samples were washed twice to remove any disturbing substances (cell debris, organic material) and the fixative with PBS by centrifugation at 3,200xg for 5 min (10 min for activated sludge samples) and the resulting pellet was resuspended in buffer to yield an optical density of 0.033 corresponding to an average cell density of $3x10^8$ cells mL^{-1}. For activated sludge exhibiting strong floc formation it was necessary to subject the samples to 10 minutes sonication in a water bath (ultrasonic bath, Merck Eurolab, Darmstadt, Germany) prior to adjustment of the optical density.

4. Staining procedures

Table 4. Staining protocols for flow cytometry, cell sorting and microscopy. polyP: polyphosphate, Tc: tetracycline hydrochloride, n. l. l. c.: neutral lipid like compounds; for solutions A and B see Annex I

step	flow cytometric analysis / microscopy / cell sorting				
	polyP		polyP/DNA	DNA	n. l. l. c.
	Tc	DAPI	DAPI, Tc	DAPI	Nile red
1	2 mL of adjusted cell suspension				
2	centrifugation				
3	10 min 100 µL Tc	20 min 1 mL solution A			10 min
4	60 min 2 mL PBS	1 washing step			10-40 µL
5		60 min 2 mL solution B (28 µM)	10 min, 100 µL Tc		Nile red
6			60 min 2 mL solution B (28 µM)		
7	sample filtration (pore diameter: 30 µm)				
8	measurement				

4.1 DNA

Adjusted cell suspensions (2 mL) were treated with 1 ml solution A (0.11 M citric acid/4.1 mM Tween 20 in bidistilled water, see Annex I) for 20 min. Then, the cells were washed and resuspended carefully in 2 mL solution B (0.24 µM or 1 µM 4',6-diamidino-2'-phenylindole (DAPI, SIGMA), 400 mM Na_2HPO_4, pH 7.0, see Annex I) for at least 60 min in the dark at room temperature using a modification of a standard procedure [MEISTRICH et al., 1978]. A DAPI solution of 0.24 µM was used for DNA staining of activated sludge samples and a 1 µM solution for *M. phosphovorus* NM1.

4.2 Polyphosphates

For cellular polyphosphate staining, two different dyes were applied.

The first one was DAPI, known to stain polyphosphates at high concentrations. Two mL adjusted cell suspension were centrifuged and treated with 1 mL solution A (see above) for 20 min. Then, the cells were washed and resuspended carefully in 2 mL of a 28 µM DAPI stock solution.

The second dye was the antibiotic tetracycline hydrochloride (Fluka, Switzerland or Roth, Germany indicated as follows: Tc_{Fluka} and Tc_{Roth}). It was applied as a 2 mg mL^{-1} stock solution in bidistilled water to give a final concentration of 0.225 mM in the cell suspension. Stock solutions were prepared freshly before each experiment. Stained samples were stored for 60 min at 20°C in the dark prior to flow cytometric measurement. For all experiments unstained cells served as controls. The number of particles displaying green autofluorescence was subtracted from the fluorescence counts from Tc stained samples to obtain polyphosphate related fluorescence information.

4.3 DNA versus polyphosphates

For dual staining of the DNA and polyphosphate granules by DAPI and Tc, the cells were subjected first to solution A for 20 min, centrifuged, washed and the pellet treated with 0.225 mM Tc for 10 min before 2 mL solution B (0.24 µM and 1 µM for activated sludge and *M. phosphovorus*, respectively) were added. Stained samples were incubated for another 60 min at 20°C in the dark before flow cytometric measurement.

4.4 PHB and neutral lipid like compounds

To visualize cellular PHB contents, Nile red (Sigma, USA) was applied as a stock solution of 1 mg per mL acetone. For PHB staining of *M. rhodesianum* MB126 20 µL mL^{-1} Nile red were used, for all other samples 5 µL mL^{-1} were sufficient for PHB staining. Stained cells were kept for at least 10 min in the dark at room temperature and then analyzed flow cytometrically.

5. Flow cytometry

5.1 General flow cytometry

Flow cytometry is a technique that allows simultaneous measurement and analyses of multiple physical characteristics of single particles in the size range of 0.2 to 150 µm at high speed (several thousand particles per second). Furthermore particles of interest can be separated from another and isolated for further analysis. With the use of fluorescent probes many intrinsic (measured without reagents, e.g. cell size, cell granularity, autofluorescence) and extrinsic properties (measured with reagents, e.g. DNA content, total protein, lipid content) of cells can be analyzed, giving insight into cell cycle activities, storage compounds, cell identity, activity status and many other parameters that may be of interest. Many different types of cells have so far been analyzed via flow cytometry: viruses [LAMBETH *et al.*, 2005; GATES *et al.*, 2009], bacteria [VALDIVIA and FALKOW, 2003; MÜLLER *et al.*, 2010], phytoplankton [LI *et al.*, 1993; SOSIK *et al.*, 2010], animal and plant cells [AL-RUBEAI, 1999; STANCHEWA *et al.*, 2010]. In microbiology, most papers report microscopic analysis despite the advantages flow cytometry offers in this field and although the problems which have to be faced with flow cytometry are the same for microscopy. Cell adherence and floc formation make it difficult to obtain representative cell counts. This, however, might be the bigger problem in microscopy since flow cytometry allows a higher cell count in the same amount of time, so the coverage is much higher.

The principle of flow cytometry is similar to microscopy, but the analysis is faster and more accurate than microscopy. A schematic drawing of the main parts of a flow cytometer is shown in Figure 5. Suspended particles within the sample stream (Figure 5, a), are lined up through a phenomenon called hydrodynamic focusing. This physical phenomenon is caused by the sheath stream (Figure 5, b). Both pressure driven streams do not mix up due their laminar flow. In general, the flow rate of the sample stream is determined by the velocity of the sheath stream. At the so called observation point the particles are passed through a beam of light (usually a laser beam; Figure 5, f) one at a time and the reflected and scattered light is collected, amplified and converted into voltage pulses (Figure 5, i and j). These pulses are used to generate two or three dimensional histograms which can thereafter be analyzed using specific software like Summit (DakoCytomation, Fort Collins, CO), WinList (Verity Software House, Topsham, ME) and FlowJo (Tree Star, Inc. Ashland, OR).

For the investigation of PAOs flow cytometry is especially favourable because there is no need for cultivation of the microorganisms. Additionally, it is possible to investigate and identify so far uncultivable organisms with various proteomic and genetic methods after separation of the organisms via cell sorting (see below).
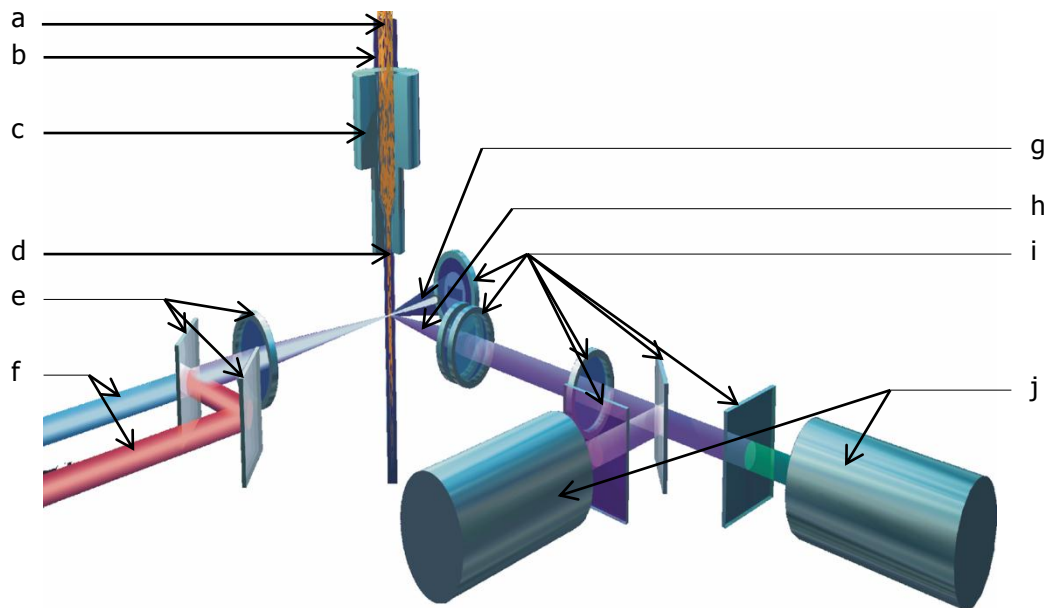
Figure 5. Schematic drawing of the most important parts of a flow cytometer (kindly provided by Prof. S. Müller). a: sample stream, b: sheath stream, c: nozzle (location of the process of hydrodynamic focussing of the sample stream), d: droplet breakoff point (formation through the action of a piezoelectric crystal oscillator; only required for cell sorting), e: optical systems (lenses and mirrors), f: laser beams, g: forward scatter (FSC), h: sideward scatter (SSC) and fluorescence signals, i: optical systems (lenses, mirrors and filters), j: detectors (photo multiplier tubes, PMTs)

5.2 Flow cytometric set-up for the experiments

Analyses were carried out using a MoFlo cell sorter (DakoCytomation, Fort Collins, CO) equipped with two water-cooled argon-ion lasers (Innova 90C and Innova 70C from Coherent, USA). Excitation of 400 mW at 488 nm was used to analyze the fluorescences of Tc and Nile red, as well as the Forward SCatter (FSC) and Sideward SCatter (SSC) signals at the first observation point. SSC was used as a trigger signal to discriminate bacterial cells from electronic noise. DAPI was excited by 100 mW of ML-UV (333-365 nm) at the second observation point. The orthogonal signal was first reflected by a beam-splitter and then recorded after reflection by a 555 nm long-pass dichroic mirror, passage by a 505 nm short-pass dichroic mirror and a band pass (BP) 488/10. Blue (DAPI) fluorescence was passed through a 450/65 BP filter, green (Tc, DAPI) fluorescence through BP 520/15, and red (Nile red) fluorescence through BP 620/45. Photomultiplier tubes were obtained from Hamamatsu Photonics (models R 928 and R 3896; Hamamatsu, Japan). Amplification was carried out at linear or logarithmic scales, depending on the application. Fluorescent beads (yellow-green fluorescent beads: 2 µm, FluoSpheres 505/515, F-8827, blue fluorescent beads: 1 µm, FluoSpheres 350/440, F-8815, crimson fluorescent beads: 1 µm, FluoSpheres 625/645, F-8816, Molecular Probes Eugene, Oregon, USA) were used to align the MoFlo. Also, an internal DAPI-stained bacterial cell standard was introduced for tuning the device up to a Coefficient of Variation (CV) value not higher than 5%.

5.3 Scatter behavior

FSC is roughly related to cell size whereas the SSC is related to cell granularity. Data were obtained by examining the light scattering behavior of individual, stained and unstained cells, mediated by the 488 nm line of the argon ion laser.

Before flow cytometric analysis the stained samples were filtered through filters with a pore diameter of 30 µm (CellTrics®, Partec, Munster, Germany) to prevent clogging of the nozzle by salt crystals (formed within the salt-rich sheath fluid), debris or remaining cell aggregates. As an internal fluorescence and size standard a bead suspension (Fluoresbrite BB Carboxylate microspheres, 1 µm, Polyscience, USA) was added to at least one DAPI stained sample per experiment.

5.4 General cell sorting

As mentioned above, some flow cytometers offer the possibility to separate particles of interest from the sample stream. This is done via flow sorting and very basically carried out like follows.

After careful calibration of the instrument the particles of interest are selected from the histograms by gates (see gate setting strategy, Figure 6, p. 21). These gates are marked for sorting and given a direction in which the so marked cells are to be directed (left, half-left, half-right and, right in the case of the flow cytometer used in this study). Then the sample stream is required to break up into droplets where, ideally, each drop contains one single particle. The droplet generation requires the action of a piezoelectric crystal oscillator (Figure 5, d) that subjects the sample stream to vibrations which lead to the formation of single drops at the droplet breakoff point. If a droplet contains a particle of interest (one that is within the selected gate), it gets electrically charged (--, -, +, or ++). After the application of the either negative or positive electric charge the droplets pass an electric field (at the deflection plates) and are deflected into respective collection vessels.

5.5 Flow cytometric set-up for the cell sorting experiments

Sorting of Tc or DAPI stained bacterial cells was done using the most accurate sort mode (single and one drop mode: highest purity 99%) at a rate not higher than 1,500 cells per second. 3 µm yellow-green fluorescent beads (YG Fluoresbrite Microspheres 441/486, Polyscience, Pennsylvania, USA) were used for calibration of the sort parameters. Cell sorting was performed using the four-way-sort-option at high speed (12 ms^{-1}). The cells were sorted into nucleic acid free glass flasks. Cells were separated from the mixed cultures using either Tc-polyphosphate fluorescence or DAPI-DNA fluorescence intensity and the respective forward scatter signals (see Figure 6, histogram D). To obtain sufficient DNA for the generation of 16S rRNA gene clone libraries, at least 10^6 cells were sorted.

6. Data evaluation and gate setting strategy

For each sample up to 500,000 events (cells and electronic noise) were recorded at a rate not exceeding 1000 events per second and the data obtained were evaluated using Summit software v3.1 (DakoCytomation, Fort Collins, CO). Sub-populations/sub-communities comprising individuals with similar properties in fluorescence (DNA content-related blue fluorescence standing for chromosome contents) and forward scatter (cell size) were marked with gates and the cell numbers therein estimated. Cell numbers usually ranged from 80,000 to 350,000 cells per dot plot. Gates were chosen according to cells with similar fluorescence and size properties. Each gate confines either a sub-population in pure cultures (Figure 11, a-f) or a sub-community in mixed cultures (Figure 11, g, h).
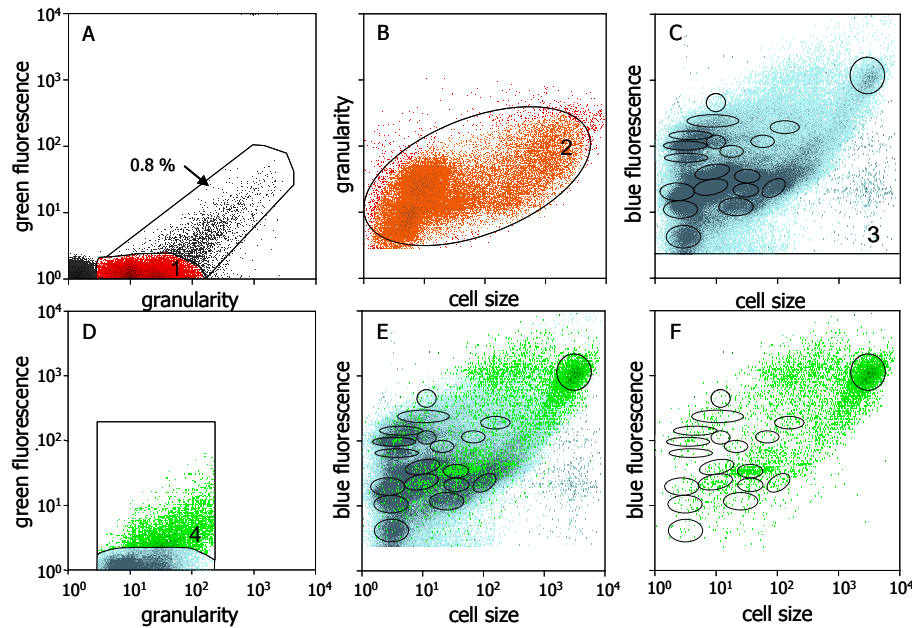
Figure 6. Gating strategy for activated sludge samples. In dot plot A unstained cells were recorded for side scatter and green autofluorescence. Dot plot B presents the SSC vs. FSC of the red region (1) of A. Histogram B was the basis for the DNA gating: electronic noise and signals outside the SSC vs. FSC gate (2) were excluded. Histogram C presents the DAPI vs. FSC features (3). Dominating clusters in dot plot C were gated and counted. The numbers of Tc stained cells in dot plot E and F were determined using the gate strategy (4) of dot plot D.

7. Microscopy

7.1 Fluorescence microscopy

To verify reliable staining and purity and to inspect cell morphologies, the cells were subjected to microscopy and image analysis (microscope: Axioskop, Zeiss; camera: DXC-9100P; software: Openlab 3.1.4., Improvision, USA) using light from a 100 W mercury arc lamp. The Zeiss filter set 02 (excitation G 365, BS 395, emission LP 420) was used for examining blue fluorescence of DAPI stained cells and filter set 09 (excitation BP 450-490, BS 510, emission LP 515) for the green fluorescence of Tc (0.225 mM) stained cells. Red fluorescence from Nile red stained cells (PHB detection) was observed using the Zeiss filter set 15 (excitation 546/12, BS 580, emission LP 590). For better visualization of cell properties, phase contrast and fluorescence images were merged using Openlab.

7.2 Transmission electron microscopy

For transition electron microscopy the cells were fixed with 3% glutaraldehyde (Sigma, Germany) in 0.1 M sodium cacodylate buffer (SCB; pH 7.2) for 1 h at 20°C. Thereafter the cells were immobilized with 4% Agar (Roth, Germany) in SCB and thoroughly washed 4 times with SCB. Polyphosphate staining was done as described by JENSEN et $al.$ (1968). Instead of a 20% $Pb(NO_3)_2$ solution a 2% $Pb(NO_3)_2$ solution was used. Samples were dehydrated in a graded ethanol series and embedded in epoxy resin [SPURR et $al.$, 1969]. Ultrathin sections (80 nm) were transferred to formvar coated copper grids and examined without further staining using an EM 900 transmission electron microscope (Zeiss SMT, Germany) at an acceleration voltage of 80 kV. Electron micrographs were taken with a slow scan camera (Variospeed SSCCD camera SM-1k-120, TRS, Germany). The size of the polyphosphate particles was determined using the iTEM software (Olympus SIS, Germany)

21

8. Statistical theory and analysis

8.1 Equivalence tests

Two main classes of hypothesis testing can be distinguished: significance tests and equivalence tests. Most studies in medicine and pharmacology, biology and related fields use significance tests to detect statistically significant differences between two or more data sets [STREINER, 2003]. In this study the criterion for the effectiveness of fixatives (i.e. sample stability) is the equivalence of data sets created at different times after the fixation. To prove the equivalence of two data sets an equivalence test needs to be applied.

The null hypothesis is that two data sets are not equal

[1] $H_0: n_1 \neq n_2$

and the corresponding alternative hypothesis is

[2] $H_A: n_1 = n_2$

So, if H_0 can be rejected the two data sets are taken as equivalent. Since for several reasons (sampling faults, natural variability of the parameters in biological systems) two data sets can never be truly identical. For reliability of data evaluation the variation between two data sets ($\Delta_{experiment}$) should be equal/lower than a predefined tolerable variation ($\Delta_{predefined\ tolerance}$, [GARRETT, 1997]).

[3] $H_A: n_1 = n_2; \Delta_{experiment} \leq \Delta_{predefined\ tolerance}$

In this study, a two-tailed test which is appropriate for data sets of largely invariable size [BARKER *et al.*, 2002; STREINER, 2003] was applied. The method requires setting a positive and negative limit for the unavoidable technically caused variations between the data sets. This so called confidence interval ($\Delta_{confidence}$) is expected to encompass the parameter of interest with a defined degree of certainty.

To determine the confidence intervals first the standard deviation (σ) of the data sets has to be estimated (for reference see WELLEK, 2003).

[4] $\sigma = \sqrt{(f_0(1 - f_0)/n_o) + (f_x(1 - f_x)/n_x)}$

wherein f_0 is the relative frequency of cells within a respective sub-population/sub-community at day 0, f_x the relative frequency of cells within the respective sub-population/sub-community at day x, n_0 the number of all analysed cells at day 0 and n_x the number of all analysed cells at day x.

Second, the CV-value (probability of error) of flow cytometric analyses needs to be considered, which is already stated to be below 5%. In this case for samples with a high number of individuals (n) there is a factor called quantile z with $z = 1.645$ (WELLEK, 2003).

So the confidence intervals of the data sets are estimated as follows

[5] $\left[f_0 - f_x - \sigma * z; f_0 - f_x + \sigma * z \right]$

For rating data sets as equivalent additionally a tolerance interval has to be set, which gives information about natural variability of the samples. If the confidence interval is contained in the tolerance interval, the two compared data sets are said to be equivalent.

The tolerance interval ($\Delta_{\text{predefined tolerance}}$; -$\Delta$, Δ) was estimated using equation [6], wherein p is the maximum proportion to which the sub-population/sub-community is allowed to vary. As we included highly complex activated sludge the maximally acceptable tolerance was set to 25%.

[6] $\Delta = p * f_0$

Hence, confidence intervals [5] were calculated for every sub-population/sub-community of every fixation at every sampling point. If the proportions of the cells of all sub-populations or sub-communities of one sample (day 0 to day x) are within the 25% range then the confidence interval fits into the tolerance interval and the sample is regarded as *stable*. If in contrast a single confidence interval of only one sub-population or sub-community lies outside the tolerance interval then the whole sample is non-equivalent meaning that the community is regarded as *unstable* (sample labelled with ----; see Results, section 1.1 and 1.2, Table 6 and 7, p. 36 and 38).

Higher resolution was addressed by defining a strict tolerance value of 10% from day 0 to day x. Sub-populations/sub-communities whose confidence interval fit into the resulting strict tolerance interval were stated as *exceptionally stable*. This led to the following classification of results: When the cell number variation of 100-75% of all sub-populations/sub-communities in a sample stayed below the strict 10% tolerance value (= *exceptionally stable* sub-populations/sub-communities) the sample was marked with + +, and if only 74-50% of a samples' sub-population/sub-communities stayed stable the sample was labelled with +, followed by 49-25% with - and 24-0% with - - , respectively (see Results, section 1.1 and 1.2, Table 6 and 7, p. 36 and 38). A summary of the behaviours of sub-populations/sub-communities of all samples regarding the 25% and the 10% stability criteria is given in Table 10 (pure cultures, p. 112) and Table 11 (mixed cultures, p. 114) of Annex II.

For the stability analysis of samples from the WWTP Eilenburg (Results, section 3.2.1, Figure 33, p. 57) equivalence tests with a maximally acceptable tolerance of 25% were used. The procedure was the same as for the analysis of the fixation stability (as described above).

8.2 Spearman's rank-order correlation coefficient and Kendall's rank correlation coefficient

Since multiparametric correlation analyses of complex samples cannot be done manually by comparing graphs of plotted parameters statistical correlation tests have to be applied. They are exceptionally useful for evaluation and quantification of correlations between almost all kinds of parameters [BOLBOACA and JÄNTSCHI, 2006] and provide a good statistical tool for description of community dynamics in complex samples such as activated sludge.

In this study correlation analyses were done using two closely related statistical tests: Spearman's rank-order correlation coefficient (r_S) and Kendall's rank correlation coefficient tau (τ).

Rank correlation is useful for evaluating information ordering because it is a well-understood and widely used measure of the strength of association between two variables.

Given the fact that both tests use the same amount of information in the data, both have the same sensitivity to detect the existence of association (i.e. both tests will lead to rejection of the null hypothesis at the same level of significance). Numerically, they cannot be directly compared since they have different underlying scales. According to SIEGEL and CASTELLAN (1988) the relationship of the two coefficients is as follows:

[7] $-1 < 3\tau - 2r_S < 1$

For each parameter to be compared, both tests require the conversion of the values (x_i, y_i; x_j, y_j;...) to ranks (Rx_i, Ry_i; Rx_j, Ry_j;...). In the rank process the lowest value gets the lowest rank. In case there are two equal values for two different variables (tied/fixed ranks), the associated rank had equal values and is calculated as means of corresponding ranks. In this study non-numerical parameters like week-days or the aeration regime (aerated vs. non-aerated) were converted into numbers: week-days were assigned numbers from 1 to 5 (respectively for Monday to Friday) and the aeration regime the numbers 0 and 1 (non-aerated and aerated).

8.2.1 Spearman's rank-order correlation coefficient

This coefficient was named after Charles Spearman (1863 - 1945), a psychologist well-known for his work in statistics (factor analysis, and Spearman's rank correlation coefficient). It provides a non-parametric measure of correlation, without making an assumption about the distribution of the variables and it does not require the variable to be measured on interval or ration scale [BOLBOACA and JÄNTSCHI, 2006]. Spearman's rank-order correlation coefficient and significance testing were calculated using the program PAST (PAleontological STatistics, Version 2.02, distributed by Øyvind Hammer at the Natural History Museum, University of Oslo [HAMMER and HARPER, 2006]).

The formula for Spearman's rank-order correlation coefficient with tied ranks is:

[8] $r_S = \Sigma(x_i - \overline{x})(y_i - \overline{y}) / \sqrt{((\Sigma(x_i - \overline{x})^2)(\Sigma(y_i - \overline{y})^2))}$

where $\overline{x}$ and $\overline{y}$ are the mean values for the variables x and y.
The null hypothesis (H_0) vs. the alternative hypothesis (H_1) for Spearman's rank-order correlation coefficient is:

[9] H_0: $r_S = 0$ (there is no correlation between the ranked pairs)

[10] H_1: $r_S \neq 0$ (ranked pairs are correlated)

Statistical significance is tested by PAST with a two tailed Student t-test with n-2 degrees of freedom at a significance level of 5% (confidence interval 0.05). For n<10 the program switches to an exact test that compares the observed r_S to the values obtained from all possible permutations of the first parameter using Monte Carlo permutation (limited to 10000 possible permutations).

8.2.2 Kendall's correlation coefficient for tied ranks in both parameters

The correlation coefficient is named after Maurice George Kendall (1907 - 1983). Kendall's tau (τ) is a non-parametric correlation coefficient that can be used to assess and test correlations between non-interval scaled ordinal variables. While Spearman's rank-order correlation coefficient is similar to the Pearson correlation coefficient but computed from ranks, the Kendall tau correlation represents a probability. Furthermore it is more accurate for analysis of samples with a low amount of data points [LAPATA, 2006]. Kendall's tau (τ) and significance testing were calculated using the program PAST.

Kendall's correlation coefficient for tied ranks in both parameters is calculated as follows:
x_i, y_i and x_j, y_j are a pair of measured parameters. First the respective values are subtracted (x_j - x_i and y_j - y_i). When x_j - x_i and y_j - y_i have the same sign (e.g. both -1) the pair is *concordant*, if have opposite signs (e.g. 1 and -1) the pair is *discordant*.

[11] $\tau = (C-D) / \sqrt{((C+D+T_x)(C+D+T_y))}$

where C is the number of concordant pairs, D the number of discordant pairs, T_x the number of pairs with $y_i = y_j$ ($T_x = \sum_{i=1}(t_{ix}(t_{ix}-1)/2)$), T_y the number of pairs with $x_i = x_j$ ($T_y = \sum_{i=1}(t_{iy}(t_{iy}-1)/2)$) and t_{ix}, t_{iy} the length of the tied rankings.

The null hypothesis vs. the alternative hypothesis for Kendalls tau correlation coefficient with tied ranks in both parameters is:

[12] H_0: $\tau = 0$ (there is no correlation between the two variables)

[13] H_1: $\tau \neq 0$ (the two variables are correlated)

Statistical significance of the Kendall's tau correlation coefficient is done by the Fischer's Z-test, at a significance level of 5%.

8.2.3 Interpretation of the results

Both coefficients vary between -1 (inverse ranks) and 1 (identical ranks).
If r_S or τ values are 0.8< or <-0.8 the samples show a high positive or negative correlation.
Values from 0.6 to 0.8 or -0.6 to -0.8 represent samples with good positive or negative correlation and values from 0.4 to 0.6 or -0.4 to -0.6 represent samples with moderate positive or negative correlation.
All values between 0.2 to 0.4 and -0.2 to -0.4 represent samples with low correlation, whereas values between 0.2 and -0.2 represent samples with no significant correlation [STEWART, 2010].
The following 3 graphs serve as examples for high and good positive / negative correlation or no correlation.

I) positive correlation
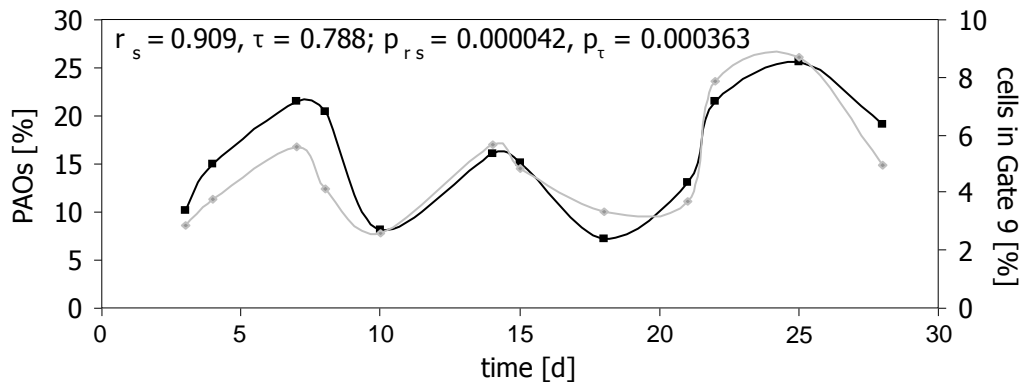
Figure 7. Example for a positive correlation. Changes in abundance of PAOs (squares, black line) and cells in the Gate (i.e. sub-community) 9 (diamonds, grey line) within the aeration tank (AT) 1 of the WWTP Eilenburg over a time span of 29 days. Spearman's rank-order correlation coefficient (r_S) is 0.909 and Kendall's tau (τ) is 0.788 corresponding to a high positive correlation. The respective probabilities, that the parameters are uncorrelated, are as follows: $p_{rs} = 0.000042$ and $p_\tau = 0.000363$

II) negative correlation
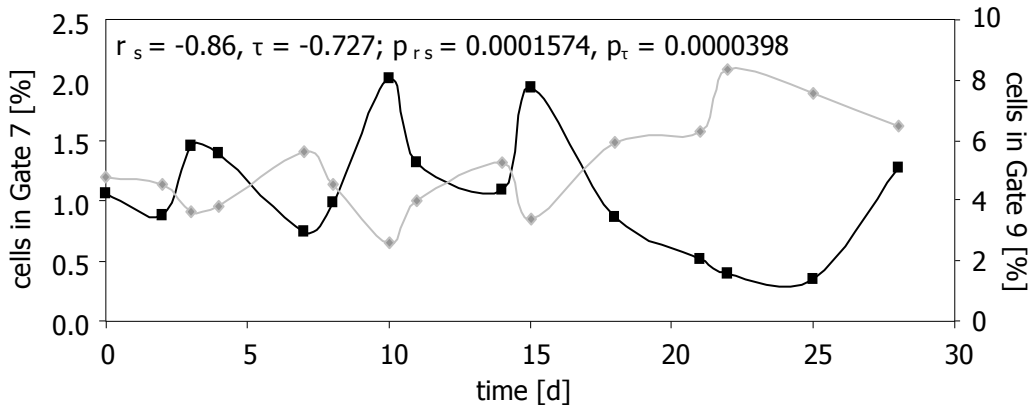
Figure 8. Example for a negative correlation. Changes in abundance of cells in the Gates (i.e. sub-communities) 7 (squares, black line) and 9 (diamonds, grey line) within the aeration tank (AT) 2 of the WWTP Eilenburg over a time span of 29 days. Spearman's rank-order correlation coefficient (r_s) is -0.86 and Kendall's tau (τ) is -0.727 corresponding to a high negative correlation. The respective probabilities, that the parameters are uncorrelated, are as follows: $p_{rs} = 0.0001574$ and $p_\tau = 0.0000398$.

III) low or no correlation
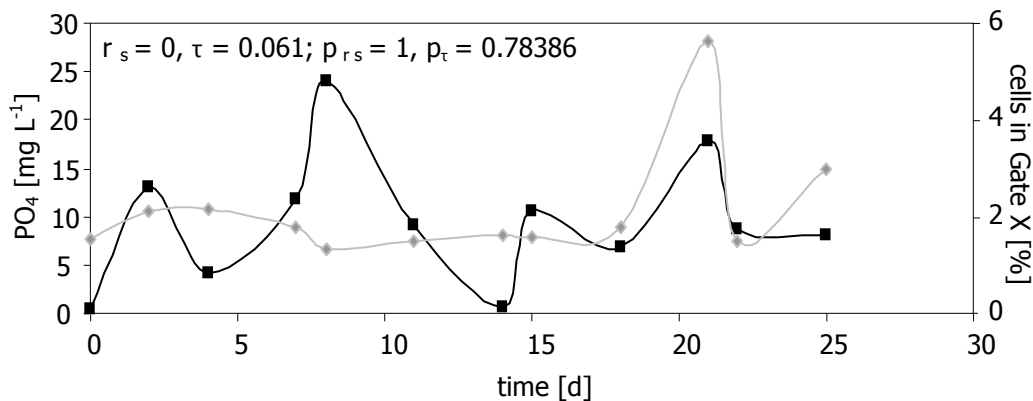
Figure 9. Example for low or no correlation. Changes in abundance of cells in Gate (i.e. sub-community) X (diamonds, grey line) and the orthophosphate concentration (PO_4; squares, black line) within the primary clarifier (PC) of the WWTP Eilenburg over a time span of 28 days. Spearman's rank-order correlation coefficient (r_s) is 0 and Kendall's tau (τ) is 0.061 corresponding to no correlation. The respective probabilities, that the parameters are uncorrelated, are as follows: $p_{rs} = 1$ and $p_\tau = 0.78386$.

8.3 Euklidian distance measurement

Euklidian distances were calculated for data obtained from the WWTP Eilenburg. The Program PAST (see section 8.2.1, p. 24) was used for the calculation. For better comparability the distance measurements of biotic and abiotic parameters were merged (Figure 31, p. 55).

9. Fluorescence spectra

All experiments were carried out using the spectrophotometer F-4500 from Hitachi, which is equipped with a xenon lamp for excitation. Excitation and emission slits were set at 10 nm and the PMT voltage at 950 V. Spectra of Tc stained cells were recorded at a speed 2400 nm per minute and corrected using spectra derived from tetracycline dissolved in PBS. Since Tc from two manufacturers was used the actually applied Tc is marked as Tc_{Fluka} or Tc_{Roth}. Excitation wavelengths were recorded from 250 to 490 nm and the corresponding emission from 480 to 700 nm.

9.1 Dependency of the fluorescence on the tetracycline manufacturer and the solvent

Tetracycline hydrochloride from two different manufacturers (Roth and Fluka, both in stock solutions at a concentration of 2 mg mL^{-1} bidestilled water) was tested. For the recording of the fluorescence spectra 3 mL PBS were incubated in the dark with 300 µL Tc_{Roth} or Tc_{Fluka} for at least one hour and then measured as indicated above. Irrespective from the fluorescence, the tetracycline stock solutions differed in their solubility and the colour. Tetracycline hydrochloride obtained from Roth could be quickly dissolved in bidestilled water yielding a bright yellow coloured solution, whereas the tetracycline from Fluka takes longer time to be dissolved and yields a weak yellow coloured solution.

9.2 Dependency of the fluorescence on the availability of cations

Tetracycline hydrochloride from two different manufacturers (Roth and Fluka, both in stock solutions at a concentration of 2 mg mL^{-1} bidestilled water) was measured and the influence of cation addition tested. For the recording of fluorescence spectra 3 mL PBS were incubated in the dark with 300 µL Tc_{Roth} or Tc_{Fluka} for at least one hour and then measured as indicated above. As cation $CaCl_2$ was used and dissolved in PBS at a concentration of 0.33 mg mL^{-1}. The experimental procedure was the same as for sole PBS (addition of 300 µL of the Tc stock solution, incubation in the dark at RT for 1 h).

9.3 Fixation effects on the fluorescence

A. calcoaceticus 69-V was cultivated batch wise on M9 medium for 4 d (30°C and 150 rpm) and harvested after 4 d. After microscopic confirmation of polyphosphate granules within the cells (DAPI and Tc_{Roth} staining, see section 4) cells were fixed with 10% NaN_3, 5 mM $BaCl_2$ and 5 mM $NiCl_2$ (dissolved in PBS) for at least 3 h. Unfixed cells were meanwhile stored at 4°C in the dark. To meet the demands of the experiment (high cell density required for fluorescence spectrophotometric analysis), the cells were after two washing steps (with PBS) adjusted to cell densities of 0.08. Two millilitres of each cell suspension were then centrifuged and the pellet incubated with 300 µL Tc_{Roth} or Tc_{Fluka} for 1 h in the dark at room temperature. Prior to measurement 3 mL of PBS were added.

10. Chemical analyses of activated sludge samples

10.1 Chemical analyses of the bench top bioreactor experiments

All chemical analyses were done at the Institute of Food Technology and Bioprocess Engineering and the Institute of Microbiology, TU Dresden (Dresden, Germany). Inorganic phosphate and nitrate were measured by ion chromatography (IC, Dionex Corporation, USA). IC analysis was performed on an IC DX 320 with an EG40 eluent generator and an IonPac NG1 guard column (4x35 mm) connected to an IonPac AS15 (4 mm) separation column. The separation was obtained at a flow rate of 0.4 mL min^{-1} with a gradient program (KOH and water) rising from 5 mM to 30 mM in the first 7 min and to 45 mM in the next 10 min. Then the concentration of KOH was kept constant for 5 min and finally decreased to 5 mM within 2 min. MLSS values (Mixed Liquor Suspended Solids [gTSS L^{-1}], TSS: Total Suspended Solids), MLVSS values (Mixed Liquor Volatile Suspended Solids [gVSS L^{-1}], VSS: Volatile Suspended Solids), COD values (Chemical Oxygen Demand [mg L^{-1}]; [CLESCERI *et al.*, 1998]) and the ash contents [g L^{-1}] were determined by standard methods [EATON *et al.*, 1995].

10.2 Chemical analyses in samples from WWTP Eilenburg

10.2.1 General information about the measured parameters

Electrical conductivity (DIN 38404 C8): Electrical conductivity is used as a general measure of the ionic concentration of fluids and is measured in µS/cm. It is a quantitative measurement of all ionizable substances which is not able to distinguish particularly between conductive substances. Since electrical conductivity is highly influenced by temperature, the measurement is conventionally done at 25°C. The typical value for domestic wastewater is usually around 500-1000 µS/cm [IMHOFF and IMHOFF, 2006]. To avoid altered results the sample should be analyzed within 4 hours after sampling. Samples can be stored at 4°C for a maximum of 48 hours. For determination of the electrical conductivity the supernatant of the sample is analyzed with a Microprocessor WTW Conductivity Meter LF96 equipped with a LF-Electrode Tetra Con 96 WTW.

pH (DIN 38404 C5): The log scale unit pH is used to express the degree of acidity (index of the chemical activity of hydrogen ions) of a solution. The pH range of wastewater varies greatly, but for most WWTPs it is between 6.5 and 8.5 [ALBERTA ENVIRONMENT, 2000]. To avoid altered results the sample should be analyzed within 4 hours after sampling. Samples can be stored at 4°C for a maximum of 48 hours.

Oxidation-reduction potential (DIN 38404 C6): The tendency of a substance to acquire electrons and thereby be reduced is measured by the oxidation-reduction potential (ORP, [mV]). A higher (more positive) ORP value indicates a greater tendency to be reduced. In some experimental WWTPs the ORP is partly used as control strategy for the biological treatment steps [LI and BISHOP, 2001]. Values commonly found in WWTPs range from <-200 to >+200 mV [INNISS, 2005], depending on the influent wastewater, the location (at which station of treatment the sample was taken) and the general procedure/technique with which the wastewater is treated. To avoid altered results the sample should be analyzed within 4 hours after sampling. Samples can be stored at 4°C for a maximum of 48 hours.

Ammonia-nitrogen (DIN 38405 E5): In aqueous environments the highly toxic ammonia-nitrogen (NH_4-N) exists in two forms: as ammonium ion or as ammonia (depending on the pH). The more alkaline a solution the more ammonia is present and for measurements ammonia is usually detected via a colorimetric reaction. Ammonia-nitrogen values found in wastewater samples vary highly between 12 and 50 mg L^{-1} [METCALF and EDDY, 1991]. To avoid altered results the sample should be kept at 4°C and analyzed within 3 hours after sampling. Due to the high temperature dependency of the measurement it is important that all reagents are used at temperatures between 20-30°C.

Diverse Carbon species (TC, IC TOC, DIN 1484): The Total Carbon (TC) is a measure for all the carbon in the sample, including both inorganic (IC) and organic carbon (TOC). In WWTPs the measurement of the abundance of several carbon species plays an important role since the quality of the plant operation could be directly judged by the measurement of the respective carbon species. Values for TOC in wastewater are often found to be between 80 and 290 mg L^{-1} [METCALF and EDDY, 1991]. To avoid altered results the sample vessels should be filled completely and closed tightly. Samples should be kept at 4°C and analyzed within 3 hours after sampling. Storage of the samples at 4°C is possible, but a measurement should be completed before 24 h.
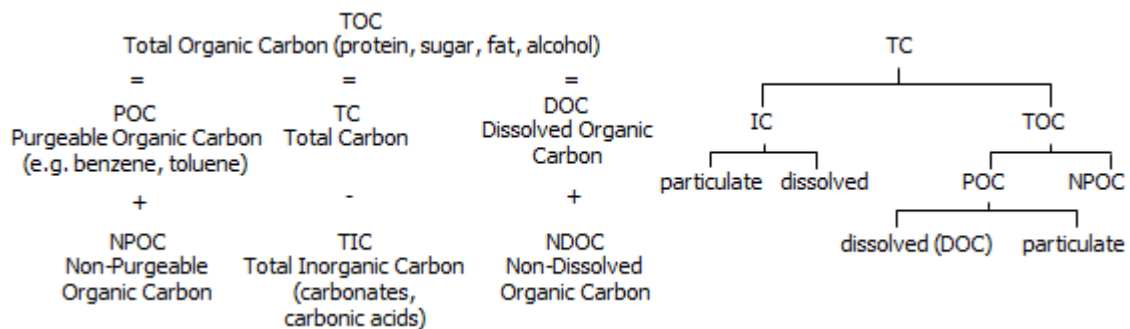
Figure 10. Relationships between different carbon species found in untreated (raw) wastewater (derived from www.hach-lange.co.uk.: Practice Report, Laboratory Analysis, Sum Parameter, TOC).

Chemical Oxygen Demand (COD, DIN 38 409 part 43): The chemical oxygen demand is a measure for all compounds that can be oxidized with a strong oxidizing agent under acidic conditions. It is close to similar to the total organic carbon (TOC), but not exactly the same because the TOC is independent of the oxidation state of the organic matter and excludes inorganic or organically bound carbon. In domestic wastewater the COD can range between 250-1000 mg L^{-1} [METCALF and EDDY, 1991] whereas in industrial wastewater the range goes up to 350,000 mg L^{-1} [ECKENFELDER *et al.*, 1989]. To avoid altered results the sample vessels should be filled completely and closed tightly. Samples should be kept at 4°C and analyzed within 3 hours after sampling. Storage of the samples at 4°C is possible, but a measurement should be completed before 24 h.

TN (Total Nitrogen, DIN 1484): Total Nitrogen is often measured together with the various carbon species. It comprises organic nitrogen, ammonia-nitrogen, nitrate and nitrite. The nitrogen concentrations may vary highly (20 to 85 mg L^{-1}) and depend on the type of discharge and the conditions in the wastewater collection system.

The average concentration in domestic wastewater is 40 mg L^{-1} [METCALF and EDDY, 1991]. To avoid altered results the sample vessels should be filled completely and closed tightly. Samples should be kept at 4°C and analyzed within 3 hours after sampling. Storage of the samples at 4°C is possible, but a measurement should be completed before 24 h.

Nitrate and nitrite (DIN 38 405-D20 and EN 26777): Nitrate and nitrite are subspecies of the afore mentioned TN. Like ammonia-nitrogen they can be toxic (nitrite is regarded as highly toxic for aquatic species) and their discharge from WWTPs in surface water bodies is not allowed and strictly observed. Normal concentrations of both nitrogen species should be around 0 L^{-1} [METCALF and EDDY, 1991], but an increase in the concentration can be measured during nitrification phase in the WWTP. To avoid altered results the sample vessels should be filled completely and closed tightly. Samples should be kept at 4°C and analyzed within 3 hours after sampling. Storage of the samples at 4°C is possible, if the pH in the sample is kept below 2.

Inorganic phosphate (DIN 38 405-D11): Inorganic phosphate is together with the organic phosphate, derived from various kinds of organic molecules, part of the total phosphorous. Within the wastewater the inorganic phosphorous can either be attached to particulate matter or dissolved. The typical values for inorganic phosphate in domestic wastewater are between 3 and 10 mg L^{-1} [METCALF and EDDY, 1991], but higher concentrations from industrial wastewaters are common as well (e.g. 132 mg L^{-1} in industrial wastewater [JØRGENSEN, 1979]). To avoid altered results the sample should be kept at 4°C and analyzed within 3 hours after sampling.

10.2.2 Chemical parameters of the WWTP Eilenburg

All analyses were carried out at the Helmholtz Centre for Environmental Research in Leipzig using the standard methods indicated in Table 5. All samples were analysed after transport and storage times shorter than 2 hours. Samples were treated as indicated in section 1.2.3, p. 14.

Table 5. Measured parameter and methods used.

parameter	unit	method
pH		DIN 38404-C5
redox potential	mV	DIN 38404-C6
electrical conductivity	mS cm^{-1}	DIN EN 27888-C8
COD	mg L^{-1}	DIN 38409 part 43, Dr. Lange cuvette test (LCK114), photometric
TC	mg L^{-1}	TOC/TN-analysator (Shimadzu), DIN EN 1484
IC	mg L^{-1}	TOC/TN-analysator (Shimadzu), DIN EN 1484
TOC	mg L^{-1}	TOC/TN-analysator (Shimadzu), DIN EN 1484
TN	mg L^{-1}	TOC/TN-analysator (Shimadzu), DIN EN 1484
NH$_4$	mg L^{-1}	DIN 38405 E5, ammonium test (Merck, 1.14752), photometric
NO$_3$	mg L^{-1}	DIN 38405-D20
NO$_2$	mg L^{-1}	EN 26777
inorganic phosphate	mg L^{-1}	DIN 38405-D11, photometric

11. DNA preparation, 16S rRNA gene cloning and sequencing

DNA preparation for the Tc control experiments (Results, section 2.4, p. 50)

For preparation of genomic DNA, sorted cells were harvested from the sheath buffer by centrifugation (25 min, 25,000xg at 6°C) and resuspended in 10 µL 10 mM Tris-HCl pH 9.0. Cells were disrupted by 10 min microwave treatment at 95°C in a thermostat microwave device BP-111-RS-IR (Microwave Research and Applications Inc., USA), immediately chilled on ice for 10 min and then centrifuged for 10 min at 23,100xg and 4°C.

DNA preparation for the application experiments (Results, section 3.2.3, p. 58 and 3.2.4, p. 60)

DNA was extracted from Tc and DAPI stained, cytometrically sorted cells. The cells were harvested from the sheath buffer by centrifugation (25 min, 25,000xg at 6°C) and stored at -20°C. DNA extraction was performed with a chelex based extraction method [GIRAFFA *et al.*, 2000]. Between 0.22 and 1.0 x 10^6 sorted cells were suspended in 70 µL of 10% (wt/vol) chelex solution (Chelex 100 Resin, Bio-Rad), vortexed for 10 s at highest speed and then incubated for 45 min at 95°C. Afterwards, the samples were again vortexed for 10 s and then centrifuged at 7,000xg for 5 min at 4°C. The supernatant was carefully transferred to a new, pre-chilled tube and directly used for PCR analysis or stored at -20°C. For the unsorted cell fractions 0.8 or 1 mL sheath buffer with stained cells was collected. The DNA was extracted as described above with the only difference that 150 µL of 10% (wt/vol) chelex solution was used. Sheath buffer (0.8 or 1 mL) without any introduced sample was included as control at every sorting day and handled in the same way as sorted cells.

From the supernatant of the extractions, bacterial 16S rRNA gene fragments were amplified by PCR using the universal primers 27F and 1492R [LANE, 1991]. PCR was performed in a 12.5 µL reaction containing 6.25 µL Taq PCR Master Mix (QIAGEN, Germany), 5 pmol of each primer (supplied by Microsynth, Switzerland) and 4 µL template DNA with a PTC-200 Thermal Cycler (MJ Research, USA). For cycle parameters and cloning strategy see [KLEINSTEUBER *et al.*, 2006]. Positive clones were screened by double digestion with the restriction enzymes HaeIII and RsaI (New England Biolabs, Germany). Partial DNA sequencing of representative clones displaying different restriction patterns was performed with BigDye RR Terminator AmpliTaq FS Kit 1.1 (Applied Biosystems, Germany) and the sequencing primers 27F and 519R [LANE, 1991]. Capillary electrophoresis and data collection were carried out on an ABI PRISM 3100 Genetic Analyzer (Applied Biosystems). Data were analyzed by ABI PRISM DNA Sequencing Analysis software and 16S rRNA gene sequences were assembled using Sequencher 4.8 (Gene Codes Corp., USA). The BLASTN tool (www.ncbi.nlm.nih.gov/BLAST; [ALTSCHUL *et al.*, 1990]) was used to search for similar sequences in the GenBank database, and the Seqmatch tool was used to search for similar sequences compiled by the Ribosomal Database Project (RDP) Release 10.0 Beta (http://rdp.cme.msu.edu; [COLE *et al.*, 2007]).

The determined 16S rRNA gene sequences were deposited in the GenBank database under accession numbers EU850352-EU850394 (Tc control experiments; Results, section 2.4, p. 50) and JN000704-JN000818 (application experiments; Results, section 3.2.3, p. 58 and 3.2.4, p. 60).

12. T-RFLP analyses

Bacterial 16S rRNA gene fragments were PCR-amplified with the primers 27F-FAM (labeled at the 5' end with phosphoramidite fluorochrome 5-carboxyfluorescein) and 1492R [LANE, 1991]. Labeled oligonucleotides were purchased from biomers.net (Germany). PCR was performed as described above. PCR products were purified using the Wizard® SV PCR Clean-Up System (Promega, Germany) and quantified after agarose gel electrophoresis and ethidium bromide staining using the GeneTools program (Syngene, UK). Purified PCR products were digested with the restriction endonucleases AluI, HaeIII or Sau3AI, respectively (New England Biolabs, Germany). A 10 µL reaction contained 1 ng DNA (for T-RFLP analyses of single clones) or 20 ng DNA (for T-RFLP analyses of the entire sample of sorted cells) and 10 units of restriction enzyme. Samples were incubated at the appropriate temperature for 3 h and then precipitated with sodium acetate (pH 5.5) and ethanol. Dried DNA samples were resuspended in 20 µL HiDi formamide containing 1.5% (vol/vol) GeneScan-500 ROX standard (Applied Biosystems). Samples were denatured at 95°C for 5 min and chilled on ice. The fragments were separated by capillary electrophoresis on an ABI PRISM 3100 Genetic Analyzer (Applied Biosystems). The lengths of the fluorescent terminal restriction fragments (T-RF) were determined using the GeneMapper V3.7 software (Applied Biosystems), and their relative peak areas were determined by dividing the individual T-RF area by the total area of peaks within the threshold of 35 to 650 bp. Only peaks with relative fluorescence intensities of at least 20 units were included in the analysis. Theoretical T-RF values of the dominant phylotypes represented in the clone library were calculated using the NEB cutter (http://tools.neb.com/NEBcutter2/index.php) and confirmed experimentally by T-RFLP analysis using the corresponding clones as template. Relative T-RF abundances of representative phylotypes were determined based on the relative peak areas of the corresponding T-RF.

Results

1. Fixation

For investigation of population dynamics in very diverse specimen like activated sludge it is important to keep the cells in an as near as life-like state as possible for reliable subsequent analysis. The fixed specimens should be capable of withstanding further preparative steps, transport and storage without changes in cell number, morphology or biochemical status [HOPWOOD, 1985].

So prior to the analysis of population dynamics a fixation strategy suitable for flow cytometric measurements is required. Fixatives for flow cytometric analysis should not increase autofluorescence, which frequently arises when aldehydes are used [SHAPIRO, 2002]. Also, the fixative in question should not cause cell aggregation, which is often induced by treatment with alcohols [SCHIMENTI and JACOBBERGER, 1992]. Aggregate formation obstructs analysis of the properties of single cells within a population and endangers the measurement itself by clogging the nozzle of the flow cytometer. This aspect is of great consequence when dealing with specimens like activated sludge or microbial species, which tend to form flocs [GÜDE, 1982]. An increased occurrence of cell debris [SCHIMENTI and JACOBBERGER, 1992] and changed uptake behaviour of dyes [JANATPOUR *et al.*, 2002] are other negative aspects of traditional fixatives like alcohols. In addition to this, fixatives composed of alcohols or aldehydes alter the refractive indices of the cells which leads to a distortion of the light scatter signals and thus hinder a reliable separation of a bacterial population from cell debris and the background noise of a flow cytometer [CUCCI and SIERACKI, 2001; SHAPIRO, 2002].

Although a 10% (1.54 M) sodium azide solution is advantageous as a fixative for aerobic bacteria and other aerobic organisms, since it preserves cells without increasing autofluorescence and effectively prevents cell aggregation [MÜLLER, 2007], it is only occasionally applied. Azide inhibits the terminal enzyme of the respiratory chain (cytochrome *c* oxidase, complex IV) causing lack of energy which leads, in combination with the osmotic effects of this concentrated salt solution, to cell death and preservation [PALMIERI and KLINGENBERG, 1967]. Unfortunately, sodium azide is ineffective for anaerobic organisms such as the methanogens as well as sulphate, iron and nitrate reducing bacteria frequently found in groundwater or activated sludge. Though nitrate reducers (about 70%) are the most abundant anaerobes in activated sludge, iron reducers (3%), sulphate reducers (1-2%), and methanogens (0.5%, [NIELSEN *et al.*, 2004]) ought to be fixed too, preventing changes in community composition. Some fixation protocols for anaerobic bacteria have been published that do not use aldehydes or alcohols. Molybdenum for instance has been used together with hydrogen peroxide and sodium azide for the fixation of sulphate reducing bacteria [VOGT *et al.*, 2005].

To surmount the limitations in available fixation procedures, species of aluminium, barium, bismuth, cobalt, molybdenum, nickel, and tungsten salts were tested for their capabilities to stop cell metabolism and growth of five pure cultures (*Desufovibrio desulfuricans, Shewanella putrefaciens, Paracocus denitrificans* (aerobic culture conditions), *Paracocus denitrificans* (anaerobic/denitrification culture conditions), *Methanomonas methylovora, Methanosarcina barkeri*) and a highly heterogenic microbial community (see Figure 11, p. 34).

Stained cellular DNA served as an indicator for fixation stability in the flow cytometric analysis since, in intact cells, it changes only under conditions where cell cycle activities occur.

In a pure culture (Figure 11, a-f) each sub-distribution (gate, here indicated as an ellipse) groups cells similar in numbers of chromosome equivalents, i.e. cells in the same phase of the cell cycle. In highly diverse microbial communities, sub-distributions (Figure 11, g, h) cluster various cell types that have certain DNA contents in common. In both cases, changes of cell numbers within a sub-distribution result from losses or gains of this group indicating low overall fixation efficiency (e.g. due to cell cycle activity). The degree of change in cell number within sub-distributions is thus a derived measure of fixation efficiency.

Pure cultures were harvested from the early exponential phase of growth. Activated sludge served as a highly diverse microbial community sample. It was harvested from anaerobic and aerobic periods of the cultivation aimed to imitate the WWTP process (Material and Methods, section 1.2.1, p. 14). All samples were microscopically inspected in parallel to confirm the flow cytometric results. The leading criterion was that fixed samples should maintain their sub-population (pure cultures) or sub-community (mixed cultures) pattern distribution with regard to the aforementioned parameters, while unfixed samples were expected to change.
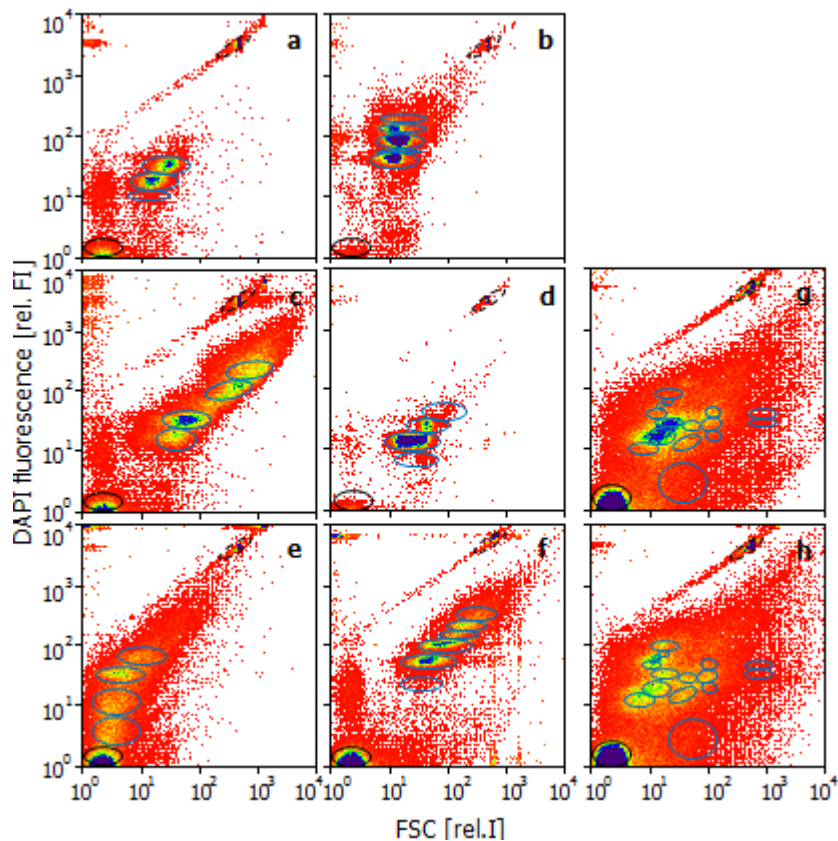
Figure 11. Dot-plots of DAPI stained cells (pure cultures: a-f; mixed cultures: g, h). The cells were fixed for 1 day in a sodium azide solution (10%) containing 5 mM $BaCl_2$ and 5 mM $NiCl_2$. Blue ellipses indicate distinct sub-populations or sub-communities, black ellipses mark the electronic noise and the dotted ellipse the blue fluorescent beads used as a standard for flow cytometric measurements. The ellipses (gates) represent all the sub-populations or sub-communities that were found during the time span of the fixation experiments, so that not every marked subpopulation or subcommunity is always present. a) *Desufovibrio desulfuricans,* b) *Shewanella putrefaciens,* c) *Paracocus denitrificans* (aerobic culture conditions), d) *Paracocus denitrificans* (anaerobic culture conditions), e) *Methanomonas methylovora,* f) *Methanosarcina barkeri,* g) activated sludge (aerobic culture conditions), h) activated sludge (anaerobic culture conditions)

The obtained flow cytometric data sets were too complex to rely solely on cell counts of sub-populations and variations in their dye uptake steadiness (verified by mode value comparison). Therefore equivalence testing was additionally performed for statistical validation (see Material and Methods, section 8.1, p. 22).

1.1 Fixation of pure cultures

DNA patterns of pure microbial cultures were analysed flow cytometrically after DAPI staining.

Fractions of the population that where distinguishable by their contents of chromosome equivalents are given in per cent (of all DAPI stained cells within the sample) as follows: *Desulfovibrio desulfuricans* (Figure 12, a, sulphate reducer; 3 sub-populations: 45%, 44%, 10%), *Shewanella putrefaciens* (Figure 12, b, iron reducer; 5 sub-populations: 28%, 27%, 35%, 6%, 6%), *Paracoccus denitrificans* (Figure 12, c and d; nitrate reducer under anaerobic conditions, 4 sub-populations (aerobic conditions): 38%, 45%, 6%, 7% and 4 sub-populations (anaerobic conditions): 1%, 86%, 12%, 1%), *Methanomonas methylovora* (Figure 12, e, methylotrophic; 4 sub-populations: 3%, 59%, 26%, 9%), and *Methanosarcina barkeri* (Figure 12, f, methanogenic; 6 sub-populations: 5%, 36%, 33%, 8%, 11%, 7%).
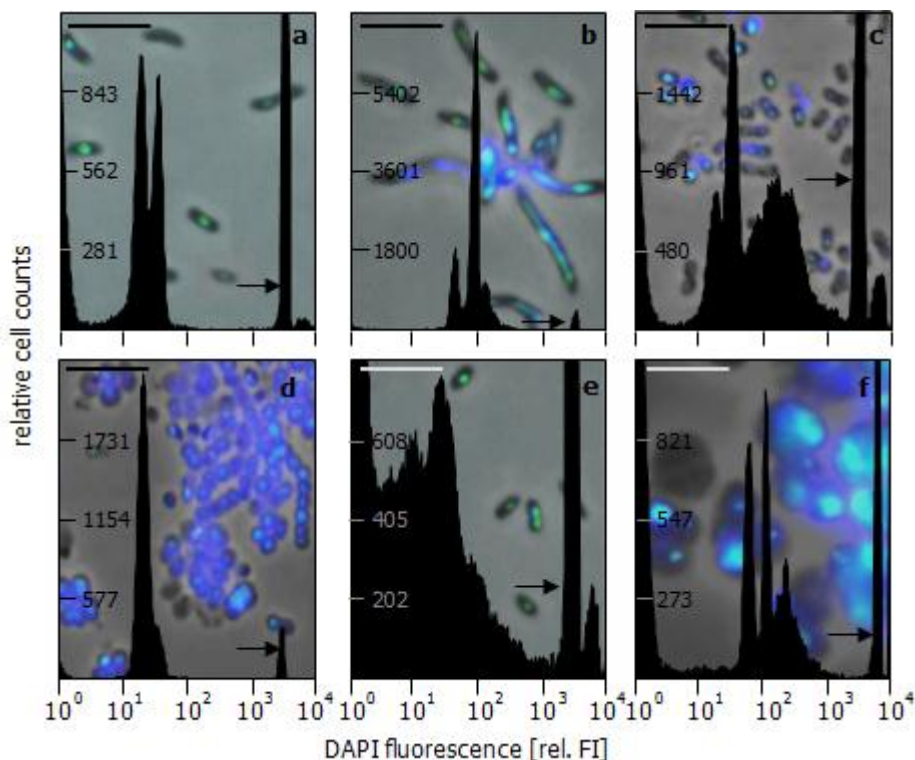
Figure 12. Fluorescence histograms and microscopic images of DAPI stained cells from pure cultures (bars: 5 µm). The relative cell counts within the histograms differ highly and are not directly comparable. The population marked with an arrow are the blue fluorescent beads used here as standard. a) *Desufovibrio desulfuricans,* b) *Shewanella putrefaciens,* c) *Paracocus denitrificans* (aerobic culture conditions), d) *Paracocus denitrificans* (anaerobic culture conditions), e) *Methanomonas methylovora,* f) *Methanosarcina barkeri*

Results of fixation efficiencies, i.e. stable sub-populations fitting in both the 10% and the 25% tolerance interval (*x* (sub-populations within 25% and 10% tolerance interval) *out of y* (all sub-populations)) are summarized in Table 6 (for further details see Annex II, Table 10).

Table 6. Fixative effects of metal solutions on pure cultures. Samples fitting in the 10% tolerance interval with 100-75% of the sub-populations are marked with + +, those fitting to 74-50% with +, 49-25% with - and those fitting to 24-0% are marked with - -. Samples where at least one sub-population does not fit into the 25% tolerance interval are marked with - - -. n.d.: not determined, [1]: in PBS with 10% sodium azide

type of metabolism	sulphate reduction	iron reduction	denitrification	aerobic growth	methane oxidation	methanogenic
organism (culture condition)	*D. desulfuricans* (anaerobic)	*S. putrefaciens* (aerobic)	*P. denitrificans* (anaerobic)	*P. denitrificans* (aerobic)	*M. methylovora* (aerobic)	*M. barkeri* (anaerobic)
Al[1]	- - -	- - -	- - -	- - -	- - -	n. d.
Ba[1]	+ +	+ +	+ +	+	+ +	n. d.
Bi[1]	- -	+	- - -	- - -	- - -	n .d.
Co[1]	- - -	- - -	- - -	- - -	- - -	n. d.
Mo[1]	+ +	- - -	- - -	- - -	- - -	n. d.
Ni[1]	+ +	+	- - -	+	+	n. d.
W[1]	- - -	- - -	+	+	+	n. d.
NaN$_3$	- - -	- - -	- - -	- - -	- - -	- - -
Ba, Ni, Bi[1]	+ +	+	- - -	+	- -	-
Ba, Ni[1]	+ +	+ +	+	+ +	+ +	+ +

Aluminium: Sodium azide solution with 5 mM aluminium showed no fixative effect on the sulphate reducer *Desulfovibrio desulfuricans* (not even one sub-population fitting into the 25% tolerance interval) and only weak fixative effects on the other test species. Changes within the sub-populations were found within less than 7 days, therefore the fixation was classified as *unstable*.

Barium: In contrast to aluminium, barium showed *exceptionally stable* fixation qualities for all tested strains with only slightly reduced stability of aerobically grown *Paracoccus denitrificans* (3/4 sub-populations within the 10% tolerance interval). All strains were effectively fixed a minimum of 7 days (all sub-populations fitting at least into the 25% tolerance interval).

Bismuth: Bismuth which had been shown previously to inhibit nitrate reducers (see Table 9, p. 68), showed only a low fixative effect on *Paracoccus denitrificans* in this study. Other species were also not influenced by bismuth addition except for some effect on the iron reducer *Shewanella putrefaciens* (3/5) and the sulphate reducer *Desulfovibrio desulfuricans* (1/3). Therefore the fixation efficiency was classified *unstable*.

Cobalt: Like aluminium, cobalt showed no sufficient fixative effect on the investigated strains and for some strains (*Shewanella putrefaciens*, *Paracoccus denitrificans* (anaerobic), *Methanomonas methylovora*) even less fixative effects than aluminium. Because of the insufficient fixative effects the fixation efficiency was classified *unstable*.

Molybdenum: Molybdenum fixed *Desulfovibrio desulfuricans* was *exceptionally stable* (3/3) for at least 7 days. This inhibition of sulphate reducers is in agreement with the results of other groups (Table 9, p. 68). However, molybdenum failed to fix any of the other test strains better than aluminium or cobalt and therefore the fixation efficiency for these test strains is regarded as *unstable*.

Nickel: Fixation with nickel was *exceptionally stable* for *Desulfovibrio desulfuricans* (3/3) and *stable* for *Shewanella putrefaciens* (3/5), *Methanomonas methylovora* (2/4) and the aerobic grown *Paracoccus denitrificans* (3/4) for at least 7 days.

Tungsten: As a known inhibitor of nitrate reducers (see Discussion, Table 9, p. 68), tungsten exhibited *stable* fixation of *Methanomonas methylovora* (2/4) and *Paracoccus denitrificans* (aerobic: 3/ 4; anaerobic: 2 /4), but not on the other test organisms. No fixative effect could be measured for *Desulfovibrio desulfuricans*.

Sodium azide: Sole sodium azide, known otherwise as a potent fixative of aerobic bacteria, failed to fix the test strains sufficiently so that every sub-population of one strain at least fits into the 25% tolerance interval. Yet, with exception of *Desulfovibrio desulfuricans*, some fixative effects were detected for all tested strains.

Combination 1: A combination of barium, nickel and bismuth (each 5 mM) showed *exceptionally stable* fixative effects for *Desulfovibrio desulfuricans* for 17 days (3/3). *Stable* fixation (9 days) was also found for *Shewanella putrefaciens* (3/5) and the aerobic grown *Paracoccus denitrificans* (2/4).

Combination 2: Most effective was a combination of 5 mM barium and nickel, in 10% sodium azide solution. All sub-populations remained within the 25% tolerance interval for at least 9 days, with reduced effects for *Paracoccus denitrificans* (anaerobic: 2/4) and *Methanosarcina barkeri* (5/6).

For an example of *exceptional stable* and *unstable* fixation see Figure 13.
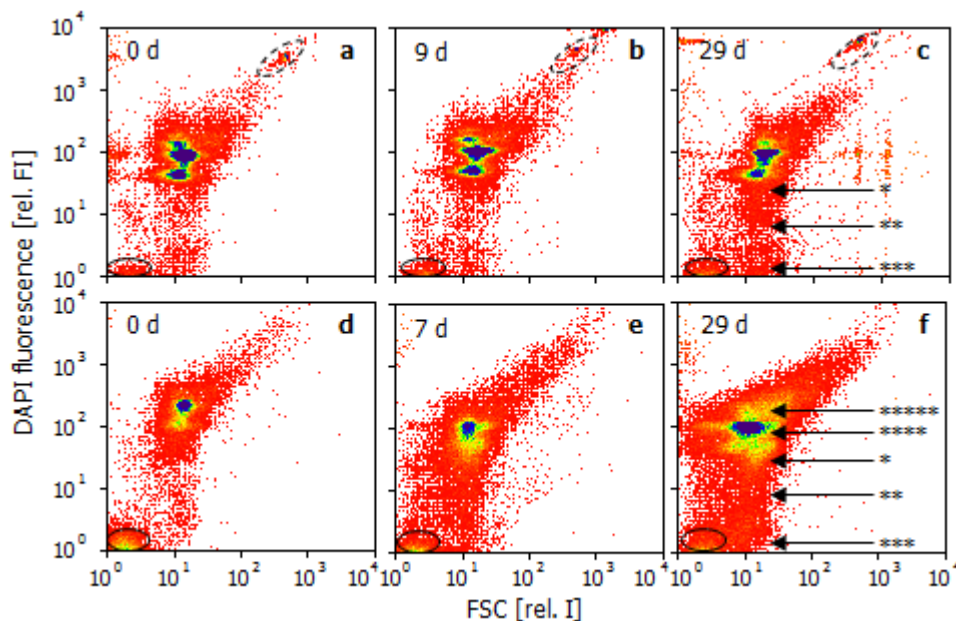
Figure 13. Dot-plots of DAPI stained cells from *Shewanella putrefaciens* fixed with either sodium azide solution (10%) with 5 mM $BaCl_2$ and 5 mM $NiCl_2$ (a-c) or sole sodium azide (d-f). Cells were measured after 0, 7/9 and 29 days after fixation. Black ellipses mark the electronic noise and the dotted ellipse indicates the blue fluorescent beads used as fluorescence standard. The following changes could be observed in the samples: *: appearance of new sub-populations with lower DNA content, **: appearance of cells with low DNA content (without formation of a separate sub-population), ***: increase in cell debris and/or salt crystals, ****: changes in sub-population size, *****: appearance of new sub-populations with higher DNA content

Changes observed within the *unstable* samples could be classified into 5 categories. First, an appearance new of sub-populations with low DNA content (i.e. lower DAPI fluorescence, Figure 13, *) could be observed. An increasing number of nearly unstained cells with low DNA content, which do not cluster in a distinct sub-population (Figure 13, **) was found to occur with prolonged duration of the fixation. In addition to this, an increasing content of dell debris and/or salt crystals was observed (Figure 13, ***) on the one hand and changes in the size of the sub-population (Figure 13, ****) or the development of new sub-populations with higher DNA content on the other (Figure 13, *****). Generally, a diminished dye uptake was noticeable for *unstable* samples (see Figure 13, d and e/f).

1.2 Fixation of highly diverse cultures

Those metal salt combinations proven to be useful fixatives for pure cultures by the experiments described under 1.1 were used in two different concentrations (5 and 15 mM) to fix samples of the highly diverse bacterial community present in activated sludge. Such samples were tested with and without addition of a detergent (Tween 20) expected to accelerate the penetration of the fixatives. Fixation by cryopreservation of the cells at -20 °C with and without addition of glycerine as a cryoprotective agent was also investigated.

Unfixed specimens of both cultivation phases (aerobic/anaerobic) served as controls and were preserved in 10% NaN_3 30 min prior to DNA staining and cytometric analysis to ensure reliable DAPI-DNA staining.

The chosen activated sludge samples showed up to 15 different sub-communities (Figure 14, p. 40). Their proportions ranged between 0.2 and over 20% of all cells analysed within the community, depending on fixation efficiency and aerobic or anaerobic phase in the cultivation reactor. Results of these experiments are summarized in Table 7 and details given in Annex II Table 11.

Table 7. Fixative effects of metal solutions on mixed cultures. Samples fitting in the 10 % tolerance interval with 100-75% of the sub-communities are marked with + +, those fitting to 74-50% with +, 49-25% with - and those fitting to 24-0% are marked with - -. Samples where at least one sub-community did not fit in the 25% tolerance interval are marked with - - -. [1]: in PBS with 10% sodium azide, [2]: 0.5 g L^{-1} Tween 20, [3]: 15% glycerine

culture condition	aerobic	anaerobic
unfixed	- - -	- - -
5 mM Ba, Ni[1]	+ +	+ +
15 mM Ba, Ni[1]	-	+
5 mM Ba, Ni[1,2]	- - -	- - -
15 mM Ba, Ni[1,2]	- - -	- - -
PBS (-20°C)	- - -	- - -
PBS[3] (-20°C)	- - -	- - -
NaN_3	- - -	- - -

Unfixed: As was to be expected, the sub-community patterns of unfixed samples greatly changed after just 1 day, regardless of whether the samples were taken from the aerobic or anaerobic cultivation phase. For instance new sub-communities developed whereas others changed in abundances.

Sodium azide: Samples treated with pure 10% sodium azide showed no sufficient smple stability. Most of the 15 sub-communities changed quickly especially in the samples from the aerobic cultivation phase.

Combination 1 (5 mM barium and nickel): A mixture of 5 mM barium and nickel salts in the presence of 10% sodium azide resulted in a good fixative effect (*stable* fixation) for about 9 days, regardless of the cultivation conditions (anaerobic: 11/15, aerobic: 12/15 sub-communities within the 10% tolerance interval).

Combination 2 (15 mM barium and nickel): When the mixture of barium and nickel salts was higher concentrated (15 mM), samples were *stable* up to 7 days for cells harvested in the aerobic growth phase (7/15) and anaerobic growth phase (11/15). Compared to the combination 1 with the lesser concentrated salts combination 2 was less successful.

Combination 3 (5 mM barium and nickel with 0.41 mM Tween 20): Addition of 0.5 g L^{-1} Tween 20 (0.41 mM) to the mixture of 5 mM barium and nickel salts resulted in noticeable but not sufficient fixation of the samples. Therefore the status of the samples was classified *unstable*.

Combination 4 (15 mM barium and nickel with 0.41 mM Tween 20): For the higher concentrated salt solution (15 mM) the results were comparable to those obtained from the lower concentrated solution of barium, nickel and sodium azide amended with 0.41 mM Tween 20. Some sub-communities were stable over the whole time range, but most of them changed after even 1 day.

Cryopreservation at -20°C: Cryopreservation without cell protecting agent resulted in a low stability of most sub-communities, regardless from which cultivation phase. Changes could be detected after just 1 day of storage.

Cryopreservation at -20°C with 15% glycerine: The addition of glycerine as cell protecting agent prior to storage at -20°C had no positive effects on the fixation efficiency. As without the glycerine significant changes could be detected after 1 day.

As an example for stable and unstable fixation the DNA/FSC patterns of samples harvested during the aerobic and anaerobic phase of activated sludge batch cultures (fourth run; see Material and Methods, section 1.2.1, p. 14) are shown in Figure 14 (p. 40).
Nearly no changes of sub-community patterns could be observed when the cells of the aerobic cultivation phase were fixed with a mixture of 5 mM $BaCl_2$ and 5 mM $NiCl_2$ in 10% sodium azide solution for 1 day (Figure 14, a) and 9 days (Figure 14, b), except for the increased abundance of cell debris and/or salt crystals.
However, cells stored with 15% glycerine at -20C (Figure 14, d-e) showed significant changes in sub-community abundances after just one day of storage at 4°C (Figure 14, d).
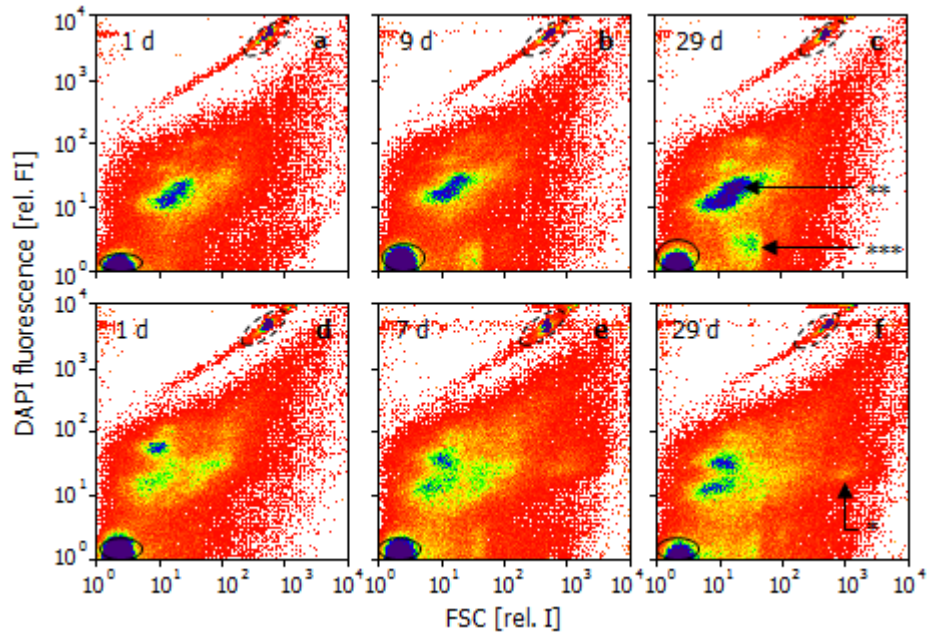
Figure 14. Dot plots of DAPI stained cells from activated sludge (aerobic (a-c) and anaerobic (d-f) cultivation phase) fixed with either sodium azide solution (10%) with 5 mM $BaCl_2$ and 5 mM $NiCl_2$ (a-c) or PBS with glycerine (15%) (d-f). Cells were measured after 0, 7/9 and 29 days after fixation. The black ellipses mark the electronic noise and the dotted ellipse indicates the blue fluorescent beads used as fluorescence standard. The following changes could be observed in the samples: *: appearance of new sub-communities **: changes in sub-community size, ***: increase in cell debris and/or salt crystals

The main changes that could be observed were similar to those of the pure cultures, namely: the increase in cell debris and/or salt crystals, changes in sub-population sizes and the development of new sub-populations

2. Evaluation of the tetracycline staining method

For evaluation of the polyphosphate content in various pure and mixed cultures the cells were stained either traditionally with DAPI in a polyphosphate probing concentration (28 μM) or, using a newly developed staining method, with the antibiotic tetracycline hydrochloride (Tc, 0.225 mM) as fluorescent dye.

An example for this new staining method is shown in Figure 15. Green fluorescent polyphosphate granules were detected and quantified by flow cytometry (see Figure 17, b) and fluorescence microscopy (Figure 15, a-d). Granules were clearly visible in *M. phosphovorus*, *Pseudomonas* sp., and *Paracoccus* sp., all harvested after 3 days of alternating aerobic/anaerobic shifts at the end of an aerobic phase.
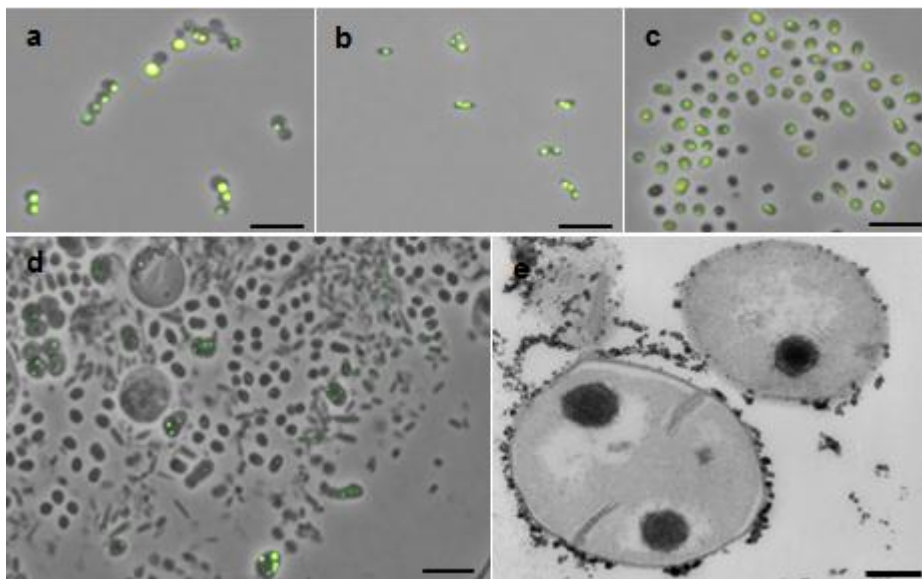
Figure 15. Tc$_{Fluka}$ stained cells of *M. phosphovorus* NM-1 (a), *Pseudomonas* sp. (b), *Paracoccus* sp. (c) and activated sludge (d) harvested from the aerobic cultivation phase. For an improved visualization of the polyphosphate granules distribution within the cells the fluorescent images were merged with the respective light microscopic images (bars: 5 μm). Cells of *M. phosphovorus* were stained for polyphosphates and analysed by TEM (e; bar: 0.2 μm)

Using Transition Electron Microscopy (TEM, Figure 15, e) and fluorescence microscopy subsequent to Tc staining the distribution, amount and size of the polyphosphate granules within the cells of three pure cultures and one mixed culture were determined. Within these samples the granule diameters varied between 0.25 and 1.33 μm, with average sizes of 0.69 μm for *M. phosphovorus*, 0.48 μm for *Pseudomonas* sp., and 0.39 μm for *Paracoccus* sp. (average of 17 granules, each). The size of the granules in *M. phosphovorus* (Figure 15, e) and *Pseudomonas* sp. obtained by fluorescence microscopy was verified by TEM (average of 100 granules, each). The granule sizes measured by TEM were significantly smaller. *M. phosphovorus* showed granule sizes varying from 0.08 to 0.52 μm with an average size of 0.26 μm (± 0.10) and *Pseudomonas* sp. showed granule sizes varying from 0.04 to 0.17 μm with an average size of 0.10 μm (± 0.03). Differences between both technologies may partly be an artefact of epifluorescence based sizing and the spatial position of the granule within the 80 nm slices analysed by TEM.

2.1 Comparison of the new and the traditional polyphosphate staining method

Analysing cytometric proliferation patterns of bacteria after DNA staining with DAPI gives information about the growth rate of a species. Since the interest of this study is in the abundance and community dynamics of PAOs, the analysis of polyphosphate contents by Tc staining and the analysis of growth activity based on DNA pattern analyses using DAPI (1 µM) were combined. For comparison the traditional DAPI staining method with a high concentration of DAPI (28 µM) was applied.
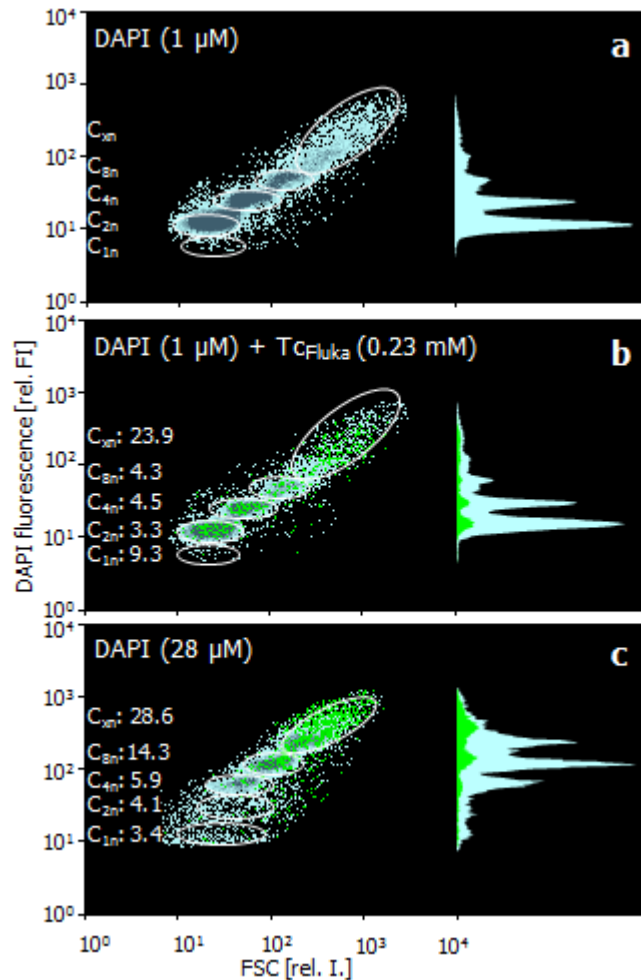
Figure 16. Dot plots of *M. phosphovorus* NM-1 cells subjected to 3 different staining procedures. To determine the DNA based sub-population pattern of the sample the cells were stained with 1 µM DAPI (a). For the measurement of the polyphosphate content in the second sample the cells were additionally stained with Tc$_{Fluka}$ (b). DAPI (28 µM) was applied to the third sample (c). The numbers at each sub-population indicate the quantity of chromosomal equivalents and the amount of green fluorescent cells within that sub-population.

To obtain simultaneously information about growth activities and polyphosphate accumulation of individual cells in a population, it was important that the DAPI and the Tc stains did not interfere. Actually, reliable information on DNA pattern distributions was obtained with cells that had been exposed to Tc prior to the addition of 1 µM DAPI solution (Figure 16, b). With this biphasic staining, it was intended that Tc binds to the polyphosphate granules before DAPI molecules would bind there. To detect possible influences of Tc on the apparent distribution of the chromosome numbers, cells were stained with DAPI only (Figure 16, a) or in combination with Tc$_{Fluka}$ (Figure 16, b).

The obtained DAPI fluorescence intensities and distributions of chromosome equivalents (in brackets) with DAPI only were C_{1n}: 6 (2%), C_{2n}: 12 (48%), C_{4n}: 24 (30%), C_{8n}: 47 (7%), and C_{xn}: 183 (13%, Figure 16, a). With DAPI applied in combination with Tc_{Fluka} the following values were found C_{1n}: 6 (3%), C_{2n}: 12 (47%), C_{4n}: 25 (30%), C_{8n}: 47 (7%), and C_{xn}: 179 (13%). The similarity shows that Tc did not influence quantitative DNA staining with DAPI. The Tc stained cells (6.1%) were determined after gating and shown as green dots in the DAPI-FSC plots (Figure 16, b; see gating strategy: Material and Methods section 6, Figure 6, p. 21). The polyphosphate containing cells were distributed over the entire population, but the relative presence of polyphosphate-accumulating individuals was higher in sub-populations with a higher number of chromosome equivalents. The percentage of polyphosphate containing cells decreased from 23.9% (C_{xn}) to 4.3% (C_{8n}), 4.5% (C_{4n}), 3.3% (C_{2n}) and increased again in C_{1n} (9.3%), respectively.

When polyphosphate granules were stained the traditional way (high concentrations of DAPI: 28 µM), some of the dye obviously also interacts with the DNA. It was therefore checked whether DAPI staining alone could be used to infer both the DNA and the polyphosphate contents from the respective blue and yellow-green fluorescence. Using the same sample of *M. phosphovorus* as above (Figure 16, c), a comparable fraction of polyphosphate containing cells (6.2%) was found. Also, the previously observed five main sub-populations based on chromosome equivalents were found and characterized by almost the same mean DAPI fluorescence intensity of each individual sub-population as before. However, the apparent distribution of cell numbers between these sub-populations was shifted towards higher fluorescence intensities as follows: C_{1n}: 8 (3%), C_{2n}: 13 (3%), C_{4n}: 26 (15%), C_{8n}: 55 (18%), and C_{xn}: 240 (61%). These results verified that the linkage of cell proliferation to polyphosphate synthesis using high DAPI concentrations alone was not reliable.

To further test the comparability of the two polyphosphate staining methods in terms of detection of polyphosphate containing cells, cells of *M. phosphovorus* NM1 were stained either with Tc (Figure 17, a, grey bar) or DAPI in a polyphosphate probing concentration (Figure 17, a, white bar). Both dyes were found to be comparable in the amount of stained cells.
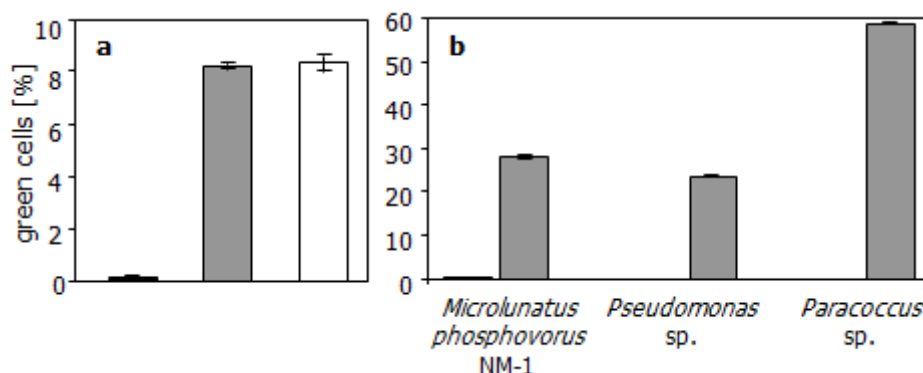
Figure 17. Comparison of Tc and DAPI staining. a) *Microlunatus phosphovorus* NM-1 cells, harvested in the aerobic phase of cultivation, were fixed and stained with 0.225 mM Tc_{Fluka} (grey) or 28 µM DAPI (white). b) Tc_{Fluka} stained cells of *Microlunatus phosphovorus* NM-1, *Pseudomonas* sp., and *Paracoccus* sp. harvested from the aerobic phase of growth. All samples were analyzed flow cytometrically and the amount of green fluorescent cells was determined (grey bars). Unstained cells served as autofluorescence controls (a, b: black).

2.2 Calibration of the staining method and fluorescence spectra of tetracycline

2.2.1 Calibration

The tetracycline staining procedure was optimized with cells *M. phosphovorus* NM-1 (Figure 18, a) and a bacterial community derived from activated sludge (Figure 18, b; see Material and Methods, section 1.2.1, p. 14). Influences of incubation times (0 to 180 min) and Tc concentrations (0.023 to 1.35 mM) on staining results were tested. This was necessary to minimize unspecific staining or dye interactions as a prerequisite for obtaining quantitative information on individual polyphosphate contents.

Microscopically, stained granules within the cells were already visible after 10 min exposure to 0.225 mM Tc. In flow cytometric measurements, the amount of stained cells was almost constant after about 40 to 60 minutes. The staining was found to be stable in fixed as well as living samples for 3 hours and there was no sign of efflux pumping of Tc.
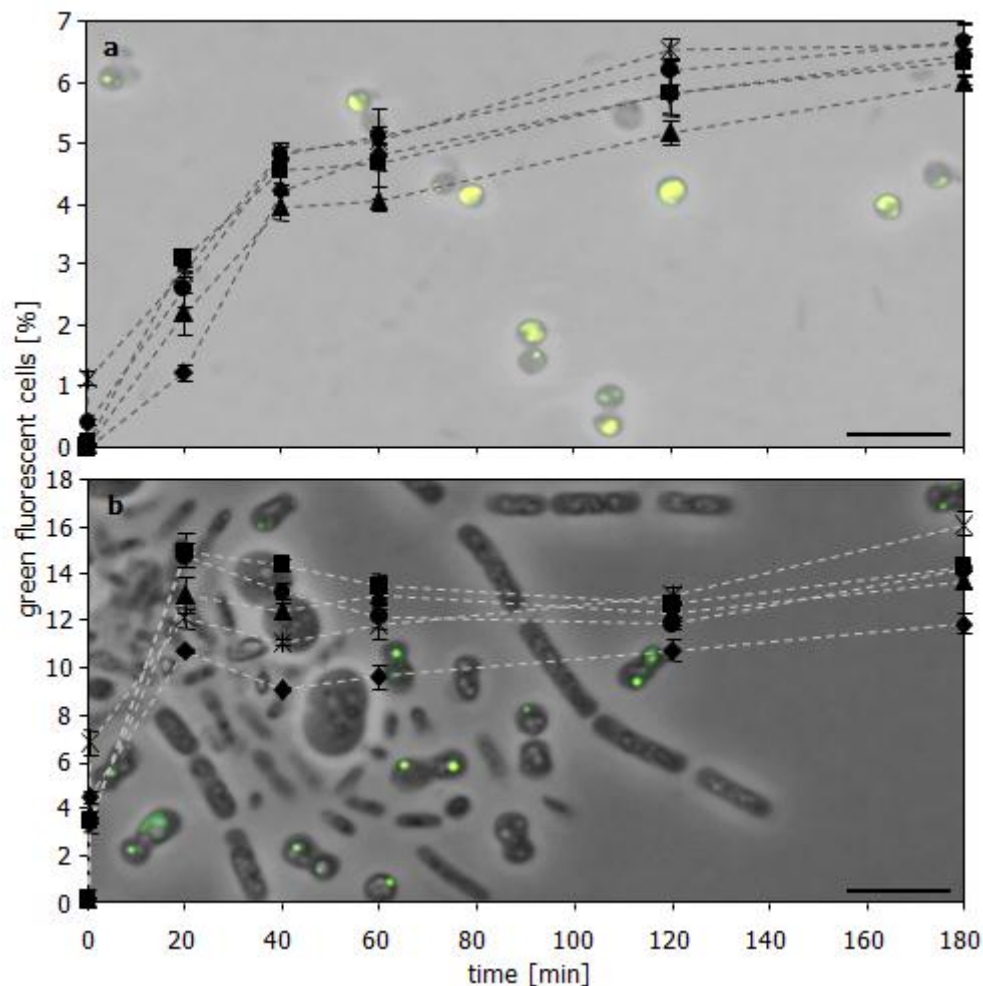
Figure 18. Optimization of the Tc$_{Fluka}$ concentration for polyphosphate staining of living cells of *M. phosphovorus* (a) and activated sludge (b) harvested in the aerobic phase of cultivation. The cells were stained with five different Tc$_{Fluka}$ concentrations (mM): 0.023 (diamonds), 0.14 (triangles), 0.225 (squares), 0.45 (circles), 1.35 (asterisks) and the fluorescence development was observed over a time range of 180 minutes. Bars in a and b represent 5 µm.

2.2.2 Fluorescence spectra

To verify that Tc can be excited by the available excitation source and to choose the right filter sets for flow cytometric analysis bound and unbound Tc was analysed spectrophotometrically. Since Tc from two manufacturers was used, the actually applied Tc is marked as Tc_{Fluka} or Tc_{Roth}.

If not stated otherwise, the shown data are derived from 3D spectra. The Rayleigh scatter peaks which occur at the excitation wavelength (first order peak) and at the doubled excitation wavelength (second order peak) were manually removed from the respective 3D spectra to avoid misinterpretation.

A summary of the results is given at the end of this section in Table 8 (p. 49).

Dependency of the fluorescence on the tetracycline manufacturer and the solvent
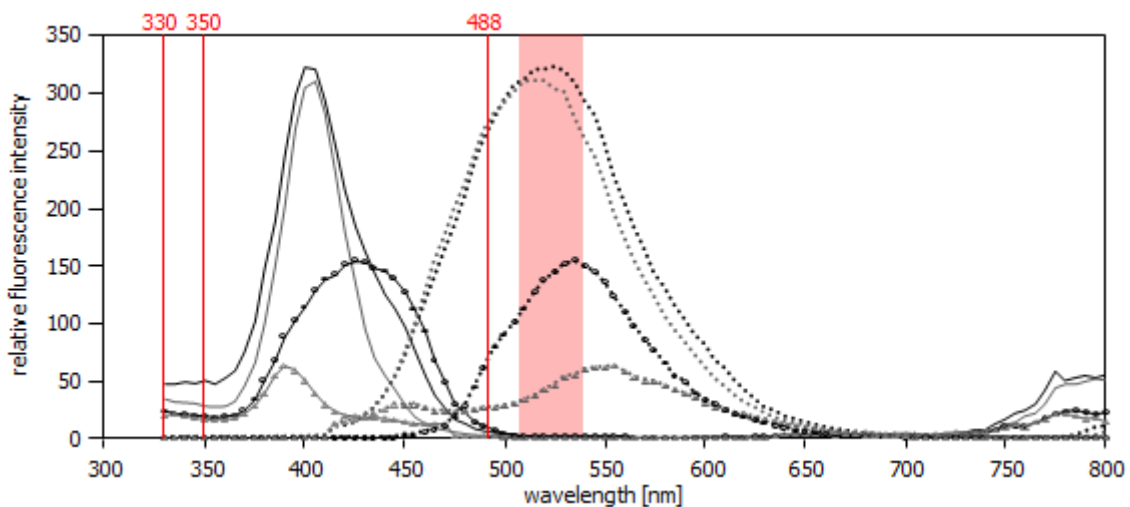
Figure 19. Fluorescence of Tc from Roth (black) and Fluka (grey) dissolved in PBS (lines without symbols) or bidestilled water (b. w., lines with symbols: circle for Tc_{Roth} and triangle for Tc_{Fluka}). The excitation wavelengths (nm) of the lasers used in this study are marked with red lines and the band pass filter for green fluorescence with light red background. ex.: excitation (solid line), em.: emission (dotted line)

When Tc_{Roth} was dissolved in water maximum excitation was reached at 425 nm with emission at 535 nm (intensity $_{em.\ max}$: 154.85). For Tc_{Fluka} dissolved in water the maximum intensity value for the emission was significantly lower, being 62.88 at the maximum excitation wavelength of 390 nm, with the emission at 555 nm. Tc_{Roth} showed 2.46 times higher fluorescence intensities than Tc_{Fluka} when dissolved in bidestilled water.

Maximum excitation for Tc_{Roth}, which was dissolved in PBS, was reached at 400 nm with maximum emission at 525 nm (intensity $_{em.\ max}$: 323.7). For Tc_{Fluka} the maximum intensity value for the emission of the solution in PBS was only slightly lower, being 311.04 at the maximum excitation wavelength of 405 nm, with the maximum emission at 520 nm. Tc_{Roth} showed 1.04 times higher fluorescence intensities than Tc_{Fluka} when dissolved in PBS. Tc_{Roth} showed 2.09 times higher fluorescence intensities when dissolved in PBS rather than in bidestilled water. For Tc_{Fluka} the difference between the two solvents was even more prominent (4.95).

In contrast to Tc dissolved in water the excitation maxima of Tc_{Roth} and Tc_{Fluka} varied only slightly when they were dissolved in PBS (variance $_{b.\ w.}$: 35 nm, variance $_{PBS}$: 5 nm). The same hold true for the emission maxima: variance $_{b.\ w.}$: 20 nm, variance $_{PBS}$: 5 nm.

Dependency of the fluorescence on the availability of cations
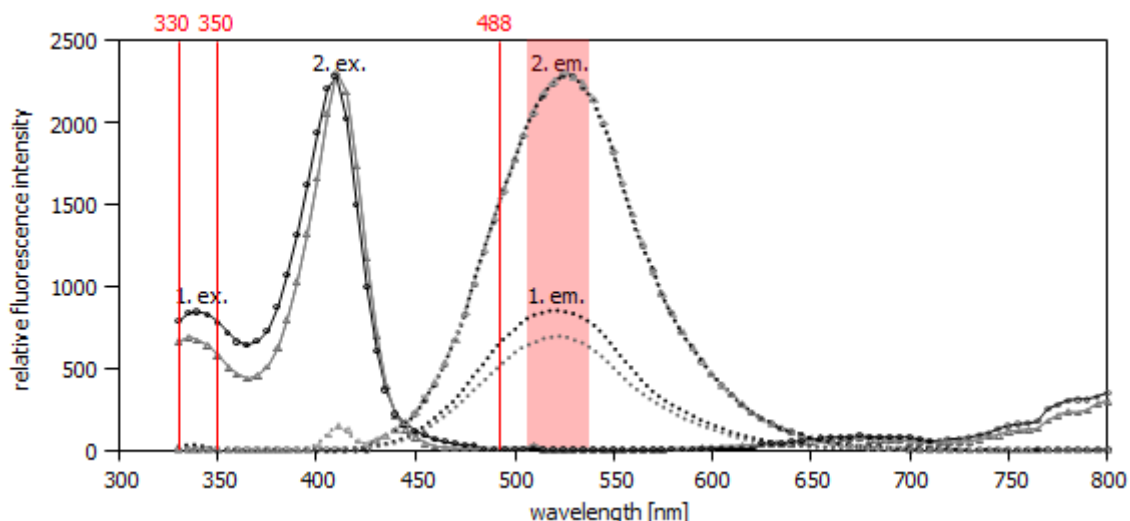
Figure 20. Fluorescence of Tc from Roth (black) and Fluka (grey) dissolved in PBS with added CaCl$_2$ (2.97 mM). The excitation wavelengths (nm) of the lasers used in this study are marked with red lines and the band pass filter for green fluorescence with light red background. ex.: excitation (solid line), em.: emission (dotted line)

Both dyes showed two excitation and emission peaks when cations were available. The first excitation peak for Tc$_{Roth}$ is to be found at 340 nm with the corresponding emission at 520 nm (intensity $_{em. max}$: 853.83). A maximum emission intensity of 2281 was recorded for the second excitation peak (2.67 times higher than the first excitation peak) with maximum excitation at 410 nm and emission at 525 nm. In case of Tc$_{Fluka}$ the first excitation peak is situated at an excitation wavelength of 335 nm and an emission wavelength of 525 nm, with a maximum emission intensity of 693.08. The location of the second excitation peak is identical to the location of the respective peak from Tc$_{Roth}$ only varying in the maximum emission intensity: 2310 (0.99 times higher than Tc$_{Roth}$).

The excitation (1. ex. and 2. ex.) and second emission peaks (2. em.) of the respective dyes showed an almost identical course, whereas the emission peaks (1. em.) of the first excitation peak differed in their fluorescence intensity (Tc$_{Roth}$ being 1.23 times higher than Tc$_{Fluka}$). When compared to the fluorescence emission of Tc$_{Roth}$ dissolved in sole PBS the solution showed a 7.05 times higher fluorescence intensity (second excitation peak) when CaCl$_2$ (2.97 mM) was added. For Tc$_{Fluka}$ the difference between the two solutions was even higher: 7.43.

Fixation effects on the fluorescence

a) Fixed cells: Cells of *Acinetobacter calcoaceticus* 69-V with intracellular polyphosphate granules were fixed and stained with either Tc$_{Roth}$ or Tc$_{Fluka}$ (Figure 21). Unstained, fixed cells with neglect able fluorescence served as controls. A broad excitation peak was measured for cells stained with Tc$_{Roth}$ exhibiting a maximum excitation at 405 nm and maximum emission at 525 nm (intensity $_{em. max}$: 337.66). The excitation peak for cells stained with Tc$_{Fluka}$ was smaller and located at 400 nm. Highest corresponding emission was measured at 515 nm with an intensity of 294.37.
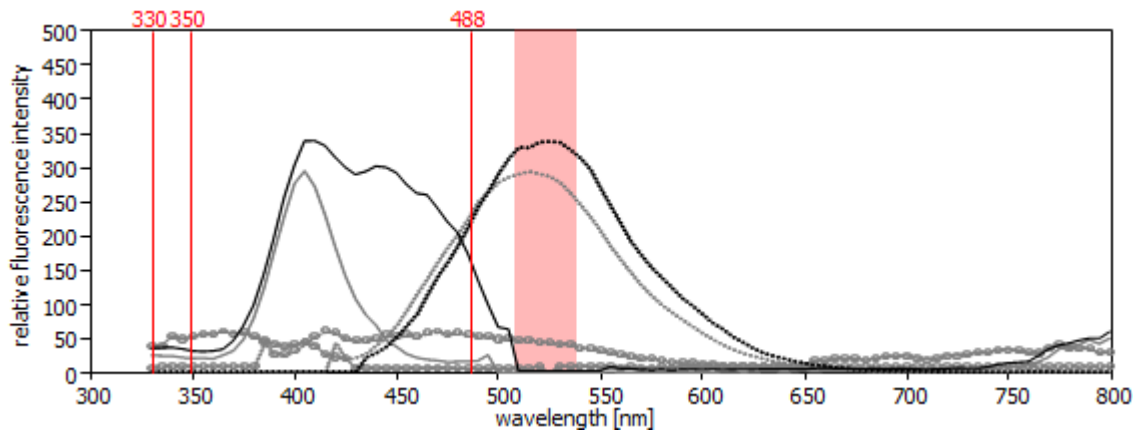
Figure 21. Fluorescence spectra of fixed *Acinetobacter calcoaceticus* 69-V cells. Cells were fixed and stained with Tc$_{Roth}$ (black) or Tc$_{Fluka}$ (grey). Unstained, fixed cells (grey with circles) served as controls. The excitation wavelengths (nm) of the lasers used in in this study are marked with red lines and the band pass filter for green fluorescence with light red background. ex.: excitation (solid line), em.: emission (dotted line)

Both dyes showed alike excitation and emission maxima but differed in the fluorescence intensity. Cells stained with Tc$_{Roth}$ emitted 1.15 times more fluorescence than cells stained with Tc$_{Fluka}$.

b) Unfixed cells: The same cells used for the previous experiment were stained alive with both dyes (with unstained cells as controls).
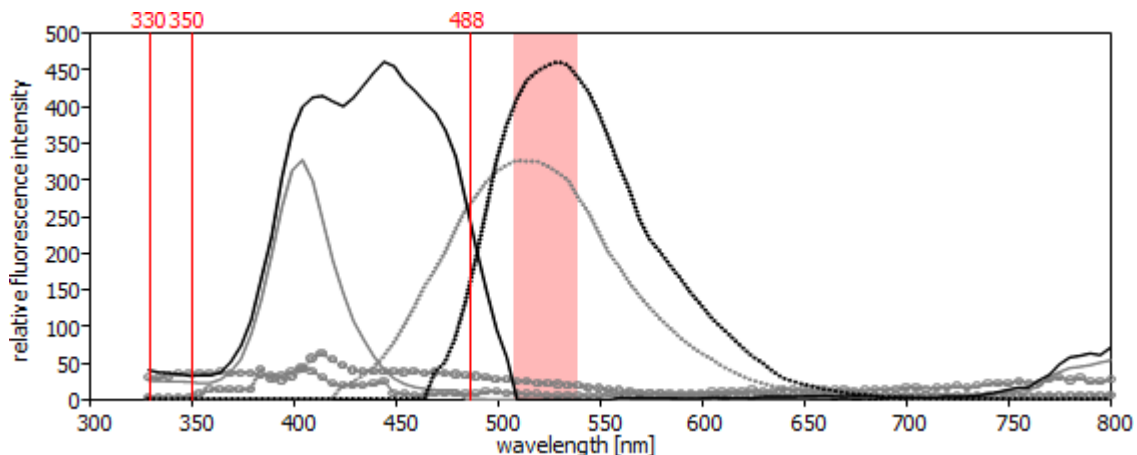
Figure 22. Fluorescence spectra of unfixed *Acinetobacter calcoaceticus* 69-V cells. Unfixed cells were stained with Tc$_{Roth}$ (black) or Tc$_{Fluka}$ (grey). Unstained cells are depicted in grey with circles. The excitation wavelengths (nm) of the lasers used in in this study are marked with red lines and the band pass filter for green fluorescence with light red background. ex.: excitation (solid line), em.: emission (dotted line)

Again Tc$_{Roth}$ showed a broad excitation peak. Maximum excitation was recorded at 445 nm with maximum emission at 530 nm (intensity $_{em.\ max.}$: 457.99). Tc$_{Fluka}$ was maximally excited at 400 nm with the highest emission at 510 nm (intensity $_{em.\ max.}$: 324.78). As with the fixed cells, staining with Tc$_{Roth}$ caused higher fluorescence emission (1.41 times higher) than staining with Tc$_{Fluka}$. Unlike the spectrum of fixed cells, the excitation peaks differed in their maximum by 45 nm and the emission peaks by 20 nm.

A comparison of the maximum emission intensities of unfixed and fixed cells showed reduced fluorescence intensities in fixed cells for both dyes. Unfixed cells stained with Tc$_{Roth}$ had a 1.36 times higher fluorescence than fixed cells and cells stained with Tc$_{Fluka}$ a 1.1 times higher fluorescence.

Fluorescence at different excitation wavelengths and granule fluorescence
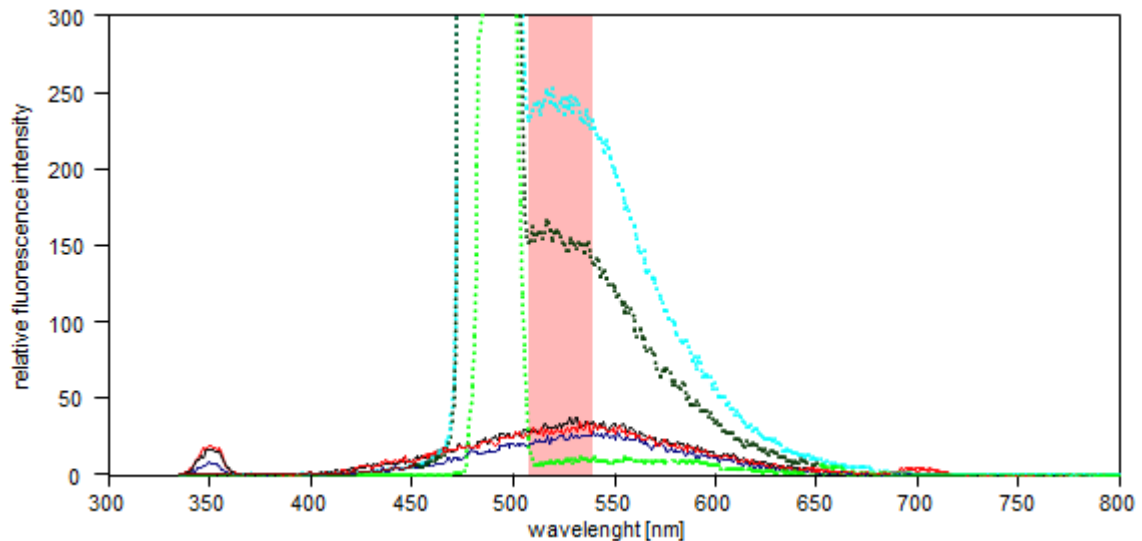
Figure 23. Emission spectra of Tc_{Roth} in PBS (blue$_{350\ nm}$ and green$_{488\ nm}$) and fixed (red$_{350\ nm}$ and dark green$_{488\ nm}$) as well as unfixed (black$_{350\ nm}$ and cyan$_{488\ nm}$) *A. calcoaceticus* 69-V cells which were stained with Tc_{Roth} and excited at either 350 (solid lines) or 488 nm (dotted lines) which are the respective laser lines of the flow cytometer.

When Tc_{Roth} in PBS was excited at 350 nm, the highest fluorescence intensity was 27.94 at an emission of 540 nm. The emission wavelength changed to 536 nm at excitation of 488 nm and dropped to 10.79. The intensity was 2.56 times higher for excitation at 350 nm then 488 nm.

Unfixed cells stained with Tc_{Roth} and excited at 350 nm, showed highest fluorescence intensity at 531 nm (intensity: 37.08; 1.33 times higher than sole Tc_{Roth} in PBS). When the same cells were subjected to excitation at 488 nm the intensity increased 6.8 fold (intensity: 252.3; emission maximum: 520 nm, 23.38 times higher than sole Tc_{Roth} in PBS). The intensities decreased when fixed cells were used.

If fixed cells were excited at 350 nm the maximum emission was recorded at 537 nm (intensity: 34.18; 1.22 times higher than sole Tc_{Roth} in PBS). For the excitation wavelength of 488 nm the emission shifted to 517 nm with 165.13 as the highest intensity (15.33 times higher than sole Tc_{Roth} in PBS). The emission was 1.53 times higher for unfixed cells than for fixed cells if these were excited at 488 nm.

To measure the fluorescence properties of Tc stained polyphosphate granules cells of *Acinetobacter calcoaceticus* 69-V were cultivated on M9-media (medium 9, Annex I) until the culture showed a significant amount of polyphosphate containing cells. Cells from the same pre-culture were also cultivated on M9-media but without a source of phosphate for polyphosphate accumulation. After measuring the fluorescence properties of both cell cultures (which were stained with Tc_{Roth}) the values for the culture without granules were subtracted from the values obtained with the granule exhibiting culture. As a result, the fluorescence properties of the stained granules remained without interferences from cell background staining and fluorescence of Tc_{Roth} in the stained cells solutions.
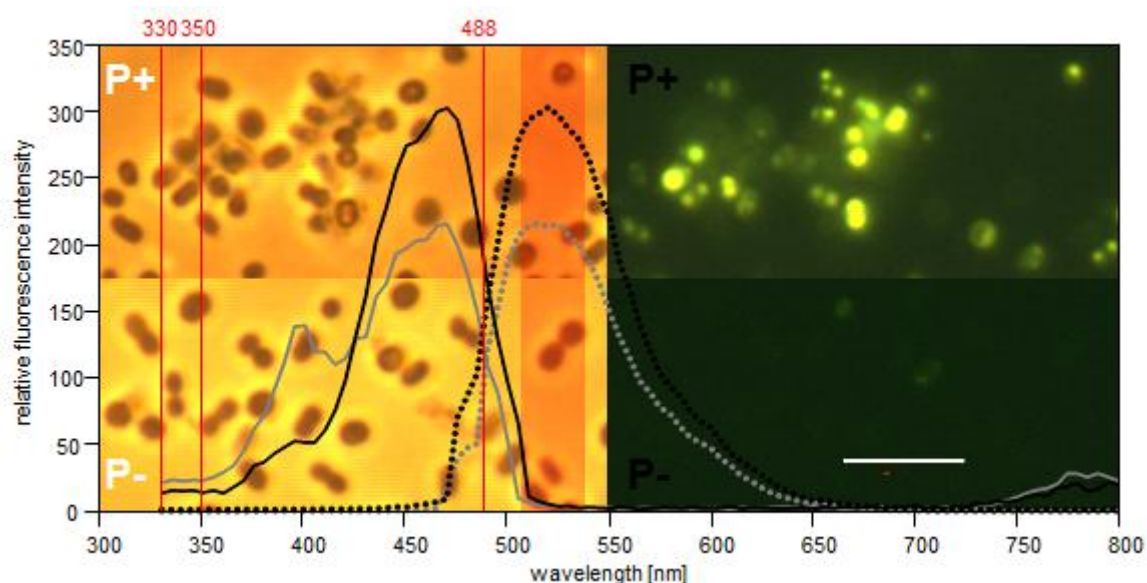
Figure 24. Fluorescence of the polyphosphate granules. Unfixed (black) and fixed (grey) cells of *Acinetobacter calcoaceticus* 69-V, cultivated in two different media (with and without a phosphate source) were stained with Tc$_{Roth}$. The excitation wavelengths (nm) of the lasers used in in this study are marked with red lines and the band pass filter for green fluorescence with light red background. Pictures show fixed cells of the two media stained with Tc$_{Roth}$ (bar on the lower right side: 5 µm). ex.: excitation (solid line), em.: emission (dotted line)

Granules of fixed and unfixed cells showed maximum excitation at 470 nm and maximum emission at either 515 nm (fixed cells, intensity $_{em.\ max.}$: 216.12) or 520 nm (unfixed cells, intensity $_{em.\ max.}$: 303.63). Unfixed cells had a 1.41 times higher fluorescence intensity than fixed cells.

Table 8. Summary of excitation and emission maxima of tetracycline hydrochloride from the two manufacturers. n. d.: not determinded, rel. I.: relative intensity

	tetracycline hydrochloride from Roth			tetracycline hydrochloride from Fluka		
	excitation [nm]	emission [nm]	intensity [rel. I.]	excitation [nm]	emission [nm]	intensity [rel. I.]
water	425	535	154.9	390	555	62.9
PBS	400	525	323.7	405	520	311.0
PBS + Ca	340 410	520 525	853.8 2281	335 410	525 525	693.1 2310
unfixed cells	445	530	457.9	400	510	324.8
fixed cells	405	525	337.7	400	515	294.4
granules (unfixed cells)	470	520	303.6	n. d.	n. d.	n. d.
granules (fixed cells)	470	515	216.1	n. d.	n. d.	n. d.

2.3 Controls to verify specific and quantitative staining

After evaluation of the fluorescence properties, the stability of the tetracycline staining solution was tested on polyphosphate containing cells of *Microlunatus phosphovorus* NM-1 (Figure 25, a). A significant reduction in the amount of green fluorescent cells was measured after just three days of storage of the staining solution at RT in the dark. Possible unspecific staining of cellular constituents by Tc was tested using *Escherichia coli* K12, a bacterium that does not produce significant amounts of polyphosphate granules without genetic manipulation [RAO *et. al.*, 1985].

Tc (0.225 mM) caused no fluorescence labeling of *E. coli* (0.03%, ± 0.01), whereas DAPI (28 µM) caused greenish fluorescence of 1.30% (± 0.03) of the treated cells (Figure 25, b). In addition to this, *Methylobacterium rhodesianum* MB126 was used to test for possible binding of Tc to Poly-*ß*-HydroxyButyrate (PHB) granules (Figure 25, b). The presence of PHB was verified using Nile red staining which caused bright red fluorescence, whereas Tc caused no fluorescence with PHB (0.03%, ± 0.01).
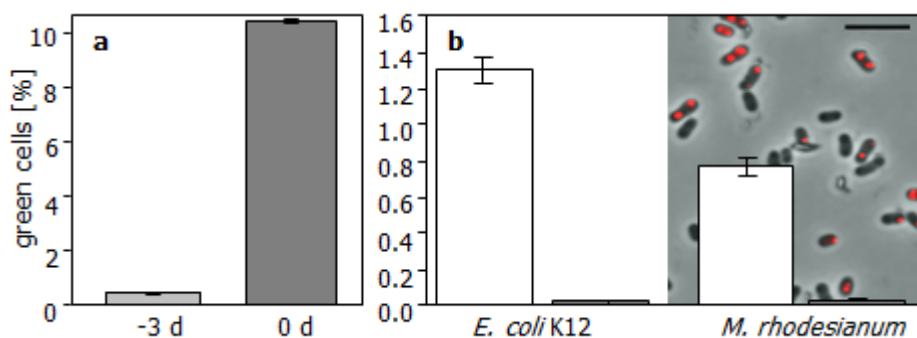
Figure 25. Tetracycline aging and fluorescence controls. a) To determine the effect of tetracycline aging, living cells of *Microlunatus phosphovorus* NM-1 were stained with 0.23 mM Tc$_{Fluka}$, which was either prepared right before starting the experiment (dark grey) or 3 days in advance (light grey) and stored in the dark at 20°C. b) polyP free cells of *Escherichia coli* K12 and *Methylobacterium rhodesianum* MB126 were fixed and treated with 0.225 mM Tc$_{Fluka}$ (grey) or 28 µM DAPI (white). They served as DNA- (*E. coli* K12) and PHB- (Microphotograph: *M. rhodesianum*, stained with Nile red, bar: 5 µm) negative controls.

Finally, also the glycogen accumulating strain *M. glycogenica* which does not produce polyphosphates was tested for green unspecific staining of glycogen granules but showed no Tc fluorescence (0.03%, ± 0.01, data not shown). Also spores of *Bacillus subtilis*, known to have a high content of divalent cations, were tested negative for Tc staining (Figure 26).
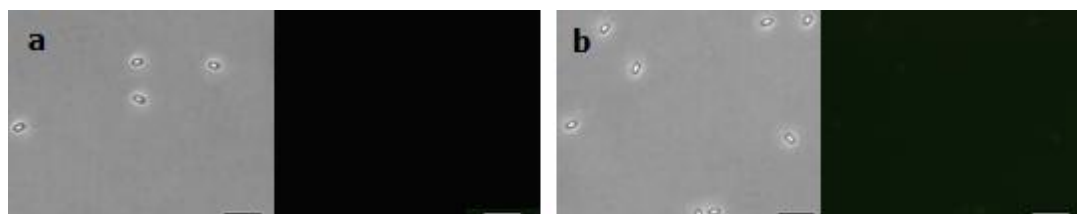
Figure 26. Tetracycline staining of spores. Spores of *Bacillus subtilis* (DSM 347, UFZ strain collection, harvested from peptone media) dispensed in PBS and stained with Tc$_{Fluka}$ for more than 2 hours (bars 5 µm). a) unstained spores, b) Tc$_{Fluka}$ stained spores

2.4 Verification of the method by phylogenetic analysis

The reliability of the dual labelling technique was also tested by analysis of a sample harvested from the aeration tank of the WWTP Elsterwerda. The sample was aerated and kept on ice until flow cytometric analysis. Tc staining revealed that 10.2% of the cells contained polyphosphate granules. The polyphosphate positive cells were sorted and subjected to DNA extraction for the phylogenetic identification of PAOs. To verify if the sorted cells can be phylogenetically affiliated to PAOs a 16S rRNA gene clone library of 78 clones was generated and screened by ARDRA (Amplified rDNA Restriction Analysis).

Based on different ARDRA patterns, 43 representative clones were partially sequenced. Phylogenetic affiliation of the sequences based on the RDP taxonomy and the highest BLAST hit is given in Annex III. The most frequent phylotype comprising 27 clones was affiliated with the *Rhodocyclaceae*. These sequences showed high similarity to clones retrieved from EBPR sludge, among them those affiliated to the *'Candidatus* Accumulibacter' lineage [HE *et al.*, 2007]. The second most frequent phylotype with 13 clones was assigned to the genus *Pseudomonas*. A third group, comprising seven clones, was a phylotype belonging to the *Gammaproteobacteria* and related to Glycogen Accumulating Organisms (GAO) retrieved from an EBPR WWTP (acc. no. DQ201885). A phylotype assigned to the genus *Nitrospira* was also represented by seven clones. Four clones were assigned to the genus *Tetrasphaera* and closely related to actinobacterial PAOs detected in an EBPR plant [KONG *et al.*, 2005]. The genus *Dechloromonas* was also represented by four clones. Other phylotypes present in minor proportions were affiliated to another group of the *Actinomycetales* (two clones) and the candidate division TM7 (two clones), 12 other phylotypes were represented only by single clones (Annex III). Most of these organisms are described as potential polyphosphate accumulators.

In addition, Terminal-Restriction Fragment Length Polymorphism (T-RFLP) was applied to strengthen the data obtained from the clone library and to establish a method which reveal data on phylogenetic affiliation much easier and on the basis of the clone library. The T-RFLP analysis showed Terminal-Restriction Fragments (T-RFs) assigned to *Pseudomonas* sp. were most frequent and comprised more than 50% of the total peak area (Figure 27). The *Rhodocyclaceae* phylotype related to *Accumulibacter* as well as the *Tetrasphaera*- and *Nitrospira*-like phylotypes were also detected in the T-RFLP profiles but with lower percentages than expected from the clone library. These results indicate that *Pseudomonas* spp. was the predominant polyphosphate containing organism in the EBPR community analyzed here and also, in general, that the established method is well suited to detect PAOs in pure as well as natural microbial communities.
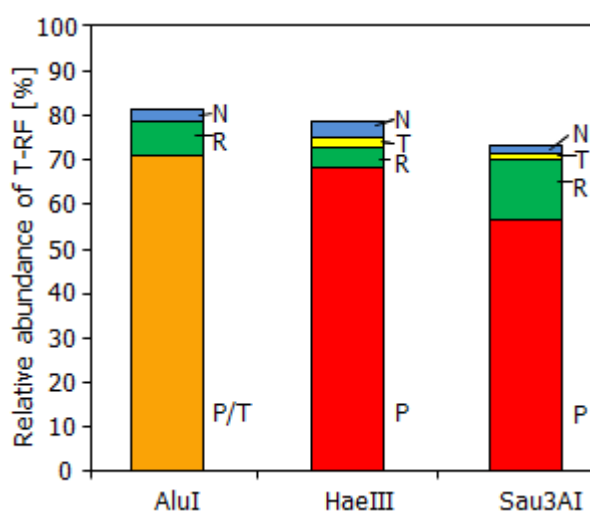
Figure 27. Relative abundances of T-RFs after digestion with the restriction endonucleases AluI, HaeIII, and Sau3AI, respectively. The T-RF values were assigned to phylotypes according to the experimentally determined T-RF values of the respective clones. P – *Pseudomonas* sp.; R – *Rhodocyclaceae*; T – *Tetrasphaera* sp.; N – *Nitrospira* sp. With AluI, the T-RF values of *Pseudomonas* sp. and *Tetrasphaera* sp. were identical and therefore their relative abundances are summarized.

3. Application experiments

After the development of the appropriate fixation and staining technique for flow cytometric analysis of polyphosphate (polyP) accumulating organisms the techniques were verified on mixed microbial cultures. Tests were conducted either with a community harvested from a bench top bioreactor or directly from a WWTP. In addition to the results obtained by flow cytometric analysis abiotic parameters were measured as well to obtain a more detailed view on the community dynamics and possible reasons behind them.

3.1 Activated sludge community dynamics in bench top bioreactor experiments

For evaluation of the staining method, the dual staining technique of DAPI and Tc_{Fluka} was tested by analysing PAO dynamics in activated sludge as a-proof-of-principle study in a bench top bioreactor. DAPI staining provides information on sub-community dynamics within natural communities, whereas the Tc staining distinguishes polyphosphate accumulating community members.

Activated sludge was cultivated in a sequenced batch mode and subjected to alternating aerobic and anaerobic conditions (as described in Material and Methods, section 1.2.2, p. 14). Samples were harvested from both cultivation phases and biotic as well as abiotic parameters analysed. Biomass was found to be produced at constant rates, sometimes floc formation was observed after several aerobic/anaerobic cycles. MLSS (Mixed Liquor Suspended Solids), MLVSS (Mixed Liquor Volatile Suspended Solids), and ash contents did not change much during the bioreactor cultivation. The following values were measured: 3.0 (± 0.02) g L^{-1} MLSS, 2.4 (± 0.00) g L^{-1} MLVSS and 0.6 (± 0.02) g L^{-1} ash for the aerobic phase as compared to 2.7 (± 0.58) g L^{-1} MLSS, 2.2 (± 0.41) g L^{-1} MLVSS, and 0.5 (± 0.18) g L^{-1} ash for the anaerobic phase. The nitrite/nitrate concentration was close to zero during the anaerobic phases, indicating nitrate-reducing conditions (Figure 28).
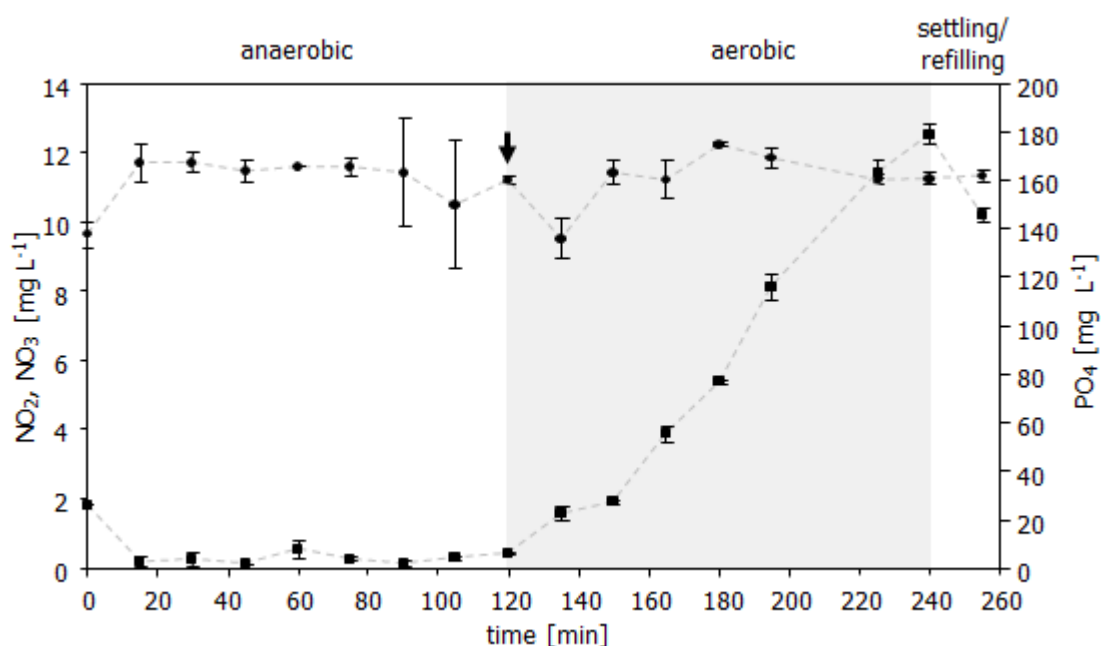
Figure 28. Orthophosphate (circles) and nitrite/nitrate (squares) contents of the bench top bioreactor during one anaerobic/aerobic/refilling cycle. The aerobic phase is marked with a light grey background, the refilling phase is only partly shown.

The stationary orthophosphate concentration was set to relatively high values up to nearly 180 mg L^{-1} to stimulate the polyphosphate accumulation for convenient fluorescence measurement.

To visualize changed polyphosphate granule accumulation during the anaerobic and aerobic phases, cells were harvested 5 min after entering the anaerobic phase and 105 min after entering the subsequent aerobic phase (158 mg orthophosphate L^{-1} in this sample). They were fixed and stained with DAPI and Tc_{Fluka}. Higher quantities of polyphosphate containing cells were found during the aerobic cultivation phase (2.9%, Figure 29) than in the anaerobic phase (0.8%).
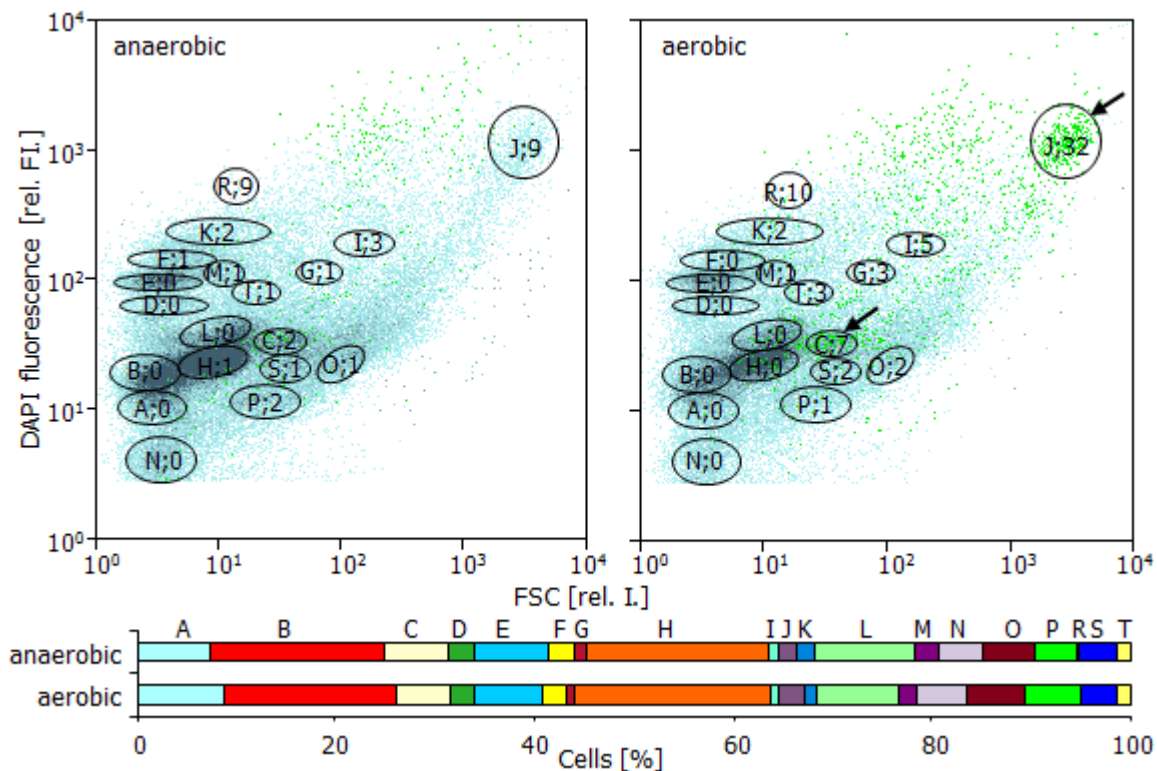
Figure 29. Pattern of DNA distributions (blue, with dominant sub-communities marked with black gates) and PAO distribution (green dots and numbers within the gates [%]) of cells harvested from the anaerobic and aerobic cultivation phase and double stained with DAPI and Tc_{Fluka}. Sub-communities with a high PAO content are marked with arrows. The amount of cells within each sub-community is shown in the lower part.

Up to 19 sub-communities differing in either polyphosphate or DNA contents as well as cell size were found. The bars at the bottom of Figure 29 give their relative abundances. The numbers and letters in this Figure indicate percentages of PAOs within the gates and the denomination of the sub-communities. It is noteworthy, that neither the number of distinct sub-communities nor the corresponding cell abundances changed much between the aerobic and anaerobic phases. However, it was interesting that high abundances of PAOs were found in only a few of the sub-communities in the sample. These sub-communities were characterized by intermediate to high forward scatter and intermediate to high DNA contents. It was not observed that the PAOs where members of the very small and low DNA content sub-communities at the left side of the histogram (gates: A, B, D, E, N). The majority of the PAOs was present in two sub-communities (C and J, arrows) to which they contributed 2% and 9% in the anaerobic phase or 7.3% and 32% in the aerobic phase, respectively. One sub-community (gate R) comprising cells with medium forward scatter and high DNA content showed a high PAO abundance (9% to 10%) irrespective of the cultivation phase.

Additionally, the activated sludge cultivation regime was modified by altering stationary orthophosphate and carbon concentrations to prove the effectiveness of the new PAO detection technique (Figure 30) and identify possible influences on the PAOs within the system. PAO abundances were followed in dependence of phosphate concentrations in the feed increasing from 57 mg L^{-1} (days 11, 14; 1 x P) to 74 mg L^{-1} (days 15, 18; 1.3 x P), 97 mg L^{-1} (days 26, 27; 1.7 x P), and, 151 mg L^{-1} (days 28, 32; 2.6 x P) in combination with elevated carbon contents from 583 mg L^{-1} (days 11, 14, 15, 18; 1 x C) to 1166 mg L^{-1} (days 27, 27 and 28, 32; 2 x C). Samples were taken during the aerobic phases only, on different days separated by several shifts of the oxygen regime. Consequently, increased phosphate concentrations led to increased fractions of PAOs within the sludge from about 0.3% with 57 mg phosphate L^{-1} to 4% with 151 mg phosphate L^{-1}. Otherwise, the relative abundances of bacterial cells in the 19 pre-defined sub-communities remained nearly unchanged during the cultivation on 583 mg L^{-1} (1 x C, Figure 30) carbon content.
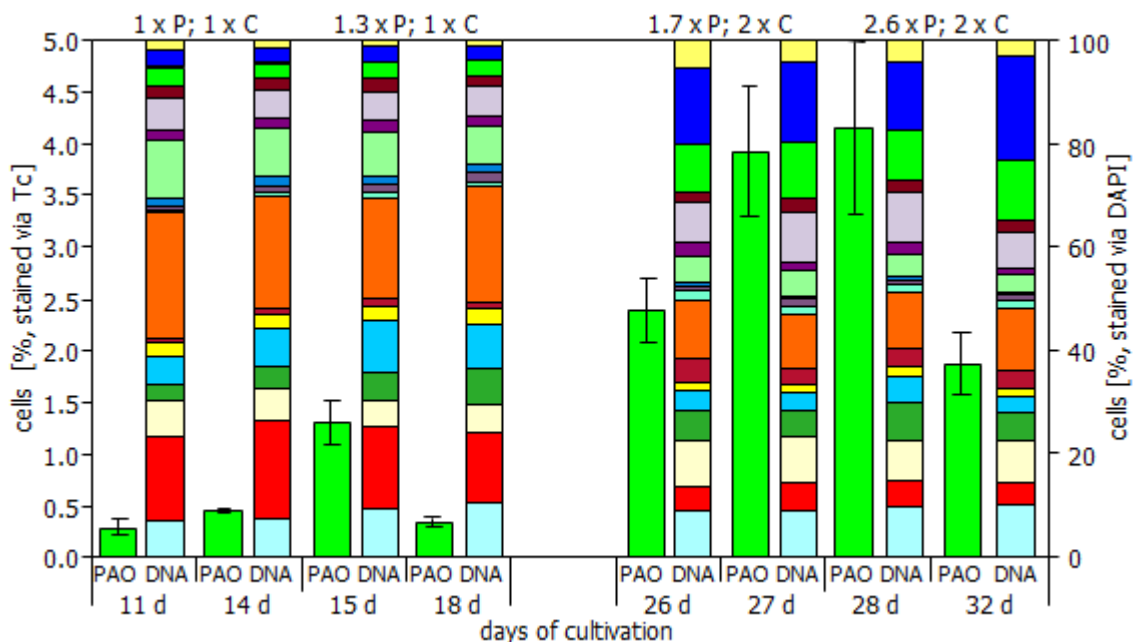
Figure 30. DNA pattern (right column, labels corresponding to those in Figure 29) and proportions of PAOs (left column) of an activated sludge community cultivated in the bench top bioreactor for 32 d. The cells were harvested from the aerobic cultivation phase and double stained with DAPI and Tc$_{Fluka}$. Phosphorous (P) and carbon (C) concentrations were varied as indicated at the top of the Figure.

Seven major sub-communities (A, B, C, E, H, L, N; each above 5%) comprised together nearly 80% of the whole community. When the carbon concentration was doubled to 1165 mg L^{-1} COD (2 x C), a different distribution of the community's individuals developed. Although the total number of the distinguishable 19 sub-communities remained constant, changed dominance patterns were observed. Now eleven main sub-communities (A, B, C, D, E, G, H, N, P, S, T; each above 5%) comprised together 90% of all cells in the 19 sub-communities. This shows the massive influence of the carbon concentration on the community structure. Nevertheless, the general abundances of the PAO containing key sub-communities C and J stayed nearly constant during cultivation on low carbon concentrations with J slightly increasing in cell number.

A similar stability was observed on higher carbon concentrations although the abundance of C increased from 6 to 9%, whereas cell numbers in J slightly decreased to 2%. The sub-community R with low general abundance (about 0.05% of all DAPI stained cells) but high PAO content, showed no significant changes towards altered phosphate and carbon contents.

3.2 Activated sludge community dynamics in the WWTP Eilenburg

As a final point, community dynamics within a WWTP were investigated. Since the dynamics in a WWTP were assumed to reflect altering abiotic conditions and varying substrate inflow, a large number of abiotic and biotic parameters were measured at three sampling points: primary clarifier (PC) and the aeration tanks 1 and 2 (AT 1 /2). During the monitoring campaign of 29 days (June - July 2010) the weather was warm and dry. Average maximum temperature was 25.3°C (minimum: 12.5°C), with 0.8 mm rain and more than 10 hours sunshine per day (Annex IV).

Due to the detected differences in fluorescence from the two suppliers, the dual staining method was here replaced by a combination of the two single staining techniques (DAPI for DNA, Tc for PAOs) with the statistical technique of correlation analysis. This combination gives the same information as the double staining technique and assures the highest measurement accuracy possible.

3.2.1 Comparability of the three sampling points

The measured data sets for abiotic and biotic parameters were compared for overall similarity (Figure 31) using n-MDs (Non-parametric MultiDimensional Scale) analysis.
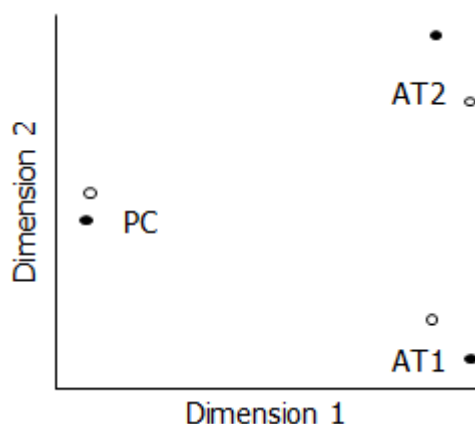
Figure 31. N-MDS plot of all abiotic (black circles) and biotic (white circles) parameters (mean values) for the three sampling points at the WWTP Eilenburg: primary clarifier (PC), aeration tank 1 (AT 1) and aeration tank 2 (AT 2). The plot is based on Euclidian distance measurement. Stress values for the two merged n-MDS plots were both 0 and the R^2 values: 1 (axis 1) and 0 (axis 2).

Euclidian distance measurement analysis of the abiotic and biotic parameter revealed a pattern which stated high similarity of the measured parameters with regard to the sampling site. The data obtained from the primary clarifier were clearly different from those of aeration tanks 1 and 2, although these two were not as similar as could be expected from the mode of plant operation (see Material and Methods, section 1.2.3, p. 14). Generally, the distance between the abiotic data points was higher than for the biotic data (for data values included in this Figure see Annex IV).

3.2.2 Sub-community stability at the three sampling points

Community dynamics were described using results derived from flow cytometrical measurements. Parameters measured of every cell were FSC (information related to cell size), SSC (information on cell granularity), DNA content (information on community structure), Nile red fluorescence (information on the amount of cells with neutral lipid like substances), and Tc fluorescence (information on polyP accumulation). Since many WWTPs are prone to break downs and suffer instabilities during the water treatment process the stability of the microbial community is a precondition for a reliable EBPR process operation. Thus, the microbial community can be seen as a kind of whole cell biocatalyst and, even more important for control applications, a biosensor which allows judgment on the process functionality.

At the WWTP Eilenburg the primary clarifier receiving carbon and energy rich substrate is located upstream of the aeration tanks 1 and 2 (see Material and Methods, Figure 4, p. 15). Tanks 1 and 2 obtain the same kind and amount of primary-clarifier-water and are operated identically.

To investigate the stability of the community within the three sampling sites over a time period of 29 days the samples were stained with DAPI and analyzed flow cytometrically (for respective dot plots of these measurements see Annex V). Main sub-communities were gated and their cell number measured (Figure 33, given in % of all DAPI stained cells).

As shown in the dot plots of Annex V, fifteen distinct clusters were found in total. The number of all cells within gates varied between 37 and 45% of all DAPI stained cells. Generally, the cells varied by several orders of magnitude in DNA fluorescence and the cell size-related FSC signal (blue gates in Figure 32). As is highlighted by the blue gates in the dot plot of e.g. day 8 (Figure 32) the cells in the left gate lack a significant FSC signal indicating small size and low DNA content. The blue gate on the upper right side contains cells with twenty-fold higher DNA content and 10^3 times more light scattering. The enormous range of these characteristics within the wastewater community facilitates the distinction of community patterns to a great extent. Although all sub-communities were present within the 29 days of sampling, the proportion of cells within distinguishable clusters differed over time. For example, the green gate in the dot plot of day 8 comprised 10.2% of all DAPI-stained cells but decreased to 2.77% within 3 days (day 11, Figure 32).
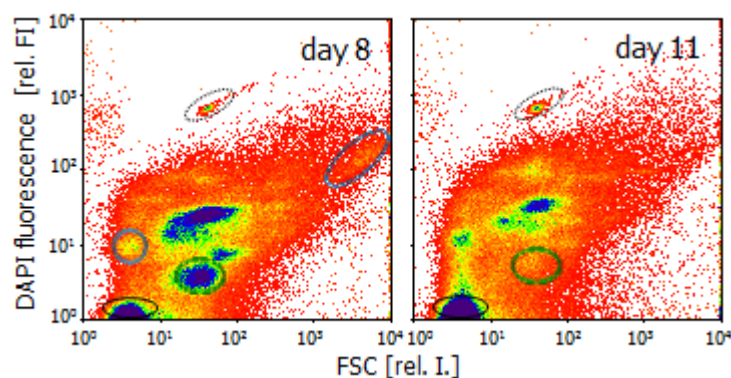
Figure 32. Example for the variance in cell abundances during the sampling period. black ellipses indicate electronic noise, dotted ellipses indicate blue fluorescent beads
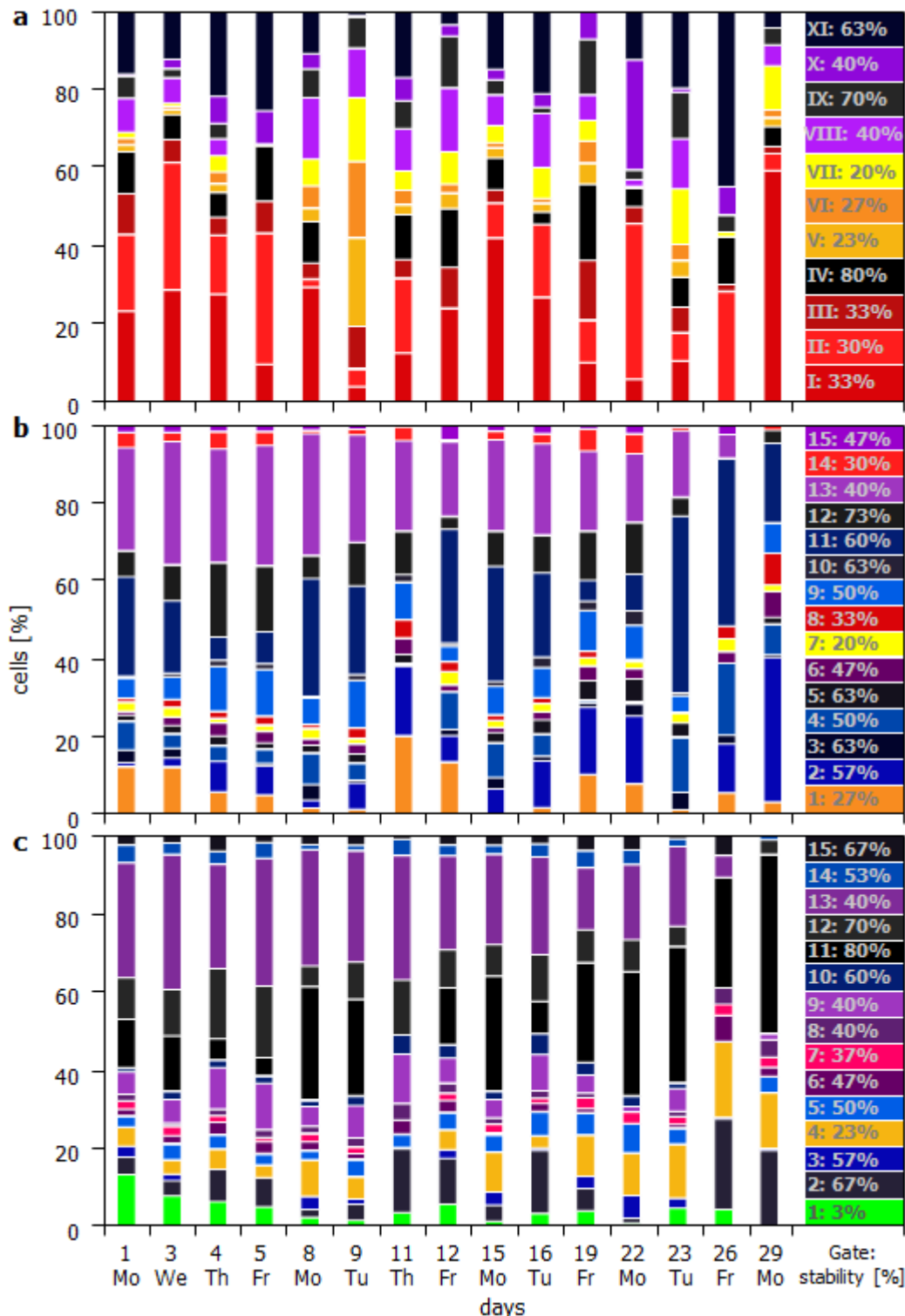
Figure 33. Sub-community profile of the PC (a) and of the AT 1 (b) and 2 (c) over 29 days. The relative abundances of cells (in %, height of bars on y-axis) in dominant sub-communities (PC: numbers I-XI; AT 1 and 2: numbers 1-15) are shown. The percentage value after every gate number (see color legend: e.g. At 2, 1: 3%) means that the cells in AT 2 within the sub-community number 1 are present over the sampling time with a stability of 3% (for 3% of the days the cell number of this sub-community was within the 25% tolerance interval and therefore stable (see Materials and Methods, section 8.1, p. 22)). Stability of the sub-communities is further indicated by colours: sub-communities in dark colours had a high and those with light colours a low stability. To highlight the changes, the base line of cell number estimation was specifically determined by the lowest cell number for every gate during the whole sampling period.

Stability of each sub-community at every sampling point was determined using an equivalence test. All sub-communities that were within a 25% tolerance interval (with the values of the first day of sampling as the reference point) were regarded as stable. The number of stable days (15 days of sampling) per sub-community was expressed as a percentage. High percentages indicate stable sub-communities and are defined by dark colors in varying degrees whereas cells in yellow or green clusters showed low stability (= low percentages of stability) and almost vanish within certain time frames.

As a first result, sub-communities and cell numbers therein differed in the samples from the primary clarifier (sub-communities I-XI, Figure 33, a) as well as aeration tanks 1 and 2 (sub-communities 1-15, Figure 33, b and c; for dot plots of these measurements see Annex V). Second, within aeration tanks 1 and 2 a higher stability (6 and 7 sub-communities out of 15 with stability percentages higher than 50%) can be stated in comparison to the primary clarifier (only 3 sub-communities out of 11 with percentages higher than 50%). Most clusters emerging in the aeration tank 2 resembled those in aeration tank 1 while some differed partly e.g. on days 19 and 22. Differences were also detected in the sub-community stability. For instance, sub-community 1 in the aeration tanks showed 27% stable days in AT 1 and only 3% in AT 2. This further confirms the similarity analysis in Figure 31 that also shows significant differences between the two aeration tanks (for sub-community numerations see Figures 38-40).

3.2.3 Taxonomic affiliation of WWTP organisms

For further insight into the community dynamics and performance of metabolic sub-groups like the PAOs more detailed information about the organisms present at the sampling site is needed.

Initially, to identify the organisms dominating the whole WWTP community a 16S rRNA gene clone library of the aeration tank 1 at day 54 was constructed. One-hundred sixteen clones were partially sequenced and taxonomically assigned by RDP database retrieval. The clone library of this sample was dominated by *Sphingobacteriales* and *Rhodocyclaceae* with 12.9% each. In total, 20 phylotypes belonging to 9 different phyla, all common in WWTPs were found (including candidate phylum TM7, details see Annex VI). For 68% of the clones, the taxonomic affiliation below the phylum level could be determined. Results of the T-RFLP profiling of selected clones are shown in Annex VI.

The composition of the whole community was also investigated using the T-RFLP approach. Restriction digestion with RsaI is given for the days 23, 54, and 57 by the first three bars in Figure 34. Similar results were obtained with HaeIII (not shown). These T-RFLP analyses confirmed the results of the clone library as *Sphingobacteriales* and *Rhodocyclaceae* were dominant with 20 and 52%, respectively. However, the clone library construction and whole community T-RFLP analysis lack the knowledge on the impact of certain cell abundances in the community seen by cytometric clustering.

The limited sensitivity and poor quantitative resolution using the T-RFLP technique and the lack of phylogenetic information in quantitative cytometric community patterns can be overcome with combining both approaches by cell sorting. Therefore, the phylogenetic identities were assigned to distinct sub-communities by cell sorting followed by T-RFLP (digested with RsaI and HaeIII) analysis.
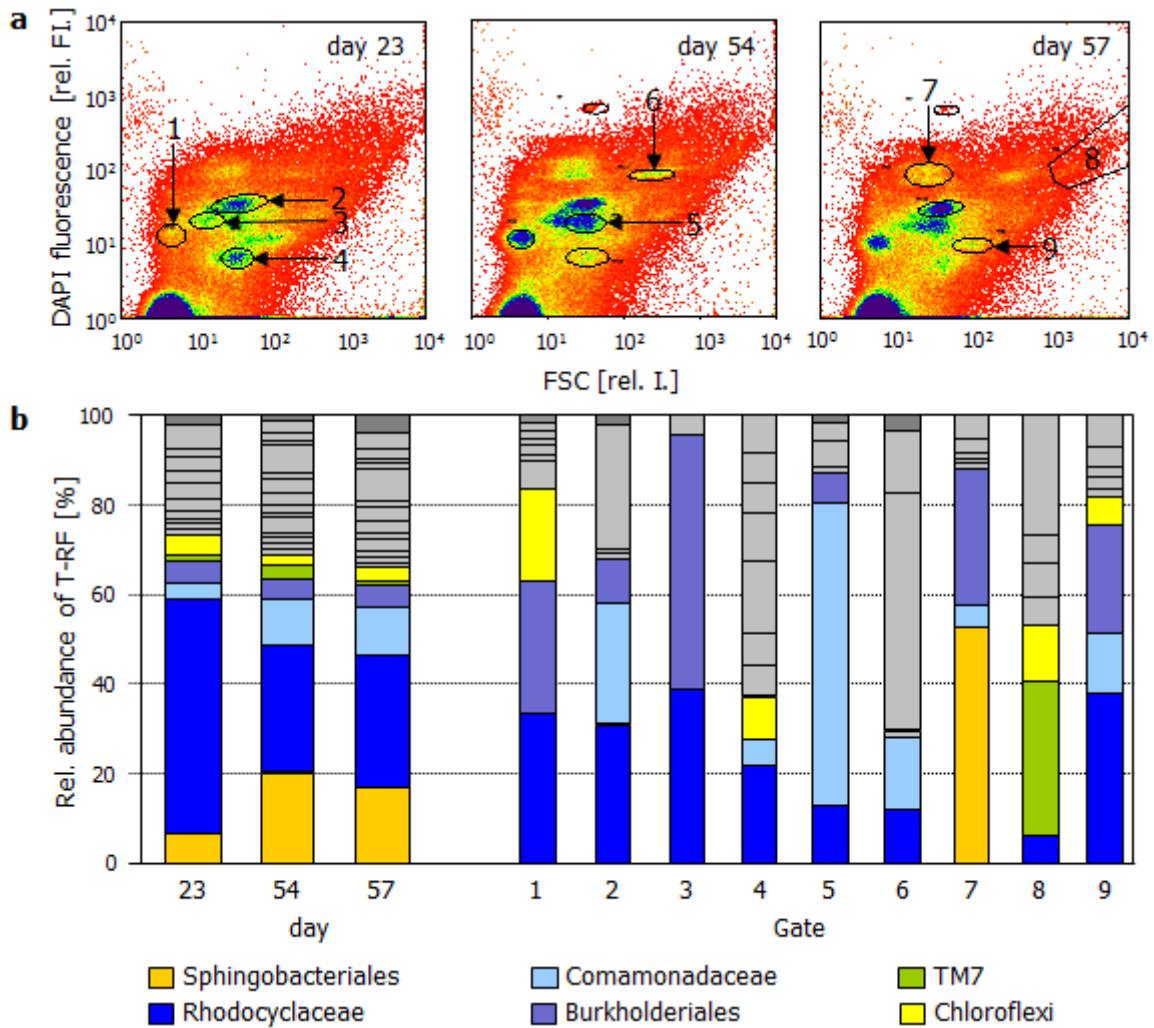
Figure 34. DNA/FSC pattern distributions of cells harvested from the activated sludge tank 1 after 23, 54, 57 days (a). Gates were selected virtually and between 0.22 and 1.0 x 10^6 cells locally separated per gate by cell sorting. The sorted cells were digested with RsaI for T-RFLP analyses and the phylogenetic affiliation is documented (b). For comparison the whole community composition is shown for every day (left bars, b).

Samples from days 23, 54, and 57 of tank 1 were cytometrically analysed (Figure 34, a) with nine sub-communities chosen and sorted in total. The sub-communities 2, 3 and 5 are those with the highest cell abundances in the community, which show numbers that are in maximum 5.7, 2.8 and 3.9 times higher than in the other sub-communities (evaluated for cells shown in Figure 34). According to the T-RFLP analysis, *Rhodocyclaceae*, *Burkholderiales*, and *Comamonadaceae* were the chief representatives in these three central sub-communities, but they can also be detected in the sub-communities 1, 4 and 9 to a smaller amount. The cells in the latter sub-communities with abundances of 6.44%, 4.88%, and 2.57% of all DAPI stained cells, respectively, contained low DNA quantities but were diverse in cell size. *Chloroflexi* emerged as additional phylotype here. Organisms belonging to this phylotype are known to act in WWTPs with carbon removal as well as nitrification and denitrification processes [KRAGELUND *et al.*, 2007], but were non-detectable with the HaeIII digestion in this study and present with only one clone in the clone library (Annex VI).

A clearly different composition was found for sub-communities 6 (1.34%), 7 (3.53%), and 8 (1.05%). All those cells contained high DNA contents as well as medium to large cell sizes but their abundances were low. The clone library was not capacious enough to determine the chief organisms in sub-community 6 but found *Shingobacteriales* in sub-community 7 and TM7 in sub-community 8 as main phylotypes. It is worth to note that not all T-RFs could be assigned to a representative from the clone library. Reasons for that might have been the limited number of clones but also method dependent problems like pseudo peak formation. From the T-RFLP data (Figure 34) it is apparent that the chief sub-communities 2, 3 and 5 showed high species consistency and mirrored the main abundant groups from the total community. The diversity in the low and high DNA sub-communities seemed more elevated due to raised T-RF numbers.

3.2.4 Polyphosphate accumulating organisms in the WWTP

Microbial cells containing polyphosphates were detected by Tc staining, leading to green fluorescence exemplarily shown for day 19 in Figure 35 and for the whole sampling period in Figure 36.
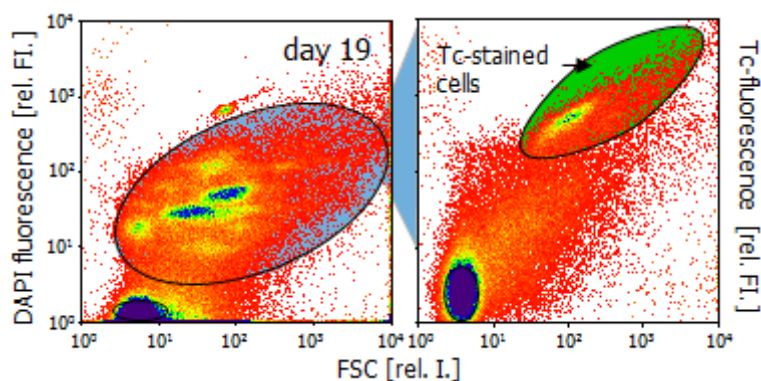
Figure 35. Determination of PAOs using Tc$_{Roth}$-staining of unfixed cells. Depicted here is the sub-community distribution (left side) and the amount of green fluorescent cells (right side) of AT 1 at day 19. DAPI stained cells are marked with a blue background and indicate all those cells analysed by tetracycline staining.

Among the cells with green fluorescence were those with bright green fluorescence (marked in Figure 35 by an ellipse with green background) and those with low or medium tetracycline fluorescence. Bright fluorescence indicates either big or a high number of polyphosphate granules within the cells whereas lower green fluorescence serves as an indication for small granules. Very low green fluorescence is either due to very small granules or to background staining.

For example, at day 26 (AT 1) up to 25.62% of all cells determined by FSC/SSC stored polyphosphates. These cells were of medium size as were those in Figure 35. Phylogenetic affiliation of the Tc stained and sorted cells (see Figure 35, day 19, green fluorescent cells) was also determined. The main phylotypes found were the *Rhodocyclaceae* (15.7% RsaI, also found by HaeIII) and *Chloroflexi* with 50.46% (only by RsaI).
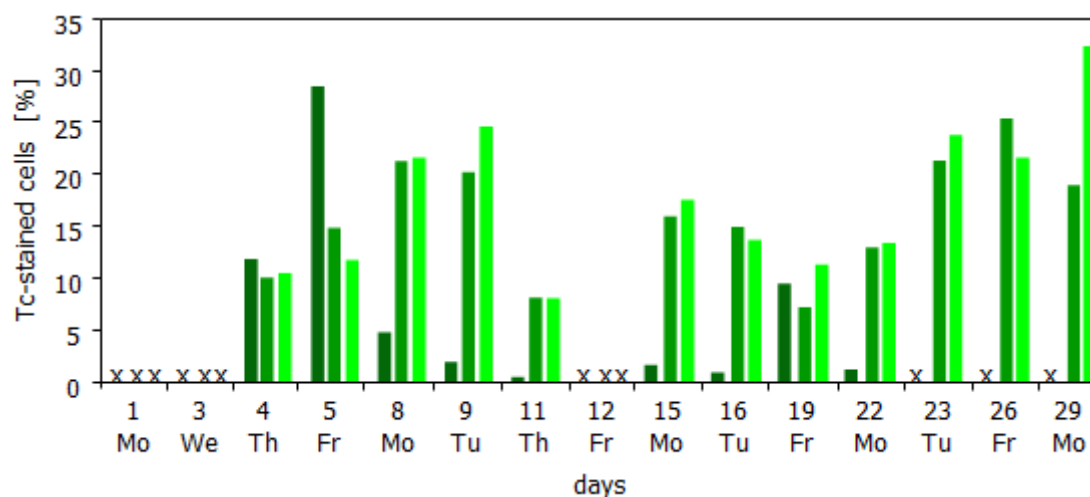
Figure 36. Percentage of fixed, tetracycline stained cells with polyP granules at the three sampling sites. dark green: primary clarifier, green: aeration tank 1, light green: aeration tank 2, X: no data

While the abundance of PAOs in AT1 and 2 did not vary to a great extent, the variation in the primary clarifier was high (e.g. day 5 and 11). Nevertheless, the abundance of PAOs was between 0.44% - 28.52% for the primary clarifier and 7.25% - 25.62% for AT1 and 8.04-34.4% for AT2 during the investigated time span of 29 days.

3.2.5 Correlation of biotic and abiotic data sets

Although much information about the WWTP Eilenburg and the organisms present there was gained by flow cytometric analysis combined with cell sorting and phylogenetic analysis the main reasons for changes in the community structure and performance of the WWTP remained vague.

Therefore, multivariate statistics were applied to correlate cytometrically measured microbial community dynamics (Annex V) with fluctuating abiotic data sets (Annex IV).

Spearman's rank-order correlation coefficient and the Kendall's rank correlation coefficients were used to combine and interpret all abiotic and biotic datasets (for the respective correlation values see Annex VII). Those coefficients are described to be exceptionally useful for evaluation and quantification of correlations between almost all kinds of parameters [LAPATA, 2006]. The approach offers a non-parametric measure of correlation, without making an assumption about the distribution of the variables and it does not require the variable to be measured on interval or ratio scale.

General correlations

Various general positive and negative correlations were found between weather parameters and WWTP-related parameter (Figure 37). For instance the values for rain positively correlated with many WWTP-related parameters like turbidity, amount of influent, pH of the influent and even the temperature of the influent. Negative correlations were found between rain and temperature as well as for rain and sunshine.
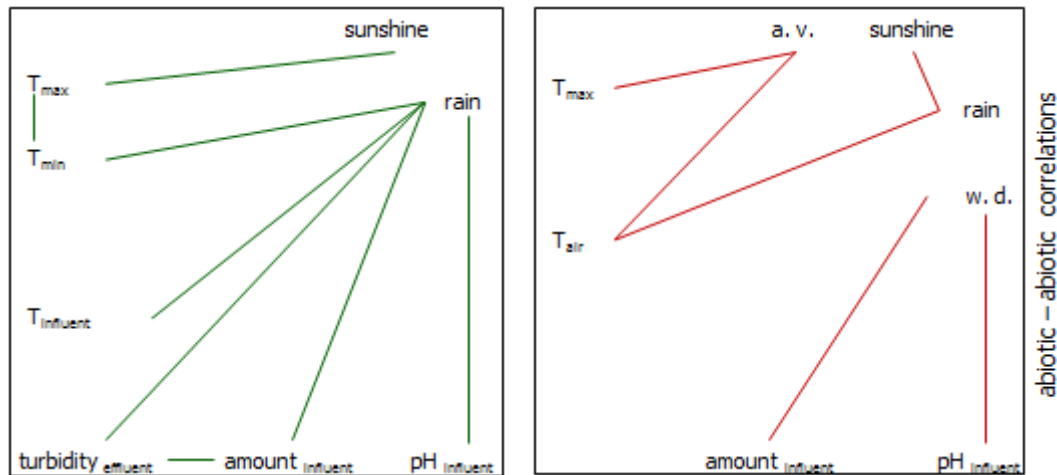
Figure 37. General abiotic correlations found for WWTP Eilenburg during a warm and dry sampling period (positive correlations: green, left side, negative: red, right side). Only correlations with r_S values higher than 0.4 or lower than -0.4 were included. T: temperature, a. v.: air velocity, w. d.: week day, max.: maximum, min.: minimum

In the following, main correlations of abiotic and biotic data at the three sampling points are shown. Correlations between the sampling points, for instance between the PC and the ATs, are not shown.

Primary clarifier

Complex correlation patterns were found in the Primary Clarifier). Figure 38 shows some of those positive and negative correlations, drawing a complex network between abiotic and biotic datasets.

Most of the correlations found for the PC were either abiotic-abiotic (e.g. rain and COD or NH_4-N and TC) or biotic-abiotic (e.g. Tc stained cells and week day or nitrate/nitrite content with cells that contained neutral lipid like substances). Only a few correlations between biotic parameters (sub-communities) were present. Sub-community III (gates highlighted in black) changed the cell number concurrently with the Tc stained (= polyP) cells. The sub-communities in the grey gates (VII and VIII) behaved reciprocally to polyP cells, whereas cell abundances in the white gates showed no correlation with polyP cells. Brewery discharge positively correlated with the cell numbers of sub-communities V, VI and VII and negatively with: II, X and XI.
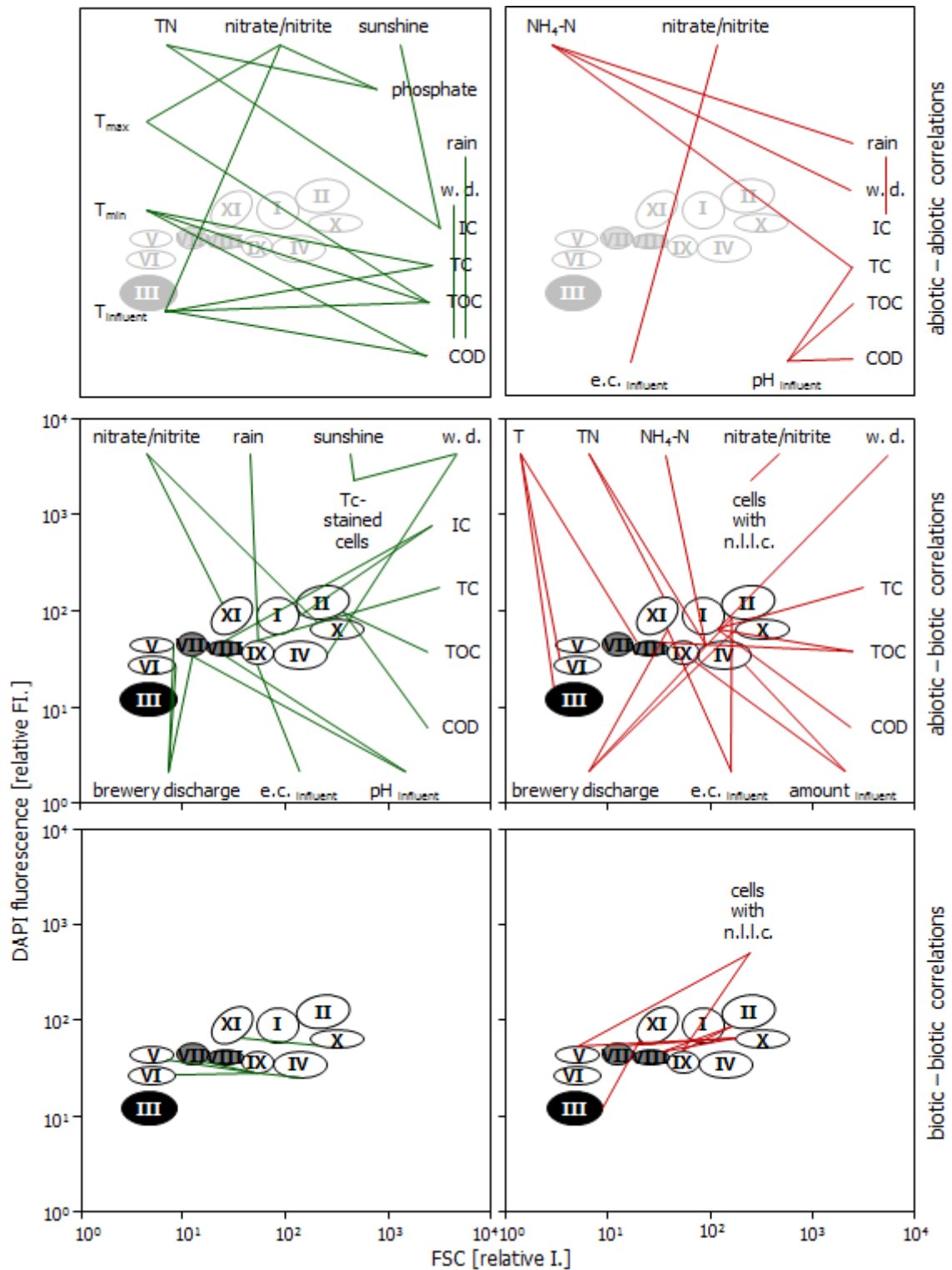
Figure 38. Positive (green, left side) and negative (red, right side) correlations in the PC. Only correlations with r_S values higher than 0.4 or lower than -0.4 were included. Ellipses mark the gates of sub-communities found during the 29 days of sampling (dot plots in Annex V, a). Filled black ellipses indicate sub-communities that showed a positive correlation with the PAO content and grey filled ellipses a negative correlation with the PAO content. T: temperature, WW: wastewater, IC: inorganic carbon, TOC: total organic carbon, TC: total carbon, COD: chemical oxygen demand, TN: total nitrogen, NH$_4$-N: ammonia-nitrogen, n. l. l. c.: neutral lipid like compounds, max.: maximum, min.: minimum, e.c.: electrical conductivity, w. d.: week day

Aeration tank 1 and 2

Correlations between the kind of inflow were also found in the Aeration Tank 1 (AT 1, Figure 39). For instance the inflow of blackwater had a negative correlation with TN and redox-potential whereas the latter correlated positively with brewery discharge (Figure 39, abiotic - abiotic correlations). As could be expected, strong positive correlations were found between the different measured modi of temperature and the N-species as well as humidity and rain thus verifying the sensitivity of the used correlation approach.

In the abiotic-biotic correlations, the influence of the kind of wastewater could also be detected. For example the influx of blackwater went along with increasing abundances of cells in sub-communities 1 and 6. In contrast, the influx of the brewery discharge coincided with increased abundances in gates 4 and 8. Negative correlation were found for the sub-communities in gates 1, 5, 13, and cells containing neutral lipid like compounds for brewery discharge and the sub-communities in gates 4, 9 and polyP cells for the blackwater inflow. These gates have thus a diagnostic value for the wastewater type and are defined as index-gates in the following. The concentration of Inorganic Carbon (IC) was found to correlate with abundances of cells in gates 7, 14, and 15 whereas high nitrate and nitrite concentrations went along with high abundances of polyP cells. Interestingly, rainfall went along with reduced abundances in gates 2, 3, 5, 7, 13, 15, whereas the cell abundances in gate 4 were increased. Other parameters positively correlated with cell abundances in certain gates were temperature and redox potential whereas negative correlations prevailed for other parameters like Total Organic Carbon (TOC), and Total Nitrogen (TN, all correlations shown in Annex VI, additional with the Monte Carlo permutation values).

In contrast to the primary clarifier there were many biotic-biotic correlations between the fifteen sub-communities. Interestingly the sub-communities which positively correlated with the amount of Tc stained cells (black filled gates) showed positive correlations only among each other and sub-community 10 whereas their counterparts in grey filled gates correlated with many other sub-communities.

Most of the correlations present in AT 1 were also present in AT 2. This was not surprising since the similarity analyses in Figure 31 (p. 55) stated a significant similarity between abiotic and biotic parameter measured in AT 1 and 2.
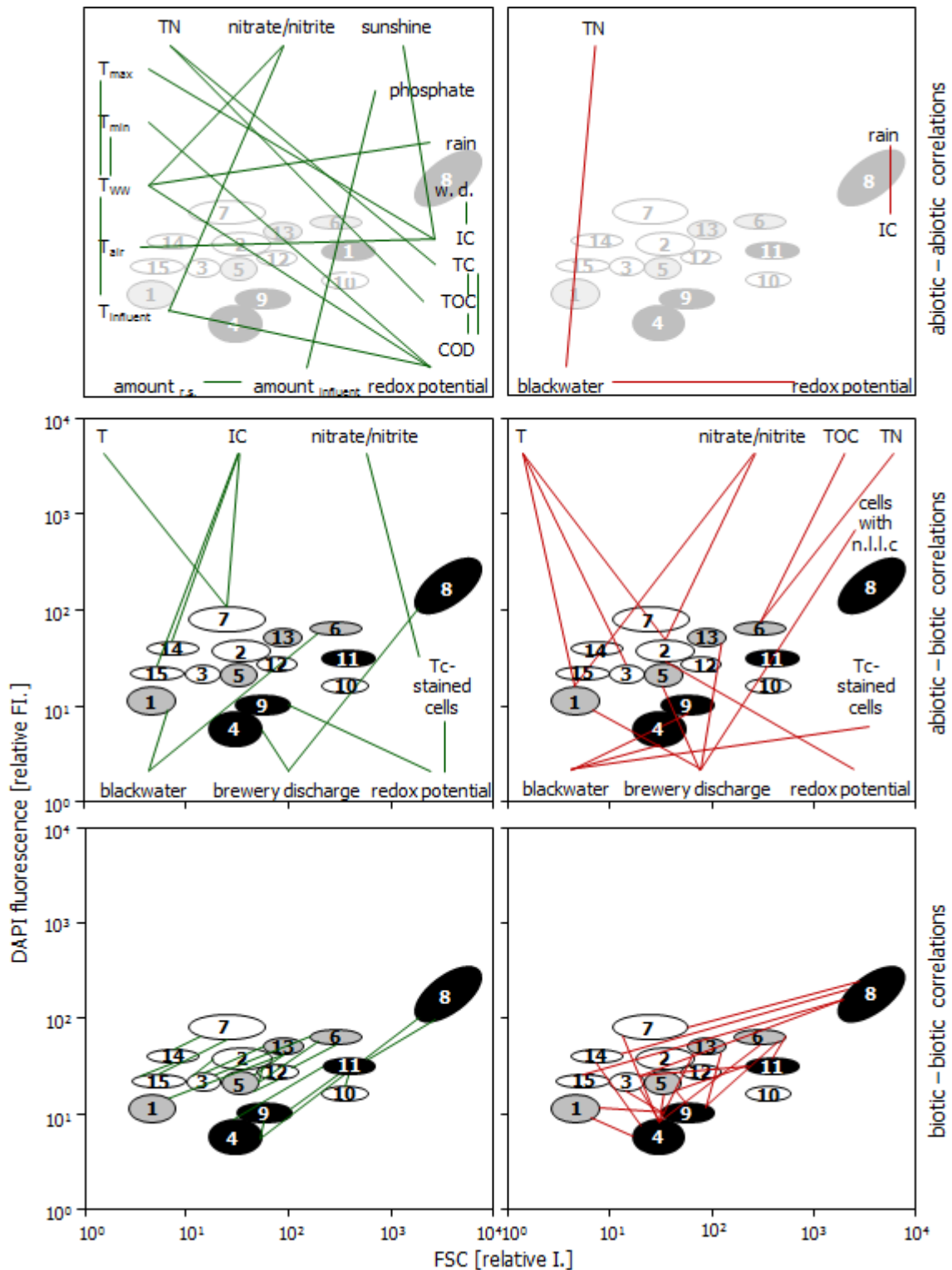
Figure 39. Positive (green, left side) and negative (red, right side) correlations in the AT 1. Only correlations with r_S values higher than 0.4 or lower than -0.4 were included. Ellipses mark the gates of sub-communities found during the 29 days of sampling (dot plots in Annex V, b). Filled black ellipses mark sub-communities that showed a positive correlation with the PAO content and grey filled ellipses a negative correlation with the PAO content. T: temperature, WW: wastewater, IC: inorganic carbon, TOC: total organic carbon, TC: total carbon, COD: chemical oxygen demand, TN: total nitrogen, Tc: tetracycline hydrochloride, n. l. l. c.: neutral lipid like compounds, max.: maximum, min.: minimum, amount $_{r.s.}$: amount return sludge (reused sludge from the secondary clarifier 1), w. d.: week day
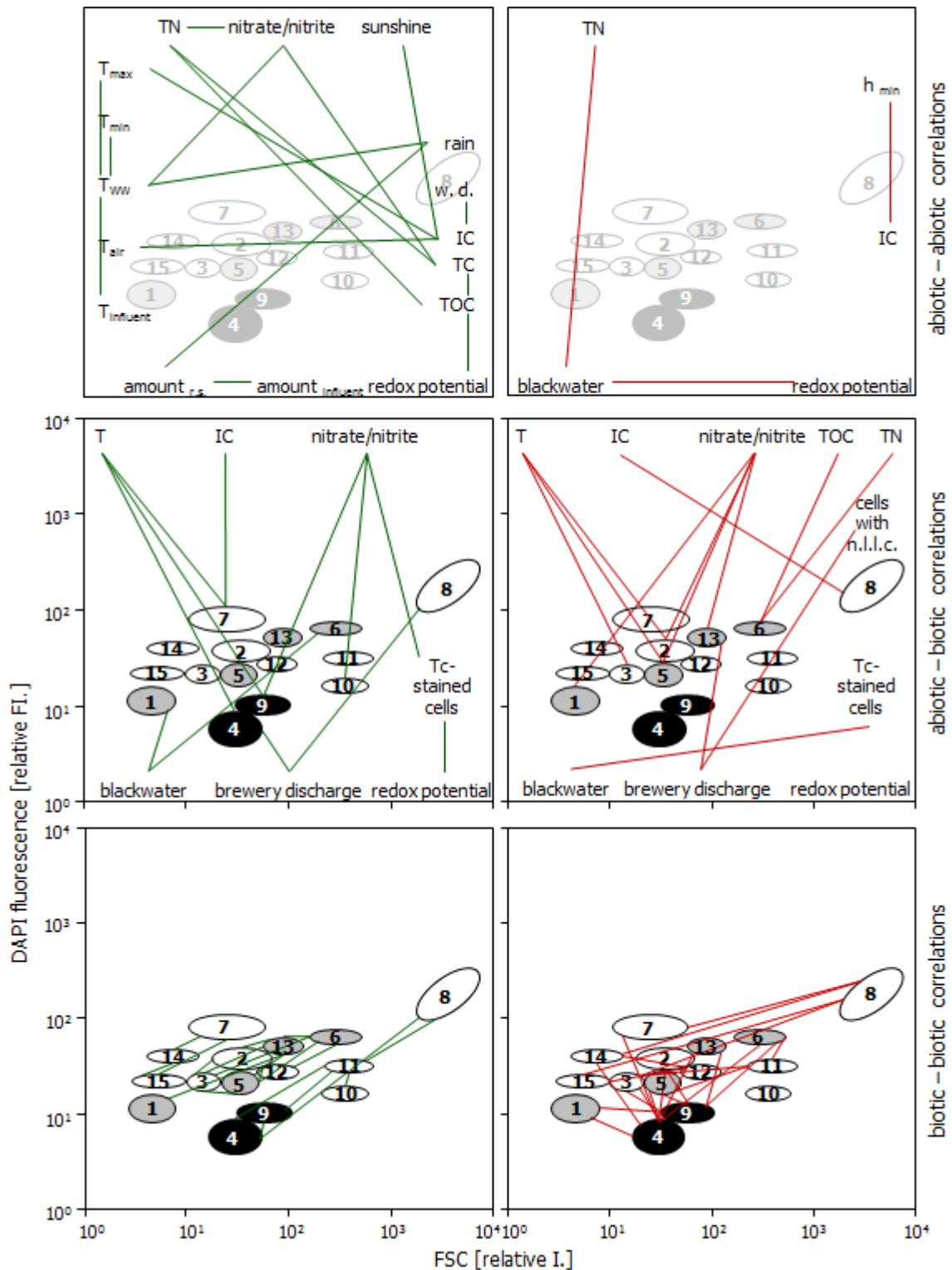
Figure 40. Positive (green, left side) and negative (red, right side) correlations in the AT 2. Only correlations with r_S values higher than 0.4 or lower than -0.4 were included. Ellipses mark the gates of sub-communities found during the 29 days of sampling (dot plots in Annex V, c). Filled black ellipses mark sub-communities that showed a positive correlation with the PAO content and grey filled ellipses a negative correlation with the PAO content. T: temperature, WW: wastewater, IC: inorganic carbon, TOC: total organic carbon, TC: total carbon, TN: total nitrogen, h.: humidity, Tc: tetracycline hydrochloride, n. l. l. c.: neutral lipid like compounds, max.: maximum, min.: minimum, amount $_{r.s.}$: amount return sludge (reused sludge from the secondary clarifier 2), w. d.: week day

Discussion

1. Fixation

Proper fixation of samples for subsequent analysis is crucial for the validity of experiments carried out with fixed specimens. Owing to the history of fixation there are a multitude of fixatives in existence for all kinds of tissues [HOPWOOD, 1969; SRINIVASAN *et al.*, 2002] and cell types [MOLLENHAUER, 1959; TREILHOU-LAHILLE *et al.*, 1981; SRINIVASAN *et al.*, 2002; VOGT *et al.*, 2005].

For microbial cells the most widely used fixatives are alcohols or aldehydes, although they are not appropriate for fixation of some species. For instance ethanol fixation of cells from the anaerobic bacterium *Desulfobacula toluolica* induces massive cell destruction [VOGT *et al.*, 2005]. In addition to this, they frequently cause cell aggregation and enhanced autofluorescense. Whereas these shortcomings may not hinder microscopical observation to a great extent, they can cause many severe problems in flow cytometric analysis.

To avoid these problems, new fixation procedures specifically designed for flow cytometric analysis and the specimen of interest are a necessity.

Flow cytometry is a quick and reliable tool for single cell analysis and able to provide information on the physiology of bacteria [MÜLLER, 2007]. Due to that, it was used here to test the fixation efficiency of various metal solutions based on the cell's DNA. Cell cycle activities and other cell related properties such as cell size and sideward light scatter behaviour were followed and used for differentiation between active and dead (fixed) cells. The leading criterion was that fixed samples should maintain their sub-population pattern distribution with regard to the above-mentioned parameters, while unfixed samples were expected to undergo changes.

For the development of a fixation procedure compatible with the demands of flow cytometric measurements the fixation effects of seven metal salts (aluminium, barium, bismuth, cobalt, molybdenum, nickel, and tungsten) on the sample stability of quickly growing microbial populations / communities cultivated under anaerobic or aerobic conditions and harvested from the early exponential phase were investigated.

Under natural conditions most of the tested metals are needed in nanomolar concentrations as trace elements. Their transport into the cell is mainly driven by constitutively expressed uptake systems for divalent cations with a rather broad specificity, but specific and high affinity uptake systems have also been reported (e.g. uptake of nickel in *Alcaligenes eutrophus*; [NIES *et al.*, 1992]). Since the uptake systems are constitutively expressed, it is not possible for the cells to avoid uptake of high metal concentrations.

For most of the metals the mechanisms of action is currently unknown, but nevertheless they are used as potent inhibitors of anaerobic respiration and/or metabolic pathways [PRINS *et al.*, 1980; TAKAHASHI *et al.*, 1989; THOMAS *et al.*, 1998; CUCCI and SIERACKI, 2001; BOGAN *et al.*, 2004]. The metals are reported to act against components of the cell envelope and to interfere with cell division, energy and general metabolism (cell growth and substrate utilisation). Table 9 gives a referenced overview of how the tested metals act on cells.

Table 9. Metals and their action on microbial cells as reported in literature. [1] STRATTON *et al.*, 1999; [2] ZHANG *et al.*, 2006; [3] DOMENICO *et al.*, 1996; [4] MARTIN, 1986; [5] GUTTERIDGE 1985; [6] WOOD, 1995; [7] ILLMER and ERLEBACH, 2003; [8] AMONETTE *et al.*, 2003; [9] BOGAN *et al.*, 2004; [10] CRAWFORD *et al.*, 1974; [11] SUZUKI *et al.*, 1978; [12] THEODOTOU *et al.*, 1976; [13] MCKILLEN and SPENCER, 1970; [14] PRINS *et al.*, 1980; [15] WILSON and BANDURSKI, 1958; [16] CARR and FERGUSON, 1990; [17] PALMIERI and KLINGENBERG, 1967; [18] PETERSEN, 1977; [19] SELL, 2001; [20] SELL, 2004; [21] BOSWELL *et al.*, 1998; [22] LOMBRANA *et al.*, 1993; [23] SAI RAM *et al.*, 2000; [24] SIGEE and AL-RABAEE, 1986; [25] DENG *et al.*, 1989; [26] JOHNSON *et al.*, 1974; [27] TAKAHASHI *et al.*, 1989; [28] KELLY *et al.*, 2004; [29] INTERNATIONAL PROGRAMME ON CHEMICAL SAFETY, 1990

	cell envelope	cell division	general metabolism	energy metabolism	respiratory chain	sulphate reduction	nitrate reduction	methano-genesis
Al	+ [5, 7, 8]	+ [6, 7, 8]	+ [8]	+ [4, 7, 8]				
Ba		+ [29]	+ [29]					
Bi	+ [1]	+ [3]	+ [2]	+ [3]			+ [9]	
Co		+ [10, 12]		+ [11]				+ [23]
Mo	+ [13]		+ [9]			+ [9]		
Ni	+ [21, 24]	+ [24]	+ [22]	+ [28]		+ [23]		+ [23]
W			+ [14]				+ [14, 24, 26, 27]	
NaN$_3$				+ [17, 18]	+ [19, 20]		+ [16, 18]	

To rate the fixation efficiency equivalence testing of the flow cytometric data sets was used because it is able to prove the stability of the multivariate samples over time (see Material and Methods, section 8.1, 22-24). A firm 25% and a much stricter 10% tolerance interval were used to judge fixation efficiency. These tolerance intervals were applied to every sub-population or sub-community of every data point, detecting changes that might not be easily optical discernible from sole data analysis. Figure 41 is a good example for this.
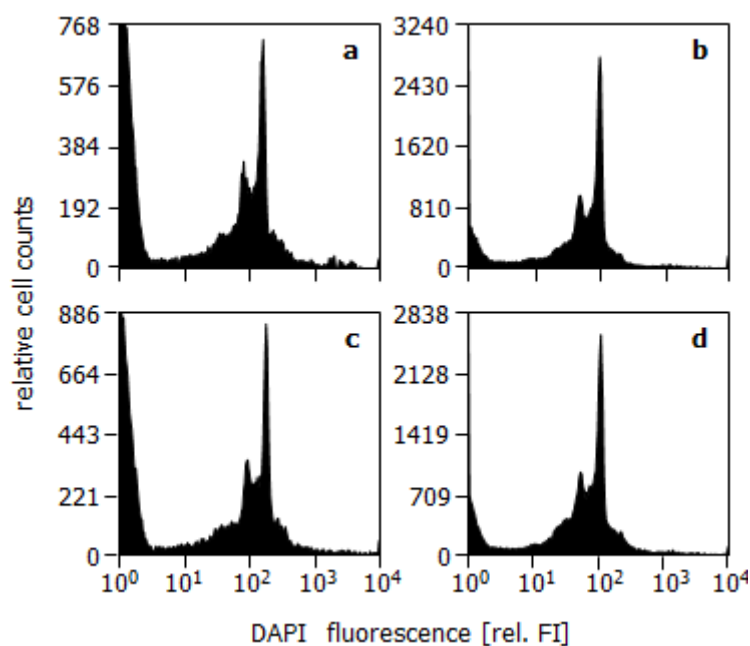
Figure 41. Histograms of *Shewanella putrefaciens* cells treated either with a 10% solution of sodium azide with 5 mM molybdate (a, b) or 5 mM bismuth (c, d). DAPI stained cells were measured after 1 (a, c) and 7 (b, d) days.

The histograms show cells of *Shewanella putrefaciens* either treated with a solution of 5 mM molybdate in 10% sodium azide (a and b) or with 5 mM bismuth (c and d) in 10% sodium azide solution. The cells were measured after 1 and 7 days with DAPI staining prior to measurement.

Optically the histograms do not seem to differ very much, but the statistical analysis via equivalence tests showed that they differed significantly. Cells of *Shewanella putrefaciens* that were treated with molybdate had only 2 out of 5 sub-populations that were still within the 25% tolerance interval (1/5 within the 10% tolerance interval) whereas cells treated with bismuth had 5 out of 5 sub-populations within the 25% tolerance interval (3/5 within the 10% tolerance interval). Therefore the fixation with bismuth was rated more stable than with molybdate.

Another important fact is that although the applied classification allows the judgement if one sub-population or sub-community is stable or not, it gives no direct quantification of the changes (see Figure 42). When the changes from the reference sub-population / sub-community (Figure 42, 0 d) are within the 25% tolerance interval, the sub-population / sub-community (Figure 42, 1 d) is regarded as *stable* (Figure 42, bars a and b) otherwise as *unstable* (Figure 42, bars c and d).
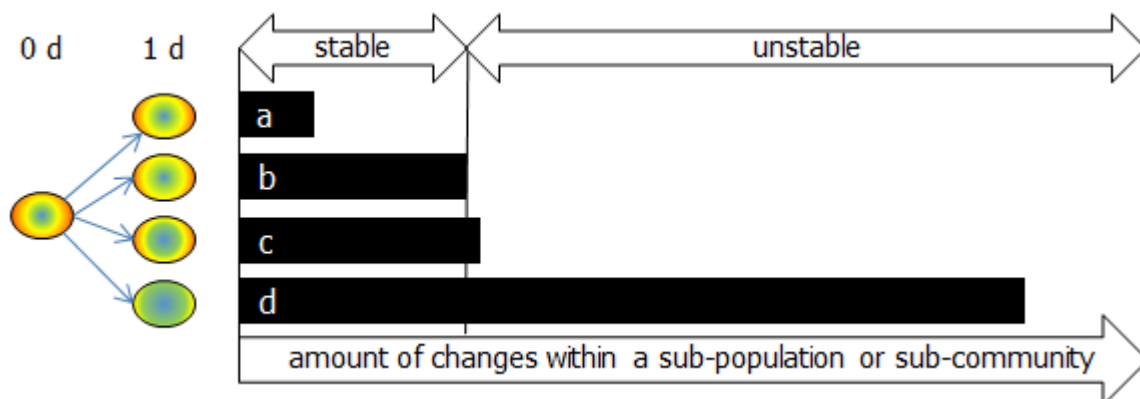
Figure 42. Schematic drawing of the stability judgment method using equivalence tests. Bars a to d represent the possible changes of one gated sub-population (in a pure culture) or sub-community (in a mixed culture) with various degrees of changes from the original sub-population / sub-community. The original sub-population / sub-community is termed 0 d, the altered 1 d.

1.1 Fixation of pure cultures

As can be seen from the results section 1.1 (Table 6, p. 36) not all metal-azide solutions were suited for fixation of the tested microbial cultures. The fixative effects of the metals and their possible action on the test microorganisms are discussed below.

Aluminium: Illmer and Erlebach (2003) list various effects of aluminium on microorganisms. According to them aluminium ions are able to chelate important ions like phosphorous, bind to cell walls or membranes causing structural und functional losses, adhere to enzymes or their substrates. Furthermore, aluminium is described to substitute magnesium in enzyme complexes and adhere to DNA and ATP molecules. In *Arthrobacter* sp. it is described to cause inhibition of cell growth and malfunction of osmoregulation at a concentration rage of 30 to 90 µM [Illmer and Erlebach, 2003].

However, a 5 mM concentration of aluminium salts in a 10% sodium azide solution did not result in fixation of some but not all sub-populations found within the tested pure cultures. It is important here to differentiate between growth inhibition measured by optical density or cell counts and changes in the sub-population ratios. Cells within a culture may stop cell division and therefore appear to be stable, but changes in the DNA dependant sub-population pattern distribution nevertheless indicate cell cycle activities. So aluminium may show inhibitory effects on the increase in cell density / cell numbers but not on the overall stability of the DNA pattern.

Barium: Most convincing results were obtained by treatment of the pure cultures with barium salt in sodium azide solution. Barium is described to cause a decrease in enzyme formation, and inhibiting dehydrogenases and lipolytic enzyme activity [INTERNATIONAL PROGRAMME ON CHEMICAL SAFETY, 1990]. Barium salts were also shown to be antagonistic to K^+ and Ca^{2+} concentrations and to cause loss of polyribosomes [BALDI *et al.*, 1996] as well as a reduction in the amount of monoribosomes [REISNER *et al.*, 1975]. Even though full broad-band activity was not observed, 5 species (*Desulfovibrio desulfuricans*, *Shewanella putrefaciens Paracoccus denitrificans* (anaerobic grown), *Methanomonas methylovora* and *Methanosarcina barkeri*) were susceptible to barium salt fixation and showed good stability over 7 days of fixation. For unknown reasons aerobic grown *Paracoccus denitrificans* showed a limited stability after fixation. This might be due to a resistance, although there is currently no reference in literature on this.

Bismuth: Bismuth salt, which showed a sufficient fixation only for the iron reducer *Shewanella putrefaciens*, has been reported to interfere with iron transport due to similar electronic valence. This antagonism to iron via non-specific competitive interference leads to iron starvation of cells [DOMENICO *et al.*, 1996]. In addition to the iron antagonism, bismuth salt also exhibits a high affinity for thiol groups. This affinity leads to interference with iron-sulphur centres of enzymes involved in ATP synthesis (F_1-ATPase) and therefore to energy depletion of cells [DOMENICO *et al.*, 1996]. STRATTON *et al.* (1999) reported increased cell permeability after bismuth treatment due to disruption of the glycocalix cell wall structure via displacement of divalent cations (Mg^{2+}, Ca^{2+}).

Cobalt: Cobalt is described by CRAWFORD and colleagues 1974 to inhibit cell division of *E. coli* cells and induce the formation of elongated cells. This is in accordance with the results obtained in this study, because the flow cytometric data showed significant changes in the sub-population ratios of all test strains. Inhibition of cell division is not similar to inhibition of DNA synthesis and so the formation of elongated cells lead to an increased amount of DNA molecules within one cell. So since the addition of cobalt did not result in stable sub-population pattern distribution it is not suited for fixation.

Molybdenum: Molybdenum salt, in contrast to tungsten, obviously stimulates growth of *Paracoccus denitrificans* (anaerobically grown) instead of having a fixative effect as has been suggested by COLE *et al.* (1986). This is because moybdenum is an essential component of several enzymes of this organism (for instance nitrogenase and nitrate reductase).

An opposite effect is found in the sulphate reducer *Desulfovibrio desulfuricans,* which was readily fixed with molybdenum salt, known to be a useful inhibitor of sulphate reduction [YADAV and ARCHER, 1989] although the mode of action is still not clear. It was stated that molybdenum leads to irreversible cleavage of ATP (molybdolysis, [MCKILLEN and SPENCER, 1970]), which prevents enzymatic activation of sulphate [WILSON and BANDURSKI, 1958]. According to literasture, there is also a competitive transport of molybdenum, sulphate and thiosulfate, preventing the accumulation of sulphate in the cells [MCKILLEN and SPENCER, 1970].

Nickel: Next to barium, nickel salt was the second best fixative. The literature lists several possible modes of action: Membrane permeabilisation, growth inhibition due to inhibited peptide synthesis (nickel nitrate, [BOSWELL *et al.*, 1998]), and plasmolysis (nickel chloride, [SIGEE and AL-RABAEE, 1986]) were common reactions of nickel treated cells. Occasionally such cell destruction as indicated by cell debris was noticed. However, changed cell morphology as described by some authors could not be observed. It may be speculated that the PBS buffer used for dissolving the metal salt enhanced the osmotic stability of the cells. According to SAI RAM *et al.* (2000) nickel chloride salt also causes an overall inhibition of anaerobic degradation processes due to inhibited H_2 uptake and hindered acetate/propionate utilization. Anaerobic processes most affected are described to be methane production and sulphate reduction. The inhibition of sulphate reducers was confirmed in our experiments, because *Desulfovibrio desulfuricans* was successfully fixed. Good fixation was also observed for *Shewanella putrefaciens*, *Paracoccus denitrificans* (aerobic grown) and *Methanomonas methylovora*.

Tungsten: Another metallic compound partly suited for fixation was tungsten salt. This compound acts homologous to molybdenum salt, which is commonly found as a constituent of enzymes involved in redox-reactions [JOHNSON *et al.*, 1974]. Because of chemical similarity, tungsten is able to replace molybdenum in the active sites of molybdenum enzymes, causing enzyme inactivation, and a deregulation of gene expression of structural genes in higher plants [DENG *et al.*, 1989]. Enzymes containing molybdenum as a cofactor are widespread in nature, including xanthine oxidase, formate oxidase, sulphite oxidase and the nitrate reductase needed for denitrification. Although KAJIKAWA *et al.* (2003) did not find general inhibition of methane oxidation by tungsten salts, in our experiment the compound evidently inhibited the methylotrophic bacterium *Methanomonas methylovora*. Also, the denitrifying strain *Paracoccus denitrificans* (aerobically and anaerobically grown) was inhibited which is in accordance with results of PRINS *et al.* (1980).

Sodium azide: Sodium azide is a known inhibitor of the terminal enzyme of the respiratory chain (cytochrome c oxidase, complex IV). This, in addition to the osmotic effects of the concentrated salt solution, is normally sufficient for fixation of aerobic bacteria. So it was to be expected that the sodium azide solution showed no fixative effect on the anaerobic sulphate reducer *Desulfovibrio desulfuricans*. Surprisingly, the 10% sodium azide solution had also only a low fixative effect on the other tested strains.

In almost all strains some sub-populations remained stable whilst others changed. For all strains (the anaerobic sulphate reducer *Desulfovibrio desulfuricans* excluded) it was the sub-population with 2 chromosome equivalents (abundances varying between 27 and 88% of all DAPI stained cells) and in 2 strains additionally the sub-population with 4 chromosome equivalents that showed *stable* fixation with sodium azide. This indicates a different susceptibility of the sub-populations towards the sodium azide solution. Since sodium azide acts on the respiratory chain and not, as some of the tested metals, on enzymes within the cell, some of the enzymes (which were not inhibited by the high osmolality) might have been still functional. Functional enzymes, not expressed in all of the sub-populations, may have led to the changes that were detected by flow cytometric measurements.

Other than that, the reasons for the low overall efficiency might also be partly explained by the following findings of other authors. Some *Escherichia coli* mutants are reported to exhibit an azide tolerance due to enhanced expression of the inducible cytochrome a_2, which makes the cells insensitive towards azide [ARIMA and OKA, 1965]. Furthermore, *Paracoccus denitrificans* was shown by CALDER *et al.* (1980) to grow in the presence of azide when cultivated under low oxygen conditions. Presence of 0.1 mM sodium azide in these cultures induced not only a higher amount of cytochrome b but also an increased expression of nitrate reductase.

Since genes for metal resistance are wide spread in nature and have so far been found on plasmids of every eubacterial group tested and in some species on the chromosome as well [SILVER *et al.*, 1996] the ineffectiveness of some metals against the used test species might be due to the expression of resistance genes. Most of these genes encode for proteins either used for efflux pumping or enzymatic detoxification. Resistances against the two most promising metals barium and nickel have been found in isolates of nearly every ecosystem; including WWTPs. FILALI *et al.* (2000) tested pure culture isolates from sewage samples for barium resistance and found minimal inhibitory concentrations ranging between 0.16-0.32 mM. Especially in environments with high metal contents most of the bacteria show broad band resistance against many metals. Pure cultures isolated by ABOU-SHANAB *et al.* (2007) from soil with high nickel content exhibited resistance against nickel to a high extent. At a concentration of 5 mM only 7% of the 45 isolated pure cultures were susceptible. A complete inhibition of all strains was found for concentrations higher than 20 mM. In addition to the probability of resistance genes there are mutants in existence with e.g. altered enzyme structures (for instance see ARIMA and OKA, 1965) that display insensitivity to otherwise effective antimicrobial agents.

For a specimen as diverse as activated sludge, it seemed most promising to test a combination of metals. So prior to testing the fixation of activated sludge samples, a 5 mM (each) solution of bismuth, nickel, barium supplemented with 10% sodium azide as well as a 5 mM (each) solution of nickel, barium, and 10% sodium azide were tested on the microbial strains described above. The 5 mM solution of nickel, barium, and 10% sodium azide turned out to be most effective, allowing good fixation of *Desulfovibrio desulfuricans*, *Shewanella putrefaciens*, *Paracoccus denitrificans* (aerobic grown), *Methanomonas methylovora* and *Methanosarcina barkeri* as well as sufficient fixation of *Paracoccus denitrificans* (anaerobically grown) for at least 9 days.

1.2 Fixation of highly diverse cultures

After finding the most promising metal combination for a fixative suitable for flow cytometric measurements to be composed of barium and nickel the combination was tested on highly diverse activated sludge samples in further variations.

Samples from wastewater treatment plants are known to tolerate higher metal concentrations than pure cultures isolated from activated sludge. This is due to trapping of the metals in the floc matrix, binding to extracellular polymers, metabolism, accumulation in dead organisms, and precipitation as sulphide complexes [KELLY *et al.*, 2004]. Toxicity towards activated sludge samples is additionally influenced by diverse factors such as the metal itself, soluble concentration, amount of suspended organic material, sludge age, concentration of other ions and bacterial community structure [BROWN and LESTER, 1979]. To reduce those negative effects on the fixation procedure, the cells have to be washed thoroughly and suspended at a rather low density within the fixative to assure that enough soluble metal ions are available for the fixation reaction.

Further strategies for enhanced fixation efficiency that were tested:

Detergent Tween 20: Detergents are known to accelerate the penetration of the fixatives through cell walls and membranes (HOPWOOD, 1985).The unexpectedly low stability of cells treated with mixtures of Ba, Ni (each 5 mM), 10 % sodium azide (in PBS) and 0.5 g L^{-1} Tween 20 may be explained by the observation that Tween 20 can used as a growth substrate by some species [IMPALLOMENI *et al.*, 2000]. Furthermore cell destruction by the detergent Tween 20 could also lead to changed sub-community patterns which indicate low fixation efficiency. Application of Tween 20 as detergent to facilitate fixation could consequently not be recommended for activated sludge samples.

Cryopreservation: Another approach chosen was freezing of the activated sludge. As cryopreservation in the absence of vitrifying solutions is reported to increase cell damage [THOMAS *et al.*, 1998] glycerine was added during freezing and thawing. However, cryopreservation turned out to be less suited for fixation purposes than for common freeze storage. Though only a minor amount of cell debris was detected after freezing, the cells were poorly preserved in terms of the fixation criteria.

Combination of metal salts: Samples of anaerobically and aerobically grown species and activated sludge as an example for highly diverse bacterial communities comprising nitrate reducers, iron reducers and various other anaerobic and aerobic bacteria were effectively fixed with a suspension of Ba and Ni salts (each 5 mM) and 10% sodium azide. Cell morphology as well as structural properties (DNA contents) of the cells and cell numbers in a community remained stable for at least 9 days, indicating successful fixation of the microbial consortium and their predators. For unknown reasons higher concentrations of the metal salts Ba and Ni did not result in more stable sub-community preservation. A possible explanation might be the precipitation of the salts due to the enhanced concentration.

With the combination of the metals barium and nickel in a 10% sodium azide solution a flow cytometric - compatible fixation protocol of activated sludge samples for subsequent analysis was established, providing a sound basis for all following experiments.

As could be shown, the effects of fixation and storage vary highly with the organism under investigation and the cell status. Therefore the fixation method in question should always be tested for suitability prior to any experiment. This is especially important, when the fixed samples are supposed to be subjected to further analysis after flow cytometric measurement (for instance the phylogenetic analysis of sorted cells). Although the combination of barium and nickel provides good fixation of microbial cultures it is not suited for samples which ought to be subjected to subsequent genetic analysis. This is mainly due to the effects of barium which, as already described above, influences the cellular ribosomal content. So, when in the following samples ought to be analysed genetically, they were fixed with sole 10% sodium azide solution and then processed further as soon as possible.

2. Evaluation of the tetracycline staining method

According to literature, most of the bacterial species that are thought to be responsible for the polyphosphate accumulation can still not be cultivated in pure cultures to date [KAWAHARASAKI *et al.*, 1999]. Monitoring of these organisms requires thus cultivation-independent techniques directed at specific characteristics such as the accumulated polyphosphate granules of PAOs. For the selective analysis of PAOs within complex communities, single cell-based methods like fluorescence microscopy and flow cytometry appear most appropriate. Particularly promising seems the detection of PAOs by flow cytometry in combination with cell sorting for further phylogenetic identification.

2.1 Comparison of the new and the traditional polyphosphate staining method

Polyphosphate granules were first identified in *Saccharomyces cerevisiae* in 1888 [LIEBERMANN, 1888]. Since then, the ability to store polyphosphates as granules within the cell was found to be widespread among microorganisms. Nowadays, polyphosphate accumulation is studied by bulk measurements like ^{31}P-NMR analysis [RÖSKE *et al.*, 1989] or even more frequently by quantifying the activity of the polyphosphate kinase (Ppk; [AULT-RICHE *et al.*, 1998]). Also, single cell approaches have been applied for a long time, examples being phase contrast or bright field microscopy. Neisser's staining and Loeffler's methylene blue techniques are the traditional non-fluorescent stains for microscopic analysis of PAOs [SERAFIM *et al.*, 2002]. Electron microscopic analysis made use of labelled antibodies to facilitate the detection of phosphate granules [SAITO *et al.*, 2005]. Another compound that is widely used to visualize polyphosphate granules is the fluorescent dye 4',6-DiAmidino-2-PhenylIndole (DAPI; [TIJSSEN *et al.*, 1982]), which stains cells with polyphosphate contents higher than 400 µmol g^{-1} dry weight when applied at a concentration of at least 18 µM (5 to 50 µg mL^{-1}; [STREICHAN *et al.*, 1990; KLAUTH *et al.*, 2006]). DAPI staining depends on a polyphosphate-mediated metachromatic reaction which causes a shift in the emitted fluorescence from blue to a bright yellow-green (λ_{ex}: 360 nm, λ_{em}: 515 nm; [KLAUTH *et al.*, 2006]). When DAPI is applied at lower concentrations (0.24 to 5 µM), the resulting blue fluorescence is related to bacterial DNA (λ_{ex}: 360 nm, λ_{em}: 465 nm; [KLAUTH *et al.*, 2006]). Unfortunately, also unspecific fluorescence of other cellular constituents like lipids was reported when DAPI was applied at high concentrations (180 µM; [STREICHAN *et al.*, 1990]). This unspecific fluorescence is reported to fade after a short time of microscopic observation, but may constitute nevertheless a severe problem for the flow cytometric analysis, since the analysis (i.e. the decision if the cell exhibits a bright green fluorescence or not) is much faster. Another, but not commonly used fluorescent dye is 9-AminoAcridine (9-AA), which has similar properties like DAPI as it emits blue fluorescence when binding to DNA and green fluorescence when binding to polyphosphate granules [KULAEV and KULAKOVSKAYA, 2000].

A few applications of flow cytometry to determine polyphosphate granules have been reported. They involved DAPI alone [ZILLES *et al.*, 2002a] or in combination with fluorescence in situ hybridization (FISH; [KAWAHARASAKI *et al.*, 1999]).

However, the aforementioned un-specific DAPI staining may spoil somehow the quantitative and possibly even the qualitative determination of PAOs in natural communities. Therefore a new staining technique, relying on tetracycline hydrochloride was established in this study.

The fluorescent antibiotic tetracycline (Tc) and its derivatives are frequently used in medicine as a label for calcium deposition in bone or teeth and as a marker for membrane-associated divalent cations [HALLET *et al.*, 1972]. Although several mechanisms have been discussed, the binding mode is still unclear (for review see NELSON, 1998). When Tc is bound to diamagnetic divalent cations such as calcium and magnesium, its fluorescence intensity is enhanced with excitation and emission maxima at 390 nm and 515 nm, respectively (at pH 7.5, [LEE *et al.*, 2003]). Using this effect, it was assumed that it is possible to stain polyphosphate granules for the quantitative determination of polyphosphate granules in individual bacterial cells, since they contain among others the divalent cations calcium and magnesium as counter ions.

The new *in vivo* Tc staining method was tested against the traditional DAPI method and found to be comparable in terms of the numbers of labelled cells and the fluorescence intensities of their phosphate granules. However, the Tc stain proved to be superior to the DAPI stain in flow cytometric analysis due to a 15 times lower unspecific background labelling. This was regardless of the fact that the Tc fluorescence originates from the strong chelation of divalent cations, which are not only present in polyphosphate granules but also at considerable amounts in the cell wall, protein complexes and in the cytoplasm [CHANG *et al.*, 1986; SMITH, 1995].

A very important advantage of Tc as opposed to DAPI staining of polyphosphate was the possibility to combine it with DNA analysis. Staining of the bacterial DNA gives information on bacterial growth rates [MÜLLER, 2007; PAWELCZYK *et al.*, 2008] and therefore on activity states of PAOs when analysed in combination with Tc. DAPI staining alone of both DNA and polyphosphate granules did not result in a reliable analysis of the two characteristics as was shown for cells of *M. phosphovorus*. However, the dual stain with Tc and DAPI proved to be a quantitative method for PAO detection and DNA content analysis.

2.2 Calibration of the staining method and fluorescence spectra of tetracycline

Binding of tetracycline hydrochloride to polyphosphate granules inside living cells of *M. phosphovorus* and an activated sludge community was found to be very stable within the observed time span. Although 8 different classes of efflux genes [SPEER *et al.*, 1992] and 29 resistance genes [CHOPRA and ROBERTS, 2001] have been described in various strains to protect the cells against the action of Tc, no sign of efflux could be found at a concentration of 0.225 mM over a time range of 180 minutes in living cells of pure and mixed culture

It is known from literature that Tc molecules strongly chelate with divalent cations. This allows them to enter various bacterial species driven by the cells' Donnan potential across the outer membrane that acts on the cations [CHOPRA and ROBERTS, 2001]. In the periplasm the amphoteric Tc molecules are then liberated and diffuse in the cytoplasm, where they probably bind to the cations neutralizing the negative charge of the polyphosphate granules (Figure 43).
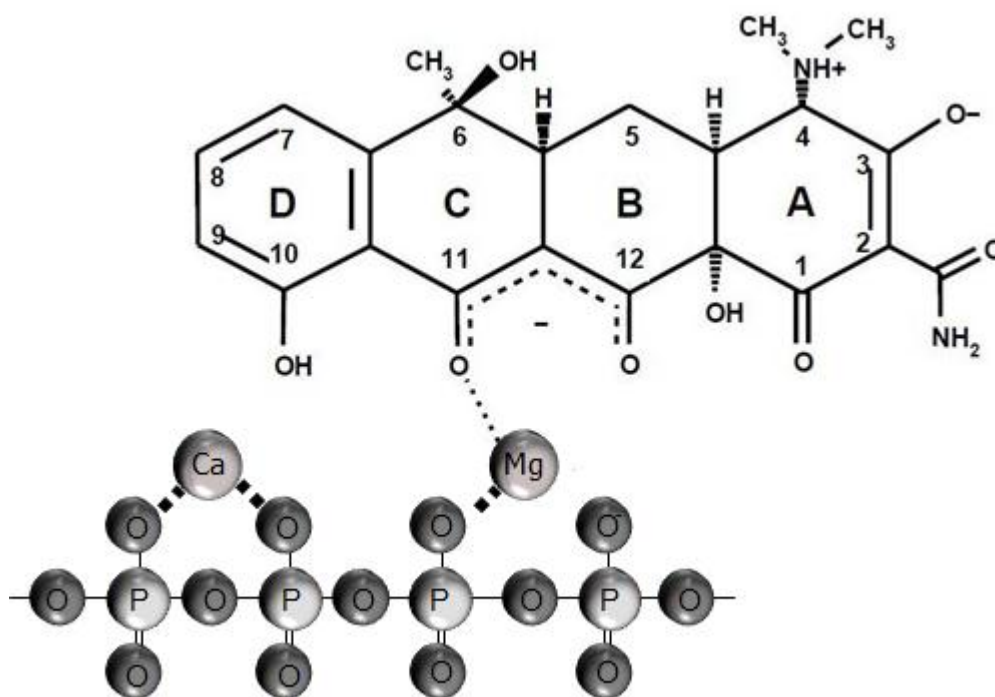
Figure 43. Possible mechanism for Tc binding to the polyphosphate granules.

Tetracycline hydrochloride from the two suppliers Fluka (LOT 1164780) and Roth (LOT 419110229) was used in this study. Both had mostly similar properties according to their certificate of analysis, only differing slightly in the following points: color (Fluka: light yellow, Roth: yellow), purity (Fluka: 97.1%, Roth: 96.8%), specific rotation (Fluka: -247°, Roth: -246°), and pH (Fluka: 2.3, Roth: 2.5). As could be expected, both showed for most of the experiments similar excitation and emission properties in terms of the location and the height of the respective maxima, which were in accordance with the literature [LEE et al., 2003]. The fluorescence intensities varied with the solvent (2 to 5 times higher fluorescence emission in PBS than in water) and were highest in the presence of calcium ions (about 7 times higher than in sole PBS). In contrast to solutions without added calcium (λ_{ex}: ~410 nm, λ_{em}: ~525 nm) the presence of metal ions resulted in the formation of a second excitation peak in the UV region (λ_{ex}: 340 nm, λ_{em}: 520 nm).

Surprisingly, the analysis of stained, polyphosphate carrying cells of *Acinetobacter calcoaceticus* 69-V revealed differences between the tetracyclines from Fluka and Roth. Although the same cell culture was used for the experiment, the fluorescence intensities obtained by application of Tc_{Roth} were generally higher than those of Tc_{Fluka} and only Tc_{Roth} showed the formation of a second excitation peak. This excitation peak was located around 445 nm with emission at 530 nm.

The unexpected variation of the tetracyclines from the two manufacturers in stained cell suspensions cannot be easily explained by the listed differences from the certificate of analysis. It can only be speculated that the purity values could eventually explain the differences. A widely known and often found decomposition product of tetracycline hydrochloride is the so called anhydrotetracycline. This anhydrotetracycline has, when bound to calcium ions, an excitation maximum at 460 nm and corresponding emission at 530 nm (solvent: 50% chloroform in absolute ethanol at an approximate concentration of 1×10^{-4} M; [STOEL *et al.*, 1976]), which is fairly close to the second peak observed in cells stained with Tc_{Roth} (λ_{ex}: 445 nm, λ_{em}: 530 nm, solvent: PBS). Additionally, tetracycline is a product obtained by *Streptomyces* species and not synthesized chemically. It is known by several other applications of similar substances that such natural products can consist of several nearly similar derivatives as is known e.g. for nystatin with differing parts of the biological active components of nystatin A1, A2, and A3 [MCGUIRE, 2000].

To determine the fluorescence properties of the stained polyphosphate granules within the cells, a stained cell suspension consisting of cells without granules was also measured and the resulting spectrum subtracted from one derived from stained, polyphosphate carrying cells. The resulting difference-spectrum showed an excitation maximum at 470 nm and the corresponding emission at 520 nm. At these wavelengths the argon-ion laser (emission at 488 nm) and the optical filters used here in flow cytometric analysis are ideally suited for measurement of cells containing polyphosphate granules.

Excitation at 488 nm was also confirmed when the fluorescence emission of Tc_{Roth} at different excitation wavelengths was recorded. The bathochromic shift of the tetracycline fluorescence after binding to the polyphosphate granules to these wavelengths is probably due to a metachromatic reaction, but this is only a speculation.

In all experiments with polyphosphate carrying cells of *Acinetobacter calcoaceticus* 69-V unfixed cells emitted higher fluorescence intensities than fixed cells. As stated by literature, tetracycline molecules enter the cell by diffusion through the membrane and by an energy dependent transport [SPEER *et al.*, 1992]. Therefore the failure of the energy dependent transport or the changed microenvironment within the cell could be responsible for the observed variance in tetracycline fluorescence.

As a result, the fluorescence properties of tetracycline hydrochloride should be tested on polyphosphate carrying cells for every new LOT to ensure comparable measurements.

2.3 Controls to verify specific and quantitative staining

The specificity for polyphosphate granules was tested with known polyphosphate accumulating bacteria like *M. phosphovorus, Paracoccus* sp. and *Pseudomonas* sp. serving as positive controls as well as against a non-phosphate accumulating strain of *E. coli* , the glycogen producing strain *M. glycogenica* Lg2^T and a strongly PHB-accumulating strain of *M. rhodesianum* serving as negative controls. All of the negative controls showed nearly no background staining with Tc neither with microscopic observation nor flow cytometric measurement, whereas the positive controls exhibited bright green fluorescent granules.

Tetracycline is therefore considered to be highly specific for polyphosphate granules inside PAOs. Even spores of *Bacillus subtilis*, used as a further negative control and known to contain a considerable amount of divalent cations showed only a very slight background staining.

2.4 Verification of the method by phylogenetic analysis

The results of 16S rRNA gene sequencing verified the specificity of the tetracycline staining technique as the clone library generated from separated Tc stained cells displayed a rather low diversity and was basically composed of phylotypes known as PAOs such as the 'Candidatus Accumulibacter'-like phylotype, members of the genus *Pseudomonas* and the *Tetrasphaera*-related actinobacteria. Although the clone library probably does not reflect the complete phylogenetic spectrum present in the sorted gate of highly green fluorescent cells, as indicated by several unique clones, its composition confirms that predominantly PAOs were captured. Moreover, T-RFLP profiles revealed the predominance of a single phylotype belonging to the genus *Pseudomonas*. Surprisingly, this phylotype was only the second most one in the clone library, but T-RFLP profiles recorded with three different restriction enzymes clearly showed the predominance of this sequence type. This bias might be explained by the low coverage of the clone library that led to an underestimation of the *Pseudomonas* sequence type. On the other hand, the relative T-RF peak areas might overestimate the relative abundances of the corresponding phylotypes, as sequence types with restriction sites outside the 35-650 bp thresholds are not considered and therefore not included in the total peak area. Nevertheless, sequencing and T-RFLP profiling of 16S rRNA genes verified that PAOs were specifically detected and captured out of a complex community.

Thus, the staining approach using tetracycline in combination with high-throughput techniques like T-RFLP fingerprinting enables the quick and reliable detection and quantification of distinct PAO groups. In contrast to the FISH technique, it can also detect PAOs of not yet known phylogenetic affiliation without the drawbacks common for the traditional DAPI staining method. The staining procedure for polyphosphate granules using tetracycline hydrochloride is easy to perform, quick and cultivation-independent.

Since DAPI as well as Tc are inexpensive dyes that do not change the features of the cells and can be applied quickly and without complicated sample handling, they are ideally suited for analysis of community dynamics with special regard to the PAOs present in the system.

3. Application experiments

Determination and quantification of PAOs in highly diverse bacterial communities such as activated sludge is of high interest because of the need for improved, reliable phosphorus removal from domestic wastewater. First, the methods developed in this study were used to follow polyphosphate accumulation within a bioreactor where abiotic conditions were controlled and changeable. Abiotic conditions were altered to induce an increase or decrease the number of polyP accumulating organisms within the bioreactor. Second, the techniques were used to determine abundances and phylogenetic affiliation of polyP accumulating organisms directly in the WWTP Eilenburg. The cell by cell measurements using flow cytometry allowed a quantitative investigation of all, mostly unknown and uncultivable, microbial members [MÜLLER and NEBE-VON-CARON, 2010].

Community dynamics were analysed based on DNA-related DAPI staining of microbial cells. Due to their individual, cell cycle stage dependant DNA content the cells bind different amounts of the blue fluorescent dye DAPI and cluster cells with similar properties (not necessarily cells of the same species) in sub-communities. Owing to this clustering of cells into sub-communities, they produce a fingerprint like pattern of the microbial community where changes in abiotic parameters tend to induce altered patterns. The alterations can be a changed position of sub-communities within the dot plot, increase or decrease of cells within the sub-community, the presence of new or the absence of sub-communities. Each microbial community, like for instance activated sludge, comprises a unique sub-community pattern that changes according to the kind and strength of external influence.

3.1 Activated sludge bench top bioreactor experiments

The bioreactor experiments were the first practical test for the combined dual-staining technique. The cultivation dependant community dynamics and the PAO abundances were followed under various conditions. Over the 32 days of sampling 19 sub-communities could be distinguished within the DAPI fluorescence / FSC patterns, a few of them apparently comprising PAOs (Figure 29, p. 53).

Despite the high orthophosphate concentration in the medium the amount of polyphosphate accumulating organisms in the bioreactor experiments was quite low when compared with values usually obtained from WWTPs. Only three sub-communities showed high amounts of polyP containing cells under aerobic conditions and most of them had high DAPI fluorescence intensities. This was also the case for most of the PAOs that did not cluster to distinct sub-communities. The overall amount of PAOs in the bench top bioreactor was between 0.29 and 0.46% when 56.95 mg L^{-1} orthophosphate were added. However, if under stationary carbon concentration the amount of orthophosphate was increased to 75.7 mg L^{-1} the number of polyP bearing microorganisms increased in their relative abundance 2.2 fold. With regard to this, it was interesting to observe that the increase in orthophosphate concentration and the accumulation of polyP did not change the community structure. Albeit the changed substrate and phosphate concentration the number of cells in the three clusters with the highest amount of Tc stained cells stayed relatively constant (Figure 30, p. 54).

Apart from the substrate induced community changes the sub-community patterns remained stable regardless of the aerobic and anaerobic cultivation modes within the bioreactor. This behaviour seems to be typical for activated sludge communities, as previously shown by bulk single-strand conformation polymorphism analysis [ZHAO *et al.*, 2008]. In contrast to the phosphate concentration, the doubled substrate concentration had a high influence and changed the structure of the community, as was seen by altered abundances in the 19 sub-communities. It is known that high community diversity is a prerequisite for high resilience, as diverse communities can flexibly react to environmental fluctuations because of the ecological complementarity of functionally redundant groups. This has been demonstrated particularly in wastewater and activated sludge communities [KINDAICHI *et al.*, 2004, REID *et al.*, 2008].

It is subject of speculation why the amount of PAOs in this system is that low in spite of the favourable external conditions (aerobic − anaerobic shifts, high orthophosphate concentration, and presence of carbon sources in the anaerobic phase). An explanation might be the existence of so called Glycogen Accumulating Organisms (GAOs) within the system. Both, the PAOs and the GAOs, are described in literature to use intracellular stored polymers (polyP or glycogen) as source of energy for the storage of polyhydroxyalcanoates in the anaerobic stage which are then in the subsequent aerobic stage used as growth substrate. On the assumption that both groups are already present in the system, this could be an explanation. The GAOs are more active under conditions with low phosphate concentrations in the feed whereas the PAOs are active when there is excess of phosphate [LIU *et al.*, 1997].

Elevated carbon levels in the feed resulted in massive changes in the community structure, but only to a slight increase in the PAO containing sub-community. Hence, it can be concluded, that in the investigated bioreactor system the availability of phosphorous was more important for the establishment of PAO activity than the increase in carbon concentration.

3.2 Activated sludge community dynamics in the WWTP Eilenburg

Supporting biological polyP accumulation to promote fertilizer production is going to be of growing importance for WWTP operators. Another already important task is to guaranty wastewater clearing with high reliability and quality. Unfortunately, many WWTPs occasionally suffer serious breakdowns with reasons often unknown [BLACKALL *et al.*, 2002]. Models developed in the past to control WWTPs probably failed mainly because the modelling parameters used were obtained from pure culture and artificial reactor schemes [WENTZEL *et al.*, 1989, PETERSEN *et al.*, 2002]. Therefore, new monitoring tools for reliable process control of the complex and particular WWTP systems need to be developed and, additionally, they should be cheap and quick for routine application.

3.2.1 Comparability of the three sampling points

To get a first idea of the whole WWTP system and the conditions therein, the focus in the following section is on the abiotic parameters characterizing the three sampling points at the WWTP Eilenburg.

A comparison of the main abiotic parameters showed that the primary clarifier (PC), were the incoming wastewater is initially treated, is with the exception of only two abiotic parameter, completely different from the next step in the wastewater treatment process: the aeration tanks (AT 1 and 2; Figure 31, p. 55 and Annex IV). For instance the values for phosphate and ammonia-nitrogen in the PC are higher whereas the concentrations of diverse carbon species are lower. The differences in the phosphate content are probably due to the uptake by organisms in the activated sludge for growth processes, biosorption and polyphosphate storage. Ammonia-nitrogen, produced by hydrolysis from nitrogen containing sewage (urea and faecal matter) during transport of the raw wastewater through the sewers, is eliminated by the action of nitrifying bacteria present in the activated sludge community inhabiting the aeration tanks.

A higher content of diverse carbon species in the aeration tanks than in the primary clarifier might at first seem controversial to the role of the aeration tanks: the degradation and elimination of organic compounds from the wastewater. However, biosorption of suspended organic compounds to the biomass (single bacteria as well as flocs) is a well described, quick process in wastewater treatment plants [FUJIE et al., 1997]. It is important for the carbon removal capacity of the WWTP and enables the compensation of fluctuating carbon concentrations. Since the concentration of biomass is many times higher in the aeration tanks than it is in the PC, reversible biosorption might be an explanation for the increased carbon values (desorption of pre-sorbed organic matter during sample preparation) and also leading to an increased value of total nitrogen. According to GUELLIL et al. (2001) three types of organic matter play a role in the biosorption process: particulate (45%, of total COD), colloidal (31%) and soluble (24%). The soluble fraction is slowly transported and incorporated into the flocs and usually irreversibly bound to the biomass, whereas there is a bidirectional, reversible transfer between the flocs and colloidal or even particulate organic matter. The biosorption capacity of activated sludge is described to vary to a great extend 40 to 100 mg COD per g dried sludge, depending on the amount of activated sludge present in the system.

An n-MDS analysis of abiotic and biotic data sets obtained from the three sampling points PC, AT 1 and AT 2 showed significant differences between the different stages of wastewater treatment as well (Figure 31, p. 55). Due to the differences in abiotic and operational conditions, the biotic parameters (i.e. community pattern) were different between the PC and the ATs (see below). In addition to this, it was interesting to find, that there were abiotic (e.g. redox potential) as well as biotic (community stability, see Figure 32, p. 56) differences between the two aeration tanks, which are, apart from the oxygen regime, operated identically. This might be caused by minor differences in the abiotic parameters or parameter not covered by this study. Another explanation might be a slightly different community structure which is not directly reflected by the flow cytometric community pattern.

In the following sections the focus will mainly be on the biotic parameters and their interaction with the abiotic ones.

3.2.2 Sub-community stability at the three sampling points

As already stated above, the DAPI stained microbial community comprises individual sub-communities that cluster according to their DNA content and forward scatter. These sub-communities react to changes in the surrounding environment and are therefore useful biosensors in pure cultures and in multispecies systems (as an example see Bᴏᴍʙᴀᴄʜ *et al.*, 2011). In this study the community structure was analysed flow cytometrically for judgement of process stability. Stability of the microbial community in the process stages following the treatment in the primary clarifier is presumed to be the main precondition for the stability of the phosphorous removal within the wastewater treatment process. Some authors have stated that changes in the community composition had serious influences on the EBPR and WWTP performance [for instance see Wᴀɢɴᴇʀ and Lᴏʏ, 2002; Oᴋᴜɴᴜᴋɪ *et al.*, 2004; Gɪᴄʜ *et al.*, 2000]. Others found, that the microbial composition had only a minor effect on the overall WWTP stability [see for instance Wᴀɴɢ *et al.*, 2010]. In general the community structure in the investigated WWTP was, like the bioreactor system, found to be very stable for a system which exists under highly variant environmental conditions. All sub-communities at all three sampling points found initially remained present during the sampling period of 29 days although varying in cell number (Figure 33, p. 57). Nevertheless the small and swift changes in community dynamics in a WWTP system were successfully monitored using the fingerprint like sub-community patterns. The primary clarifier clearly differed from the two aeration tanks being more prone to changes in sub-community abundances (just 3 sub-communities with a stability over 50% compared to 7 sub-communities in the aeration tanks) due to its position in the WWTP operation process. The wastewater only remains about 30 minutes in the PC and is then treated further in the aeration tanks (see Material and Methods, section 1.2.3, p. 14). This short time span and the resulting quick changes in wastewater composition probably impair the formation of stable microbial communities in the PC.

3.2.3 Taxonomic affiliation of WWTP organisms

In general, the structure of WWTP communities varies with type of influent and WWTP operation [Wᴀɢɴᴇʀ and Lᴏʏ, 2002; Gɪᴄʜ *et al.*, 2000]. In this study the flow cytometric analysis of the community pattern was the first step towards the investigation of the microbial community within the WWTP Eilenburg. More detailed information on the individual sub-communities was gained using phylogenetic information derived of sorted cells (Figure 34, p. 59). Consequently, cell sorting of main sub-communities (= gates in the Figure 34) was performed and combined with phylogenetic T-RFLP analysis of separated cells resulting in information on potential function and substantiating the cytometric analyses. Organisms within the gates 1, 6, 4, 8 were well-known WWTP phylotypes like *Rhodocyclaceae, Burkholderiales, Chloreflexi,* and *Comamonadaceae*. The gate 8 was clearly different from the others comprising mainly *Chloroflexi* and TM7 (with 8.6 % of all clones in the clone library and a typical member of wastewater communities, [Hᴜɢᴇɴʜᴏʟᴛᴢ *et al.*, 2001]). The main organisms found in the combined approach were *Rhodocyclaceae, Burkholderiales* and *Comamonadaceae*. These groups are well described members of wastewater communities [Mᴜʟʟᴀɴ *et al.*, 2002; Zɪʟʟᴇs *et al.*, 2002b; Sᴘʀɪɴɢ *et al.*, 2005].

3.2.4 Polyphosphate accumulating organisms in the WWTP

Since the focus of this study is on the dynamics of polyphosphate accumulating organisms cellular polyP was also cytometrically analyzed and gave information on active cellular phosphate accumulation [GÜNTHER *et al.*, 2009]. As can be seen from the pure culture in Figure 16 (p. 42), of all cells containing the PolyPhosphate Kinase gene (*ppk*) only a few started to accumulate the polymer. The reason for this heterogeneity is still unknown although the phenomenon of cell heterogeneity even in clonal cultures is well described [MÜLLER *et al.*, 2010].

However, the abundance of polyP accumulating cells was exceptionally high (up to 25%, Figure 36) in this WWTP, whereas the average amount of PAOs within a WWTP system is around 4-13% [MEHLIG, 2010]. The variation between the sampling points was high and most prominent between the primary clarifier and the aeration tanks. This is probably because the initial stage of biologic wastewater treatment, the primary clarifier, is subjected to highly variable conditions (e.g. substrate composition, temperature and pH). A lower variance was present between the aeration tanks because they are operated identically. Differences here are caused by minor differences in the community composition, or abiotic parameters like the aeration efficiency.

Using cell sorting the polyP containing cells were found to belong to *Rhodocyclaceae* and *Chloroflexi* which cover sub-groups able to synthesize polyP [KAWAHARASAKI *et al.*, 2002; ZILLES *et al.*, 2002a]. Regarding the fact that *Chloroflexi* are photosynthetic bacteria which can be metabolically active under both oxic and anoxic conditions in WWTPs [MIURA *et al.*, 2007] this affiliation might be reasonable although the peak confirmation with HaeIII was missing. Especially the *Rhodocyclaceae* can be defined as marker organisms for a good polyP accumulation in the studied WWTP and stand for a good EBPR process regime. Their involvement in polyP accumulation is well described [BLACKALL *et al.*, 2002; KAWAHARASAKI *et al.*, 2002; ZILLES *et al.*, 2002a] and their presence confirmed with both restriction enzymes in this study.

3.2.5 Correlation of biotic and abiotic data sets

In order to find the reasons for shifts within the microbial community or altered functions like polyphosphate accumulation abiotic and biotic data sets were correlated.

Various correlations were found to exist between abiotic and biotic parameters (Figure 44, as well as Annex VII).

Most of the abiotic correlations served as a kind of positive control for the overall strategy. For instance, the positive correlation of the amount of sunshine with the temperature, or the negative correlation of the amount of rain with sunshine.
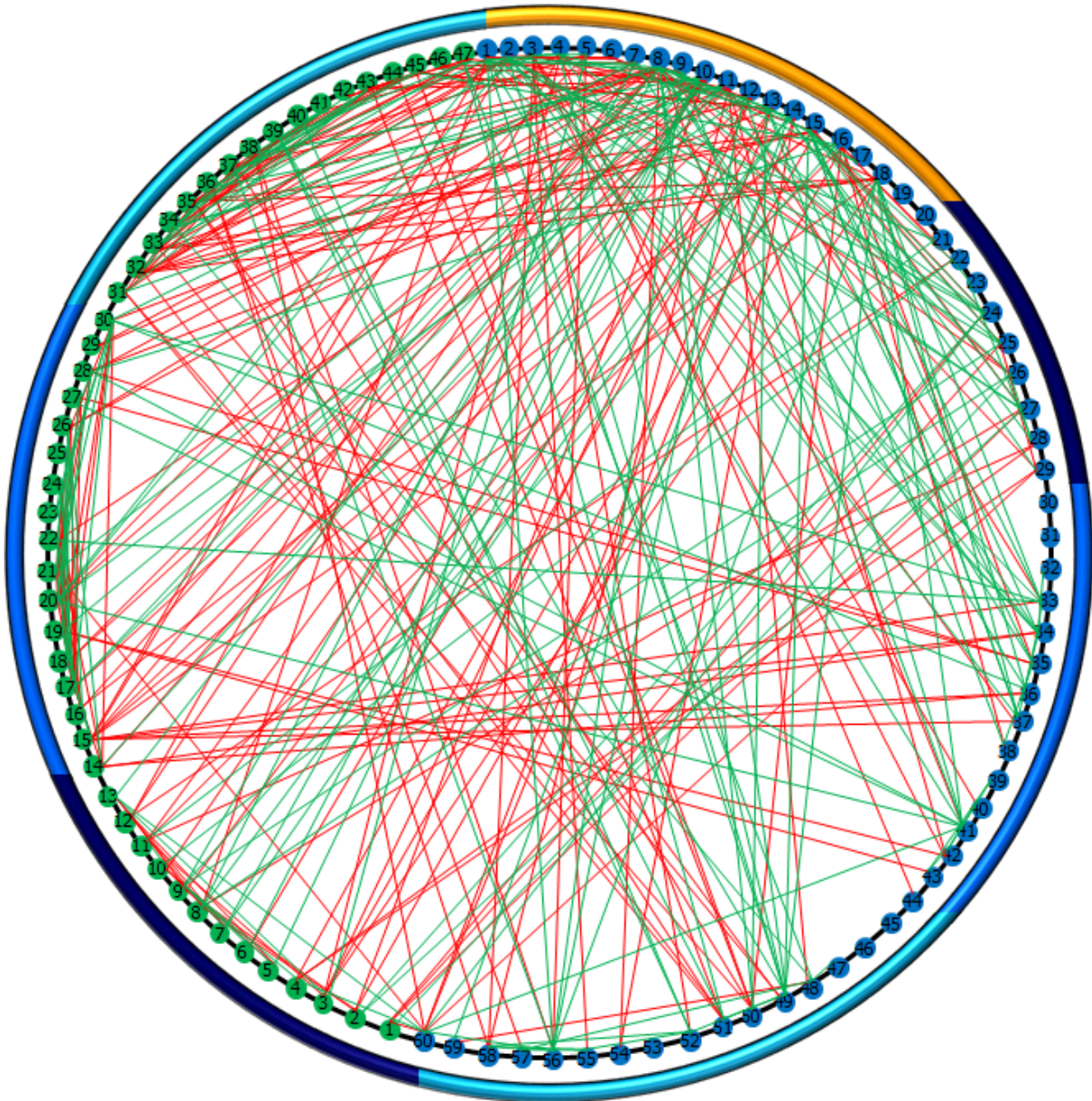
Figure 44. Correlations between abiotic and biotic parameters within the WWTP Eilenburg. Positive (green lines) and negative (red lines) correlations between abiotic (blue dots) and biotic (green dots) parameter measured in the PC (dark blue), AT 1 (blue) and AT 2 (light blue) as well as weather data and parameter obtained from the WWTP Eilenburg (orange). Numbers in the circles correspond to those in Annex IV.

Some of the correlations, which appeared most important, will be discussed in the following. First, the kind of the carbon source seems to severely influence the community structure and composition. The strong positive correlation of cell abundances in certain gates clearly points to dependences between sub-community manifestation (denoted as index-gates) and kind of substrate inflow as is obvious for blackwater or brewery discharge inflow. The composition of blackwater is known to be subjected to large variations in e.g. the COD values [VAN VOORTHUIZEN *et al.*, 2008]. These values are described to be higher for brewery discharges [BRITO *et al.*, 2008], and also acidifying emissions might play a role here. In the bioreactor experiment it was shown that carbon quantities change cell abundances in certain sub-communities.

Here in the WWTP, it could be observed that not only quantities but also the quality of the substrates led to specific changes in community structure, and this could be documented in an industrial process nearly on-line.

In addition, polyP accumulation was found to be positively correlated to the presence of nitrite and nitrate. Nitrate is known to reduce the polyP granule release into sludge [Schön et al., 1993]. Nitrate can also serve as electron acceptor under anaerobic conditions and is involved in anaerobic polyP accumulation [Meinhold et al., 1999]. This is supported by Tsuneda and colleagues (2005) describing Denitrifying PolyP Accumulating Organisms (DPAO) which can utilize both oxygen and nitrite/nitrate as electron acceptors. They identified a nirS fragment sequence which showed high similarities to sequences of *Thauera mechernichensis* and *Azoarcus tolulyticus* which belong to the *Rhodocyclus* group. *Rhodocyclaceae* comprised a large part of the AT 1 community in our WWTP according both to the clone library and the T-RFLP analysis and was found to be one of the two major groups of the tetracycline stained polyP containing cells.

After the bioreactor experiments it was quite unexpected that oxygen did not support the aerobic PAOs abundance but high nitrite concentrations at about 8 mg NO_2-N L^{-1} were described to inhibit phosphate uptake into PAOs and, at the same time, might allow DPAOs to accumulate phosphate [Rowe et al., 1979; Meinhold et al., 1999]. Also, the quick and successive change of the aerobic and anaerobic process regime in the WWTP (see description in Material and Methods, section 1.2.3) might support facultative anaerobic organisms such as the DPAOs which were also described by other authors to overtake a large amount of EBPR additional to denitrification [Meinhold et al., 1999, Shoji et al., 2003].

Other positive correlations are obvious by IC positively acting on cell abundances in gate 7. T-RFs directing to the betaproteobacteria *Burkholderiales* and the *Sphingobacteriales* were found in this gate. Since the betaproteobacteria comprise chemolithotrophic members they might be the correlating partners [Dworkin et al., 2006]. The redox potential correlated positively to the PAO abundances due to the decreased release of polyP when it is increasing - a process which was already described earlier [Schön et al., 1993]. Rain fall caused a decrease in cell abundances in many sub-communities probably because of wastewater dilution. The available datasets obtained in the study are most extensive and not all correlation information can be shown here.

As an outcome, certain sub-community index-gates mirrored bioprocess schedules such as substrate inflow. Also, functional information can be drawn as was shown by the observation that the main polyP accumulation was presumably driven by DPAOs instead of PAOs in this WWTP. New techniques like pyro-sequencing are also able to resolve microbial communities on a high level. However, those approaches are still PCR based techniques with limited quantitative information and, more importantly, they are highly expensive especially if dynamics need to be analysed [Newton et al., 2011].

Therefore, the new approach present in this study has several advantages. It

- analyses microbial community dynamics quickly in a high-through-put manner and with high statistical reliability (about 250,000 cells per sample),
- allows phylogenetic affiliation of the sub-communities in index-gates thus leading to information about the main (potential) biochemical capacities,
- allows additional functional information using fluorescent techniques like the polyP staining without the need for double staining methods, and
- allows combination of abiotic parameter variations with performances of cells in emerging sub-communities.

Also worth to mention is that phylogenetic affiliation of index-gate organisms may become less and less important if increasing sample numbers of the same WWTP are analysed (as was shown to be possible using the Dalmatian-plot analysis: BOMBACH *et al.*, 2011).

Outlook

With data sets obtained from the WWTP over longer intervals it might be possible to construct an empirical, WWTP-specific, model for phosphate removal optimization. Although mechanistic models (e.g. the ASM-series) are considered more powerful since they allow extrapolation to a great extent, they require precise and accurate knowledge about the system and the processes involved [VANHOOREN *et al.*, 2003]. It is the opinion of this studys author, that it is feasible to use such models for the investigation and control of metabolic related questions in a WWTP, but the usefulness is doubtful with regard to the PAOs since so little is known about them. Despite great efforts they have evaded cultivation in pure cultures up to now and are therefore unavailable for further investigations needed for the development of reliable mechanistic models. The alternatives are empirical models, also often described as 'models based on experience' [LINDBLOOM *et al.*, 2005] are derived from actual measurements, treating the system in question as a black box system and using only measured parameters to describe and predict the system. According to HENZE and LOOSDRECHT (2008) empirical models are based on recognition of parameters essential to describe the process pattern and linking these by relationships based on observation. They are strictly WWTP specific due to different operational parameters, wastewater composition and bacterial community composition. A general modelling procedure based on 4 steps is given by THAM (2000) as follows:

1. collection of data

2. specify correlations by means of e.g. polynomials, time-series, artificial neural networks

3. maximise correlation for parameter of interest using a numerical technique

4. validation of the model against a different dataset

If the validation is not satisfactory, then step 2 is to be reconsidered. Special attention has to be paid to the reliability of the data used for these are the basis of the model.

Using flow cytometric analysis for measurement of single cell properties in combination with measurement of other important wastewater parameters and statistical analysis an empirical model could be developed as the next step to enhance and stabilize the phosphate removal capacity of the investigated WWTP.

Summary

It was the aim of this study to investigate the populationstructure and -dynamics of polyphophate accumulating organisms (PAOs) in a wastewater treatment plant (WWTP). PAOs are responsible for the removal of phosphate from the wastewater, which is necessary to prevent eutrophication of surface water systems. The phosphate is reversibly stored in the PAOs in form of osmotic inert polyphosphate granules which fulfill many functions within the cell. Despite several years of intense research, only little is known about the PAOs and the process of polyphosphate accumulation. Although the potential PAOs are known, the central problem remains that these organisms are up to date not cultivable in pure cultures and therefore not available for investigation. Owing to this, the process of phosphate elimination is still prone to failure and malfunctions.

To make the process of phosphate removal more reliable, better knowledge about the PAOs and their interaction with abiotic and biotic factors is needed. Towards this, many abiotic and biotic parameters were measured in this study. In addition to chemical measurement of samples from the communal WWTP Eilenburg, the cells in the WWTP samples were analyzed using flow cytometry, cell sorting and subsequent phylogenetic analysis.

As a first precondition for reliable measurements of population dynamics, a fixation procedure for activated sludge cells suitable for flow cytometric analyses was developed. Since WWTP samples comprise a highly heterogenic microbial community, a fixation method for all kinds of organisms was necessary. Existing fixation methods relying on the action of alcohols or aldehydes are known to cause problems when the cells are analyzed by flow cytometry (floc formation, increased autofluorescence, changes in scatter behaviour and dye uptake). Different metals were tested for their fixative effects on pure and mixed cultures in combination with the respiratory-chain-inhibitor sodium azide. A 5 mM combination of barium, nickel and 10% sodium azide yielded the highest fixative effects on all tested cultures, resulting in sample stability of at least 9 days. No interference with flow cytometric measurement could be observed.

The next step was the development of a new *in vivo* staining method for the polyphosphate granules within PAOs. Traditional fluorescent staining of the granules is done using DAPI (4',6-Diamidin-2-phenylindole). Using high concentrations of this dye, the granules emit green fluorescence when excited with ultra violet light. In addition to this, DAPI is used at low concentrations in this study for analysis of population dynamics. It binds to the cellular DNA which is then measured flow cytometrically. According to their individual DNA content the cells cluster into sub-communities comprised of cells with similar properties in cell size and DNA content. Those sub-communities form fingerprint-like pattern which allow the investigation of population dynamics. Since the analysis of both, DNA and polyphosphate content, with DAPI alone is not possible, a new staining technique for polyphosphate granules was needed.

The green fluorescent antibiotic tetracycline hydrochloride was found in this study to stain polyphosphate granules with high specificity. Various experiments were done to verify staining of PAOs with tetracycline. It could be shown that staining with tetracycline yielded results comparable to DAPI staining in terms of stained cell numbers and fluorescence intensities, but with reduced unspecific staining.

As an example, tetracycline stained cells from a WWTP sample (WWTP Elsterwerda) were sorted and their phylogenetic affiliation determined. Results showed that known PAOs related to `Candidatus Accumulibacter phosphatis´ were captured. In addition to this, a dual staining technique for simultaneous staining of polyphosphates (tetracycline) and DNA (DAPI) was established. This allows the quick, reliable and cheap analysis of PAO population dynamics.

Finally, population dynamics in a communal WWTP were investigated. For this, a multitude of abiotic and biotic parameters were measured and subjected to correlation analysis using Spearmans rank order correlation coefficient and Kendalls tau. A high number of positive and negative correlations were found between abiotic and biotic datasets indicating a complex network of relationships between the microorganisms and their environment. These correlations gave information about possible parameters influencing PAO abundance and population dynamics even without the necessity of a double staining. For example, the influent of discharge from a local brewery positively correlated with an increase in PAO abundances whereas inflow of blackwater correlated with a decrease in PAO abundances. Furthermore, the nitrate content was found to be positively correlated with the abundances of PAOs. This, and the results from the phylogenetic analysis of sorted (polyphosphate containing) cells, led to the conclusion that denitrifying PAOs are responsible for phosphate removal in the WWTP Eilenburg.

The methods developed in this study allow the quick and reliable investigation of wastewater communities and the PAOs therein. They enable the identification and observation of PAO population dynamics without the need for cultivation and are useful for the elucidation of abiotic and biotic parameters influencing PAO activity in a WWTP.

Zusammenfassung

Ziel der vorliegenden Arbeit war die Untersuchung von Populationsstruktur und -dynamiken von polyphosphatspeichernden Organismen (PAOs) in einer Kläranlage. PAOs entfernen das im Abwasser enthaltene Phosphat und verhindern damit eine Eutrophierung von Oberflächengewässern. Das dem Abwasser entzogene Phosphat wird reversibel, in osmotisch stabiler Form, als Polyphosphatgranula gespeichert. Trotz jahrelanger, intensiver Forschung ist bis heute nur wenig über die PAOs und den Prozess der Polyphosphatspeicherung bekannt. Die Hauptursache hierfür liegt in der Unkultivierbarkeit der PAOs. Der Mangel an Informationen führt dazu, dass der Prozess der biologischen Phosphatelimination noch immer sehr störanfällig und teilweise wenig effizient ist.

Um die biologische Phosphatelimination effizienter und besser kontrollierbar zu machen ist eine eingehendere Untersuchung der daran beteiligten Mikroorganismen und deren Zusammenwirken mit abiotischen und biotischen Faktoren nötig. Hierfür wurden neben der chemischen Analyse der Abwasserproben aus der Kläranlage Eilenburg auch die darin enthaltenen Mikroorganismen durchflusszytometrisch untersucht. Potentielle PAOs wurden dabei heraussortiert und identifiziert.

Eine wichtige Voraussetzung für genaue Messdaten ist die richtige Fixierung der Belebtschlammproben aus dem Abwasser. Dies ist besonders schwierig, da sich die Organismengemeinschaft im Belebtschlamm aus einer Vielzahl an Arten zusammensetzt. Bekannte Fixierungsmethoden, die auf der Wirkung von Alkohol oder Aldehyden basieren, verursachen häufig Probleme in der Durchflusszytometrie (Zellverklumpung, erhöhte Eigenfluoreszenz, veränderte Lichtstreuung und Farbstoffaufnahme). Deshalb ist es vor allem wichtig eine Fixierungsmethode zu finden, bei der keine Probleme für die Messung der Proben mit der Durchflusszytometrie entstehen. Hierfür wurde die Wirkung verschiedener Metalle auf Rein- und Mischkulturen in Kombination mit dem Atmungsketteninhibitor Natriumazid getestet.

Eine 5 mM Mischung aus Barium und Nickel in einer 10%igen Azidlösung erzielte dabei die besten Ergebnisse. Alle Mikroorganismen konnten für 9 Tage effektiv fixiert werden ohne dass es zu Problemen für die durchflusszytometrische Messung kam.

Der nächste Schritt war die Entwicklung einer neuen Färbetechnik für die Polyphosphatgranula.

Traditionell wird für die fluoreszenzbasierte Untersuchung von PAOs eine hochkonzentrierte DAPI-(4',6-Diamidin-2-phenylindol) Lösung verwendet. Eine Anregung im ultravioletten Bereich führt hierbei zu einer grünen Fluoreszenz der Granula. Im Rahmen dieser Studie wurde DAPI jedoch in geringerer Konzentration auch zur Messung des zellulären DNS-Gehaltes genutzt. Zellen mit ähnlicher Größe und Fluoreszenzintensität (d. h. DNS-Gehalt) werden dann in der durchflusszytometrischen Messung zu Sub-Communities zusammengefasst. Die Fingerabdruck-artigen Muster die dadurch entstehen, geben Auskunft über die Populationsdynamiken der Organismen im Belebtschlamm. Weil eine gleichzeitige Untersuchung von DNS- und Polyphosphatgehalt durch die Konzentrationsunterschiede in den Färbelösungen nicht möglich war, musste eine neue Färbetechnik für Polyphosphatgranula entwickelt werden. Hierfür wurden verschiedene Fluoreszenzfarbstoffe an polyphosphatspeichernden Reinkulturen getestet.

Eine spezifische Färbung von Polyphosphatgranula durch das grün fluoreszierende Antibiotikum Tetrazyklin konnte in dieser Arbeit nachgewiesen werden. Die Färbung von PAOs auf Basis von Tetrazyklin erzielte Ergebnisse, die mit der traditionellen DAPI-Färbung hinsichtlich Anzahl und Fluoreszenzintensität der gefärbten Zellen vergleichbar waren. Zusätzlich wurde eine geringere unspezifische Färbung von nicht-Polyphosphatgranula-haltigen Zellen mit Tetrazyklin beobachtet. Um die PAO-Spezifität der Färbung zu prüfen wurden Tetrazyklin-gefärbte Zellen einer Belebtschlammprobe der Kläranlage Elsterwerda heraussortiert und phylogenetisch untersucht. Die Untersuchungen ergaben, das vor allem bekannte PAOs wie "Candidatus Accumulibacter phosphatis" isoliert wurden. Weiterhin konnte gezeigt werden, dass eine Doppelfärbung von Zellen mit DAPI und Tetrazyklin möglich ist. Dies ermöglicht die schnelle, präzise und kostengünstige Untersuchung der PAO-Populationsdynamiken.

Abschließend wurden die entwickelten Methoden bei der Untersuchung einer kommunalen Kläranlage eingesetzt. Eine Vielzahl an abiotischen und biotischen Faktoren wurde dafür gemessen und Korrelationsanalysen nach Spearman und Kendall unterzogen. Als Ergebnis dieser Analysen wurden viele positive und negative Korrelationen zwischen abiotischen und biotischen Faktoren gefunden. Dies zeigt deutlich die Komplexität der Beziehungen von Mikroorganismen untereinander und mit ihrer Umwelt. Faktoren welche die Anzahl und damit die Populationsdynamiken der PAOs beeinflussten konnten damit sogar ohne Doppelfärbung sichtbar gemacht werden. So korrelierte die Einleitung von Brauereiabwasser positiv mit der PAO-Anzahl, während Fäkalieneinleitung eine negative Korrelation zur Folge hatte. Weiterhin korrelierte der Nitratgehalt positiv mit der Anzahl der PAOs im Belebtschlamm der Kläranlage. Mit diesem Wissen und der phylogenetischen Untersuchung Polyphosphatgranula-tragender Zellen konnte ermittelt werden, dass in der Kläranlagen Eilenburg hauptsächlich denitrifizierende PAOs für die biologische Phosphatelimination zuständig sind.

Die in der vorliegenden Arbeit entwickelten Methoden ermöglichen die schnelle, zuverlässige und kostengünstige Untersuchung der mikrobiellen Gemeinschaft im Belebtschlamm und der darin enthaltenen, bislang nicht kultivierbaren PAOs. Weiterhin können potentielle PAOs identifiziert, ihre Populationsdynamiken untersucht und mögliche aktivitätsfördernde Faktoren ermittelt werden, mit dem Ziel, den Prozess der biologischen Phosphatelimination stabiler und effizienter zu machen.

References

1. Abou-Shanab, R.A.I., van Berkum, P., Angle, J.S. Heavy metal resistance and genotypic analysis of metal resistance genes in gram-positive and gram-negative bacteria present in Ni-rich serpentine soil and in the rhizosphere of *Alyssum murale*. Chemosphere 2007, 68, 360-367.

2. Alberta Environment. Guidelines for municipal wastewater irrigation. 2000, ISBN 0-7785-1150-2, p. 7.

3. Al-Rubeai, M. Monitoring animal cell growth and productivity by flow cytometry. Animal Cell Biotechnology. Method. Biotechnol. 1999, 8, 145-153.

4. Altschul, S.F., Gish, W., Miller, W., Myers, E.W., Lipman, D.J. Basic local alignment search tool. J. Mol. Biol. 1990, 215, 403-410.

5. Amonette, J.E., Russell, C.K., Carosino, K.A., Robinson, N.L., Ho, J.T. Toxicity of Al to *Desulfovibrio desulfuricans*. Appl. Environ. Microbiol. 2003, 69, 4057-4066.

6. Arima, K. and Oka, T. Cyanide resistance in *Achromobacter* - I. Induced formation of cytochrome a2 and its role in cyanide-resistant respiration. J. Bacteriol. 1965, 90, 734-743.

7. Ault-Riche, D., Fraley, C.D., Tzeng, C.M., Kornberg, A. Novel assay reveals multiple pathways regulating stress-induced accumulations of inorganic polyphosphate in Escherichia coli. J. Bacteriol. 1998, 180, 1841-1847.

8. Baldi, F., Pepi, M., Burrini, D., Kniewald, G., Scali, D., Lanciotti, E. Dissolution of barium from barite in sewage sludges and cultures of *Desulfovibrio desulfuricans*. Appl. Environ. Microbiol. 1996, 62, 2398-2404.

9. Barker, L.E., Luman, E.T., McCauley, M.M., Chu, S.Y. Assessing equivalence: an alternative to the use of difference tests for measuring disparities in vaccination coverage. Am. J. Epidemiol. 2002, 156, 1056-1061.

10. Blackall, L.L., Crocetti, G.R., Saunders, A.M., Bond, P.L. A review and update of the microbiology of enhanced biological phosphorus removal in wastewater treatment plants. A. Van. Leeuw. 2002, 81, 681-691.

11. Blum, E., Py, B., Carpousis, A.J., Higgins, C.F. Polyphosphate kinase is a component of the *Escherichia coli* RNA degradosome. Mol. Microbiol. 1997, 26, 387-398.

12. Bogan, B.W., Lamb, B.M., Husmillo, G., Lowe, K., Paterek, J.R., Kilbane II, J.J. Development of an environmentally benign microbial inhibitor to control internal pipeline corrosion. Final Report 2004, Gas Technology Institute, Des Plaines, IL. 60018.

13. Bolboaca, S.D. and Jäntschi, L. Pearson versus Spearman, Kendall's Tau correlation analysis on structure-activity relationships of biologic active compounds. Leonardo J. Sci. 2006, 9, 179-200.

14. Bombach, P. *et al.* Insight into natural microbial community dynamics using a combined approach of community fingerprinting, flow cytometry and trend interpretation analysis. In: Advances in Biochemical Engineering and Biotechnology: 'High Resolution Microbial Single Cell Analytics'; Müller, S.; Bley, T., eds.; Springer: Berlin 2011.

15. Boswell, C.D., Hewitt, C.J., Macaskie, L.E. An application of bacterial flow cytometry: Evaluation of the toxic effects of four heavy metals on *Acinetobacter* sp. with potential for bioremediation of contaminated wastewaters. Biotechnol. Lett. 1998, 20, 857-863.

16. Brito, A. G. Winery and brewery wastewater treatment: some focal points of design and operation. In: Residues from the food industry as 'by'-products; Oreopoulou, V.; Russ, W., Eds.; Springer: Hamburg 2007; pp. 1-22.

17. Brown M.R.W. and Kornberg, A. Inorganic polyphosphate in the origin and survival of species. PNAS 2004, 101, 16085-16087.

18. Brown, M.J. and Lester, J.N. Metal removal in activated sludge: the role of bacterial extracellular polymers. Water Res. 1979, 13, 817-837.

19. Buchan, L. The location and nature of accumulated P in activated sludge. D. Sc. Dissertation 1980, University of Pretoria

20. Calder, K., Burke, K.A., Lascelles, J. Induction of nitrate reductase and cytochromes in wild type and chlorate-resistant *Paracoccus denitrificans*. Arch. Microbiol. 1980, 126, 149-153.

21. Carr, G.J. and Ferguson, S.J. The nitric oxide reductase of *Paracoccus denitrificans*. Biochem. J. 1990, 269, 423-429.

22. Chang, C.-F., Shuman, H., Somlyo, A.P. Electron probe analysis, X-ray mapping, and electron energy-loss spectroscopy of calcium, magnesium, and monovalent ions in log-phase and in dividing *Escherichia coli* B cells. J. Bacteriol. 1986, 167, 935-939.

23. Chapin, F.S., Zavaleta, E.S., Eviner, V.T., Naylor, R.L., Vitousek, P.M., Reynolds, H.L., Hooper, D.U., Lavorel, S., Sala, O.E., Hobbie, S.E., Mack, M.C., Díaz, S. Consequences of changing biodiversity. Nature 2000, 405, 234-242.

24. Chopra, I., and Roberts, M. Tetracycline antibiotics: mode of action, applications, molecular biology, and epidemiology of bacterial resistance. Microbiol. Mol. Biol. Rev. 2001, 65, 232-260.

25. Clesceri, L.S., Greenberg, A.E., Eaton, A.D. Standard methods for the examination of water and wastewater. 20th ed. 1998, American public health association, Washington.

26. Cloete, T.E. and Steyn, P.L. A combined fluorescent antibody membrane filter technique for enumerating *Acinetobacter* in activated sludges, pp. 335-338. In: R. Ramadori, (ed.), Biological Phosphate Removal from Wastewater 1987, Pergamon, Oxford.

27. Cole, J.J., Howarth, R.W., Nolan, S.S., Marino, R. Sulfate inhibition of molybdate assimilation by planktonic algae and bacteria: some implications for the aquatic nitrogen cycle. Biogeochemistry 1986, 2, 179-196.

28. Cole, J.R., Chai, B., Farris, R.J., Wang, Q., Kulam-Syed-Mohideen, A.S., McGarrell, D.M., Bandela, A.M., Cardenas, E., Garrity, G.M., Tiedje, J.M. The ribosomal database project (RDP-II): introducing myRDP space and quality controlled public data. Nucleic Acids Res. 2007, 35 (Database issue): D169-D172; doi: 10.1093/nar/gkl889.

29. Crawford, B.J., Talburt, D.E., Johnson, D.A. Effects of cobalt (III) complexes on growth and metabolism of *E. coli*. Bioinorg. Chem. 1974, 3, 121-123.

30. Crocetti, G.R., Banfield, J.F., Keller, J., Bond, P.L., Blackall, L.L. Glycogen-accumulating organisms in laboratory-scale and full-scale wastewater treatment processes. Microbiology 2002, 148, 3353-3364.

31. Crocetti, G.R., Hugenholtz, P., Bond, P.L., Schuler, A., Keller, J., Jenkins, D., Blackall, L.L. Identification of polyphosphate-accumulating organisms and design of 16S rRNA-directed probes for their detection and quantitation. Appl Environ Microbiol. 2000, 66, 1175-1182.

32. Cucci, T.L. and Sieracki, M.E. Effects of mismatched refractive indices in aquatic flow cytometry. Cytometry 2001, 44, 173-178.

33. Dabert, P., Fleurat-Lessard, A., Mounier, E., Delgenès, J.P., Moletta, R., Gordon, J.J. Monitoring of the microbial community of a sequencing batch reactor bioaugmented to improve its phosphorus removal capabilities. Water Sci. Technol. 2001, 43, 1-8.

34. Deng, M., Moureaux, T., Caboche, M. Tungstate, a molybdate analog inactivating nitrate reductase, deregulates the expression of the nitrate reductase structural gene. Plant Physiol. 1989, 91, 304-309.

35. Domenico, P., Reich, J., Madonia, W., Cunha, B.A. Resistance to bismuth among gram-negative bacteria is dependent upon iron and its uptake. J. Antimicrob. Chemother. 1996, 38, 1031-1040.

36. Dworkin, M.; Falkow, S.; Rosenberg, E.; Schleifer, K. H.; Stackebrandt, E. The Prokaryotes: a handbook on the biology of bacteria. Proteobacteria: alpha and beta subclasses; 3rd ed., 5, Springer, 2006, p. 17.

37. Eaton A.D., Clesceri L.S., Greenberg A.E. Standard methods for the examination of water and wastewater. 19th ed. 1995, American Public Health Association, Washington, DC.

38. Eckenfelder, W.W. Jr. Industrial water pollution control. 2nd ed. 1989, McGraw-Hill, New York.

39. Filali, B.K., Taoufik, J., Zeroual, Y., Dzairi, F.Z., Talbi, M., Blaghen, M. Waste water bacterial isolates resistant to heavy metals and antibiotics. Curr. Microbiol. 2000, 41, 151-156.

40. Fujie, K., Hu, H.-Y., Lim, B.-R., Xia, H. Effect of biosorption on the damping of influent fluctuation in activated sludge aeration tanks. Water Sci. Technol. 1997, 35, 79-87.

41. Garrett, K.A. Use of statistical tests of equivalence (bioequivalence tests) in plant pathology. Phytopathology 1997, 87, 372-374.

42. Gates, I.V., Zhang, Y., Shambaugh, C., Bauman, M.A., Charles, T., Bodmer, J.-L. Quantitative measurement of Varicella-Zoster virus infection by semiautomated flow cytometry. Appl. Environ. Microbiol. 2009, 75, 2027-2036.

43. Gavigan, J.-A., Leonard, M.M., Dobson, A.D.W. Regulation of polyphosphate kinase gene expression in *Acinetobacter baumannii* 252. Microbiology 1999, 145, 2931-2937.

44. Gich, F.B., Amer, E., Figueras, J.B., Abella, C.A., Balaguer, M.D., Poch, M. Assessment of microbial community structure changes by amplified ribosomal DNA restriction analysis (ARDRA). Internatl. Microbiol. 2000, 3, 103-106.

45. Giraffa, G., Rossetti, L., Neviani, E. An evaluation of chelex-based DNA purification protocols for the typing of lactic acid bacteria. J. Microbiol. Meth. 2000, 42, 175-184.

46. Global Carbon Project. Carbon budget and trends 2009. www.globalcarbonproject.org/carbonbudget released on 21 November 2010 (last accessed: May 2011).

47. Gloess, S., Grossart, H.-P., Allgaier, M., Ratering, S., Hupfer, M. Use of laser microdissection for phylogenetic characterization of polyphosphate-accumulating bacteria. Appl. Environ. Microbiol. 2008, 74, 4231-4235.

48. Güde, H. Interactions between floc-forming and nonfloc-forming bacterial populations from activated sludge. Curr. Microbiol. 1982, 7, 347-350.

49. Guellil, A., Thomas, F., Block, J.-C., Bersillon, J.-L., Ginestet, P. Transfer of organic matter between wastewater and activated sludge flocs. Water Res. 2001, 35, 143-150.

50. Günther, S., Trutnau, M., Kleinsteuber, S., Hause, G., Bley, T., Röske, I., Harms, H., Müller, S. Dynamics of polyphosphate-accumulating bacteria in wastewater treatment plant microbial communities detected via DAPI (4',6'-Diamidino-2-Phenylindole) and tetracycline labeling. Appl. Environ. Microbiol. 2009, 75, 2111-2121.

51. Gutteridge, J.M.C., Quinlan, G.J., Clark, I., Halliwell, B. Aluminium salts accelerate peroxidation of membrane lipids stimulated by iron salts. Biochim. Biophys. Acta 1985, 835, 441-447.

52. Hallett, M., Schneider, A.S., Carbone, E. Tetracycline fluorescence as calcium-probe for nerve membrane with some model studies using erythrocyte ghosts. J. Membr. Biol. 1972, 10, 31-44.

53. Hamady, M., and Knight, R. Microbial community profiling for human microbiome projects: Tools, techniques, and challenges. Genome Res. 2009, 19, 1141-1152.

54. Hammer, Ø. and Harper, D.A.T. Paleontological Data Analysis; Blackwell Publishing Ltd, Wiley-Blackwell, 2006, ISBN: 978-1-4051-1544-5.

55. He, S., Gall, D.L., McMahon, K.D. 'Candidatus accumulibacter' population structure in enhanced biological phosphorus removal sludges as revealed by polyphosphate kinase genes. Appl. Envir. Microbiol. 2007, 73, 5865-5874.

56. Henze M. and Van Loosdrecht, M.C.M. Biological wastewater treatment: principles, modelling and design. IWA Publishing 2008, 363-364.

57. Hesselmann, R.P.X., Werlen, C., Hahn, D., van der Meer, J.R., Zehnder, A.J.B. Enrichment, phylogenetic analysis and detection of a bacterium that performs enhanced biological phosphate removal in activated sludge. Syst. Appl. Microbiol. 1999, 22, 454-465.

58. Hirota, R., Kuroda, A., Kato, J., Ohtake, H. Bacterial phosphate metabolism and its application to phosphorus recovery and industrial bioprocesses. J. Biosci. Bioeng. 2010, 109, 423-432.

59. Hopwood, D. Cell and tissue fixation, 1972-1982. Histochem. J. 1985, 17, 389-442.

60. Hopwood, D. Fixatives and fixation: a review. Histochem. J. 1969, 1, 323-360.

61. Hrenovic´, J., Tibljaš, D., Büyükgüngör, H., Orhan, Y. Influence of support materials on phosphate removal by the pure culture of *Acinetobacter calcoaceticus*. Food Technol. Biotechnol. 2003, 41, 331-338.

62. Hugenholtz, P., Tyson, G.W., Webb, R.I., Wagner, A.M., Blackall, L.L. Investigation of candidate division TM7, a recently recognized major lineage of the domain bacteria with no known pure-culture representatives. Appl. Environ. Microbiol. 2001, 67, 411-419.

63. Illmer, P. and Erlebach, C. Influence of Al on growth, cell size and content of intracellular water of *Arthrobacter* sp. PI/1-95. A. Van. Leeuw. 2003, 84, 239-246.

64. Imhoff, K. and Imhoff, K.R. Taschenbuch der Stadtentwässerung. Oldenbourg Industrieverlag, 2006, p. 121.

65. Impallomeni, G., Guglielmino, S.P.P., Carnazza, S., Ferreri, A., Ballistreri, A. Tween 20 and its major free fatty acids as carbon substrates for the production of polyhydroxyalkanoates in *Pseudomonas aeruginosa* ATCC 27853. J. Polymer. Environ. 2000, 8, 97-102.

66. Inniss E.C. Considerations for the use of ORP in wastewater treatment applications. http://web.missouri.edu/~innisse/presentations/WEAT051806.pdf (last accessed: May 2011).

67. ILEC: International Lake Environment Committee. Survey of the State of the World's Lakes. Volumes I-IV. 1988-1993, Otsu and United Nations Environment Programme, Nairobi. http://www.unep.or.jp/ietc/publications/insight/fal-94/2.asp (last accessed: May 2011).

68. International Programme on Chemical Safety. Environmental health criteria for barium. World Health Organization Publications, Geneva 1990, 107, ISBN 92 4 157107 1.

69. Janatpour, K., Paglieroni, T.G., Schuller, L., Foley, K., Rizzardo, T., Holland, P.V. Interpretation of atypical patterns encountered when using a flow cytometry-based method to detect residual leukocytes in leukoreduced red blood cell components. Cytometry 2002, 50, 254-260.

70. Jensen, T.E. Electron microscopy of polyphosphate bodies in a blue-green algae, *Nostoc pruniforme*. Arch. Microbiol. 1968, 62, 144-152.

71. Johansson, L. and Gustafsson, J.P. Phosphate removal using blast furnace slags and opoka-mechanisms, Water Res. 2000, 34, 259-265.

72. Johnson, J.L., Rajagopalan, K.V., Cohen, H.J. Molecular basis of the biological function of molybdenum. Effect of tungsten on xanthine oxidase and sulfite oxidase in the rat. J. Biol. Chem. 1974, 249, 859-866.

73. Jørgensen, S.E., Industrial wastewater management. Elsevier 1979, p. 368.

74. Kajikawa, H., Valdes, C., Hillman, K., Wallace, R.J., Newbold, C.J. Methane oxidation and its coupled electron-sink reactions in ruminal fluid. Lett. Appl. Microbiol. 2003, 36, 354-357.

75. Kawaharasaki, M., Manome, A., Kanagawa, T., Nakamura, K. Flow cytometric sorting and RFLP analysis of phosphate accumulating bacteria in an enhanced biological phosphorus removal system. Water Sci. Technol. 2002, 46, 139-144.

76. Kawaharasaki, M., Tanaka, H., Kanagawa, T., Nakamura, K. In situ identification of polyphosphate-accumulating bacteria in activated sludge by dual staining with rRNA-targeted oligonucleotide probes and 4',6-diamidino-2-phenylindol (DAPI) at a polyphosphate-probing concentration. Water Res. 1999, 33, 257-265.

77. Kelly, C.J., Tumsaroj, N., Lajoie, C.A. Assessing wastewater metal toxicity with bacterial bioluminescence in a bench-scale wastewater treatment system. Water Res. 2004, 38, 423-431.

78. Kindaichi, T., Ito, T., Okabe, S. Ecophysiological interaction between nitrifying bacteria and heterotrophic bacteria in autotrophic nitrifying biofilms as determined by microautoradiography-fluorescence in situ hybridization. Appl. Environ. Microbiol. 2004, 70, 1641-1650.

79. Klauth, P., Pallerla, S.R., Vidaurre, D., Ralfs, C., Wendisch, V.F., Schoberth, S.M. Determination of soluble and granular inorganic polyphosphate in *Corynebacterium glutamicum*. Appl. Microbiol. Biotechnol. 2006, 72, 1099-1106.

80. Kleinsteuber, S., Riis, V., Fetzer, I., Harms, H., Müller, S. Population dynamics within a microbial consortium during growth on diesel fuel in saline environments. Appl. Environ. Microbiol. 2006, 72, 3531-3542.

81. Kong, Y., Nielsen, J.L., Nielsen, P.H. Identity and ecophysiology of uncultured actinobacterial polyphosphate-accumulating organisms in full-scale enhanced biological phosphorus removal plants. Appl. Environ. Microbiol. 2005, 71, 4076-4085.

82. Kornberg, A., Rao, N.N., Ault-Riché, D. Inorganic polyphosphate: a molecule of many functions. Annu. Rev. Biochem. 1999, 68, 89-125.

83. Kragelund, C., Levantesi, C., Borger, A., Thelen, K., Eikelboom, D., Tandoi, V., Kong, Y., Van Der Waarde, J., Krooneman, J., Rossetti, S., Thomsen, T.R., Nielsen, P.H. Identity, abundance and ecophysiology of filamentous *Chloroflexi* species present in activated sludge treatment plants. FEMS Microbiol. Ecol. 2007, 59, 671-682.

84. Kulaev, I. and Kulakovskaya, T. Polyphosphate and phosphate pump. Annu. Rev. Microbiol. 2000, 54, 709-734.

85. Kulaev, I.S., Vagabov, V.M., Kulakovskaya, T.V., Lichko, L.P., Andreeva, N.A., Trilisenko, L.V. The development of A. N. Belozersky`s ideas in polyphosphate biochemistry. Biochemistry (Moscow) 2000, 65, 271-278.

86. Kusano S. and Ishihama, A. Functional interaction of *Escherichia coli* RNA polymerase with inorganic polyphosphate. Genes Cells 1997, 2, 433-441.

87. Lambeth, C.R., White, L.J., Johnston, R.E., de Silva, A.M. Flow cytometry-based assay for titrating Dengue Virus. J. Clin. Microbiol. 2005, 43, 3267-3272.

88. Lane, D.J. 16S/23S rRNA sequencing. In: Stackebrandt, E. and Goodfellow, M. (ed.), Nucleic Acid Techniques in Bacterial Systematics, Wiley 1991, Chichester.

89. Lapata, M. Automatic evaluation of information ordering: Kendall's Tau. Comput. Linguist. 2006, 32, 471-484.

90. Lawton, J.H., May R.M. Extinction rates. Oxford University Press, 1995.

91. Lee, T.C., Mohsin, S., Taylor, D., Parkesh, R., Gunnlaugsson, T., O'Brien, F.J., Giehl, M., Gowin, W. Detecting microdamage in bone. J. Anat. 2003, 203, 161-172.

92. Lemos, P.C., Serafim, L.S., Santos, M.M., Reis, M.A.M., Santos, H. Metabolic pathway for propionate utilization by phosphorus-accumulating organisms in activated sludge: 13C labeling and in vivo nuclear magnetic resonance. Appl. Environ. Microbiol. 2003, 69, 241-251.

93. Li, B. and Bishop, P.L. The application of ORP in activated sludge wastewater treatment processes. Environ. Eng. Sci. 2001, 18, 309-321.

94. Li, F., Hullara, M.A.J., Lampe, J.W. Optimization of terminal restriction fragment polymorphism (TRFLP) analysis of human gut microbiota. J. Microbiol. Meth. 2007, 68, 303-311.

95. Li, K.W., Zohary, T., Yacobi, Y.Z., Wood, A.M. Ultraphytoplankton in the eastern Mediterranean Sea: towards deriving phytoplankton biomass from flow cytometric measurements of abundance, fluorescence and light scatter. Mar. Ecol. Prog. 1993, 102, 79-87.

96. Liebermann, L. Über das Nuclein der Hefe und künstliche Darstellung eines Nucleins aus Eiweiss und Metaphosphorsäure. Ber. Dtsch. Chem. Ges. 1888, 21, 598-600.

97. Lindblom, E., Raduly, B., Mikkelsen, P.S. System process modelling report. Environment & Resources DTU 2005, Technical University of Denmark

98. Liu, W.-T., Nakamura, K., Matsuo, T., Mino, T. Internal energy-based competition between polyphosphate- and glycogen-accumulating bacteria. Water Res. 1997, 31, 1430-1438.

99. Lombrana, J.I., Varona, F., Mijanos, F. Biokinetics, behaviour and settling characteristics in an activated sludge under the effect of toxic Ni(II) influents. Water Air Soil Pollut. 1993, 69, 57-68.

100. Maniatis, T., Fritsch, E.F., Sambrook, J. Molecular cloning, a laboratory manual 1st ed. Cold Spring Harbor Laboratory Press 1982, p. 68.

101. Martin Garcia, H., Ivanova, N., Kunin, V., Warnecke, F., Barry, K.W., McHardy, A.C., Yeates, C., He, S., Salamov, A.A., Szeto, E., Dalin, E., Putnam, N.H., Shapiro, H.J., Pangilinan, J.L., Rigoutsos, I., Kyrpides, N.C., Blackall, L.L., McMahon, K.D., Hugenholtz, P. Metagenomic analysis of two enhanced biological phosphorus removal (EBPR) sludge communities. Nat. Biotechnol. 2006, 24, 1263-1269.

102. Martin, R.B. The chemistry of aluminium related to biology and medicine. Clin. Chem. 1986, 32, 1797-1806.

103. McGuire, J.L. Pharmaceuticals: classes, therapeutic agents, areas of application. Band 1, Wiley-VCH 2000, p. 1237.

104. McKillen, M.N. and Spencer, B. Molybdate toxicity in *Salmonella typhimurium*. Biochem. J. 1970, 118, 27.

105. Mehlig, L. Analyse und Vergleich der Biodiversität in der Gemeinschaft Polyphosphat-akkumulierender Mikroorganismen (PAO) an Belebtschlämmen kommunaler Kläranlagen. Dissertation 2010, Fakultät Mathematik und Naturwissenschaften, Institut für Mikrobiologie, Technische Universität Dresden.

106. Meinhold, J., Arnold, E., Isaacs, S. Effect of nitrite on anoxic phosphate uptake in biological phosphorous activated sludge. Water Res. 1999, 33, 1871-1883.

107. Meistrich, M.L., Göhde, W., White, R.A., Schumann, J. Resolution of x and y spermatids by pulse cytophotometry. Nature 1978, 274, 821-823.

108. Metcalf and Eddy. Wastewater Engineering. Treatment, Disposal, Reuse. Tchobanoglous G. and Burton, F.L. (eds.), 1991, McGraw-Hill, New York.

109. Miura, Y., Watanabe, Y., Okabe, S. Significance of *Chloroflexi* in performance of submerged membrane bioreactors (MBR) treating municipal wastewater. Environ. Sci. Technol. 2007, 41, 7787-7794.

110. Mollenhauer, H.H. Permanganate fixation of plant cells. J. Biophysic. Biochem. Cytol. 1959, 6, 431-436.

111. Montag, D., Gethke, K., Pinnekamp, J. Erhebung zum Stand der Phosphorelimination bei der kommunalen Abwasserreinigung sowie Realisierungspotential einer Phosphorrückgewinnung in Deutschland. GWF – Wasser/ Abwasser, Oldenbourg Industrieverlag München 2008, 149, ISSN 0016-3651.

112. Moriyama, K., Kojima, T., Minawa, Y., Matsumoto, S., Nakamachi, K. Development of artificial seed crystal for crystallization of calcium phosphate, Environ. Technol. 2001, 22, 1245-1252.

113. Mullan, A., Quinn, J.P., McGrath, J.W. Enhanced phosphate uptake and polyphosphate accumulation in *Burkholderia cepacia* grown under low-pH conditions. Microbial Ecol. 2002, 44, 69-77.

114. Müller, S. and Nebe-von-Caron, G. Functional single-cell analyses – flow cytometry and cell sorting of microbial populations and communities. FEMS Microbiol. Rev. 2010, 34, 554-587.

115. Müller, S. Modes of cytometric bacterial DNA pattern: a tool for pursuing growth. Cell Prolif. 2007, 40, 621-639.

116. Müller, S., Harms, H., Bley, T. Origin and analysis of microbial population heterogeneity in bioprocesses. Curr. Opin. Biotechnol. 2010, 21, 100-113.

117. Müller, S., Vogt, C., Laube, M., Harms, H., Kleinsteuber, S. Community dynamics within a bacterial consortium during growth on toluene under sulfate-reducing conditions. FEMS Microbial. Ecol. 2009, 70, 586–596.

118. Nagamine, S., Ueda, T., Masuda, I., Mori, T., Sasaoka, E., Joko, I. Removal of phosphorus from wastewater by crystallization on the surface of macroporous TiO2 with a fibrous microstructure. Ind. Eng. Chem. Res. 2003, 42, 4748-4752.

119. Nakamura, K., Hiraishi, A., Yoshimi Y., Kawaharasaki, M., Masuda, K., Kamagata, Y. *Microlunatus phosphovorus* gen. nov., sp. nov., a new gram-positive polyphosphate-accumulating bacterium isolated from activated sludge. Int. J. Syst. Bacteriol. 1995, 45, 17-22.

120. Nelson, M.L. Chemical and biological dynamics of tetracyclines. Adv. Dent. Res. 1998, 12, 5-11.

121. Newton, R.J., Jones, S.E., Eiler, A., McMahon, K.D., Bertilsson, S. A guide to the natural history of freshwater lake bacteria. Microbiol. Mol. Biol. Rev. 2011, 75, 14-19.

122. Nielsen, P.H., Thomsen, T.R., Nielsen, J.L. Bacterial composition of activated sludge importance for floc and sludge properties. Water Sci. Technol. 2004, 49, 51-58.

123. Nies, D.H. Resistance to cadmium, cobalt, zinc, and nickel in microbes. Plasmid 1992, 27, 17-28.

124. Okunuki, S., Kawaharasaki, M., Tanaka, H., Kanagawa, T. Changes in phosphorus removing performance and bacterial community structure in an enhanced biological phosphorus removal reactor. Water Res. 2004, 38, 2433-2439.

125. Oosthuizen D.J. and Cloete T.E. SEM-EDS for determining the phosphorus content in activated sludge EPS. Water Sci. Technol. 2001, 43, 105-112.

126. Palmieri, F. and Klingenberg, M. Inhibition of respiration under the control of azide uptake by mitochondria. Eur. J. Biochem. 1967, 1, 439-446.

127. Pawelczyk, S., Abraham, W.R, Harms, H., Müller, S. Community based degradation of 4-chorosalicylate tracked on the single cell level. J. Microbiol. Methods 2008, 75, 117-126.

128. Petersen, B., Vanrolleghem, P.A., Gernaey, K., Henze, M. Evaluation of an ASM1 model calibration procedure on a municipal–industrial wastewater treatment plant. J. Hydroinform. 2002, 4, 15-38.

129. Petersen, L.C. The effect of inhibitors on the oxygen kinetics of cytochrome c oxidase. Biochim. Biophys. Acta 1977, 460, 299-307.

130. Pimm, S.L., Russell, G.J., Gittleman, J.L., Brooks, T.M. The future of biodiversity. Science 1995, 269, 347-350.

131. Prins, R.A., Cliné-Theil, W., Malestein, A., Counotte, G.H. Inhibition of nitrate reduction in some rumen bacteria by tungstate. Appl. Environ. Microbiol. 1980, 40, 163-165.

132. Rao, N.N., Roberts, M.R., Torriani, A. Amount and chain length of polyphosphates in *Escherichia coli* depend on cell growth conditions. J. Bacteriol. 1985, 162, 242-247.

133. Reid, N.M., Bowers, T.H., Lloyd-Jones, G. Bacterial community composition of a waste water treatment system reliant on N2 fixation. Appl. Microbiol. Biotechnol. 2008, 79, 285-292.

134. Reisner, A.H., Bucholtz, C., Chandler, B.S. Studies on the polyribosomes of *Paramecium* - II. Effect of divalent cations. Exp. Cell Res. 1975, 93, 1-14.

135. Richey, J.E., Wollast, R., Duce, R.A., SCOPE 21 -The Major Biogeochemical Cycles and Their Interactions: Chapter 2: C, N, P, and S Cycles: Major Reservoirs and Fluxes, Scope 21: http://www.icsu-scope.org/downloadpubs/scope21/chapter02.html (last accessed: May 2011).

136. Ritz, K. The plate debate: Cultivable communities have no utility in contemporary environmental microbial ecology. FEMS Microbiol. Ecol. 2007, 60, 358-362.

137. Roinestad, F.A. and Yall, I. Volutin granules in *Zoogloea ramigera*. Appl. Microbiol. 1970, 19, 973-979.

138. Röske, I., Bauer, H.-D., Uhlmann, D. Nachweis phosphorspeichernder Bakterien im Belebtschlamm mittels Elektronenmikroskopie und Röntgenspektroskopie. GWF Wasser Abwasser 1989, 130, 73-75.

139. Rowe, J.J., Yarbrough, J.M., Rake, J.B., Eagon, R.G. Nitrite inhibition of aerobic bacteria. Curr. Microbiol. 1979, 2, 51–54.

140. Sáez, F., Pozo, C., Gómez, M.A., Rodelas, B., González-López, J. Growth and nitrite and nitrous oxide accumulation of *Paracoccus denitrificans* ATCC 19367 in the presence of selected pesticides. Environ. Toxicol. Chem. 2003, 22, 1993-1997.

141. Sai Ram, M., Singh, L., Suryanarayana, M.V.S., Alam, S.I. Effect of iron, nickel and cobalt on bacterial activity and dynamics during anaerobic oxidation of organic matter. Water Air Soil Pollut. 2000, 117, 305-312.

142. Saito, K., Ohtomo, R., Kuga-Uetake, Y., Aono, T., Saito, M. Direct labeling of polyphosphate at the ultrastructural level in Saccharomyces cerevisiae by using the affinity of the polyphosphate binding domain of *Escherichia coli* exopolyphosphatase. Appl. Environ. Microbiol. 2005, 71, 5692-5701.

143. Sanz, J.L., and Köchling, T. Molecular biology techniques used in wastewater treatment: An overview. Process Biochem. 2007, 42, 119-133.

144. Schimenti, K.J. and Jacobberger, J.W. Fixation of mammalian cells for flow cytometric evaluation of DNA content and nuclear immunofluorescence. Cytometry 1992, 13, 48-59.

145. Schön, G., Geywitz, S., Mertens, F. Influence of dissolved oxygen and oxidation-reduction potential on phosphate release and uptake by activated sludge from sewage plants with enhanced biological phosphorus removal. Water Res. 1993, 27, 349-354.

146. Schönborn, C., Bauer, H.D., Röske, I. Stability of enhanced biological phosphorous removal and composition of polyphosphate granules. Water Res. 2001, 35, 3190-3196.

147. Sell, A. Differenzierung mitochondrialer und nicht-mitochondrialer Quellen von reaktiven Sauerstoffspezies in PC12-Zellen unter Hypoxie. Dissertation 2001, Fachbereich Veterinärmedizin, Justus-Liebig-Universität Gießen.

148. Sell, D. Wege zur Online-Bestimmung der mikrobiellen Stoffwechselaktivität mittels einer neuartigen Bioaktivitätssensorik. Habilitation 2004, Universität Hannover.

149. Selman, M. and Greenhalgh, S. Eutrophication: Sources and Drivers of Nutrient Pollution. Washington, DC 2009. http://www.wri.org/publication/eutrophication-sources-and-drivers (last accessed: May 2011).

150. Selman, M., Greenhalgh, S., Diaz, R., Sugg, Z., Eutrophication and hypoxia in coastal areas: A global assessment of the state of knowledge. Washington, DC, 2008. http://www.wri.org/publication/eutrophication-and-hypoxia-in-coastal-areas (last accessed: May 2011).

151. Serafim, L.S., Lemos, P.C., Levantesi, C., Tandoi, V., Santos, H., Reis, M.A. Methods for detection and visualization of intracellular polymers stored by polyphosphate-accumulating microorganisms. J. Microbiol. Methods 2002, 51, 1-18.

152. Seufferheld, M.J., Alvarez, H.M., Farias, M.E. Role of polyphosphates in microbial adaptation to extreme environments. Appl. Environ. Microbiol. 2008, 74, 5867-5874.

153. Shapiro, H.M. Practical flow cytometry, 4th ed. In: Wiley-Liss 2002, New York NY.

154. Shively, J.M. Inclusion bodies of prokaryotes. Annu. Rev. Microbiol. 1974, 28, 167-188.

155. Shoji, T., Satoh, H., Mino, T. Quantitative estimation of the role of denitrifying phosphate accumulating organisms in nutrient removal. Water Sci. Technol. 2003, 47, 23-29.

156. Siegel, S., and Castellan, N.J. Nonparametric statistics for the behavioral sciences. 2nd ed. McGraw-Hill 1988, New York, NY.

157. Sigee, D.C., and Al-Rabaee, R.H. Nickel toxicity in *Pseudomonas tabaci*: single cell and bulk sample analysis of bacteria cultured at high cation levels. Protoplasma 1986, 130, 171-185.

158. Silver, S. Bacterial resistances to toxic metal ions - a review. Gene 1996, 179, 9-19.

159. Smith, R.J. Calcium and bacteria. Adv. Microb. Physiol. 1995, 37, 83-133.

160. Sosik, H.M., Olson R.J., Armbrust, E.V. Flow cytometry in plankton research. In: Suggett, D.J., Prasil, O., Borowitzka, M.A. (eds.), Chlorophyll a fluorescence in aquatic sciences: methods and applications. 2010, Springer

161. Speer B.S., Shoemaker, N.B., Salyers, A.A. Bacterial resistance to tetracycline: mechanisms, transfer, and clinical significance. Clin. Microbiol. Rev. 1992, 5, 387-399.

162. Spring, S., Wagner, M., Schumann, P., Kämpfer, P. *Malikia granosa* gen. nov., sp. nov., a novel polyhydroxyalkanoate- and polyphosphate-accumulating bacterium isolated from activated sludge, and reclassification of *Pseudomonas spinosa* as *Malikia spinosa* comb. nov. Int. J. Syst. Evol. Microbiol. 2005, 55, 621-629.

163. Spurr, A.R. A low-viscosity epoxy resin embedding medium for electron microscopy. J. Ultrastruct. Res. 1969, 26, 31-43.

164. Srinivasan, M., Sedmak, D., Jewell, S. Effect of fixatives and tissue processing on the content and integrity of nucleic acids. Am. J. Pathol. 2002, 161, 1961-1971.

165. Stancheva, N., Weber, J., Schulze, J., Alipieva, K., Ludwig-Müller, J., Haas, C., Georgiev, V., Bley, T., Georgiev, M. Phytochemical and flow cytometric analyses of Devil's claw cell cultures. Plant Cell Tiss. Org. 2010, 105, 79-84.

166. Stewart, A. Basic Statistics and Epidemiology: A Practical Guide. Radcliffe Publishing 2010, p. 65

167. Stoel, L.J., Newman, E.C., Asleson, G.L., Frank, C.W. Potentiometric and spectral investigations of anhydrotetracycline and its metal-ion complexes. J. Pharm. Sci. 1976, 65, 1794-1799.

168. Stratton, C.W., Warner, R.R., Coudron, P.E., Lilly, N.A., 1999. Bismuth- mediated disruption of the glycocalyx-cell wall of Helicobacter pylori ultrastructure evidence for a mechanism of action for bismuth salts. J. Antimicrob. Chemother. 43, 659-666.

169. Streichan, M., Golecki, J.R., Schön, G. Polyphosphate accumulating bacteria from sewage plants with different processes for biological phosphorus removal. FEMS Microbiol. Ecol. 1990, 73, 113-124.

170. Streiner, D.L. Unicorns do exist: a tutorial on 'proving' the null hypothesis. Can. J. Psychiatry 2003, 48, 756-761.

171. Stumpf, A. Phosphorrecycling durch MAP-Fällung im kommunalen Faulschlamm. In: Publikationen des Umweltbundesamtes, 2007. http://www.umweltdaten.de/publikationen/fpdf-l/3471.pdf.

172. Suzuki, S., Higashiyama, T., Nakahara, A. Nonenzymatic hydrolysis reactions of adenosine 5'-triphosphate and its related compounds-III: catalytic aspects of some cobalt (II1) complexes in ATP-hydrolysis. Bioinorg. Chem. 1978, 8, 277-289.

173. Takahashi, J., Johchi, N., Fujita, H. Inhibitory effects of sulphur compounds, copper and tungsten on nitrate reduction by mixed rumen micro-organisms. Br. J. Nutr. 1989, 61, 741-748.

174. Tandoi, V., Majone, M., May, J., Ramadori, R. The behavior of polyphosphate accumulating Acinetobacter isolates in an anaerobic aerobic chemostat. Water Res. 1998, 32, 2903-2912.

175. Tham M. Overview of mechanistic modelling techniques. Department of Chemical and Process Engineering, 2000, University of Newcastle upon Tyne. http://lorien.ncl.ac.uk/ming/dynamics/modelling.pdf

176. Theodotou, A., Stretton, R.J., Norbury, A.H., Massey, A.G. Morphological effects of chromium and cobalt complexes on bacteria. Bioinorg. Chem. 1976, 5, 235-239.

177. Thomas, C.A., Garner, D.L., DeJarnette, J.M., Marshall, C.E. Effect of cryopreservation on bovine sperm organelle function and viability as determined by flow cytometry. Biol. Reprod. 1998, 58, 786-793.

178. Tijssen, J.P.F., Beekes, H.W., Van Steveninck, J. Localization of polyphosphates in *Saccharomyces fragilis*, as revealed by 46-diamidino-2-phenylindole fluorescence. Biochim. Biophys. Acta 1982, 721, 394-398.

179. Treilhou-Lahille, F., Cressent, M., Taboulet, J., Moukhtar, M.S., Milhaud, G. Influences of fixatives on the immunodetection of calcitonin in mouse 'C' cells during pre- and post-natal development. J. Histochem. Cytochem. 1981, 29, 1157-1163.

180. Tsuneda, S., Miyauchi, R., Ohno, T., Hirata, A. Characterization of denitrifying polyphosphate accumulating organisms in activated sludge based on nitrite reductase gene. J. Biosci. Bioeng. 2005, 99, 403-407.

181. Valdivia, R.H. and Falkow, S. Bacterial genetics by flow cytometry: rapid isolation of *Salmonella typhimurium* acid-inducible promoters by differential fluorescence induction. Mol. Microbiol. 1996, 22, 367-378.

182. Van Groenestijn, J.W., Vlekke, G.J.F.M., Anink, D.M.E., Deinema, M.H., Zehnder, A.J.B. Role of cations in accumulation and release of phosphate by *Acinetobacter* strain 210A. Appl. Environ. Microbiol. 1988, 54, 2894-2901.

183. Van Voorthuizen, E., Zwijnenburg, A., van der Meer, W., Temmink, H. Biological black water treatment combined with membrane separation. Water Res. 2008, 42, 4334-4340.

184. Vanhooren, H., Meirlaen, J., Amerlinck, Y., Claeys, F., Vangheluwe, H., Vanrolleghem, P.A. WEST: Modelling biological wastewater treatment, J. Hydroinform. 2003, 5, 27-50.

185. Vogt, C., Lösche, A., Kleinsteuber, S., Müller, S. Population profiles of a stable, commensalistic binary bacterial culture grown with toluene under sulphate-reducing conditions. Cytometry A 2005, 66, 91-102.

186. Wagner, M. and Loy, A. Bacterial community composition and function in sewage treatment systems. Curr. Opin. Biotechnol. 2002, 13, 218-227.

187. Wagner, M., Erhart, R., Manz, W., Amman, R., Lemmer, H., Wedi, D., Schleifer, K.H. Development of an rRNA-targeted oligonucleotide probe specific for the genus *Acinetobacter* and its application for in situ monitoring in activated sludge. Appl. Environ. Microbiol. 1994, 60, 792-800.

188. Wagner, M., Nielsen, P.H., Loy, A., Nielsen, J.L., Daims, H. Linking microbial community structure with function: fluorescence in situ hybridization-microautoradiography and isotope arrays. Curr. Opin. Biotechnol. 2006, 17, 83-91.

189. Wang, X., Wen, X., Criddle, C., Yan, H., Zhang, Y., Ding, K. Bacterial community dynamics in two full-scale wastewater treatment systems with functional stability. J. Appl. Microbiol. 2010, 109, 1218-1226.

190. Wellek, S. Testing statistical hypotheses of equivalence. In: Chapman and Hall, 2003, New York, NY.

191. Wentzel, M.C., Ekama, G.A., Loewenthal, R.E., Dold, P.L., Marais, G.v.R. Enhanced polyphosphate organism cultures in activated sludge systems. Part II: Experimental behavior. Water SA 1989, 15, 71-88.

192. Wilson, L.G. and Bandurski, R.S. Enzymatic reactions involving sulfate, sulfite, selenate and molybdate. J. Biol. Chem. 1958, 233, 975-981.

193. Wollast, R. SCOPE 21 -The major biogeochemical cycles and their interactions: Chapter 14: interactions in estuaries and coastal waters. http://www.icsu-scope.org/downloadpubs/scope21/chapter14.html.

194. Wood, M. A mechanism of aluminium toxicity to soil bacteria and possible ecological implications. Plant Soil 1995, 171, 173-179.

195. Yadav, V.K. and Archer, D.B. Sodium molybdate inhibits sulphate reduction in the anaerobic treatment of high-sulphate molasses wastewater. Appl. Microbiol. Biotechnol. 1989, 31, 103-106.

196. Zhang, L., Mulrooney, S.B., Leung, A.F.K., Zeng, Y., Ko, B.B.C., Hausinger, R.P., Sun, H. Inhibition of urease by bismuth(III): implications for the mechanism of action of bismuth drugs. Biometals 2006, 19, 503-511.

197. Zhao, Y.G., Wang, A.J., Ren, N.Q., Zhao, Y. Microbial community structure in different waste water treatment processes characterized by single-strand conformation polymorphism (SSCP) technique. Front. Environ. Sci. Engin. 2008, 2, 116-121.

198. Zilles, J.L., Hung, C.H., Noguera, D.R. Presence of *Rhodocyclus* in a full-scale waste water treatment plant and their participation in enhanced biological phosphorus removal. Water Sci. Technol. 2002a, 46, 123-128.

199. Zilles, J.L., Peccia, J., Kim, M.W., Hung, C.H., Noguera, D.R. Involvement of *Rhodocyclus*-related organisms in phosphorus removal in full-scale wastewater treatment plants. Appl. Environ. Microbiol. 2002b, 68, 2763-2769.

Acknowledgments

Annex I: List of media and solutions (all values given in g or mL)

1: *ATCC* 436 (methanol medium)

Methanol medium	pH 7.0
Methanol	5 mL
Trace element solution I	3 drops
Solution A	10 mL
Solution B	1 mL
Solution C	5 mL
Distilled water	ad up to 1000 mL
Solution A	
KH_2PO_4	0.681 g
K_2HPO_4	0.871 g
Distilled water	10 mL
Solution B	
$CaCl_2$ x $2H_2O$	0.004 g
Distilled water	1 mL
Solution C	
NH_4Cl	0.764 g
Distilled water	5 mL

2: DSM 1 (nutrient agar)

DSM 1	pH 7.0
Peptone (pancreatic)	5.000 g
Meat extract	3.000 g
Agar, if required	15.000 g
Distilled water	ad up to 1000.0 mL

3: DSM 63 (*Desulfovibrio* medium)

DSM 63	pH 7.8
Solution A	
K_2HPO_4	0.500 g
NH_4Cl	1.000 g
Na_2SO_4	1.000 g
$CaCl_2$ x $2H_2O$	0.100 g
$MgSO_4$ x $7H_2O$	2.000 g
DL-Na-lactate	2.000 g
Yeast extract	1.000 g
Resazurin	0.001 g
Solution B	10 mL
Solution C	10 mL
Distilled water	ad up to 1000.0 mL
Solution B	
$FeSO_4$ x $7H_2O$	0.500 g
Distilled water	10.0 mL
Solution C	
Na-thioglycolate	0.100 g
Ascorbic acid	0.100 g
Distilled water	10.0 mL

4: Denitrification medium (SAEZ *et al.*, 2003)

Denitrification medium	pH 7.2
NaNO$_3$	3.000 g
K$_2$HPO$_4$	1.000 g
MgSO$_4$ x 7H$_2$O	0.500 g
KCI	0.500 g
FeSO$_4$ x 7H$_2$O	0.010 g
Sucrose	2.000 g
Distilled water	ad up to 1000.0 mL

5: DSM 120 (*Methanosarcina* medium)

DSM 120	pH 6.5-6.8
K$_2$HPO$_4$	0.348 g
KH$_2$PO$_4$	0.227 g
NH$_4$Cl	0.500 g
MgSO$_4$ x 7H$_2$O	0.500 g
CaCl$_2$ x 2H$_2$O	0.250 g
NaCl	2.250 g
FeSO$_4$ x 7H$_2$O	0.002 g
Yeast extract (Difco)	2.000 g
Casitone (Difco)	2.000 g
Resazurin	0.001 g
NaHCO$_3$	0.850 g
Cysteine-HCl x H$_2$O	0.300 g
Na$_2$S x 9H$_2$O	0.300 g
Methanol	10.00 mL
Trace element solution II	1.00 mL
Vitamin solution IV	10.00 mL
Distilled water	ad up to 1000.0 mL

6: Synthetic wastewater (modified, after HRENOVIC *et al.*, 2003)

Synthetic wastewater	pH 7.0
Na-propionate	0.500 g
Na-acetate	1.000 g
Peptone from meat (pancreatic)	0.100 g
MgSO$_4$ x 7H$_2$O	0.010 g
CaCl$_2$ x 6H$_2$O	0.006 g
KCl	0.030 g
Yeast extract	0.020 g
KH$_2$PO$_4$	0.220 g
Distilled water	ad up to 1000.0 mL

7: Peptone media

Peptone media	pH 7.0
Peptone from meat (pancreatic)	5.000 g
NaCl	3.000 g
K$_2$HPO$_4$	2.000 g
Meat extract	10.00 g
Yeast extract	10.00 g
Glucose	5.000 g
Distilled water	ad up to 1000.0 mL

8: DSM 776 (*Microlunatus* medium)

DSM 776	pH 7.0
Glucose	0.500 g
Peptone	0.500 g
Yeast extract	0.500 g
Na-glutamate	0.500 g
KH_2PO_4	0.500 g
$(NH_4)_2SO_4$	0.100 g
$MgSO_4$ x $7H_2O$	0.100 g
Distilled water	ad up to 1000.0 mL

9: M9 minimal medium (MANIATIS *et al.*, 1982)

M9 minimal medium	pH 7.4
Solution A	
Solution B	100 mL
$MgSO_4$ (1M)	2 mL
$CaCl_2$ (1M)	0.1 mL
Glucose (40%)	5 mL
Distilled water	ad up to 1000.0 mL
Solution B	
Na_2HPO_4	60.00 g
KH_2PO_4	30.00 g
NaCl	5.000 g
NH_4Cl	10.00 g
Distilled water	ad up to 1000.0 mL

10: OECD synthetic wastewater

OECD synthetic wastewater	pH 7.0
Peptone from meat (pancreatic)	0.160 g
Meat extract	0.110 g
Urea	0.030 g
KH_2PO_4	0.028 g
NaCl	0.007 g
$CaCl_2$ x $2H_2O$	0.004 g
$MgSO_4$ x $7H_2O$	0.002 g
Trace element solution III	2 mL
Distilled water	ad up to 1000.0 mL

I: Trace element solution I

Trace element solution I	
$MgSO_4$ x $7H_2O$	71.20 g
$ZnSO_4$ x $7H_2O$	0.440 g
$MnSO_4$ x H_2O	0.615 g
$CuSO_4$ x $5H_2O$	0.785 g
Na_2MoO_4 x $2H_2O$	0.252 g
$FeSo_4$ x $7H_2O$	4.980 g
H_2SO_4 (1N)	ad up to 100 mL

II: Trace element solution II

Trace element solution II	
$FeCl_2$ x $4H_2O$	1.500 g
$ZnCl_2$	0.070 g
$MnCl_2$ x $4H_2O$	0.100 g
H_3BO_3	0.006 g
$CoCl_2$ x $6H_2O$	0.190 g
$CuCl_2$ x $2H_2O$	0.002 g
$NiCl_2$ x $6H_2O$	0.024 g
Na_2MoO_4 x $2H_2O$	0.036 g
HCl (25%)	10.0 mL
Distilled water	ad up to 1000.0 mL

III: Trace element solution III

Trace element solution III	
$ZnCl_2$	0.070 g
$MnCl_2$ x $4H_2O$	0.100 g
$CoCl_2$ x $6H_2O$	0.200 g
$NiCl_2$ x $6H_2O$	0.100 g
$CuCl_2$ x $2H_2O$	0.020 g
$NaMoO_4$ x $2H_2O$	0.050 g
Na_2SeO_3 x $5H_2O$	0.026 g
HCl (25%)	1 mL
Distilled water	ad up to 1000.0 mL

IV: Vitamin solution IV

Vitamin solution IV	
Biotin	0.002 g
Folic acid	0.002 g
Pyridoxine-HCl	0.010 g
Thiamine-HCl x $2H_2O$	0.005 g
Riboflavin	0.005 g
Nicotinic acid	0.005 g
D-Ca-pantothenate	0.005 g
Vitamin B12	0.001 g
p-Aminobenzoic acid	0.005 g
Lipoic acid	0.005 g
Distilled water	ad up to 1000.0 mL

V: DAPI staining solution

DAPI staining solution	
Solution A	
Citric acid	2.100 g
Tween 20	0.500 g
Bidestilled water	100 mL
Solution B 0.24 µM DAPI (**1 µM** DAPI)	
Disodiumhydrogenphosphate	7.100 g
Solution C	0.17 (**0.72**) mL
Bidestilled water	99.83 (**99.28**) mL
Solution C (DAPI stock solution 143 µM)	
4`,6-diamidino-2`-phenylindole (DAPI)	0.0005 g
Dimethylformamide	0.100 mL
Bidestilled water	9.9 mL

Annex II: Fixation efficiency

Table 10. Pure cultures and their response towards tested metal solutions at different time points. Shown are the numbers of sub-populations (subp.) fitting into the 10% and the 25% tolerance interval. Stable samples where all of the sub-populations fit at least into the 25% tolerance interval have a grey background. n.d.: not determined, [1]: in PBS with 10% sodium azide

	[d]	Al[1]		Ba[1]		Bi[1]		Co[1]		Mo[1]		Ni[1]		W[1]		NaN$_3$		Ba, Ni, Bi[1]		Ba, Ni[1]	
		10%	25%	10%	25%	10%	25%	10%	25%	10%	25%	10%	25%	10%	25%	10%	25%	10%	25%	10%	25%
Desulfovibrio desulfuricans (anaerobic, 3 subp.)	1	0	0	3	3	1	3	0	0	3	3	3	3	0	0	0	0	3	3	3	3
	2	0	0	3	3	1	3	0	0	3	3	3	3	0	0	0	0	3	3	3	3
	7	0	0	3	3	1	3	0	0	3	3	3	3	0	0	0	0	3	3	3	3
	9	n. d.	n.d.	n. d.	n.d.	n. d.	n.d.	n. d.	n.d.	n. d.	n.d.	n. d.	n.d.	n. d.	n.d.	n. d.	n.d.	2	3	3	3
	13	n. d.	n.d.	n. d.	n.d.	n. d.	n.d.	n. d.	n.d.	n. d.	n.d.	n. d.	n.d.	n. d.	n.d.	n. d.	n.d.	2	3	3	3
	17	n. d.	n.d.	n. d.	n.d.	n. d.	n.d.	n. d.	n.d.	n. d.	n.d.	n. d.	n.d.	n. d.	n.d.	n. d.	n.d.	2	3	3	3
	24	n. d.	n.d.	n. d.	n.d.	n. d.	n.d.	n. d.	n.d.	n. d.	n.d.	n. d.	n.d.	n. d.	n.d.	n. d.	n.d.	2	2	3	3
	29	0	0	0	0	0	0	0	0	0	0	0	0	0	0	0	0	2	2	2	3
Shewanella putrefaciens (aerobic, 5 subp.)	1	1	4	5	5	3	5	0	1	1	2	3	5	3	3	1	2	5	5	5	5
	2	1	4	5	5	3	5	0	1	1	2	3	5	3	3	1	2	5	5	5	5
	7	1	4	5	5	3	5	0	1	1	2	3	5	3	3	1	2	3	5	5	5
	9	n. d.	n.d.	n. d.	n.d.	n. d.	n.d.	n. d.	n.d.	n. d.	n.d.	n. d.	n.d.	n. d.	n.d.	n. d.	n.d.	3	5	5	5
	13	n. d.	n.d.	n. d.	n.d.	n. d.	n.d.	n. d.	n.d.	n. d.	n.d.	n. d.	n.d.	n. d.	n.d.	n. d.	n.d.	3	4	4	4
	17	n. d.	n.d.	n. d.	n.d.	n. d.	n.d.	n. d.	n.d.	n. d.	n.d.	n. d.	n.d.	n. d.	n.d.	n. d.	n.d.	2	3	4	4
	24	n. d.	n.d.	n. d.	n.d.	n. d.	n.d.	n. d.	n.d.	n. d.	n.d.	n. d.	n.d.	n. d.	n.d.	n. d.	n.d.	0	3	3	4
	29	0	0	1	2	0	2	0	1	0	1	2	3	0	0	1	2	0	4	3	3
Paracoccus denitrificans (anaerobic, 4 subp.)	1	2	4	4	4	2	2	1	2	1	2	1	4	2	4	2	2	2	2	3	4
	2	2	4	4	4	2	2	1	2	1	2	1	4	2	4	2	2	2	2	3	4
	7	1	2	4	4	2	2	1	2	1	2	1	4	2	4	2	2	2	2	3	4
	9	1	2	4	4	2	3	1	2	1	3	1	2	2	4	1	1	2	2	2	4
	13	1	1	2	3	2	2	1	2	1	1	1	2	1	2	1	2	2	4	2	2
	17	1	2	2	3	1	2	1	3	1	2	1	2	1	2	1	2	1	3	2	3
	24	1	2	2	2	1	2	1	2	1	2	1	1	1	3	1	2	1	3	2	2
	29	1	1	2	2	1	3	1	2	1	0	1	3	1	2	1	2	1	2	2	2

Paracoccus denitrificans (aerobic, 4 subp.)	1	1	2	3	4	2	2	2	2	2	2	3	4	3	4	1	2	2	4	4	4
	2	1	2	3	4	2	2	2	2	2	2	3	4	3	4	1	2	2	4	4	4
	7	1	2	3	4	2	2	2	2	2	2	3	4	3	4	1	2	2	4	4	4
	9	n. d.	n.d.	n. d.	n.d.	n. d.	n.d.	n. d.	n.d.	n. d.	n.d.	n. d.	n.d.	n. d.	n.d.	n. d.	n.d.	2	4	4	4
	13	n.d.	n.d.	n. d.	n.d.	n. d.	n.d.	n. d.	n.d.	n. d.	n.d.	n. d.	n.d.	n. d.	n.d.	n. d.	n.d.	2	3	3	4
	17	n.d.	n.d.	n. d.	n.d.	n. d.	n.d.	n. d.	n.d.	n. d.	n.d.	n. d.	n.d.	n. d.	n.d.	n. d.	n.d.	2	4	2	3
	24	n.d.	n.d.	n. d.	n.d.	n. d.	n.d.	n. d.	n.d.	n. d.	n.d.	n. d.	n.d.	n. d.	n.d.	n. d.	n.d.	1	2	1	3
	29	1	2	2	3	2	3	1	2	1	2	1	2	2	2	1	1	0	1	0	4
Methanomonas methylovora (aerobic, 4 subp.)	1	1	1	3	4	2	2	0	1	1	1	2	4	2	4	1	2	4	4	4	4
	2	1	1	3	4	2	2	0	1	1	1	2	4	2	4	1	2	4	4	4	4
	7	1	1	3	4	2	2	0	1	1	1	2	4	2	4	1	2	0	4	4	4
	9	n. d.	n. d.	n. d.	n.d.	n. d.	n.d.	n. d.	n. d.	n. d.	n. d.	n.d.	n.d.	n.d.	n.d.	n. d.	n.d.	0	4	4	4
	13	n. d.	n. d.	n. d.	n.d.	n. d.	n.d.	n. d.	n. d.	n. d.	n. d.	n.d.	n.d.	n.d.	n.d.	n. d.	n.d.	0	1	2	3
	17	n. d.	n. d.	n. d.	n.d.	n. d.	n.d.	n. d.	n. d.	n. d.	n. d.	n.d.	n.d.	n.d.	n.d.	n. d.	n.d.	0	0	2	3
	24	n. d.	n. d.	n. d.	n.d.	n. d.	n.d.	n. d.	n. d.	n. d.	n. d.	n.d.	n.d.	n.d.	n.d.	n. d.	n.d.	0	0	1	2
	29	1	1	1	1	1	2	0	1	2	3	0	1	1	2	0	2	0	0	1	3
Methanosarcina barkeri (anaerobic, 6 subp.)	1	n. d.	n. d.	n. d.	n. d.	n. d.	n. d.	n. d.	n. d.	n. d.	n. d.	n. d.	n. d.	n. d.	n. d.	3	3	2	6	5	6
	2	n. d.	n. d.	n. d.	n. d.	n. d.	n. d.	n. d.	n. d.	n. d.	n. d.	n. d.	n. d.	n. d.	n. d.	3	3	2	6	5	6
	7	n. d.	n. d.	n. d.	n. d.	n. d.	n. d.	n. d.	n. d.	n. d.	n. d.	n. d.	n. d.	n. d.	n. d.	3	3	2	6	5	6
	9	n. d.	n. d.	n. d.	n. d.	n. d.	n. d.	n. d.	n. d.	n. d.	n. d.	n. d.	n. d.	n. d.	n. d.	3	3	1	6	5	6
	13	n. d.	n. d.	n. d.	n. d.	n. d.	n. d.	n. d.	n. d.	n. d.	n. d.	n. d.	n. d.	n. d.	n. d.	2	4	1	4	4	5
	17	n. d.	n. d.	n. d.	n. d.	n. d.	n. d.	n. d.	n. d.	n. d.	n. d.	n. d.	n. d.	n. d.	n. d.	2	4	1	4	4	5
	24	n. d.	n. d.	n. d.	n. d.	n. d.	n. d.	n. d.	n. d.	n. d.	n. d.	n. d.	n. d.	n. d.	n. d.	0	2	0	3	2	3
	29	n. d.	n. d.	n. d.	n. d.	n. d.	n. d.	n. d.	n. d.	n. d.	n. d.	n. d.	n. d.	n. d.	n. d.	0	2	0	3	2	3

Table 11. Response of the activated sludge samples towards tested metal solutions at different time points. Shown are the numbers of sub-populations fitting into the 10% and the 25% tolerance interval. Stable samples where all of the sub-populations fit at least in to the 25% tolerance interval have a grey background. A total number of 15 sub-communities were found for the activated sludge samples from aerobic and anaerobic phase. [1]: in PBS with 10% sodium azide; [2]: 0.5 g L^{-1} Tween 20; [3]: 15% glycerine

	[d]	unfixed		NaN$_3$		5 mM Ba, Ni[1]		15 mM Ba, Ni[1]		5 mM Ba, Ni[1,2]		15 mM Ba, Ni[1,2]		-20°C, PBS		-20°C, PBS/glycerine	
		10%	25%	10%	25%	10%	25%	10%	25%	10%	25%	10%	25%	10%	25%	10%	25%
activated sludge (aerobic phase, 15 sub-communities)	1	2	11	1	2	15	15	12	15	7	9	4	5	6	9	1	1
	2	0	8	1	1	14	15	9	15	7	14	4	4	6	10	1	3
	3	0	7	1	1	13	15	8	15	7	8	4	4	2	8	0	0
	7	0	8	0	0	13	15	7	15	5	8	4	5	2	7	0	2
	9	0	3	0	0	12	15	5	6	4	8	2	2	1	7	0	1
	14	0	5	0	0	8	8	4	6	3	7	2	4	1	6	0	1
	16	0	3	0	0	6	9	3	6	3	6	2	4	1	6	0	1
	21	0	5	0	0	3	4	3	7	3	9	1	1	1	6	0	1
activated sludge (anaerobic phase, 15 sub-communities)	1	4	12	3	3	13	15	14	15	6	11	7	10	5	7	4	8
	2	2	6	2	3	13	15	11	15	6	11	7	9	3	6	3	8
	3	1	12	1	2	13	15	11	15	4	10	6	10	2	6	2	8
	7	0	10	1	6	13	15	11	15	4	10	4	6	1	7	2	9
	9	0	6	1	2	11	15	12	13	1	9	4	4	0	2	2	8
	14	0	7	1	3	11	13	8	13	0	9	3	4	0	7	2	7
	16	0	6	0	0	5	8	5	8	0	5	3	11	0	4	2	10
	21	0	8	0	0	4	4	1	7	0	4	2	7	0	3	1	9

Annex III: Sequencing results of representative 16S rRNA gene clones derived from Tc stained and sorted cells of the WWTP Elsterwerda (Results, section 2.4)

Table 12. Sequencing results of 16S rRNA gene clones.

Clone	Acc. No.	Highest BLAST hit (Acc. no.) / Identity	Taxonomic affiliation according to RDP
B3 (471 bp)	EU850359	Uncultured betaproteobacterium clone S7 (AF447793) / 98%	*Rhodocyclaceae*
C10 (475 bp)	EU850366	Uncultured betaproteobacterium clone nsc151 (DQ211501) / 100%	*Rhodocyclaceae*
C11 (501 bp)	EU850367	Uncultured bacterium SA34 (AF245349) / 99%	*Rhodocyclaceae*
D7 (525 bp)	EU850371	Uncultured bacterium clone UTFS-002-12-23 (AB166771) / 99%	*Rhodocyclaceae*
D10 (483 bp)	EU850372	Uncultured bacterium clone UTFS-002-12-23 (AB166771) / 99%	*Rhodocyclaceae*
E3 (468 bp)	EU850376	Uncultured bacterium SA34 (AF245349) / 99%	*Rhodocyclaceae*
E4 (477 bp)	EU850377	Uncultured bacterium clone VIR_D5 (EF565151) / 99%	*Rhodocyclaceae*
E6 (458 bp)	EU850379	Uncultured bacterium clone VIR_D5 (EF565151) / 99%	*Rhodocyclaceae*
E8 (516 bp)	EU850381	Uncultured bacterium SA34 (AF245349) / 98%	*Rhodocyclaceae*
F5 (497 bp)	EU850384	Uncultured bacterium clone UTFS-002-12-23 (AB166771) / 99%	*Rhodocyclaceae*
F11 (485 bp)	EU850389	Uncultured bacterium clone VIR_D5 (EF565151) / 98%	*Rhodocyclaceae*
H5 (512 bp)	EU850394	Uncultured bacterium clone D07 (EF589969) / 97%	*Rhodocyclaceae*
OTU 1		27 clones	*Rhodocyclaceae*
A1 (425 bp)	EU850352	*Pseudomonas putida* KT2440 (AE015451) / 99%	*Pseudomonas* sp.
E5 (443 bp)	EU850378	*Pseudomonas putida* isolate 24 (EU438854) / 99%	*Pseudomonas* sp.
E12 (515 bp)	EU850383	*Pseudomonas putida* BM2 (DQ989291) / 99%	*Pseudomonas* sp.
OTU 2		13 clones	*Pseudomonas* sp.
B1 (291 bp)	EU850358	Uncultured *Nitrospira* sp. clone 0B11 (EU499597) / 98%	*Nitrospira* sp.
B8 (578 bp)	EU850362	Uncultured *Nitrospira* sp. clone 3 (DQ414437) / 99%	*Nitrospira* sp.
E2 (463 bp)	EU850375	Uncultured *Nitrospira* sp. clone 3 (DQ414437) / 99%	*Nitrospira sp.*
OTU 3		7 clones	*Nitrospira* sp.
A2 (407 bp)	EU850353	Uncultured gammaproteobacterium clone GB2917y (DQ201885) / 96%	*Gammaproteobacteria*
A5 (389 bp)	EU850355	Uncultured gammaproteobacterium clone GB2917y (DQ201885) / 95%	*Gammaproteobacteria*
A7 (477 bp)	EU850357	Uncultured gammaproteobacterium clone GB2917y (DQ201885) / 94%	*Gammaproteobacteria*
OTU 4		7 clones	*Gammaproteobacteria*
A3 (485 bp)	EU850354	Uncultured eubacterium clone F13.46 (AF495440) / 98%	*Tetrasphaera* sp.

E9 (451 bp)	EU850382	Uncultured bacterium clone Ebpr19 (AF255629) / 99%	*Tetrasphaera* sp.
F9 (473 bp)	EU850387	Uncultured eubacterium clone F13.46 (AF495440) / 98%	*Tetrasphaera* sp.
OTU 5		4 clones	*Tetrasphaera* sp.
A6 (447 bp)	EU850356	*Dechloromonas* sp. A34 (EF632559) / 97%	*Dechloromonas* sp.
D11 (504bp)	EU850373	Uncultured bacterium clone ORS10C_g11 (EF392932) / 99%	*Dechloromonas* sp.
E7 (535 bp)	EU850380	*Dechloromonas* sp. A34 (EF632559) / 97%	*Dechloromonas* sp.
OTU 6		4 clones	*Dechloromonas* sp.
B7 (448 bp)	EU850361	Uncultured actinobacterium clone DOK_NOFERT_clone341 (DQ829293) / 96%	*Actinomycetales*
F8 (450 bp)	EU850386	Uncultured actinobacterium clone DOK_NOFERT_clone341 (DQ829293) / 96%	*Actinomycetales*
OTU 7		2 clones	*Actinomycetales*
E1 (438 bp)	EU850374	Uncultured bacterium clone T015D (AM158382) / 91%	Candidate division TM7
H2 (428 bp)	EU850393	Uncultured bacterium clone IC-61 (AB255073) / 93%	Candidate division TM7
OTU 8		2 clones	Candidate division TM7
C12 (530 bp)	EU850368	Uncultured bacterium clone DSSD59 (AY328757) / 98%	*Alphaproteobacteria*
G12 (559 bp)	EU850392	*Derxia gummosa* (AB089482) / 95%	*Betaproteobacteria*
C2 (413 bp)	EU850365	Uncultured bacterium clone 197up (AY212650) / 99%	*Burkholderiales*
B10 (532 bp)	EU850363	*Ralstonia detusculanense* (AF280433) / 99%	*Ralstonia* sp.
D1 (452 bp)	EU850369	Uncultured bacterium clone TH-141 (AB184983) / 98%	*Comamonadaceae*
F7 (457 bp)	EU850385	Uncultured bacterium clone 44 (DQ413103) / 99%	*Rhodocyclaceae*
G10 (449 bp)	EU850391	Uncultured bacterium clone SRRB48 (AB240518) / 96%	*Nocardioidaceae*
B5 (458 bp)	EU850360	Uncultured *Sphingobacteria* bacterium clone ADK-SGe02-50 (EF520599) / 96%	*Sphingobacteriales*
B11 (522 bp)	EU850364	Uncultured bacterium clone HM15 (AM909923) / 95%	*Acidobacteriaceae*
F10 (495 bp)	EU850388	Uncultured bacterium clone LaP15L89 (EF667686) / 99%	*Caldilinea* sp.
D5 (435 bp)	EU850370	Uncultured bacterium clone mdt16a02 (AY537009) / 98%	*Bacteria*
F12 (574 bp)	EU850390	Uncultured bacterium clone 032D06_P_BA_P3 (BX294877) / 92%	*Bacteria*

Annex IV: List of measured abiotic and biotic parameters of WWTP Eilenburg

Table 13. Measured abiotic and biotic parameters. PC: primary clarifier, AT: aeration tank, T: temperature, a. v.: air velocity, h: humidity, a. p.: air pressure, WW: wastewater, IC: inorganic carbon, TOC: total organic carbon, TN: total nitrogen, amount $_{r.s.}$: amount of return sludge (reused sludge from AT 1 and 2), TC: total carbon, COD: chemical oxygen demand, NH$_4$-N: ammonium nitrogen, e. c.: electrical conductivity, aut. part.: autofluorescent particles, a. r.: aeration regime, Tc: tetracycline hydrochloride, n. l. l. c.: neutral lipid like compound

number	abiotic	mean
1	T_{max} [°C]	25.3 (± 5.2)
2	T_{min} [°C]	12.5 (± 3.5)
3	a. v. [km h^{-1}]	13.1 (± 4.3)
4	h $_{max}$ [%]	90.1 (± 5.9)
5	h $_{min}$ [%]	33.8 (± 7.0)
6	a. p. $_{max}$ [hPa]	1019.5 (± 4.1)
7	a. p. $_{min}$ [hPa]	1014.7 (± 4.7)
8	rain [mm d^{-1}]	0.8 (± 1.9)
9	sunshine [h d^{-1}]	10.3 (± 3.8)
10	brewery discharge [m³]	662.4 (± 78.6)
11	blackwater [m³]	2.3 (± 3.4)
12	T $_{air}$ [°C]	19.0 (± 3.1)
13	amount $_{influent}$ [m³]	71.2 (± 17.4)
14	pH $_{influent}$	6.9 (± 0.5)
15	T $_{influent}$ [°C]	18.0 (± 1.5)
16	e. c. $_{influent}$ [mS cm^{-1}]	1.5 (± 0.2)
17	turbidity $_{effluent}$	17.5 (± 13.2)
18	T $_{effluent}$ [°C]	20.9 (± 2.0)
19	e. c. $_{effluent}$ [mS cm^{-1}]	1.3 (± 0.1)
20	aut. part. PC [%]	0.2 (± 0.3)
21	nitrate PC [mg L^{-1}]	0.9 (± 1.1)
22	nitrite PC [mg L^{-1}]	2.4 (± 4.0)
23	phosphate PC [mg L^{-1}]	9.5 (± 6.7)
24	COD PC [mg L^{-1}]	1063.0 (± 451.0)
25	TC PC [mg L^{-1}]	502.3 (± 196.8)
26	IC PC [mg L^{-1}]	113.3 (± 26.0)
27	TOC PC [mg L^{-1}]	389.0 (± 198.8)
28	TN PC [mg L^{-1}]	56.6 (± 21.0)
29	NH$_4$-N PC [mg L^{-1}]	32.4 (± 17.5)
30	a. r. AT1	1.1 (± 0.4)
31	a. p. AT1 [%]	0.2 (± 0.3)
32	oxygen [mg L^{-1}] AT1	0.5 (± 0.5)
33	redox potential [mV] AT1	-12.5 (± 129.3)
34	T $_{WW}$ AT1 [°C]	21.7 (± 2.5)
35	amount $_{r. s.}$ AT1 [m³]	33.7 (± 7.8)
36	nitrate AT1 [mg L^{-1}]	0.1 (± 0.1)
37	nitrite AT1 [mg L^{-1}]	8.5 (± 17.8)
38	phosphate AT1 [mg L^{-1}]	2.5 (± 3.3)
39	COD AT1 [mg L^{-1}]	6197.5 (± 432.5)
40	TC AT1 [mg L^{-1}]	2339.9 (± 430.5)

41	IC AT1 [mg L^{-1}]	171.1 (± 29.5)
42	TOC AT1 [mg L^{-1}]	2143.8 (± 408.2)
43	TN AT1 [mg L^{-1}]	428.7 (± 81.1)
44	NH$_4$-N AT1 [mg L^{-1}]	0.7 (± 1.0)
45	a. r. AT2	1.9 (± 0.4)
46	a. p. AT2 [%]	0.1 (± 0.1)
47	oxygen [mg L^{-1}] AT2	0.3 (± 0.3)
48	redox potential [mV] AT2	-248.1 (± 122.9)
49	T $_{WW}$ AT2 [°C]	21.1 (± 2.4)
50	amount r. s. AT2 [m³]	34.5 (± 7.8)
51	nitrate AT2 [mg L^{-1}]	0.3 (± 0.4)
52	nitrite AT2 [mg L^{-1}]	2.4 (± 2.7)
53	phosphate AT2 [mg L^{-1}]	5.1 (± 10.1)
54	COD AT2 [mg L^{-1}]	5885.0 (± 1247.0)
55	TC AT2 [mg L^{-1}]	1933.4 (± 588.3)
56	IC AT2 [mg L^{-1}]	186.3 (± 66.3)
57	TOC AT2 [mg L^{-1}]	1747.1 (± 576.8)
58	TN AT2 [mg L^{-1}]	370.9 (± 121.3)
59	NH$_4$-N AT2 [mg L^{-1}]	1.9 (± 2.3)
60	week day	

number	biotic	mean [% of all cells]
1	I	7.2 (± 3.0)
2	II	5.8 (± 2.4)
3	III	1.7 (± 0.4)
4	IV	4.3 (± 0.7)
5	V	0.7 (± 0.8)
6	VI	0.8 (± 0.7)
7	VII	1.5 (± 0.8)
8	VIII	2.4 (± 0.8)
9	IX	2.2 (± 0.5)
10	X	2.4 (± 1.0)
11	XI	7.2 (± 2.9)
12	cells with n.l.l.c. PC	6.4 (± 7.8)
13	Tc-stained cells PC	6.7 (± 9.1)
14	1 AT1	3.7 (± 1.2)
15	2 AT1	9.0 (± 2.4)
16	3 AT1	3.7 (± 0.9)
17	4 AT1	7.2 (± 2.7)
18	5 AT1	4.5 (± 1.3)
19	6 AT1	0.9 (± 0.2)
20	7 AT1	3.6 (± 1.6)
21	8 AT1	1.0 (± 0.3)
22	9 AT1	3.1 (± 1.0)
23	10 AT1	0.9 (± 0.2)
24	11 AT1	0.8 (± 0.2)
25	12 AT1	1.8 (± 0.3)
26	13 AT1	1.3 (± 0.4)
27	14 AT1	1.2 (± 0.3)

28	15 AT1	1.1 (± 0.3)
29	cells with n.l.l.c. AT1	6.6 (± 3.3)
30	Tc-stained cells AT1	16.1 (± 5.8)
31	1 AT2	3.2 (± 0.7)
32	2 AT2	9.2 (± 2.4)
33	3 AT2	3.9 (± 0.9)
34	4 AT2	7.1 (± 2.5)
35	5 AT2	4.7 (± 1.3)
36	6 AT2	1.0 (± 0.3)
37	7 AT2	3.7 (± 1.4)
38	8 AT2	1.0 (± 0.3)
39	9 AT2	3.3 (± 1.0)
40	10 AT2	1.1 (± 0.3)
41	11 AT2	0.9 (± 0.1)
42	12 AT2	1.9 (± 0.3)
43	13 AT2	1.3 (± 0.3)
44	14 AT2	1.2 (± 0.3)
45	15 AT2	1.1 (± 0.3)
46	cells with n.l.l.c. AT2	9.4 (± 7.8)
47	Tc-stained cells AT2	17.5 (± 7.3)

Annex V: Community pattern at the three sampling points of WWTP Eilenburg

a) Primary clarifier (PC)

Figure 45. Dot plots from the flow cytometric analysis of the primary clarifier over 29 days of sampling. black ellipses indicate electronic noise, dotted ellipses indicate blue fluorescent beads
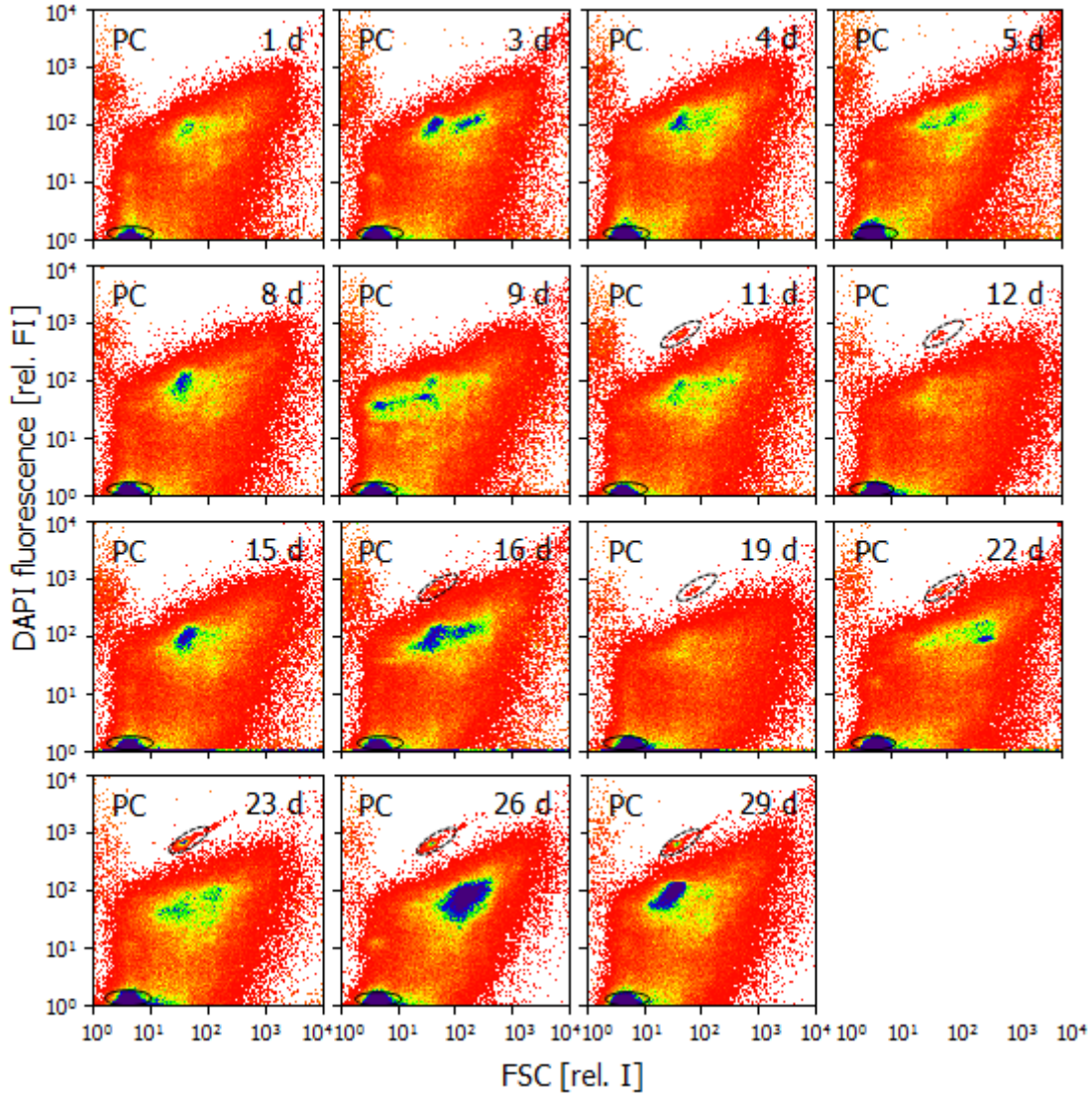
b) Aeration tank 1 (AT 1)

Figure 46. Dot plots from the flow cytometric analysis of the aeration tank 1 over 29 days of sampling. black ellipses indicate electronic noise, dotted ellipses indicate blue fluorescent beads
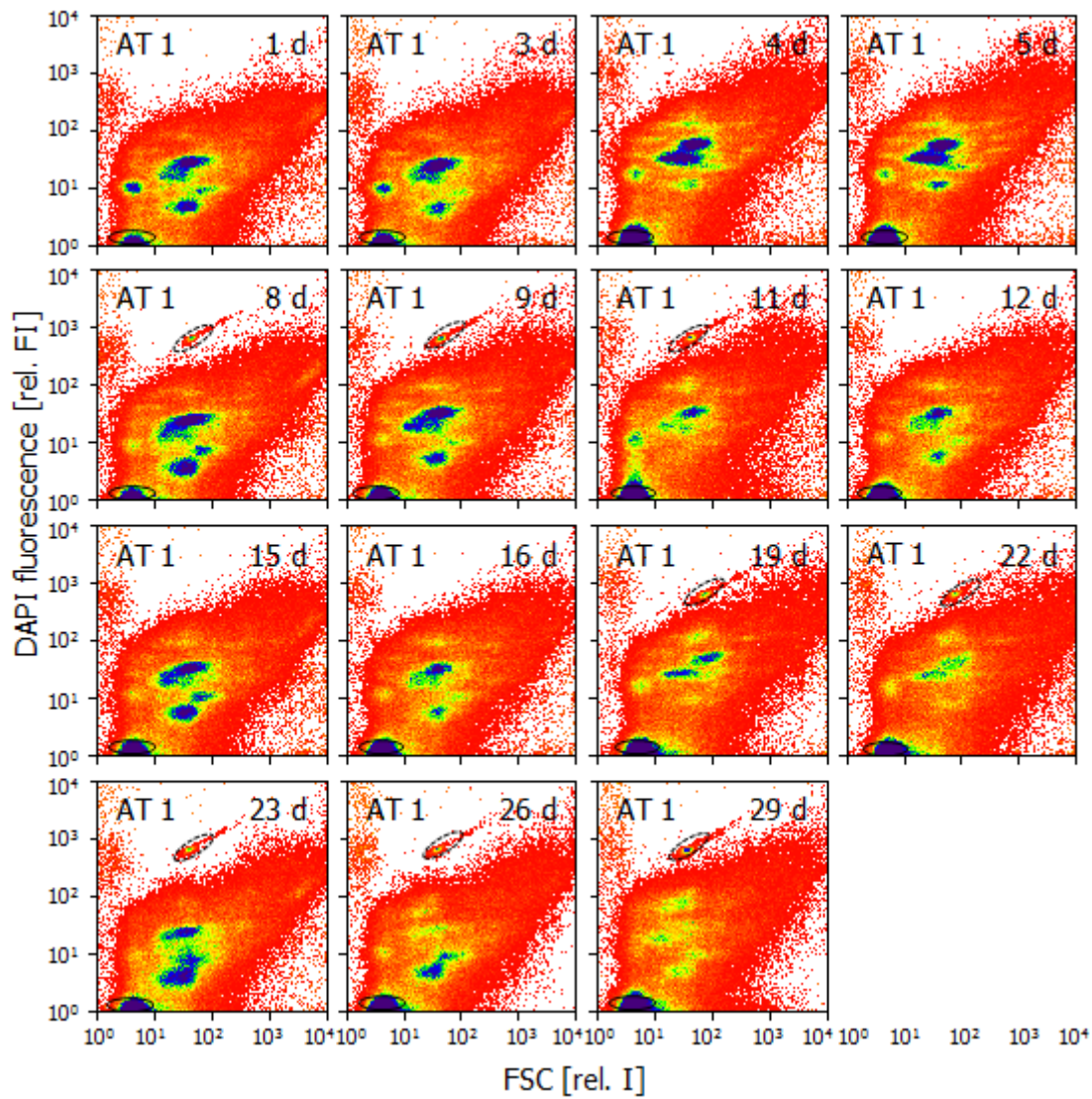
c) Aeration tank 2 (AT 2)

Figure 47. Dot plots from the flow cytometric analysis of the aeration tank 1 over 29 days of sampling. black ellipses indicate electronic noise, dotted ellipses indicate blue fluorescent beads
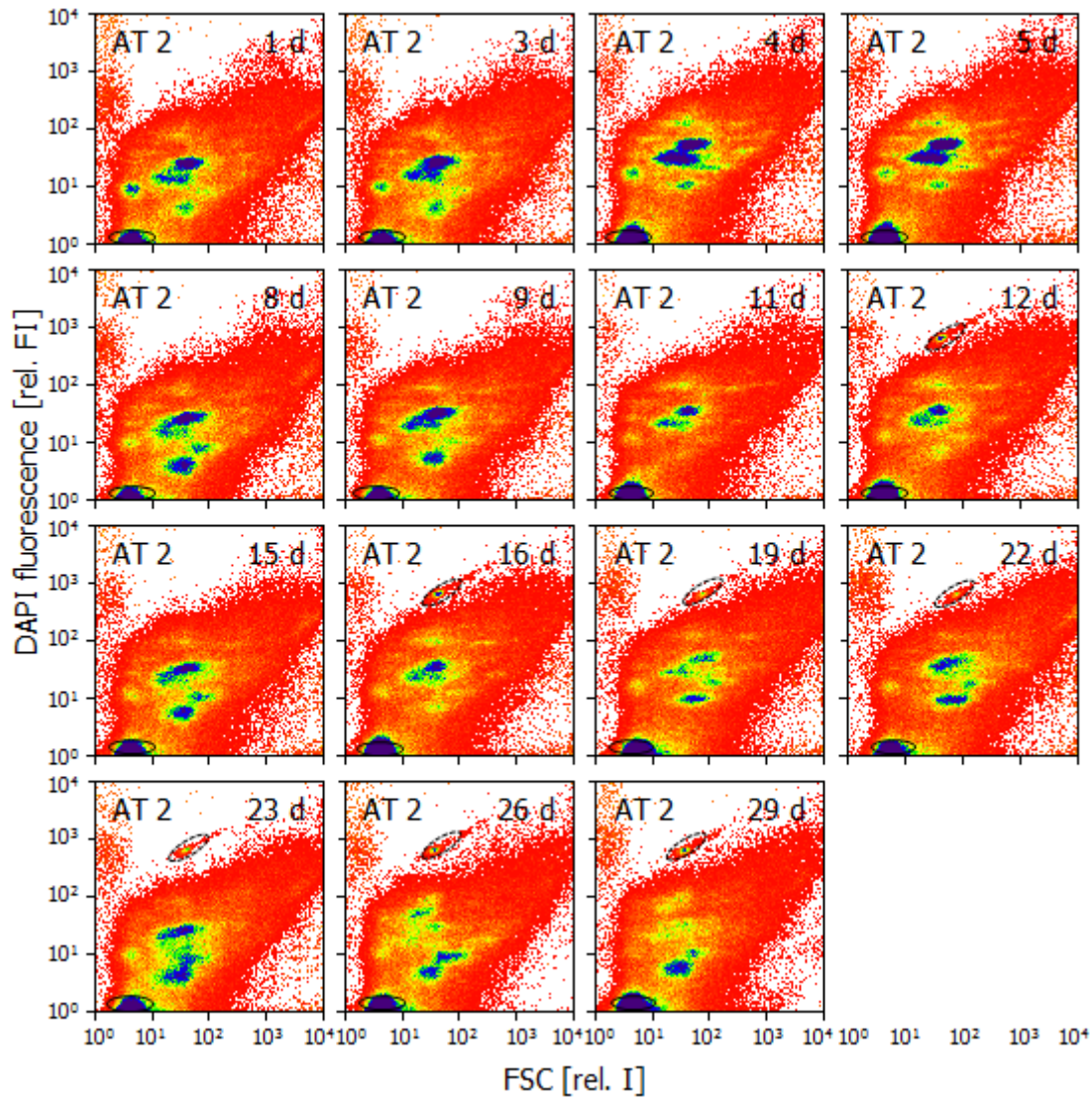
Annex VI: Clone library of sorted samples from WWTP Eilenburg

Table14. Sequencing results of 16S rRNA gene clones.

Clone	bp	Highest BLAST hit (Acc. no.) / Sequence identity	Taxonomic affiliation according to RDP 10
P1_B12	515	Uncultured bacterium clone V201-144 (HQ114159.1) / 99%	*Sphingobacteriales*
P1_C10	517	Uncultured bacterium clone AK1DE1_08E (GQ396988.1) / 99%	*Sphingobacteriales*
P1_C11	515	Uncultured bacterium clone V201-144 (HQ114159.1) / 99%	*Sphingobacteriales*
P1_C5	522	Uncultured bacterium clone ambient_uncontrolled-22 (GU454883.1) / 98%	*Sphingobacteriales*
P1_E10	502	Uncultured bacterium clone V201-144 (HQ114159.1) / 99%	*Sphingobacteriales*
P1_F6	525	Uncultured bacterium clone RBC1-68 (AB567802.1) / 97 %	*Sphingobacteriales*
P2_B6	527	Uncultured bacterium clone V201-144 (HQ114159.1) / 99%	*Sphingobacteriales*
P2_D6	545	Uncultured bacterium clone V201-144 (HQ114159.1) / 99%	*Sphingobacteriales*
P2_E8	630	Uncultured bacterium clone RBC4-10 (AB567918.1) / 98%	*Sphingobacteriales*
P2_F1	437	Uncultured eubacterium clone F13.14 (AF495420.1) / 99%	*Sphingobacteriales*
P2_F5	444	Uncultured bacterium clone RBC1-68 (AB567802.1) / 99%	*Sphingobacteriales*
P2_F6	633	Uncultured bacterium clone V201-144 (HQ114159.1) / 96%	*Sphingobacteriales*
P2_F9	527	Uncultured Bacteroidetes bacterium clone Skagenf40 (DQ640709.1) / 99%	*Sphingobacteriales*
P2_G6	495	Uncultured bacterium clone BCM3P-28B (AY102891.1)	*Sphingobacteriales*
P2_H1	519	Uncultured bacterium clone ambient_uncontrolled-60 (GU454921.1) / 99%	*Sphingobacteriales*
P1_E12	523	Uncultured Bacteroidetes bacterium clone AS64 (EU283382.1) / 99%	*Bacteroidetes*
P1_E5	507	Uncultured Bacteroidetes bacterium clone Elev_16S_1393 (EF020003.1) / 94%	*Bacteroidetes*
P2_C2	539	Uncultured Bacteroidetes bacterium clone AS100 (EU283397.1)	*Bacteroidetes*
P2_E2	471	Uncultured bacterium clone SAV07B05 (EU542338.1)	*Bacteroidetes*
P2_E6	737	Uncultured bacterium clone RBC4-13 (AB567915.1) / 99%	*Bacteroidetes*
P2_H2	456	Uncultured bacterium clone RBC4-13 (AB567915.1) / 98%	*Bacteroidetes*
P1_A2	525	Uncultured bacterium clone 135 (HQ538650.1) / 99%	*Rhodocyclaceae*
P1_A8	427	Uncultured bacterium clone BF-28 (HQ609633.1)	*Rhodocyclaceae*

P1_B2	537	Uncultured bacterium clone BXHB95 (GQ480128.1)	*Rhodocyclaceae*
P1_F1	520	Uncultured bacterium clone 135 (HQ538650.1) / 98%	*Rhodocyclaceae*
P1_F4	460	Uncultured Rhodocyclaceae bacterium clone H5 (EU850394.1) / 99%	*Rhodocyclaceae*
P1_F7	438	Uncultured bacterium clone 135 (HQ538650.1)	*Rhodocyclaceae*
P1_H10	467	Uncultured Rhodocylaceae bacterium clone TDNP_Wbc97_146_1_49 (FJ517018.1) / 99%	*Rhodocyclaceae*
P1_H4	524	Uncultured beta proteobacterium clone CB_05 (EF562548.1) / 99%	*Rhodocyclaceae*
P2_C1	564	Uncultured bacterium clone F_SBR_65 (HQ010840.1)	*Rhodocyclaceae*
P2_D2	560	Uncultured bacterium clone BXHB55 (GQ480093.1) / 100 %	*Rhodocyclaceae*
P2_F2	554	Uncultured bacterium clone S-110 (HQ132419.1) / 99%	*Rhodocyclaceae*
P2_F4	474	Uncultured Rhodocyclaceae bacterium clone H5 (EU850394.1) / 99%	*Rhodocyclaceae*
P2_G2	488	Uncultured bacterium clone A49 (FJ660557.1) / 99%	*Rhodocyclaceae*
P2_G5	502	Uncultured bacterium clone RBC4-16 (AB567914.1)	*Rhodocyclaceae*
P2_H4	425	Uncultured Rhodocylaceae bacterium clone TDNP_Wbc97_146_1_49 (FJ517018.1) / 99%	*Rhodocyclaceae*
P1_B7	523	Uncultured beta proteobacterium clone 48GS2 (EF203830.1) / 98%	*Comamonadaceae*
P1_D5	523	Uncultured beta proteobacterium clone 40GS2 (EF203828.1) / 99%	*Comamonadaceae*
P2_A4	429	Uncultured beta proteobacterium clone 65GS2 (EF203836.1)	*Comamonadaceae*
P2_B4	491	Uncultured bacterium clone C-CF-23 (AF443568.1) / 98%	*Comamonadaceae*
P2_C4	550	Uncultured Betaproteobacteria bacterium clone QEDN4AA02 (CU927369.1) / 99%	*Comamonadaceae*
P2_D5	487	Uncultured bacterium clone S1-1-CL2 (AY725246.1) / 98%	*Comamonadaceae*
P2_E5	501	Uncultured bacterium clone TH-3 (AB184982.1)	*Comamonadaceae*
P2_H6	590	Uncultured beta proteobacterium clone D1 (EF203798.1) / 98%	*Comamonadaceae*
P1_C6	523	Uncultured bacterium clone A62 (FJ660561.1) / 96%	*Burkholderiales*
P2_B2	585	Uncultured bacterium clone P092904_P1A07 (HQ385510.1) / 99%	*Burkholderiales*
P2_C3	447	Uncultured Betaproteobacteria bacterium clone QEDR2CH08 (CU922595.1)	*Burkholderiales*
P2_C6	500	Uncultured bacterium clone A62 (FJ660561.1)	*Burkholderiales*
P2_E1	482	Uncultured beta proteobacterium clone F-49 (HQ132426.1) / 99%	*Burkholderiales*

P1_A10	531	Uncultured bacterium clone PL14-3B (EU409545.1) / 98%	*TM7*
P1_C9	603	Uncultured bacterium clone RBC3-80 (AB567850.1) / 95%	*TM7*
P1_D7	443	Uncultured gamma proteobacterium clone AS137 (EU283406.1)	*TM7*
P1_D9	565	Uncultured TM7 bacterium clone QEEB2AF06 (CU917744.1)	*TM7*
P1_F2	485	Uncultured candidate division TM7 bacterium clone IC3092 (HQ595220.1) / 94%	*TM7*
P1_F8	597	Uncultured gamma proteobacterium clone AS131 (EU283403.1) / 98%	*TM7*
P1_G5	502	Uncultured bacterium clone SB1-28 (AB567933.1) / 100%	*TM7*
P2_B1	609	Uncultured bacterium clone E6 (HQ008083.1) / 97%	*TM7*
P2_C8	540	Uncultured TM7 bacterium clone QEEB1DB09 (CU917528.1)	*TM7*
P2_G1	530	Uncultured bacterium clone E6 (HQ008083.1) / 99%	*TM7*
P1_E9	334	Uncultured freshwater bacterium clone 965020C02.y1 (DQ065088.1) / 97 %	*Rhodobacteraceae*
P2_A8	500	Uncultured bacterium clone 44 (FJ623308.1) / 98%	*Rhodobacteraceae*
P1_B9	471	Uncultured bacterium clone VE08-141-BAC (GQ340352.1) / 98%	*Sphingomonadaceae*
P1_F9	475	Uncultured Alphaproteobacteria bacterium clone QEEB3BD01 (CU918333.1) / 98%	*Sphingomonadaceae*
P1_A1	518	Uncultured Firmicutes bacterium clone p1a14pool (HM104862.1) / 87%	*Clostridia*
P2_A9	514	Uncultured bacterium clone orang2_aai68b09 (EU777440.1) / 99%	*Clostridia*
P1_C3	511	Uncultured bacterium clone F5K2Q4C04IYRIT (GU912871.1) / 98%	*Myxococcales*
P2_A3	487	Uncultured bacterium clone G01-2 (FM253670.1) / 93%	*Myxococcales*
P2_B7	461	Uncultured bacterium clone F5K2Q4C04I9XV0 (GU911876.1) / 100%	*Myxococcales*
P1_C7	447	Uncultured bacterium clone T1-126 (GQ487929.1) / 93%	*Actinobacteria*
P1_H11	433	Uncultured Firmicutes bacterium clone QEDP2DB03 (CU924559.1) / 96%	*Actinobacteria*
P2_C5	446	Uncultured bacterium clone ORS25C_f06 (EF392998.1)	*Acidobacteria Gp3*
P2_E4	475	Uncultured bacterium clone I2-49 (GU325930.1) / 96%	*Acidobacteria Gp6*
P2_C7	501	Uncultured bacterium clone VE07-08-BAC (GQ340204.1) / 99%	*Campylobacteraceae*
P1_E2	438	Uncultured sludge bacterium A17 (AF234760.1) / 95%	*Planctomycetaceae*
P2_G9	479	Uncultured bacterium clone F11 (FJ230909.1) / 99%	*Planctomycetaceae*

P1_C4	500	Uncultured bacterium clone F5K2Q4C04INAWL (GU911618.1) / 98%	*Chloroflexi*
P2_C9	576	Uncultured bacterium clone d0-6 (AM409805.1) / 99%	*Chromatiales*
P2_B3	530	Uncultured bacterium clone DP7.3.68 (FJ612220.1) / 99%	*Lactobacillales*
P1_A6	399	Uncultured alpha proteobacterium clone A12-1 (FM253575.1) / 97%	*Rhizobiales*
P2_F8	300	Uncultured bacterium clone SINO708 (HM129861.1)	*Verrucomicrobiales*
P1_D3	406	Uncultured bacterium clone cc18 (EU875547.1)	*Bacteria*
P1_D11	479	Uncultured bacterium clone DP7.3.10 (FJ612210.1)	*Bacteria*
P1_G8	475	Uncultured bacterium clone BXHA102 (GQ480048.1)	*Bacteria*
P2_D1	565	Uncultured Unclassified bacterium clone QEDR1AD03 (CU922007.1)	*Bacteria*
P2_E3	475	Uncultured bacterium clone Unfilt_MembC06 (GQ247072.1)	*Bacteria*
P1_B11	524	Uncultured bacterium clone B16_B134 (GQ458142.1)	*Bacteria*
P1_H6	520	Uncultured bacterium clone RBC1-13 (AB567781.1)	*Bacteria*
P2_G3	443	Uncultured Chlorobi bacterium clone QEDN11AE07 (CU926672.1)	*Bacteria*
P2_D4	484	Uncultured Termite group 1 bacterium clone MVP-111 (DQ676373.1)	*Bacteria*
P2_F3	499	Uncultured bacterium clone Skagenf79 (DQ640692.1)	*Bacteria*
P1_E4	509	Uncultured bacterium clone Skagenf79 (DQ640692.1)	*Bacteria*
P2_A2	597	Uncultured bacterium clone P092904_P1A07 (HQ385510.1)	*Betaproteobacteria*
P2_G7	569	Uncultured prokaryote clone Fr1-12 (GU208468.1)	*Betaproteobacteria*
P2_F7	471	Uncultured bacterium clone ambient_uncontrolled-16 (GU454877.1)	*Betaproteobacteria*
P2_B9	599	Uncultured Rhodocyclaceae clone 114 (FM207944.1)	*Betaproteobacteria*
P1_F12	477	Uncultured bacterium clone d085 (AF422666.1)	*Betaproteobacteria*
P2_H5	457	Uncultured bacterium clone Kas142B (EF203189.1)	*Betaproteobacteria*
P1_B10	508	Unidentified bacterium clone M1_Rhizo_T7s_42 (EF605930.1)	*Deltaproteobacteria*
P1_G9	535	Uncultured epsilon proteobacterium clone BB-1-D9 (AY214766.1)	*Deltaproteobacteria*
P1_E6	548	Uncultured gamma proteobacterium clone GB2917y (DQ201885.1)	*Gammaproteobacteria*
P1_E8	547	Uncultured Unclassified bacterium clone QEEB3DF08 (CU918127.1)	*Gammaproteobacteria*

P1_F11	631	Uncultured gamma proteobacterium clone GB2917y (DQ201885.1)	*Gammaproteobacteria*
P2_G4	480	Uncultured bacterium clone LaP15L85 (EF667684.1)	*Gammaproteobacteria*
P2_D9	279	Uncultured bacterium clone H68 (EU529733.1)	*Gammaproteobacteria*
P2_E9	426	Uncultured gamma proteobacterium clone GB2917y (DQ201885.1)	*Gammaproteobacteria*
P2_D7	506	Uncultured Flavimonas sp. clone CL2.C72 (FM175401.1)	*Gammaproteobacteria*
P2_E7	503	Uncultured bacterium clone HF_NC_6 (FJ625345.1)	*Gammaproteobacteria*
P2_H9	437	Uncultured bacterium clone 60 (FJ623321.1)	*Gammaproteobacteria*
P1_B5	520	Uncultured bacterium clone 128 (FJ623379.1)	*Gammaproteobacteria*
P2_A7	513	Uncultured Unclassified bacterium clone QEEB3DF08 (CU918127.1)	*Gammaproteobacteria*
P1_G11	513	Uncultured gamma proteobacterium clone GB2917y (DQ201885.1)	*Gammaproteobacteria*
P1_C12	521	Uncultured bacterium clone June05-pIII-B05 (HQ592542.1)	*Gammaproteobacteria*
P1_G4	519	Uncultured bacterium clone LSC41 (EU117079.1)	*Gammaproteobacteria*
P1_G12	530	Uncultured bacterium clone 5C231050 (EU803476.1)	*Proteobacteria*
P2_G8	397	Uncultured bacterium clone 0311 (AB286384.1)	*Proteobacteria*
P2_B5	479	Uncultured bacterium clone eub62A3 (GQ390243.1)	*Proteobacteria*

Annex VII: Correlations of abiotic and biotic parameters in the WWTP Eilenburg

Table 15. General correlations between abiotic parameters (weather and WWTP influent). Given are the values for main correlations found using Spearmans correlation factor and Kendalls Tau (r_S, τ) as well as their respective significance (p) and permutation ($p_{permutation}$) values.
T: temperature, WWTP: wastewater treatment plant, h: humidity, a. v.: air velocity, a. p.: air pressure, e. c.: electrical conductivity, w. d.: week day, max.: maximum, min.: minimum

parameter 1 (abiotic)	parameter 2 (abiotic)	r_S	p	$p_{permutation}$	τ	p	$p_{permutation}$
a. v.	h $_{min}$	0.4	0.1	0.1	0.3	0.1	0.1
amount $_{influent}$	turbidity $_{effluent}$	0.4	0.1	0.1	0.3	0.2	0.2
h $_{max}$	pH $_{influent}$	0.4	0.1	0.1	0.3	0.1	0.2
rain	pH $_{influent}$	0.4	0.1	0.1	0.3	0.1	0.1
rain	T $_{influent}$	0.5	0.1	0.1	0.3	0.1	0.1
rain	amount $_{influent}$	0.4	0.1	0.1	0.4	0.1	0.1
rain	turbidity $_{effluent}$	0.4	0.1	0.1	0.4	0.1	0.1
T $_{max}$	T $_{min}$	0.6	0.0	0.0	0.5	0.0	0.0
T $_{max}$	h $_{max}$	0.6	0.0	0.0	0.4	0.0	0.1
T $_{max}$	sunshine	0.4	0.1	0.1	0.3	0.1	0.2
T $_{min}$	rain	0.5	0.1	0.1	0.4	0.0	0.1
a. p. $_{max}$	T $_{influent}$	-0.4	0.1	0.1	-0.3	0.1	0.1
a. p. $_{max}$	T $_{effluent}$	-0.5	0.1	0.1	-0.4	0.1	0.1
a. v.	T $_{air}$	-0.5	0.1	0.1	-0.4	0.0	0.1
e. c. $_{influent}$	turbidity $_{effluent}$	-0.5	0.1	0.1	-0.4	0.1	0.1
rain	sunshine	-0.4	0.1	0.1	-0.3	0.1	0.1
rain	T $_{air}$	-0.4	0.1	0.1	-0.4	0.1	0.1
T $_{max}$	a. p. $_{max}$	-0.5	0.1	0.1	-0.2	0.1	0.2
T $_{max}$	a. v.	-0.5	0.1	0.1	-0.3	0.1	0.1
T $_{min}$	a. p. $_{max}$	-0.6	0.0	0.0	-0.4	0.0	0.0
w. d.	amount $_{influent}$	-0.5	0.1	0.1	-0.4	0.1	0.1
w. d.	pH $_{influent}$	-0.4	0.1	0.1	-0.4	0.1	0.1

a) Primary clarifier

Table 16. General correlations between chemical parameters measured in the primary clarifier and abiotic parameters. Given are the values for main correlations found using Spearmans correlation factor and Kendalls Tau (r_S, τ) as well as their respective significance (p) and permutation ($p_{permutation}$) values.
T: temperature, WW: wastewater, h: humidity, a. v.: air velocity, a. p.: air pressure, e. c.: electrical conductivity, w. d.: week day, IC: inorganic carbon, TOC: total organic carbon, TC: total carbon, COD: chemical oxygen demand, TN: total nitrogen, NH$_4$-N: ammonium nitrogen, max.: maximum, min.: minimum

parameter 1	parameter 2	r_S	p	$p_{permutation}$	τ	p	$p_{permutation}$
COD	w. d.	0.5	0.1	0.1	0.4	0.1	0.0
COD	h. $_{max}$	0.4	0.2	0.2	0.3	0.2	0.2
COD	rain	0.5	0.1	0.2	0.4	0.1	0.2
COD	T $_{min}$	0.4	0.2	0.2	0.3	0.1	0.1
COD	T $_{influent}$	0.6	0.0	0.1	0.5	0.0	0.0
IC	sunshine	0.5	0.1	0.1	0.4	0.1	0.1
IC	TN	0.5	0.1	0.1	0.4	0.1	0.1
NH$_4$-N	pH $_{influent}$	0.6	0.1	0.1	0.4	0.1	0.1
nitrate	T $_{max}$	0.4	0.2	0.2	0.3	0.1	0.1
nitrite	phosphate	0.4	0.2	0.2	0.3	0.1	0.2
nitrite	T $_{influent}$	0.4	0.2	0.2	0.3	0.1	0.2
TC	T $_{min}$	0.4	0.2	0.2	0.3	0.1	0.2
TC	T $_{influent}$	0.6	0.1	0.1	0.5	0.0	0.0
TC	a. p. $_{min}$	0.4	0.2	0.2	0.3	0.2	0.2
TN	pH $_{influent}$	0.5	0.1	0.1	0.4	0.1	0.1
TN	phosphate	0.5	0.1	0.1	0.4	0.1	0.1
TOC	T $_{max}$	0.4	0.2	0.2	0.3	0.2	0.2
TOC	T $_{min}$	0.4	0.1	0.2	0.4	0.1	0.1
TOC	T $_{influent}$	0.6	0.0	0.0	0.5	0.0	0.0
COD	pH $_{influent}$	-0.5	0.1	0.1	-0.3	0.1	0.2
IC	h. $_{max}$	-0.5	0.1	0.1	-0.4	0.1	0.1
IC	rain	-0.5	0.1	0.1	-0.4	0.1	0.2
NH$_4$-N	w. d.	-0.5	0.1	0.1	-0.3	0.2	0.2
NH$_4$-N	rain	-0.5	0.1	0.2	-0.4	0.1	0.2
nitrate	e. c. $_{influent}$	-0.6	0.1	0.1	-0.4	0.0	0.1
nitrite	e. c. $_{influent}$	-0.5	0.1	0.1	-0.4	0.1	0.1
TC	NH$_4$-N	-0.6	0.1	0.1	-0.4	0.1	0.1
TC	pH $_{influent}$	-0.6	0.0	0.0	-0.4	0.1	0.1
TOC	pH $_{influent}$	-0.6	0.0	0.1	-0.4	0.1	0.1

Table 17. Spearmans correlation factor and Kendalls Tau (r_S, τ) and their respective significance (p) and permutation ($p_{permutation}$) values for the main correlations between biotic and abiotic parameters in the primary clarifier.
T: temperature, WW: wastewater, h: humidity, a. v.: air velocity, a. p.: air pressure, e. c.: electrical conductivity, w. d.: week day, IC: inorganic carbon, TOC: total organic carbon, TC: total carbon, COD: chemical oxygen demand, TN: total nitrogen, NH_4-N: ammonium nitrogen, Tc: tetracycline hydrochloride, n. l. l. c.: neutral lipid like compounds, max.: maximum, min.: minimum

parameter 1 (biotic)	parameter 2 (abiotic)	r_S	p	$p_{permutation}$	τ	p	$p_{permutation}$
Tc-stained cells	sunshine	0.4	0.3	0.3	0.3	0.2	0.3
Tc-stained cells	w. d.	0.5	0.2	0.2	0.3	0.3	0.3
I	IC	0.4	0.2	0.2	0.4	0.1	0.1
II	COD	0.4	0.2	0.2	0.4	0.1	0.1
II	TOC	0.5	0.1	0.1	0.4	0.1	0.1
III	h. min	0.5	0.1	0.1	0.3	0.1	0.1
IV	w. d.	0.4	0.1	0.1	0.3	0.1	0.2
V	brewery discharge	0.5	0.0	0.1	0.3	0.1	0.1
VI	brewery discharge	0.4	0.1	0.1	0.3	0.2	0.2
VII	brewery discharge	0.5	0.1	0.1	0.3	0.1	0.1
VII	pH influent	0.4	0.1	0.1	0.3	0.1	0.2
VIII	a. p. min	0.4	0.1	0.1	0.3	0.1	0.1
VIII	IC	0.4	0.2	0.2	0.3	0.2	0.2
VIII	pH influent	0.5	0.1	0.1	0.4	0.0	0.1
IX	TC	0.4	0.2	0.2	0.3	0.2	0.3
IX	rain	0.4	0.1	0.1	0.4	0.1	0.1
IX	e. c. influent	0.5	0.1	0.1	0.4	0.0	0.1
X	nitrite	0.6	0.0	0.0	0.4	0.0	0.1
XI	nitrate	0.6	0.0	0.0	0.4	0.1	0.1
cells with n.l.l.c.	h. max	-0.5	0.1	0.1	-0.4	0.1	0.1
cells with n.l.l.c.	a. p. min	-0.5	0.1	0.1	-0.2	0.2	0.2
cells with n.l.l.c.	nitrite	-0.5	0.1	0.1	-0.4	0.1	0.1
I	COD	-0.4	0.2	0.2	-0.3	0.1	0.2
I	TC	-0.5	0.1	0.1	-0.4	0.1	0.1
I	TOC	-0.5	0.1	0.1	-0.4	0.1	0.1
I	w. d.	-0.5	0.1	0.1	-0.4	0.1	0.1
II	brewery discharge	-0.5	0.0	0.0	-0.4	0.0	0.0
II	e. c. influent	-0.5	0.1	0.1	-0.4	0.1	0.1
III	h. max	-0.5	0.1	0.1	-0.4	0.1	0.1
III	T air	-0.5	0.1	0.1	-0.4	0.1	0.1
III	T influent	-0.4	0.1	0.1	-0.3	0.1	0.1
III	T effluent	-0.5	0.1	0.1	-0.4	0.0	0.1
IV	TN	-0.6	0.0	0.1	-0.4	0.1	0.1
IV	NH_4-N	-0.4	0.2	0.2	-0.3	0.1	0.2
IV	amount influent	-0.5	0.0	0.1	-0.4	0.1	0.1
VI	T air	-0.5	0.1	0.1	-0.3	0.1	0.1
VIII	T max	-0.4	0.1	0.1	-0.3	0.1	0.1
VIII	TOC	-0.4	0.2	0.2	-0.3	0.2	0.2
IX	amount influent	-0.5	0.0	0.0	-0.5	0.0	0.0

X	brewery discharge	-0.4	0.1	0.1	-0.3	0.2	0.2
XI	TN	-0.4	0.2	0.2	-0.3	0.2	0.2
XI	brewery discharge	-0.5	0.1	0.1	-0.4	0.0	0.0
XI	e.c. influent.	-0.5	0.1	0.1	-0.4	0.1	0.1

Table 18. Spearmans correlation factor and Kendalls Tau (r_S, τ) and their respective significance (p) and permutation (p permutation) values for the main correlations between biotic parameters in the primary clarifier. Tc: tetracycline hydrochloride, n. l. l. c.: neutral lipid like compounds

parameter 1 (biotic)	parameter 2 (biotic)	r_S	p	p permutation	τ	p	p permutation
Tc-stained cells	III	0.4	0.2	0.2	0.3	0.2	0.3
IV	IX	0.4	0.1	0.1	0.3	0.1	0.1
V	IX	0.5	0.0	0.0	0.4	0.0	0.0
VI	IX	0.4	0.1	0.1	0.4	0.1	0.1
VII	IX	0.4	0.1	0.1	0.3	0.1	0.1
X	XI	0.5	0.1	0.1	0.0	0.1	0.1
cells with n.l.l.c.	V	-0.5	0.0	0.0	-0.4	0.1	0.1
cells with n.l.l.c.	IX	-0.6	0.0	0.0	-0.4	0.1	0.1
Tc-stained cells	VII	-0.5	0.2	0.2	-0.3	0.2	0.3
Tc-stained cells	VIII	-0.5	0.2	0.2	-0.3	0.2	0.3
II	VIII	-0.5	0.1	0.1	-0.3	0.1	0.1
II	IX	-0.5	0.1	0.1	-0.3	0.1	0.1
III	XI	-0.5	0.1	0.1	-0.3	0.1	0.1
V	X	-0.6	0.0	0.0	-0.5	0.0	0.0
VII	X	-0.5	0.0	0.0	-0.4	0.0	0.0
VIII	X	-0.4	0.1	0.1	-0.2	0.2	0.2

b) Aeration tank 1

Table 19. Spearmans correlation factor and Kendalls Tau (r_S, τ) and their respective significance (p) and permutation (p permutation) values for the main correlations between abiotic parameters in the aeration tank 1. T: temperature, WW: wastewater, h: humidity, a. v.: air velocity, e. c.: electrical conductivity, IC: inorganic carbon, TOC: total organic carbon, TC: total carbon, COD: chemical oxygen demand, TN: total nitrogen, NH_4-N: ammonium nitrogen, amount r. s.: amount return sludge (reused sludge from the secondary clarifier 1), max.: maximum, min.: minimum

parameter 1 (abiotic)	parameter 2 (abiotic)	r_S	p	p permutation	τ	p	p permutation
amount influent	amount r. s	1.0	0.0	0.0	1.0	0.0	0.0
IC	w. d.	0.6	0.0	0.0	0.5	0.0	0.0
IC	sunshine	0.7	0.0	0.0	0.5	0.0	0.0
nitrate	a. p. min	0.7	0.0	0.0	0.6	0.0	0.0
phosphate	amount influent	0.8	0.0	0.0	0.7	0.0	0.0
phosphate	amount r. s	0.8	0.0	0.0	0.7	0.0	0.0
rain	amount r. s.	0.5	0.1	0.1	0.4	0.1	0.1
T air	IC	0.7	0.0	0.0	0.6	0.0	0.0
T effluent	nitrate	0.4	0.2	0.2	0.3	0.2	0.2
T effluent	nitrite	0.7	0.0	0.0	0.6	0.0	0.0
T effluent	redox potential	0.6	0.0	0.0	0.5	0.0	0.0
T effluent	IC	0.5	0.1	0.1	0.4	0.1	0.1
T influent	nitrate	0.5	0.1	0.1	0.3	0.1	0.1
T influent	nitrite	0.6	0.0	0.0	0.5	0.0	0.0
T influent	redox potential	0.6	0.0	0.0	0.5	0.0	0.0
T max	IC	0.7	0.0	0.0	0.6	0.0	0.0
T min	redox potential	0.5	0.1	0.1	0.4	0.1	0.1
T min	nitrite	0.7	0.0	0.0	0.5	0.0	0.0
T ww	T max	0.6	0.0	0.0	0.4	0.0	0.0
T ww	T min	0.7	0.0	0.0	0.5	0.0	0.0
T ww	T influent	0.8	0.0	0.0	0.6	0.0	0.0
T ww	h. max	0.5	0.1	0.1	0.3	0.1	0.1
T ww	rain	0.4	0.1	0.1	0.4	0.1	0.1
T ww	nitrate	0.5	0.1	0.1	0.4	0.1	0.1
T ww	nitrite	0.6	0.0	0.0	0.4	0.1	0.1
T ww	redox potential	0.7	0.0	0.0	0.6	0.0	0.0
T ww	oxygen	0.7	0.0	0.0	0.5	0.0	0.0
TC	COD	0.6	0.0	0.0	0.5	0.0	0.0
TC	TOC	1.0	0.0	0.0	0.9	0.0	0.0
TC	TN	0.8	0.0	0.0	0.8	0.0	0.0
TOC	COD	0.7	0.0	0.0	0.6	0.0	0.0
TOC	TN	0.9	0.0	0.0	0.8	0.0	0.0

a. v.	TN	-0.5	0.1	0.1	-0.3	0.1	0.2
a. v.	nitrite	-0.6	0.1	0.1	-0.4	0.0	0.1
a. v.	TC	-0.5	0.1	0.1	-0.3	0.2	0.2
black water	TN	-0.4	0.2	0.2	-0.3	0.1	0.2
black water	redox potential	-0.4	0.1	0.1	-0.3	0.1	0.2
e. c. influent	amount r. s	-0.8	0.0	0.0	-0.7	0.0	0.0
e. c. influent	phosphate	-0.7	0.0	0.0	-0.5	0.0	0.0
NH$_4$-N	h. max	-0.7	0.0	0.0	-0.5	0.0	0.0
rain	IC	-0.5	0.1	0.1	-0.4	0.1	0.1

Table 20. Spearmans correlation factor and Kendalls Tau (r_S, τ) and their respective significance (p) and permutation (p $_{permutation}$) values for the main correlations between biotic and abiotic parameters in the aeration tank 1. T: temperature, WW: wastewater, IC: inorganic carbon, TOC: total organic carbon, TC: total carbon, COD: chemical oxygen demand, TN: total nitrogen, Tc: tetracycline hydrochloride, n. l. l. c.: neutral lipid like compounds, max.: maximum, min.: minimum, e. c.: electrical conductivity, a. p.: air pressure, w. d.: week day, amount $_{r. s.}$: amount return sludge (reused sludge from the secondary clarifier 1)

parameter 1 (biotic)	parameter 2 (abiotic)	r_S	p	p $_{permutation}$	τ	p	p $_{permutation}$
Tc-stained cells	a. p. min	0.5	0.1	0.1	0.4	0.1	0.1
Tc-stained cells	nitrate	0.4	0.2	0.2	0.3	0.3	0.3
Tc-stained cells	redox potential	0.4	0.2	0.2	0.3	0.1	0.2
1	blackwater	0.5	0.1	0.1	0.4	0.1	0.1
4	rain	0.4	0.1	0.1	0.4	0.1	0.1
4	brewery discharge	0.6	0.1	0.1	0.4	0.1	0.1
6	blackwater	0.5	0.1	0.1	0.4	0.0	0.0
7	T max	0.8	0.0	0.0	0.6	0.0	0.0
7	T min	0.5	0.1	0.1	0.3	0.1	0.1
7	T air	0.8	0.0	0.0	0.7	0.0	0.0
7	IC	0.7	0.0	0.0	0.6	0.0	0.0
8	brewery discharge	0.6	0.1	0.1	0.4	0.1	0.1
9	redox potential	0.4	0.1	0.1	0.3	0.1	0.1
14	IC	0.7	0.0	0.0	0.5	0.0	0.0
15	IC	0.6	0.0	0.0	0.4	0.1	0.1
15	e. c. influent	0.6	0.0	0.0	0.4	0.0	0.0
Tc-stained cells	blackwater	-0.6	0.0	0.0	-0.4	0.0	0.1
cells with n.l.l.c.	brewery discharge	-0.5	0.0	0.0	-0.3	0.1	0.1
cells with n.l.l.c.	a. p. min	-0.5	0.0	0.0	-0.4	0.1	0.1
1	brewery discharge	-0.5	0.2	0.2	-0.3	0.2	0.3
1	T ww	-0.6	0.0	0.0	-0.4	0.0	0.0
1	nitrate	-0.4	0.1	0.2	-0.3	0.2	0.3
2	T max	-0.7	0.0	0.0	-0.5	0.0	0.0
2	T min	-0.8	0.0	0.0	-0.6	0.0	0.0
2	T air	-0.5	0.0	0.0	-0.4	0.0	0.0
2	T influent	-0.9	0.0	0.0	-0.7	0.0	0.0

2	T effluent	-0.8	0.0	0.0	-0.7	0.0	0.0
2	T ww	-0.6	0.0	0.0	-0.4	0.1	0.1
2	nitrate	-0.4	0.2	0.2	-0.3	0.1	0.2
2	nitrite	-0.6	0.0	0.0	-0.5	0.0	0.0
2	rain	-0.5	0.1	0.1	-0.4	0.0	0.1
2	redox potential	-0.7	0.0	0.0	-0.5	0.0	0.0
3	T influent	-0.4	0.1	0.1	-0.3	0.1	0.2
3	rain	-0.5	0.1	0.1	-0.4	0.0	0.1
4	blackwater	-0.7	0.0	0.0	-0.5	0.0	0.0
5	brewery discharge	-0.8	0.0	0.0	-0.6	0.0	0.0
5	rain	-0.5	0.1	0.1	-0.4	0.0	0.1
6	TOC	-0.4	0.1	0.1	-0.3	0.2	0.3
6	TN	-0.5	0.1	0.1	-0.4	0.1	0.1
7	rain	-0.4	0.1	0.1	-0.4	0.1	0.1
7	h. min	-0.6	0.0	0.0	-0.5	0.0	0.0
8	w. d.	-0.5	0.1	0.1	-0.3	0.1	0.1
9	blackwater	-0.8	0.0	0.0	-0.7	0.0	0.0
13	brewery discharge	-0.9	0.0	0.0	-0.7	0.0	0.0
13	rain	-0.5	0.1	0.1	-0.4	0.0	0.1
14	amount r. s.	-0.6	0.0	0.0	-0.5	0.0	0.0
15	rain	-0.4	0.1	0.1	-0.4	0.1	0.1
15	amount influent	-0.6	0.0	0.0	-0.5	0.0	0.0
15	amount r. s.	-0.7	0.0	0.0	-0.6	0.0	0.0

Table 21. Spearmans correlation factor and Kendalls Tau (r_S, τ) and their respective significance (p) and permutation (p permutation) values for the main correlations between biotic parameters in the aeration tank 1. Tc: tetracycline hydrochloride, n. l. l. c.: neutral lipid like compounds

parameter 1 (biotic)	parameter 2 (biotic)	r_S	p	p permutation	τ	p	p permutation
Tc-stained cells	4	1.0	0.0	0.0	0.8	0.0	0.0
Tc-stained cells	8	0.5	0.1	0.1	0.4	0.1	0.1
Tc-stained cells	9	0.8	0.0	0.0	0.7	0.0	0.0
Tc-stained cells	11	0.6	0.1	0.1	0.4	0.1	0.1
1	13	0.5	0.1	0.1	0.3	0.1	0.2
3	2	0.6	0.1	0.0	0.5	0.0	0.0
3	6	0.6	0.0	0.0	0.4	0.0	0.0
3	13	0.6	0.0	0.0	0.5	0.0	0.0
4	8	0.7	0.0	0.0	0.6	0.0	0.0
4	9	0.9	0.0	0.0	0.7	0.0	0.0
4	11	0.7	0.0	0.0	0.5	0.0	0.0
5	2	0.6	0.0	0.0	0.4	0.0	0.0
5	6	0.8	0.0	0.0	0.6	0.0	0.0
5	12	0.6	0.0	0.0	0.5	0.0	0.0
5	13	0.8	0.0	0.0	0.6	0.0	0.0
9	11	0.6	0.0	0.0	0.4	0.0	0.0
11	8	0.7	0.0	0.0	0.5	0.0	0.0

11	10	0.6	0.0	0.0	0.4	0.0	0.0
12	6	0.7	0.0	0.0	0.6	0.0	0.0
14	7	0.7	0.0	0.0	0.6	0.0	0.0
15	7	0.5	0.1	0.1	0.4	0.0	0.0
15	14	0.7	0.0	0.0	0.5	0.0	0.0
Tc-stained cells	1	-0.7	0.0	0.0	-0.6	0.0	0.0
Tc-stained cells	5	-0.7	0.0	0.0	-0.5	0.0	0.0
Tc-stained cells	6	-0.8	0.0	0.0	-0.6	0.0	0.0
Tc-stained cells	13	-0.9	0.0	0.0	-0.8	0.0	0.0
1	4	-0.5	0.1	0.1	-0.4	0.0	0.0
1	9	-0.5	0.1	0.1	-0.3	0.1	0.1
3	8	-0.5	0.1	0.1	-0.3	0.1	0.1
4	3	-0.6	0.0	0.0	-0.4	0.0	0.0
4	5	-0.6	0.0	0.0	-0.4	0.0	0.0
4	6	-0.7	0.0	0.0	-0.5	0.0	0.0
4	7	-0.7	0.0	0.0	-0.5	0.0	0.0
4	13	-0.7	0.0	0.0	-0.5	0.0	0.0
4	14	-0.7	0.0	0.0	-0.5	0.0	0.0
7	8	-0.7	0.0	0.0	-0.5	0.0	0.0
9	3	-0.5	0.0	0.1	-0.4	0.1	0.1
9	5	-0.6	0.0	0.0	-0.4	0.0	0.0
9	6	-0.7	0.0	0.0	-0.5	0.0	0.0
9	13	-0.7	0.0	0.0	-0.5	0.0	0.0
11	3	-0.7	0.0	0.0	-0.5	0.0	0.0
11	5	-0.5	0.0	0.0	-0.4	0.0	0.0
11	6	-0.6	0.0	0.0	-0.4	0.0	0.0
14	8	-0.8	0.0	0.0	-0.7	0.0	0.0
15	8	-0.7	0.0	0.0	-0.5	0.0	0.0

c) Aeration tank 2

Table 22. Spearmans correlation factor and Kendalls Tau (r_S, τ) and their respective significance (p) and permutation (p $_{permutation}$) values for the main correlations between abiotic parameters in the aeration tank 2. T: temperature, WW: wastewater, h: humidity, a. v.: air velocity, a. p.: air pressure, e. c.: electrical conductivity, IC: inorganic carbon, TOC: total organic carbon, TC: total carbon, COD: chemical oxygen demand, TN: total nitrogen, NH$_4$-N: ammonium nitrogen, amount $_{r. s.}$: amount return sludge (reused sludge from the secondary clarifier 2), max.: maximum, min.: minimum

parameter 1 (abiotic)	parameter 2 (abiotic)	r_S	p	p $_{permutation}$	τ	p	p $_{permutation}$
amount $_{r. s}$	amount $_{influent}$	0.8	0.0	0.0	0.8	0.0	0.0
amount $_{r. s.}$	rain	0.4	0.1	0.1	0.4	0.0	0.1
IC	w. d.	0.7	0.0	0.0	0.5	0.0	0.0
IC	T $_{max}$	0.8	0.0	0.0	0.7	0.0	0.0
IC	T $_{effluent}$	0.5	0.1	0.1	0.4	0.0	0.1
IC	T $_{air}$	0.7	0.0	0.0	0.6	0.0	0.0
IC	sunshine	0.7	0.0	0.0	0.5	0.0	0.0
NH$_4$-N	pH $_{influent}$	0.6	0.0	0.0	0.5	0.0	0.1
oxygen	redox potential	0.7	0.0	0.0	0.6	0.0	0.0
T $_{WW}$	nitrate	0.4	0.2	0.2	0.4	0.1	0.1
T $_{WW}$	nitrite	0.5	0.1	0.1	0.3	0.1	0.2
T $_{WW}$	rain	0.4	0.1	0.1	0.4	0.1	0.1
T $_{WW}$	h. $_{max}$	0.4	0.1	0.1	0.3	0.1	0.1
T $_{WW}$	T $_{influent}$	0.8	0.0	0.0	0.7	0.0	0.0
T $_{WW}$	T $_{max}$	0.5	0.0	0.1	0.5	0.0	0.0
T $_{WW}$	T $_{min}$	0.7	0.0	0.0	0.5	0.0	0.0
T $_{WW}$	T $_{effluent}$	0.8	0.0	0.0	0.7	0.0	0.0
TC	TOC	0.9	0.0	0.0	0.9	0.0	0.0
TC	TN	1.0	0.0	0.0	0.9	0.0	0.0
TC	nitrite	0.7	0.0	0.0	0.5	0.0	0.0
TN	nitrite	0.7	0.0	0.0	0.5	0.0	0.0
TOC	TN	0.9	0.0	0.0	0.8	0.0	0.0
TOC	redox potential	0.6	0.0	0.0	0.5	0.0	0.0
a. v.	TN	-0.5	0.1	0.1	-0.4	0.1	0.1
a. v.	nitrite	-0.5	0.1	0.1	-0.4	0.1	0.1
a. v.	TC	-0.4	0.2	0.2	-0.3	0.2	0.2
amount $_{r. s.}$	e. c. $_{influent}$	-0.6	0.0	0.0	-0.5	0.0	0.0
blackwater	TN	-0.5	0.1	0.1	-0.4	0.0	0.1
blackwater	redox potential	-0.5	0.1	0.0	-0.4	0.0	0.1
COD	pH $_{influent}$	-0.8	0.0	0.0	-0.6	0.0	0.0
COD	rain	-0.6	0.0	0.0	-0.5	0.0	0.0
IC	h. $_{min}$	-0.7	0.0	0.0	-0.5	0.0	0.0
redox potential	NH$_4$-N	-0.7	0.0	0.0	-0.5	0.0	0.0

Table 23. Spearmans correlation factor and Kendalls Tau (r_S, τ) and their respective significance (p) and permutation (p $_{permutation}$) values for the main correlations between biotic and abiotic parameters in the aeration tank 2. T: temperature, WW: wastewater, h: humidity, a. v.: air velocity, a. p.: air pressure, e.c.: electrical conductivity, IC: inorganic carbon, TOC: total organic carbon, TC: total carbon, COD: chemical oxygen demand, TN: total nitrogen, NH_4-N: ammonium nitrogen, max.: maximum, min.: minimum, amount $_{r.\,s.}$: amount return sludge (reused sludge from the secondary clarifier 2), Tc: tetracycline hydrochloride, n. l. l. c.: neutral lipid like compounds

parameter 1 (biotic)	parameter 2 (abiotic)	r_S	p	p $_{permutation}$	τ	p	p $_{permutation}$
Tc-stained cells	a. p. $_{min}$	0.5	0.1	0.1	0.4	0.1	0.1
Tc-stained cells	nitrate	0.6	0.1	0.1	0.4	0.1	0.1
Tc-stained cells	redox potential	0.5	0.1	0.1	0.3	0.1	0.2
1	blackwater	0.5	0.1	0.1	0.4	0.1	0.1
3	a. v.	0.6	0.1	0.0	0.5	0.0	0.0
4	T $_{WW}$	0.6	0.0	0.0	0.4	0.0	0.0
4	brewery discharge	0.5	0.1	0.1	0.4	0.1	0.2
4	rain	0.7	0.0	0.0	0.5	0.0	0.0
6	blackwater	0.5	0.1	0.1	0.4	0.0	0.0
7	IC	0.7	0.0	0.0	0.5	0.0	0.0
7	T $_{max}$	0.6	0.0	0.0	0.4	0.0	0.0
8	brewery discharge	0.5	0.2	0.2	0.4	0.1	0.1
9	T $_{WW}$	0.7	0.0	0.0	0.6	0.0	0.0
9	nitrate	0.7	0.0	0.0	0.5	0.0	0.0
9	nitrite	0.7	0.0	0.0	0.5	0.0	0.0
10	nitrite	0.6	0.0	0.0	0.5	0.0	0.0
15	e. c. $_{influent}$	0.6	0.0	0.0	0.5	0.0	0.0
cells with n.l.l.c.	brewery discharge	-0.8	0.0	0.0	-0.7	0.0	0.0
cells with n.l.l.c.	a. p. $_{min}$	-0.7	0.0	0.0	-0.6	0.0	0.0
Tc-stained cells	blackwater	-0.5	0.1	0.1	-0.4	0.1	0.1
1	nitrate	-0.8	0.0	0.0	-0.6	0.0	0.0
2	rain	-0.5	0.1	0.1	-0.4	0.0	0.0
2	T $_{influent}$	-0.9	0.0	0.0	-0.7	0.0	0.0
2	T $_{max}$	-0.7	0.0	0.0	-0.5	0.0	0.0
2	T $_{min}$	-0.8	0.0	0.0	-0.7	0.0	0.0
2	h. $_{max}$	-0.4	0.1	0.1	-0.3	0.1	0.1
2	T $_{effluent}$	-0.8	0.0	0.0	-0.7	0.0	0.0
2	T $_{WW}$	-0.7	0.0	0.0	-0.6	0.0	0.0
2	T $_{air}$	-0.6	0.0	0.0	-0.4	0.0	0.0
2	nitrate	-0.6	0.1	0.1	-0.4	0.1	0.1
3	rain	-0.5	0.1	0.1	-0.4	0.0	0.1
3	T $_{min}$	-0.7	0.0	0.0	-0.5	0.0	0.0
3	T $_{influent}$	-0.7	0.0	0.0	-0.5	0.0	0.0
3	T $_{effluent}$	-0.7	0.0	0.0	-0.6	0.0	0.0
3	T $_{WW}$	-0.6	0.0	0.0	-0.4	0.0	0.0
5	rain	-0.6	0.3	0.0	-0.5	0.0	0.0
5	nitrate	-0.6	0.0	0.0	-0.5	0.0	0.0
5	T $_{min}$	-0.7	0.0	0.0	-0.5	0.0	0.0
5	T $_{influent}$	-0.7	0.0	0.0	-0.5	0.0	0.0

5	T effluent	-0.7	0.0	0.0	-0.5	0.0	0.0
5	T ww	-0.7	0.0	0.0	-0.5	0.0	0.0
6	TOC	-0.4	0.2	0.1	-0.3	0.2	0.2
6	TN	-0.5	0.1	0.1	-0.5	0.0	0.0
7	rain	-0.4	0.1	0.1	-0.4	0.1	0.1
7	h. min	-0.4	0.0	0.1	-0.3	0.1	0.1
7	amount r. s.	-0.6	0.0	0.0	-0.4	0.0	0.0
8	w. d.	-0.6	0.0	0.0	-0.4	0.0	0.0
8	IC	-0.5	0.1	0.1	-0.4	0.1	0.1
11	a. v.	-0.7	0.0	0.0	-0.5	0.0	0.0
12	oxygen	-0.6	0.0	0.0	-0.6	0.0	0.0
13	rain	-0.4	0.1	0.1	-0.3	0.1	0.1
13	nitrate	-0.7	0.0	0.0	-0.6	0.0	0.0
13	brewery discharge	-0.8	0.0	0.0	-0.6	0.0	0.0
14	amount influent	-0.4	0.1	0.1	-0.2	0.2	0.2
14	amount r. s.	-0.4	0.1	0.1	-0.2	0.2	0.2
15	amount influent	-0.5	0.1	0.1	-0.4	0.0	0.0
15	amount r. s.	-0.5	0.1	0.1	-0.4	0.1	0.1

Table 24. Spearmans correlation factor and Kendalls Tau (r_S, τ) and their respective significance (p) and permutation (p permutation) values for the main correlations between biotic parameters in the aeration tank 2. Tc: tetracycline hydrochloride, n. l. l. c.: neutral lipid like compounds

parameter 1 (biotic)	parameter 2 (biotic)	r_S	p	p permutation	τ	p	p permutation
Tc-stained cells	4	0.8	0.0	0.0	0.6	0.0	0.0
Tc-stained cells	9	0.7	0.0	0.0	0.5	0.0	0.0
1	13	0.5	0.1	0.1	0.4	0.1	0.1
2	3	0.9	0.0	0.0	0.7	0.0	0.0
2	13	0.6	0.0	0.0	0.4	0.0	0.1
3	5	0.9	0.0	0.0	0.7	0.0	0.0
3	6	0.5	0.1	0.1	0.4	0.0	0.1
3	13	0.6	0.0	0.0	0.5	0.0	0.0
4	8	0.6	0.0	0.0	0.4	0.0	0.0
4	9	0.9	0.0	0.0	0.7	0.0	0.0
4	11	0.6	0.0	0.0	0.5	0.0	0.0
5	2	0.9	0.0	0.0	0.7	0.0	0.0
5	6	0.5	0.1	0.1	0.4	0.0	0.0
5	13	0.8	0.0	0.0	0.6	0.0	0.0
6	12	0.6	0.0	0.0	0.4	0.0	0.0
6	13	0.5	0.1	0.1	0.4	0.0	0.0
7	14	0.7	0.0	0.0	0.5	0.0	0.0
7	15	0.7	0.0	0.0	0.6	0.0	0.0
8	11	0.5	0.1	0.1	0.3	0.1	0.1
9	11	0.6	0.0	0.0	0.5	0.0	0.0
10	11	0.5	0.1	0.1	0.4	0.0	0.1
14	15	0.7	0.0	0.0	0.6	0.0	0.0

Tc-stained cells	1	0.5	0.1	0.1	-0.3	0.1	0.1
Tc-stained cells	5	-0.7	0.0	0.0	-0.5	0.0	0.0
Tc-stained cells	6	-0.7	0.0	0.0	-0.5	0.0	0.0
Tc-stained cells	13	-0.9	0.0	0.0	-0.7	0.0	0.0
1	4	-0.6	0.0	0.0	-0.4	0.0	0.0
1	9	-0.4	0.1	0.1	-0.3	0.1	0.1
2	4	-0.7	0.0	0.0	-0.5	0.0	0.0
2	9	-0.8	0.0	0.0	-0.6	0.0	0.0
3	4	-0.8	0.0	0.0	-0.6	0.0	0.0
3	8	-0.5	0.1	0.1	-0.4	0.0	0.0
3	9	-0.8	0.0	0.0	-0.7	0.0	0.0
3	11	-0.8	0.0	0.0	-0.6	0.0	0.0
4	5	-0.9	0.0	0.0	-0.7	0.0	0.0
4	6	-0.6	0.0	0.0	-0.5	0.0	0.2
4	7	-0.5	0.1	0.1	-0.5	0.0	0.0
4	13	-0.7	0.0	0.0	-0.5	0.0	0.0
4	14	-0.6	0.0	0.0	-0.4	0.0	0.0
5	9	-0.9	0.0	0.0	-0.7	0.0	0.0
5	11	-0.6	0.0	0.0	-0.4	0.0	0.0
6	9	-0.7	0.0	0.0	-0.5	0.0	0.0
6	11	-0.5	0.0	0.1	-0.4	0.0	0.0
7	8	-0.7	0.0	0.0	-0.6	0.0	0.0
8	14	-0.8	0.0	0.0	-0.6	0.0	0.0
8	15	-0.7	0.0	0.0	-0.5	0.0	0.0
9	13	-0.7	0.0	0.0	-0.5	0.0	0.0
12	14	-0.7	0.0	0.0	-0.5	0.0	0.0
12	15	-0.6	0.0	0.0	-0.5	0.0	0.0

Erklärung

Die Dissertation wurde in der Zeit von September 2006 bis September 2011 im Helmholtz-Zentrum für Umweltforschung Leipzig, unter der wissenschaftlichen Betreuung von Prof. Dr. S. Müller und Prof. Dr. I. Röske angefertigt. Die Arbeit stellt eine erweiterte Zusammenfassung folgender Veröffentlichungen dar:

1. Günther, S., Hübschmann, T., Rudolf, M., Eschenhagen, M., Röske, I., Harms, H., Müller, S. (2008) Fixation procedures for flow cytometric analysis of environmental bacteria. J. Microbiol. Methods 75, 127-134.

2. Günther, S., Trutnau, M., Kleinsteuber, S., Hause, G., Bley, T., Röske, I., Harms, H., Müller, S. (2009) Dynamics of polyphosphate accumulating bacteria in waste water communities detected via DAPI and tetracycline labelling. Appl Environm Microbiol 75/7, 2111-2121.

3. Günther, S., Koch, C., Hübschmann, T., Röske, I., Müller, R.A., Bley, T., Harms, H., Müller, S. (2011) Correlation of community dynamics and process parameters as a tool for the prediction of the stability of wastewater treatment. Environmental Science and Technology, accepted

Aus diesem Grund wurden Teile der Veröffentlichungen in diese Arbeit übernommen.

Hiermit versichere ich, dass ich die vorliegende Arbeit ohne unzulässige Hilfe Dritter und ohne Benutzung anderer als der angegebenen Hilfsmittel angefertigt habe; die aus fremden Quellen direkt oder indirekt übernommenen Gedanken sind als solche kenntlich gemacht. Die Arbeit wurde bisher weder im Inland noch im Ausland in gleicher oder ähnlicher Form einer anderen Prüfungsbehörde vorgelegt.

....

Leipzig, September 2011